BIOTECHNOLOGICAL PRODUCTION OF INSECT SEX PHEROMONES AND POTATO VIRUS Y INFECTIOUS CLONE AS TOOLS IN PLANT PROTECTION

Mojca Juteršek

MEDNARODNA PODIPLOMSKA ŠOLA JOŽEFA STEFANA
JOŽEF STEFAN INTERNATIONAL POSTGRADUATE SCHOOL

Mojca Juteršek

BIOTECHNOLOGICAL PRODUCTION OF INSECT SEX PHEROMONES AND POTATO VIRUS Y INFECTIOUS CLONE AS TOOLS IN PLANT PROTECTION

Doctoral Dissertation

BIOTEHNOLOŠKA PROIZVODNJA SPOLNIH FEROMONOV ŽUŽELK IN INFEKTIVNI KLON VIRUSA KROMPIRJA Y KOT ORODJI PRI ZAŠČITI RASTLIN

Doktorska disertacija

Supervisor: Assist. Prof. Dr. Špela Baebler

Ljubljana, Slovenia, October 2023

Acknowledgments

The work presented in this dissertation would not have seen the light of day had I not been part of an admirable and experienced group of researchers in the Department of Biotechnology and Systems Biology at the National Institute of Biology. Inputs from all my co-workers created a stimulating environment in which I was able to acquire many new skills and much knowledge. Most importantly, I was fortunate to experience a positive and friendly work environment, which I greatly appreciate. Here, I would also like to specify everyone with exceptionally important contributions.

First and foremost, I would like to thank my supervisor, Špela Baebler, for all her encouragements and guidance. She masterfully navigated me through the real-world of research work and patiently revised all my manuscripts and other outputs. Thank you for all the fruitful discussions and one-on-one meetings, especially during the social distancing times of the pandemic.

I would also like to thank Kristina Gruden, the head of the Department and "Omics Approaches" group, for all her advice, ideas, and support driving the research work, as well as for her constant care for a great atmosphere at the Department.

Most of the presented work stems from the SUSPHIRE project, in which we collaborated with outstanding researchers from Spain, Germany, and the United Kingdom, each of whom has contributed their own expertise. I would also like to highlight the contribution of co-workers from the National Institute of Biology to the project, especially Marko Petek for his proficient bioinformatics analyses and insightful discussions and Živa Ramšak for her help with the network analyses.

Lastly, I would like to express my everlasting gratitude to my family. I have the great privilege of being surrounded by the most supportive, wise, and caring people who make me who I am. This accomplishment is as much theirs as it is mine.

Abstract

Rising demands for food, instigated by population growth and urbanization, are calling for advanced agricultural approaches to increase crop yields. However, the expansion of food production should not come with an unmanageable environmental cost. Plant science is therefore challenged to provide sustainable innovations for combating the detrimental effects of unfavourable abiotic and biotic environmental factors on crop plants. In this thesis, we aimed to contribute to the development of biotechnological production of sustainable insect pest control compounds and to develop molecular tools for studying interactions between plants and viral pathogens.

Advances in synthetic biology and biotechnology can provide valuable solutions for sustainable insect pest control. One approach is the biotechnological production of alternative insecticides with less adverse effects, such as insect sex pheromones. To this end, transgenic *Nicotiana benthamiana* lines with constitutive production of moth pheromones were developed. However, high pheromone production resulted in stunted growth and development of the plant chassis. We have investigated the observed growth penalty with gene expression and network analyses and discovered a transcriptional reprogramming towards the stress response, with upregulated jasmonic acid and downregulated gibberellic acid signalling. Genetic manipulation of hardwired growth retardation in response to perceived stress could therefore improve the growth of plants with high insect sex pheromone biosynthesis. This would improve the suitability of such plants for biotechnological production in a greenhouse setting or even as living biodispensers in the field.

Additionally, we searched for coding sequences of enzymes catalysing the biosynthesis of mealybug sex pheromones. Focusing on the citrus mealybug, *Planococcus citri*, we generated long- and short-read transcriptomic data and found several candidate genes that could be involved in the biosynthesis of the rare cyclobutane structure in the *P. citri* sex pheromone. Their identification presents the groundwork for the future implementation of plant-based biotechnological production of mealybug sex pheromones.

To protect crops from the devastating effects of pathogenic infections, breeding or engineering resistant crop cultivars is essential. Therefore, it is necessary to understand the molecular mechanisms underlying successful plant immune response to infection. For this, efficient molecular tools, tailored to the pathosystem of interest are needed, such as plant virus infectious clones, which could enable functional studies of plant and viral genes. We have developed a robust protocol for mutagenesis of the monopartite infectious clone of the potato virus Y, thereby constructing a clone tagged with green fluorescent protein. The clone was able to infect potato plants and establish systemic infection, and expressed green fluorescent protein enabled microscopic evaluation of viral replication and spread *in planta*. As such it will contribute to the identification of important targets for genetic improvement of potato resistance to potato virus Y.

Povzetek

Naraščajoče potrebe po hrani, ki jih povzročata rast prebivalstva in pospešena urbanizacija, zahtevajo razvoj naprednih pristopov za izboljšanje donosa kmetijske pridelave ob hkratnem zmanjšanju okoljskih bremen. Znanost je zato postavljena pred izziv zagotavljanja trajnostnih inovacij za blaženje neugodnih abiotskih in biotskih dejavnikov na pridelke. V okviru doktorske naloge smo si prizadevali prispevati k razvoju biotehnološke proizvodnje trajnostnih spojin za zatiranje žuželčjih škodljivcev ter razviti molekularna orodja za raziskave interakcij med rastlinami in virusnimi povzročitelji bolezni.

Sintezna biologija in biotehnologija ponujata orodja za trajnostno obvladovanje žuželčjih škodljivcev. Eden izmed pristopov je biotehnološka proizvodnja insekticidov z manj škodljivimi učinki, kot so žuželčji feromoni. V ta namen so bile razvite transgene rastline vrste *Nicotiana benthamiana*, ki konstitutivno proizvajajo feromone vešč. Vendar visoka proizvodnja feromonov vodi do nezaželene upočasnitve rasti rastlin. Molekularne vzroke slabše rasti smo raziskali z analizo izražanja genov in medgenskimi interakcijskimi podatki iz rastlinskih mrež ter odkrili izrazit stresni odziv s povišanim izražanjem genov, povezanih s signalizacijo jasmonske kisline, in zmanjšanim izražanjem genov, povezanih s signalizacijo giberelinske kisline. Aktivacija stresne signalizacije jasmonske kisline je v rastlinah pogosto neločljivo sklopljena z inhibicijo signalizacije giberelinske kisline, ki spodbuja rast. Tarčni inženiring genov, vključenih v sklopitev obeh signalizacijskh poti, bi lahko vodil v izboljšanje rasti rastlin ob hkratni biosintezi žuželčjih spolnih feromonov in omogočil biotehnološko proizvodnjo v rastlinjakih ali celo uporabo rastlin kot bioloških razpršilnikov na poljih.

Poleg tega smo iskali kodirajoča zaporedja encimov, ki katalizirajo biosintezo spolnih feromonov kaparjev. Osredotočili smo se na vrsto *Planococcus citri*, za katero smo določili zaporedja transkriptov na genomskem nivoju z visoko zmogljivostnim sekvenciranjem kratkih in dolgih nukleotidnih zaporedij. Poiskali smo kandidatne gene, katerih encimski produkti bi lahko katalizirali tvorbo redke ciklobutanske strukture v spolnem feromonu vrste *P. citri*. Kandidatni geni predstavljajo temelje za razvoj biotehnološke proizvodnje spolnih feromonov kaparjev v rastlinah.

Za zaščito pridelkov pred okužbami se največkrat uporablja žlahtnjenje ali genetsko inženirstvo odpornih sort pridelkov. Pri načrtovanju in razvoju odpornih sort je ključnega pomena razumevanje molekularnih mehanizmov uspešnega imunskega odziva rastlin na okužbo. Za ta namen so potrebna učinkovita in specifična molekularna orodja, kot so infektivni kloni rastlinskih virusov, ki omogočajo funkcionalne raziskave rastlinskih in virusnih genov. Razvili smo robusten protokol za mutagenezo monopartitnega infektivnega klona virusa krompirja Y (PVY) in ga uporabili za pripravo infektivnega klona, označenega z zelenim fluorescenčnim proteinom (GFP). S klonom smo uspešno okužili rastline krompirja, v katerih se je vzpostavila sistemska okužba. Izraženi GFP je omogočil sledenje replikaciji in širjenju virusa v rastlinah krompirja, kar bo prispevalo k identifikaciji pomembnih tarč za genetsko izboljšavo odpornosti krompirja na PVY.

Contents

List of Figures

Abbreviations

cDNA	. . .	complementary deoxyribonucleic acid
DMAPP	. . .	dimethyl allyl diphosphate
EU	. . .	European Union
FAR	. . .	fatty acyl reductase
FAD	. . .	fatty acyl desaturase
GFP	. . .	green fluorescent protein
IDS	. . .	isoprenyl diphosphate synthase
IPP	. . .	isopentenyl diphosphate
PVY	. . .	potato virus Y

Chapter 1

Introduction

1.1 Biotechnological Approaches for Sustainable Plant Protection in Agriculture

Human health and well-being depend on nutrients directly or indirectly provided by plants. Due to the growing population, agriculture has been under constant pressure to boost crop production. By increasing agricultural land area and improving yields, global production has managed to meet the demands or even provide surpluses of major crops (Bailey-Serres, Parker, Ainsworth, Oldroyd, & Schroeder, 2019). However, this success, mainly fuelled by the Green Revolution's approaches of elite variety breeding, hybrid crop development, and application of fertilizers and pesticides, seems to have reached its limits (Pingali, 2012). First, the strategies failed to fully address global diversity and inequality, falling short on providing tailored solutions and equitable benefits for all communities (Pingali, 2012). Second, yield improvements have started to stagnate or even drop in the last decades, threatening food security (Ray, Ramankutty, Mueller, West, & Foley, 2012). This trend of decreasing yields is being accelerated by climate change, due to temperature increases, changes in rainfall patterns and the spread of pests and diseases (Wing, De Cian, & Mistry, 2021; C. Zhao et al., 2017). Third, the adopted practices of intensive food production have led to environmental degradation with devastating effects on biodiversity and agriculture itself (A. M. D. Ortiz, Outhwaite, Dalin, & Newbold, 2021; Pathak et al., 2022; Raven & Wagner, 2021). Emerging markets with a growing middle class and urban populations will further emphasize the abovementioned challenges. The future of food production thus depends on the implementation of sustainable and resilient crops and agricultural practices that will address the interdependent goals of sufficient supply, economic viability for all types of farmers, and conservation of natural resources (Gaffney et al., 2019).

Scientific advances over the last few decades offer novel solutions to design resilient crops with high performance or innovative plant protection strategies (Eckardt et al., 2023). Development of stress-resistant crops builds upon advances in basic plant research, i.e., improved plant genomics, functional genomics, and plant genome editing techniques. Plant genomics is a basis for the characterisation of the available genetic diversity of plant germplasm and of the loci contributing to favourable morphological, developmental, and physiological crop traits, e.g., resistance to heat, cold, drought, flooding, and pathogens (Bailey-Serres et al., 2019). Research on the molecular networks regulating plant adaptational responses to different environmental factors is further supported by extensive multiomics analyses, covering molecular phenotypes at the interconnected levels of transcripts, proteins, and small molecules (Qian & Huang, 2020). With the increasing amount of generated data, systems biology approaches can offer comprehensible insights into the complexity of molecular networks. Computational tools such as network analysis,

modelling, and machine learning are becoming indispensable for this purpose (Hayes et al., 2023; X. Yang et al., 2020).

Understanding gene function is essential for the implementation of advanced biotechnological solutions in crop protection. The new plant breeding revolution emerged from genome editing technology, which can generate transgene-free genetically engineered plants with improved performance such as disease-resistance, stress-tolerance or even improved nutritional quality (Tyczewska, Twardowski, & Woźniak-Gientka, 2023). Genome editing is faster, more accurate and more predictable than former techniques of genetic modifications. Genetically engineered plants with improved yields even under intensified environmental stresses could minimize the environmental burden of agriculture and therefore contribute to the sustainability of the food system.

Apart from breeding resilient crops with desired traits, innovations related to agricultural management practices are becoming increasingly important for future-based strategies. Carbon-neutral technologies, biological alternatives to chemical fertilizers and pesticides, efficient the supply chains, and food waste reduction are common goals in environmental and agricultural policies. In the EU, climate-smart agriculture is outlined in the European Green Deal, with its Farm to Fork and Biodiversity strategies most directly tackling sustainability issues in agriculture (European Commission, 2022). Many different lines of research and innovation are pursued that include beneficial plant symbiotic microbes (Marco et al., 2022), mixed land use and agroforestry (Low, Dalhaus, & Meuwissen, 2023), digital technologies (Hayes et al., 2023), and biological alternatives to chemical pesticides, such as biological agents (Jaiswal et al., 2022) and semiochemicals (Beck, Torto, & Vannette, 2017). The latter include chemicals produced by insects, such as sex, alarm, and aggregation pheromones, which stimulate certain behaviours and interactions between individuals and can thus be used for insect pest control.

The results presented in this dissertation are centred around two approaches of sustainable crop protection. First, we focused on improving the biotechnological production of insect sex pheromones, which are used as an environmentally friendly alternative to chemical insecticides. Second, we developed molecular biology tools for exploring the interactions between plant viruses and their hosts, knowledge that is crucial for breeding virus-resilient crops.

1.2   Insect Sex Pheromones for Plant Protection

Insect pests cause crop damage by feeding on plant sap and tissue and transmitting plant pathogens (Heck, 2018). Their sugar-rich excretions can also promote growth of sooty moulds (Ascomycetes), which cover plants with a dark powdery coating that can promote further pest attacks, and decrease the value of ornamental plants (Chomnunti et al., 2014). The importance of protection against insect pests is increasing as climate change, global trade, and travel facilitate their spread (Deutsch et al., 2018; Schneider, Rebetez, & Rasmann, 2022). The main tool for their management is the application of chemical insecticides, of which 760 000 tonnes were applied globally in 2021. Their use has been steadily increasing, starting from 460 000 tonnes in 1990 and stagnating at over 700 000 tonnes in the last decade (FAOSTAT, 2023).

Heavy insecticide use results in water and soil pollution, which threatens human health and biodiversity because of non-target effects on other organisms (Goulson, 2013; Gunstone, Cornelisse, Klein, Dubey, & Donley, 2021). Insecticide use is therefore becoming progressively restricted in the EU. One of the latest examples is the 2020 EU ban on the insecticides chlorpyrifos and chlorpyrifos-methyl (European Commission, 2020). In 2022, the European Commission adopted the Nature Restoration Law and Sustainable Use of

Pesticide Regulation, which includes the aim to reduce chemical pesticide use by 50 % by 2030 (European Commission, 2022). To reach this goal but still ensure crop protection from insects, an integrated pest management approach is proposed. It encompasses several methods for pest control, with an emphasis on prevention measures (e.g., crop rotation and use of pest resistant varieties), monitoring, and less harmful control methods. Based on the precise identification and quantification of a potential pest, an informed decision is made regarding the implementation of control measures. If needed, targeted and less risky methods are applied first, and the broad application of conventional pesticides is only used as a last resort (Dara, 2019).

Synthetic insect sex pheromones have been used in integrated pest management for insect monitoring and population control with mass trapping and mating disruption (Rizvi, George, Reddy, Zeng, & Guerrero, 2021; Witzgall, Kirsch, & Cork, 2010). Sex pheromones are semiochemicals used by insects to attract mates (Figure 1). They are species-specific compounds or blends of compounds mostly produced and emitted by females (Zou & Millar, 2015). Due to their specificity, they are non-toxic to other insect species, have a low risk of resistance development and thus represent a sustainable alternative to broad-spectrum insecticides (Rizvi et al., 2021). Insect traps with pheromones as attractants are used for monitoring population dynamics and thus facilitate early detection of infestations (Carleton et al., 2020). They are also invaluable for detecting invasive species (Žunič Kosi, Stritih Peljhan, Zou, McElfresh, & Millar, 2019), the spread of which is greatly accelerated by climate change. Besides monitoring, population control can be achieved as well, either by the attract-and-kill strategy (Luo et al., 2020) or mating disruption strategy (Franco et al., 2022). For the first strategy, larger traps at higher densities are used, aiming to reduce the population numbers of reproductively active adults. For mating disruption, sex pheromones are dispersed into the air, obscuring the attracting pheromone trail of females, and thereby preventing males from locating females.

Synthetic sex pheromones have been successfully deployed and commercialized for several insect species. However, the chemical synthesis of certain pheromones is costly and thus hinders increasing the number of target species (Petkevicius, Löfstedt, & Borodina, 2020; Zou & Millar, 2015). Sex pheromones of certain insect species also include chiral centres, requiring several stereoselective synthesis steps and the separation of the active stereoisomer from the final racemic mix (Zou & Millar, 2015), which increases the production costs. Due to higher prices, sex pheromones are currently mostly used on high-value fruits, vegetables, and nuts, as they are not economically viable for lower-value crops (Holkenbrink et al., 2020; Wang et al., 2022). This is especially true for the mating disruption approach, for which larger quantities of the compound are (Zou & Millar, 2015). Additionally, chemical synthesis requires the use of hazardous chemicals and generates polluting by-products (Hagström et al., 2013).

Therefore, the conventional production of insect sex pheromones by chemical synthesis should be replaced with cleaner biotechnological production in microbe or plant biofactories (Petkevicius et al., 2020). Plants could also be developed into on-site pheromone dispensers in the fields, bypassing the need for extraction of the accumulated compounds from the plant biomass (Petkevicius et al., 2020). Such living biodispensers would both produce and release sex pheromones at the target locations in controlled quantities and only upon a specific signal, the latter two goals achievable using robust synthetic genetic circuits.
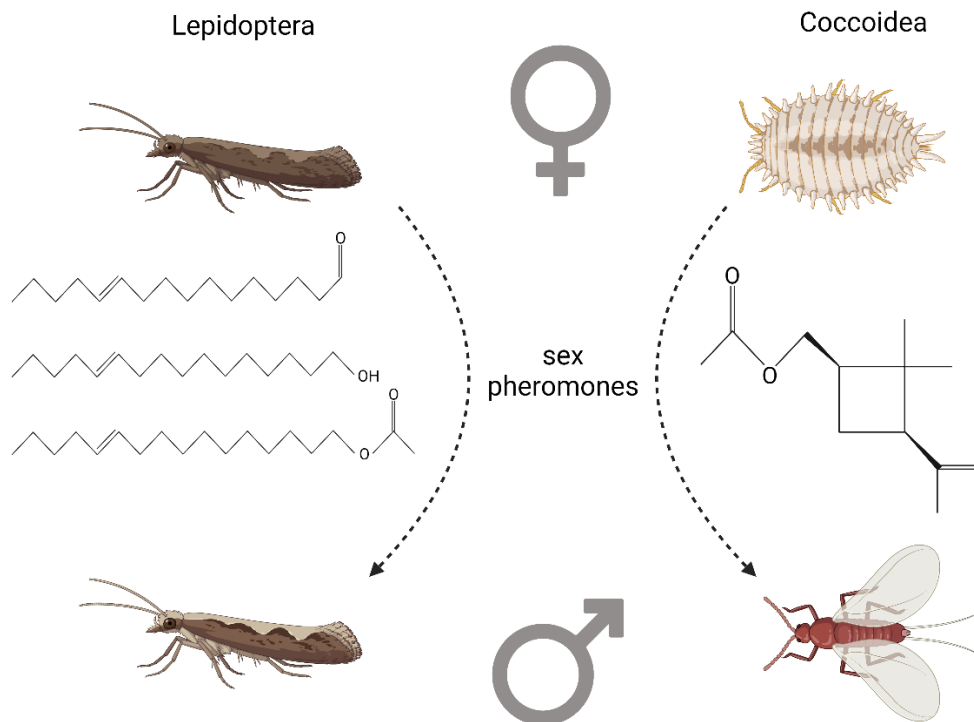
Figure 1: Insect sex pheromones are produced by females to attract males for mating. Examples of three moth (Lepidoptera) sex pheromones (*left*) and the *Planococcus citri* mealybug (Coccoidea) sex pheromone (*right*) are shown. Lepidoptera sex pheromones are fatty acid aldehydes, alcohols, and acetates with double bonds at unique positions. Mealybug sex pheromones are monoterpenoids resulting from irregular coupling of isoprene units, which can form branched chains or cyclized structures. The image was created with BioRender.com.

1.2.1   Lepidoptera pheromones and their biotechnological production

The larvae of moths (order Lepidoptera) are major agricultural pests of food and fibre crops, with abundant populations causing severe defoliations of crops and fruit trees, severely stunting growth and limiting the development of harvestable crop organs (Suckling et al., 2017). Most moth sex pheromones are unsaturated fatty acid alcohols, acetates, or aldehydes with chain lengths between 10 and 18 carbons (Löfstedt, Wahlberg, & Millar, 2016) (Figure 1). The double bonds are formed at uncommon positions (e.g., $\Delta 9$ and $\Delta 11$). Functional pheromones usually comprise a blend of components, which determine the pheromone's specificity. Pheromones are biosynthesized from palmitic (C16 saturated fatty acid) or stearic acid (C18 saturated fatty acid), followed by consecutive steps catalysed by fatty acyl desaturases (FADs), introducing *cis-* (*Z*) or *trans-*(*E*) double bonds in a regio- and stereoselective manner, and fatty acyl reductases (FARs), reducing fatty acyls to alcohols (Figure 2). Both reaction steps occur in the endoplasmic reticulum of insect cells (Holkenbrink et al., 2020). Fatty acyl alcohols can be further converted into fatty esters or aldehydes (Figure 2). Other chain lengths are synthesized through chain-elongation or chain-shortening (beta-oxidation) reactions (Löfstedt et al., 2016).

To implement the bioproduction of Lepidoptera sex pheromones in a plant chassis, insect genes coding for the enzymes involved in the fatty acid conversion reactions must be identified. Genes encoding fatty acyl desaturases and fatty acyl reductases have been identified from several moth species (Lassance, Ding, & Löfstedt, 2021; Tupec, Buček, Valterová, & Pichová, 2017). Conversely, enzymes catalysing alcohol conversion into

aldehydes (fatty alcohol oxidases or fatty alcohol dehydrogenases) or esters (acetyltransferases) have not yet been identified from any insect species (Xia et al., 2022). For ectopic production of fatty acyl ester pheromones, acetyltransferases from plants and yeast have been utilised, for example *Ea*DAcT from burning bush (*Euonymus alatus*) and ATF1 from yeast (B.-J. Ding et al., 2016).
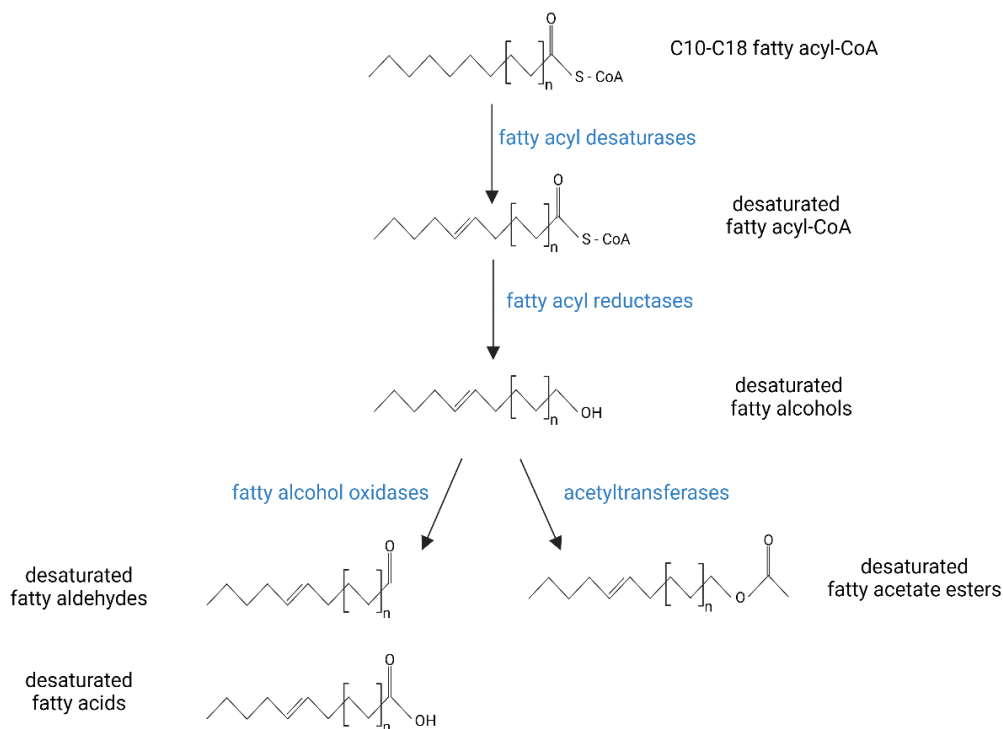
Figure 2: Moth (Lepidoptera) sex pheromone biosynthesis. Schematic representation of general steps in moth sex pheromone biosynthesis with names of enzyme families catalysing the conversions given in blue text colour. The image was created with BioRender.com.

Based on the successful characterisation of several genes, the production of moth sex pheromones and their precursors has been reported in yeasts and plants. In plants, mostly transient expression of heterologous genes has been used to demonstrate biosynthesis and release of sex pheromone compounds. Furthermore, stably transformed genetically modified plant lines have been generated as well. Examples of moth pheromone biosynthesis in plants include the production of the precursor (*Z*)-11-hexadecenyl in transgenic *Nicotiana tabacum* (Nešněrová, Šebek, Macek, & Svatoš, 2004), transient production of (*Z*)-11-hexadecenol, (*E*)-11-tetradecenol, and (*Z*)-11-tetradecenol in *Nicotiana benthamiana* (B.-J. Ding et al., 2014), and transient production and release of (*Z*)-11-hexadecenol, (*Z*)-11-hexadecenal, and (*Z*)-11-hexadecenyl in *N. benthamiana* (Xia et al., 2022). Most cases report metabolic engineering in *N. tabacum* and *N. benthamiana*, which are well-established platforms for genetic engineering (Bally et al., 2018; Molina-Hidalgo et al., 2021). However, production in *Camelina sativa* or other oil seed crops might be advantageous, as they can synthesize and store more lipid-derived compounds (R. Ortiz et al., 2020). Proof-of-concept work demonstrated production of (*E,E*)-8,10-dodecadienoic acid (a precursors of a codling moth (*Cydia pomonella*) sex pheromone) in *C. sativa* (Xia et al., 2021). Several compounds were also successfully produced by yeast fermentation, e.g., (*Z*)-11-hexadecenol in *Saccharomyces cerevisiae* (Hagström et al., 2013), and (*Z*)-11-hexadecenol and (*Z*)-tetradec-9-en-1-ol in *Yarrowia lipolytica* (Holkenbrink et al., 2020).

1.2.2 Coccoidea pheromones

Scale insects (order Hemiptera, superfamily Coccoidea) are small sap-feeding insects that form dense colonies on host plants. Many species, mostly from the families of mealybugs (Pseudococcidae), soft scales (Coccidae), and armoured scales (Diaspididae), are pests that cause economically devastating damage to food crops, fruit trees, and ornamental plants (Kakoti, Deka, Roy, & Babu, 2023). The inflicted damage mostly stems directly from phloem sap loss, resulting in nutrient loss with consequent stunted growth and leaf damage. Additionally, scale insects can also transmit plant viruses (Cabaleiro, Pesqueira, & Segura, 2022; Hommay, Alliaume, Reinbold, & Herrbach, 2021; Puig, Wurzel, Suarez, Marelli, & Niogret, 2021). As implied by their name, their bodies are covered with a waxy layer, which protects them from natural enemies but also reduces the efficiency of synthetic insecticides (Quesada, Witte, & Sadof, 2018).

Scale insects exhibit strong sexual dimorphism, with wingless and almost immobile adult females, and winged, non-feeding, short-lived adult males. The sedentary females attract males for mating by releasing sex pheromones, which for most species consist of a single compound rather than a blend of related structures. So far identified sex pheromones of armoured scales and mealybugs are monoterpenoids resulting from "irregular" non-head-to-tail coupling of the five carbon precursors, DMAPP (dimethyl allyl diphosphate) and IPP (isopentenyl diphosphate) (Zou & Millar, 2015).

The majority of natural terpenoid compounds result from "regular" (1'-4, or head-to-tail) coupling of IPP and DMAPP, whereas structures originating from irregular coupling are less frequent (Kobayashi & Kuzuyama, 2018; Nagel, Schmidt, & Peters, 2019). Besides Coccoidea sex pheromones, other examples include a few plant (Demissie, Erland, Rheault, & Mahmoud, 2013; Rivera et al., 2001), bacterial (Ozaki, Zhao, Shinada, Nishiyama, & Kuzuyama, 2014) and archaeal terpenoids (Ogawa, Emi, Koga, Yoshimura, & Hemmi, 2016). Lavandulol and lavandulyl acetate found in lavender essential oils result from 1'-2 "head-to-middle" coupling (Demissie et al., 2013), whereas pyrethrins, present in chrysanthemum flowers, result from c1'-2-3 cyclopropanation coupling of two DMAPP units (Rivera et al., 2001). Both types of irregular backbones have also been found in mealybugs and armoured scales (Zou & Millar, 2015). Additionally, there are several cases of mealybug sex pheromones in which the isoprenyl backbone forms a cyclobutane ring, resulting from a 1'-2-3-2' coupling pattern, so far not identified in any other taxonomic group (Figure 1).

Enzymes catalysing the ubiquitously present "regular" 1'-4 coupling are well known and characterised. They are grouped into two structurally and evolutionarily distinct isoprenyl diphosphate synthase (IDS) families, which generate polyprenyl diphosphate products with the different double-bond geometries: *cis* (*Z*) and *trans* (*E*) (Nagel et al., 2019). Conversely, only a few enzymes with irregular coupling activity have been isolated and characterised, none of which originate from insects (Kobayashi & Kuzuyama, 2018). The biosynthetic pathway of Coccoidea sex pheromones is therefore still completely unknown. However, to develop their biotechnological production, the identification of mealybug IDSs with irregular coupling activity is crucial.

1.3   Developing Disease-Resilient Crops

Pathogenic infections of crops lead to severe yield losses, which directly threaten food security (Ristaino et al., 2021). Plant pathogens include viruses, viroids, bacteria, fungi, and oomycetes (Juroszek, Racca, Link, Farhumand, & Kleinhenz, 2020; Patel et al., 2022). Climate change is predicted to facilitate the spread of plant diseases into new areas (Singh

et al., 2023), which is already expedited through international trade and trave land the spread of vectors, such as insects (Schneider et al., 2022). Additionally, altered weather conditions can have unfavourable effects on plant-pathogen interactions (Velásquez, Castroverde, & He, 2018; L.-N. Yang, Ren, & Zhan, 2023) that include enhanced pathogen fitness and pathogenicity and reduced plant immunity (Delgado-Baquerizo et al., 2020; Desaint et al., 2021; Son & Park, 2022; Tsai, Brosnan, Mitter, & Dietzgen, 2022).

Genetically modified crops with improved resistance to one or even several pathogens are an effective and sustainable measure for mitigating plant diseases (Dong & Ronald, 2019). Their generation is supported both by advances in our understanding of the plant immune system and determinants of pathogen infectivity, and by the development of fast and precise techniques for genetic engineering (Zaidi, Mahas, Vanderschuren, & Mahfouz, 2020). Plant immunity research has provided breeding targets based on plant receptors for pathogen recognition and components of plant defence signalling, which is mainly conveyed through plant hormones (Kim et al., 2022; Yan Zhao, Zhu, Chen, & Zhou, 2022). Other approaches employ the expression of antimicrobial compounds (Li, Hu, Jian, Xie, & Yang, 2021; Montesinos, 2007) and RNA interference against the RNA of pathogenic viruses (Yaling Zhao, Yang, Zhou, & Zhang, 2020).

Despite several advances in the field of plant immunity, much is still unknown regarding plant–pathogen interactions, especially interactions with viral pathogens, which are among the most devastating plant pathogens (Nicaise, 2014). The outcomes of plant–pathogen interactions depend on several factors, including the genotypes of the pathogenic strain and host plant cultivar and on the environmental factors (Gold, 2021). Knowledge obtained from a specific pathosystem tested under defined conditions cannot thus be easily transferred to a different experimental system. Most of the molecular biology resources and gene functional knowledge is available for model organisms, e.g., *Arabidopsis thaliana*, and thus there is a need to develop tools that enable plant immunity research also in crop plants.

1.3.1 Infectious viral clones as tools in plant biotechnology

Plant viral genomes can be used to construct infectious plant viral clones, which can be used as efficient plant vectors (Brewer, Hird, Bailey, Seal, & Foster, 2018; Cody & Scholthof, 2019). They are also an invaluable resource for studies of plant virus genomes and biology. Infectious clones are mostly designed as full-length genome sequences of plant viruses inserted into a plasmid backbone to enable cloning in *Escherichia coli*. Upstream of the viral genome is either a bacteriophage promoter, enabling *in vitro* transcription followed by plant inoculation with naked viral RNA, or a plant promoter, resulting in *in planta* transcription of the viral genome after transfecting plants with the plasmid DNA (Abrahamian, Hammond, & Hammond, 2020). Viral clones have several advantages over other plant vectors. They are faster, reach higher protein production levels, and can establish expression throughout the plant due to viral spread (Abrahamian et al., 2020).

Viral clones could be potentially used for the production of therapeutic proteins, such as vaccines and antibodies, in plants (Dhama et al., 2020; Dubey et al., 2018). Currently, they are mostly used for reverse genetics in plant gene functional studies via virus-induced gene silencing (Beyene, Chauhan, & Taylor, 2017), gene overexpression or genome editing (Uranga, Aragonés, Daròs, & Pasin, 2023) and reverse genetics of viral genes (Kežar et al., 2019; Trapani et al., 2023). They can also be tagged with a reporter protein, which enables tracking the infection in the host plant (Baulcombe, Chapman, & Santa Cruz, 1995; Bedoya, Martínez, Orzáez, & Daròs, 2012; Cordero, Mohamed, López-Moya, & Daròs, 2017; Wieczorek, Budziszewska, Frąckowiak, & Obrępalska-Stęplowska, 2020). Recently, high-throughput sequencing accelerated the discovery of new virus species and strains that

remain to be biologically characterized (Fontdevila Pareta et al., 2023). Difficulties associated with their isolation can be circumvented by the assembly of an infectious clone based on the determined vial genome sequence (Pasin, 2022).

1.3.1.1 Infectious clones of potato virus Y (PVY)

Potato virus Y (PVY, genus *Potyvirus*) is an aphid-transmitted plant pathogen with worldwide presence, causing major losses of several cultivated solanaceous species, including potato, tobacco, tomato, and pepper. Disease outcome depends on the virus and host plant genotypes, environmental conditions, developmental and physiological state of the host plant, and transmission mode (Baebler, Coll, & Gruden, 2020). Functional characterisation of PVY and related host immunity genes is fundamental for generating resistant plant cultivars.

The PVY genome is a positive single-stranded RNA with a length of 9.7 kilobases. It includes two open reading frames of which the larger translates into a polyprotein that is subsequently cleaved into ten functional proteins by viral proteases (Baebler et al., 2020). Several full-length cDNA clones of PVY have been developed, based on different PVY strains and isolates. Due to the toxicity of their cDNA in *E. coli*, first cloning attempts depended on *in vitro* amplification and transcription of the viral genome (Fakhfakh, Vilaine, Makni, & Robaglia, 1996). Later on, bipartite clones (Jakab, Droz, Brigneti, Baulcombe, & Malnoë, 1997) or clones with intron insertions (Bukovinszki, Götz, Johansen, Maiss, & Balázs, 2007; Cheng et al., 2020) were developed and enabled cloning in *E. coli*. The designs mostly include the plant constitutive promoter cauliflower mosaic virus 35S upstream of the viral cDNA, enabling *in planta* transcription to form the positive-stranded RNA genome, which can initiate viral replication and spread.

Developing stable clones, which can be maintained in *E. coli* is crucial for easy manipulation of the viral genome, either through targeted mutagenesis of viral genes or in-frame insertion of ectopic coding sequences. The first approach has been used to determine viral protein regions or amino acid residues that play a crucial role in viral infectivity, replication, and spread (Kežar et al., 2019; Stare et al., 2020). The second approach can create tagged viruses, as the inserted coding sequence of a reporter protein, such as GFP, undergoes translation and cleavage with viral replication (Rupar et al., 2015). Thus, viral replication and spread can be confirmed by detecting the reporter protein signal with fluorescent microscopy. Similar results were also obtained by insertion of the Rosea1 transcription factor, which activates anthocyanin biosynthesis, serving both as a visual marker for viral spread and a potential method for crop biofortification (Cordero et al., 2017).

1.4 Scientific Problems and Aims of the Thesis

1.4.1 Understanding the molecular background of growth penalty associated with moth sex pheromone production in *Nicotiana benthamiana*

Several studies report successful biotechnological production of moth sex pheromones in plants (Petkevicius et al., 2020). However, most of them were only proof-of-concept systems based on transient expression, reaching low yields and volatility of the pheromones (Xia et al., 2022, 2020). In the scope of an international project, we participated in the development of stable transgenic *N. benthamiana* lines constitutively producing a blend of three moth pheromone compounds: (*Z*)-11-hexadecenol, (*Z*)-11-hexadecenal, and (*Z*)-11-hexadecenyl

acetate. Although adequate yields were obtained, the use of transgenic plants was still limited due to the severe growth and developmental inhibition observed in homozygous high-producing plant lines. High producers were much smaller and, in most cases, failed to develop flowers and seeds compared to wild-type *N. benthamiana* and heterozygous lines producing much lower amounts of the moth sex pheromones.

Such inhibited growth is an obstacle for commercialization of this production system and is especially incompatible with the vision of developing the plants as biological dispensers of sex pheromones. Inhibited seed production is additionally problematic for the maintenance and propagation of the transgenic plants.

We have therefore aimed to characterise the molecular perturbations underlying the observed phenotype and thereby potentially identify possibilities for improving the growth of high producers. Starting with only a few measured phenotypic parameters (plant height and sex pheromone content in the leaf mass), we decided to implement a broad approach, which would provide insight into the physiological changes triggered by high pheromone production. RNA-Seq is an affordable method for acquiring high-density information at the genome-wide level of gene transcriptional activity. It has become indispensable for understanding signalling regulation in response to different conditions (Van Den Berge et al., 2019). We aimed to obtain RNA-Seq data for wild-type and transgenic low and high producers of moth sex pheromones. We also included a novel version of transgenic *N. benthamiana* plants, which exhibited a more moderate growth penalty, but produced higher amounts of moth sex pheromones. We included several different genotypes with varying phenotypes and compared their transcriptional profiles obtained with RNA-Seq and the data on their growth and pheromone production to detect the transcriptional changes underlying growth inhibition related to high pheromone production.

1.4.2 Identification of IDS-like sequences in the genome of *Planococcus citri*

Compared to Lepidoptera sex pheromones, Coccoidea sex pheromones are more difficult and expensive to synthesize. Their chemical structure includes chiral centres and requires stereoselective steps of synthesis to obtain the pure active compound (Zou & Millar, 2015). Development of a bioproduction system would make broader sex pheromone use viable also in scale insect pest management.

However, no mealybug IDSs capable of the irregular coupling mechanisms predicted to form the polyprenyl backbones of mealybug sex pheromones have been identified. There is also very little information on other non-insect enzymes capable of irregular coupling (Kobayashi & Kuzuyama, 2018). They seem to stem from isolated evolutionary events, mostly through diversification from ancestor IDSs with regular coupling activity (Thulasiram, Erickson, & Poulter, 2007). Therefore, it is possible that an enzyme with homology to regular IDSs also catalyses the formation of mealybug sex pheromones.

We aimed to obtain genome-wide coding sequence information from the citrus mealybug, *P. citri*, and search for sequences with homology to enzymes capable of regular coupling. *P. citri* is a widespread pest, causing significant damage in citrus orchards and other crops. Its sex pheromone, planococcyl acetate, has a cyclobutane-containing polyprenyl backbone, and has been successful synthesized and tested for monitoring purposes (Dunkelblum, Zada, Gross, Fraistat, & Mendel, 2002; Mansour et al., 2018). We aim to generate short- and long-read transcriptomic data by performing Iso-Seq and RNA-Seq, search for IDS homologs, characterise them *in silico,* and test their *in vitro* enzymatic activity after heterologous expression.

1.4.3   Generation of a GFP-tagged PVY infectious clone

PVY is one of the most important pathogens negatively impacting the production of potato worldwide. Infection of susceptible cultivars leads to reduced yields and can also cause potato tuber necrotic ringspot disease, resulting in unmarketable potatoes (Kreuze et al., 2019). To develop resistant or tolerant potato cultivars, we need to understand the molecular interactions that govern all the major steps involved in successful potato infection: the viral infection of the cell, plant sensing of the infection and initiation of defence, and viral counter defence. Importantly, plant defence is tightly regulated in a spatiotemporal manner, and thus we must develop methods that can address all aspects of defence signalling to detect the interactions crucial for resistance (Lukan et al., 2020).

Following viral spread *in vivo* is an important tool to determine points and paths of infection. We have been using a PVY clone tagged with green fluorescent protein (GFP) to follow viral replication and spread with confocal microscopy (Rupar et al., 2015). This enables comparisons of the extent and pattern of viral spread in different genetic backgrounds, helping to characterise the effectiveness of resistance and thus to deduce the role of specific genes in PVY resistance. This also enables spatially resolved analysis of plant responses, as we can distinguish between infected and non-infected cells and determine the distance of a cell from the point of infection (Lukan et al., 2018).

However, the currently available clone has a bipartite design, making its use impractical, as *in vitro* ligation is required prior to infection. We therefore aim to use a monopartite PVY infectious clone and insert the GFP-coding sequence with the mutagenesis approach. The resulting infectious clone can be maintained as a single plasmid in *E. coli*, isolated, and used directly for plant transformation through biolistic inoculation. To generate the GFP-tagged PVY clone, we aim to develop a robust mutagenesis protocol, which will enable insertion of other coding sequences of interest into the PVY genome.

1.5   Research Hypotheses

1. The growth arrest phenotype in high pheromone-producing *N. benthamiana* plants will have detectable changes on the level of gene expression.

2. Differential expression analysis will provide information on possible regulatory or metabolic perturbations as molecular mechanisms triggering the growth penalty.

3. The *P. citri* transcriptome includes IDS-like transcripts with potential for irregular coupling activity function.

4. The viral clone of PVY with the inserted GFP sequence will be able to infect potato plants and establish systemic infection, with expressed GFP enabling microscopic evaluation of viral replication and spread *in planta*.

1.6   Publications Included and Candidate's Contributions

This dissertation includes five publications, of which four are original papers and one a review. The candidate is the first author of two publications. Four of these publications have been published, whereas one has been submitted to the bioRxiv preprint server and submitted for publication in a peer-reviewed journal.

The first publication, entitled "Insect pest management in the age of synthetic biology" is a review article, describing the use of synthetic biology approaches for sustainable insect

pest management. It includes chapters on new breeding technologies for developing insect-resistant crops by exploiting different defence compounds and mechanisms, RNA interference to downregulate essential insect genes, gene drives, biotechnological production of insect control compounds, and biocontrol agents. The review also evaluates the potential societal and regulatory implications of the emerging technologies. The PhD candidate wrote the subsection "Harnessing biocontrol" on biological insect pest control, in which she reviewed different options for improving biocontrol agents such as entomopathogenic organisms or parasitoids.

The second publication, entitled "Production of Volatile Moth Sex Pheromones in Transgenic *Nicotiana benthamiana* Plants" describes the design and characterisation of two versions of transgenic *N. benthamiana* plants that produce moth sex pheromones. This work was mostly performed by our collaborators in Valencia, Spain. The transgenic plants, named the Sexy Plant, produced a blend of (Z)-11-hexadecenol, (Z)-11-hexadecenal, and (Z)-11-hexadecenyl acetate, whose high production stunted plant growth. Due to the truncation of the acetyltransferase transgene in the first generation of transgenic plants, a new generation of plants with a new insertion event was prepared. Plants of the second version accumulated even higher amounts of moth sex pheromones compared to the first version whilst also growing better. The PhD candidate contributed to this work by performing transgene expression quantification, which also revealed the truncation of the acetyltransferase transgene.

The third publication, entitled "Transcriptional deregulation of stress-growth balance in *Nicotiana benthamiana* biofactories producing insect sex pheromones" includes the results of the transcriptional analysis of the growth penalty observed in high producers of moth sex pheromones. We identified a stress-like transcriptional response and proposed the activation of jasmonic acid signalling coupled with inhibition of gibberellic acid signalling as the underlying mechanisms of the growth penalty. We discussed possible reasons for the activation of this signalling hub and interventions that could alleviate the severe growth phenotype. The PhD candidate is the first author of this publication. She contributed to the experimental planning and performed all the bioinformatic analyses of RNA-Seq data generated from Sexy Plants, including the differential expression and gene set enrichment analyses, functional annotation of the *N. benthamiana* genome, and the network visualisation analysis. She wrote the first draft of the manuscript and prepared most of the figures and tables.

The fourth publication, entitled "Identification and characterisation of *Planococcus citri cis*- and *trans*-isoprenyl diphosphate synthase genes, supported by short- and long-read transcriptome data" includes the results of the irregular IDS candidate search in the genome of *P. citri* and *in vitro* activity testing of some candidates. We used *de novo* assembled and full-length sequenced transcriptome data to complement the available genome assembly and searched for coding sequences with homology to IDS sequences. We identified and phylogenetically characterized 30 candidate sequences, of which we selected 19 as the most promising candidates for the *P. citri* sex pheromone biosynthesis. Five of them had regular coupling activity, of which one also produced low amounts of two irregular polyprenyl chains. The PhD candidate is the first co-author of the manuscript. She contributed by performing quality control analysis of the generated transcriptomic data, searching for sequences similar to IDSs, and preparing candidate sequence alignments and phylogenetic analyses. She wrote the first draft of the manuscript and prepared most of the figures and tables.

The fifth publication, entitled "Chloroplast redox state changes mark cell-to-cell signalling in the hypersensitive response" includes a detailed spatiotemporal analysis of the redox state changes and stromule formation in the hypersensitive response to viral infection in potato. Using this approach, we identified cells with oxidized chloroplasts further from

the cell death zone that may play a role in signalling for resistance and showed that stromules are induced by both cell death and PVY multiplication. The PhD candidate contributed to this work by generating the GFP-tagged PVY infectious clone, which was used to determine the viral multiplication zone and stromule formation in the chloroplasts of adjacent cells. She designed the genetic construct, performed molecular cloning, and characterised the resulting PVY-GFP infectious clone. She also wrote the methods section describing her work.

Chapter 2

Scientific Publications

2.1   Insect Pest Management in the Age of Synthetic Biology

Rubén Mateos-Fernández, Marko Petek, Iryna Gerasymenko, Mojca Juteršek, Špela Baebler, Kalyani Kallam, Elena Moreno Giménez, Janine Gondolf, Alfred Nordmann, Kristina Gruden, Diego Orzaez, and Nicola J Patron

In this review, we summarised the contemporary techniques of molecular and synthetic biology that are or could be exploited in the future for crop protection against insect pests. The first chapter describes genetically modified crops with insect resistance, mostly achieved by expressing toxins and resistance genes or by removing susceptibility genes. Discovering novel insecticidal proteins and metabolites and genome editing approaches will contribute to the development of new generations of resistant crops. The second chapter focuses on the use of RNA interference for insect control, either through host-induced or spray-induced gene silencing. Based on initial success, further improvements will rely on increased RNA stability and uptake by insects and on the determination of target specificity and potential non-target effects. The third chapter is dedicated to genetic methods for insect pest population control, namely the sterile insect technique, release of insects with a dominant lethal trait, and the most recent development — gene drives. Insect genome editing holds great promise to further accelerate the development of gene drives. The fourth chapter summarizes biomanufacturing of pest control compounds, using yeast or plant chassis, which can provide affordable large-scale production of different insecticidal compounds, sex pheromones, and other semiochemicals. The fifth chapter is dedicated to biotechnological improvement of biocontrol agents. The review also considers societal and environmental aspects of implementing novel synthetic biology approaches.

The PhD candidate contributed to this review article by participating in the writing of the subsection "Harnessing biocontrol" on biological insect pest control. She reviewed the use of natural predators, parasitoids, competitors, and pathogens of insect pests. She also reviewed synthetic biology approaches that could enhance their effects, e.g., genetic engineering that increases the toxicity or environmental stability of entomopathogenic agents.

Review

Insect pest management in the age of synthetic biology

Rubén Mateos Fernández[1,†], Marko Petek[2,†], Iryna Gerasymenko[3,†], Mojca Juteršek[2,4], Špela Baebler[2] (iD),
Kalyani Kallam[5], Elena Moreno Giménez[1], Janine Gondolf[6], Alfred Nordmann[6], Kristina Gruden[2], Diego Orzaez[1] (iD)
and Nicola J Patron[5,*] (iD)

[1]*Institute for Plant Molecular and Cell Biology (IBMCP), UPV-CSIC, Valencia, Spain*

[2]*Department of Biotechnology and Systems Biology, National Institute of Biology, Ljubljana, Slovenia*

[3]*Plant Biotechnology and Metabolic Engineering, Technische Universität Darmstadt, Darmstadt, Germany*

[4]*Jožef Stefan International Postgraduate School, Ljubljana, Slovenia*

[5]*Earlham Institute, Norwich Research Park, Norfolk, UK*

[6]*Institut für Philosophie, Technische Universität Darmstadt, Darmstadt, Germany*

Summary

Arthropod crop pests are responsible for 20% of global annual crop losses, a figure predicted to increase in a changing climate where the ranges of numerous species are projected to expand. At the same time, many insect species are beneficial, acting as pollinators and predators of pest species. For thousands of years, humans have used increasingly sophisticated chemical formulations to control insect pests but, as the scale of agriculture expanded to meet the needs of the global population, concerns about the negative impacts of agricultural practices on biodiversity have grown. While biological solutions, such as biological control agents and pheromones, have previously had relatively minor roles in pest management, biotechnology has opened the door to numerous new approaches for controlling insect pests. In this review, we look at how advances in synthetic biology and biotechnology are providing new options for pest control. We discuss emerging technologies for engineering resistant crops and insect populations and examine advances in biomanufacturing that are enabling the production of new products for pest control.

Introduction

It has been estimated that food production needs to increase by at least 50% over 2005 yields to meet the needs of the 2050 global population (Alexandratos, 2012). Improving crop yields and minimizing pre- and post-harvest losses are critical to achieving these goals. While many factors from cultivation practices to climate events and outbreaks of pathogens are influential, arthropod pests account for around 20% of global annual crop losses, valued at over US\$ 470 billion (Culliney, 2014). In developing countries, where population growth is most likely to outstrip increases in yields, pre-harvest losses of grain crops from arthropod pests range from 15 to 100% and post-harvest losses from 10% to 60% (Mihale *et al.*, 2009). Alarmingly, a warmer climate is expected to alter agriculturally relevant characteristics of many insect pests, leading yield losses to increase by an estimated 10%–25% (Deutsch *et al.*, 2018). In addition to direct damage, insect pests can also either directly transmit or facilitate secondary infections by viruses, bacteria and fungi. For example, the leafhopper, *Scaphoideus titanus*, transmits the grapevine yellows phytoplasma (Constable and Bertaccini, 2017), and the English grain aphid, *Macrosiphum avenae*, is a vector for barley yellow dwarf virus with infestations also leading to colonization by sooty moulds that establish on honeydew secretions (Fiebig *et al.*, 2004).

Humans have applied chemicals with the aim of controlling insect pests for thousands of years. The use of elements such as sulphur as well as heavy metals and salts in agriculture was recorded by the Romans and other ancient civilizations. However, it was in the late 19th and early 20th century that advances in chemistry gave rise to synthetic pesticides. The first generation of insecticides consisted of highly toxic compounds, including the arsenic-containing 'Paris Green', a copper acetoarsenite widely used in the United States between 1867 and 1900 (Hughes *et al.*, 2011). Inorganic pesticides were largely replaced in the 1940s by a new generation of synthetic organic compounds, and, subsequently, production has boomed resulting in the marketing of numerous insecticides and general pesticides. Soon after their introduction, concerns arose about the effects of pesticides on the health of farmworkers and consumers as well as their impact on ecosystems (Oerke and Dehne, 2004). However, pesticide use increased throughout the twentieth century.

In the 1990s, new biotechnologies enabled the production of genetically modified (GM) crops. The first example of a transgenic insect-resistant plant was provided by the expression of a cowpea trypsin inhibitor in tobacco (Hilder *et al.*, 1987), and in 1995, 'NewLeaf' potatoes expressing the Cry3A protein from *Bacillus thuringiensis* (Bt) became the first genetically modified crop sold by the Monsanto Company. Since then, the global area of biotech crops increased from 1.7 million hectares in 1996 to 191.7 million

hectares in 2018 with close to half of this area planted with pest resistant Bt varieties (ISAAA, 2018). In some regions, the adoption rate of Bt crops has been phenomenal. For example, in India, adoption rates for Bt cotton have been at 95% since 2015. Further, the use of GM crops has led to localized reductions in chemical pesticide use. For example, adoption of Bt eggplant in India reduced chemical pesticide applications by half while driving a 42% increase in yield (Ahmed *et al.*, 2019). Similarly, planting of Bt cotton in Australia reduced pesticide use by up to 85% (Knox *et al.*, 2006). In these contexts, one can argue that biotechnology has been successful and has provided a clear advantage over chemical products. However, in some world regions, these crops remain controversial due to differing perspectives on genetic modification as well as concerns about the emergence of resistant insect populations. Additionally, while some biotechnology crops have developed as public goods (Ahmed *et al.*, 2019), increased costs associated with the use of biotechnology limit the spread of these technologies in low-income nations.

In recent years, advances in computational technologies and biotechnologies have provided several alternatives to synthetic chemicals and first-generation GM plants. These approaches promise to provide more sustainable and durable solutions. In this review, we will assess the opportunities and challenges afforded by these new technologies, noting that, for a genuine breakthrough, biotechnological innovations need to ensure that agriculture is socially, economically and environmentally sustainable to serve societies that increasingly recognize the value of biodiversity and environment (Pellé and Reber, 2015; Sayer *et al.*, 2021).

New generations of insect-resistant crops

In insect-resistant Bt crops, insecticidal activity is provided by expression of genes encoding parasporal crystalline protoxins, commonly known as Cry proteins (Palma *et al.*, 2014). Nine different Cry proteins (Cry1Ab, Cry1Ac, Cry1A.105, Cry1Fa, Cry2Ab, Cry3Bb, mCry3A, eCry3.1Ab and Cry34/35Ab) have been used as transgenes, but insect populations have begun to evolve resistance to all of them. Interestingly, however, this has not happened in all insect species (Tabashnik and Carrière, 2017). For example, even after more than 20 years of exposure to a Bt maize in Europe, resistance has not been reported in the major pest, *Sesamia nonagrioides* (Castañera *et al.*, 2016). Regardless, it is generally predicted that crops expressing multiple toxins with different modes of action are likely to perform better and delay the development of resistance (Bravo and Soberón, 2008; Tabashnik and Carrière, 2017). This has primarily been achieved through transgene pyramiding (Zhao *et al.*, 2003). For example, three genes, *Cry1Ac*, *Cry2A* and *Gna* (snowdrop lectin), were inserted into indica rice targeting three major pests, rice leaf folder, *Cnaphalocrocis medinalis*, yellow stemborer, *Scirpophaga incertulas*, and the brown planthopper, *Nilaparvata lugens* (Maqbool *et al.*, 2001). Additionally, pyramiding Cry toxins with vegetative insecticidal protein 3A (Vip3Aa) from *B. thuringiensis* has also been shown to diminish the risk of resistance (Carrière *et al.*, 2015).

Several sources of resistance to insects have also been found within plants themselves. Many plants have evolved specialized metabolites to deter herbivores and sap feeders. Several of these have been used as ingredients in insecticidal formulations applied as foliar sprays including nicotine from tobacco, capsaicin from chilli peppers, pyrethrin from chrysanthemum and azadirachtin isolated from the Neem tree (Benelli *et al.*, 2017; Pavela, 2016).

More recently, transgenic approaches have also been demonstrated. For example, monoterpene biosynthesis in tomato fruits improved resistance against larvae of the corn earworm, *Helicoverpa zea* (Gutensohn *et al.*, 2014). Further, the biosynthetic pathway of the volatile sesquiterpene (*E*)-β-farnesene, a plant metabolite that has also been described to act as an alarm pheromone in aphids (Bowers *et al.*, 1972), was transferred to *Arabidopsis thaliana* (Beale *et al.*, 2006) and, subsequently, to wheat (Bruce *et al.*, 2015). While aphids were repelled and foraging behaviour of a natural parasite increased in laboratory conditions, these results were not replicated in the field (Bruce *et al.*, 2015). Overexpression of an endogenous terpene synthase in rice (Os*TPS46*) led to overproduction of (*E*)-β-farnesene and limonene, deterring feeding by the bird cherry-oat aphid, *Rhopalosiphum padi* (Sun *et al.*, 2017), and tobacco plants genetically engineered to produce (*E*)-β-farnesene synthase from peppermint showed decreased levels of aphid infestation (Yu *et al.*, 2013). Overexpression of (*E*)-β-caryophyllene, another volatile sesquiterpene found in plants and emitted by some insects as a semiochemical (El-Sayed, 2021), in *A. thaliana* repelled the vector of citrus disease Huanglongbing, *Diaphorina citri* (Alquézar *et al.*, 2017) and expression of the same gene in sweet orange produced similar effects (Alquézar *et al.*, 2021). Lectins, common in many plants, bind to carbohydrate structures in the midguts of phytophagous insects causing disruption of the digestive system. Lectin genes have been transferred into crops including wheat (Stoger *et al.*, 1999) and maize (Wang *et al.*, 2005) conferring some resistance to aphid pests. Protease inhibitors, which aim to inhibit insect digestive enzymes, have also been deployed using transgenic strategies with genes originating from plants (Duan *et al.*, 1996), sea anemones (Outchkourov *et al.*, 2003) and mushrooms (Šmid *et al.*, 2013).

To initiate their defence cascades, plants have evolved resistance genes (R genes). Many R genes encode nucleotide-binding site leucine-rich repeat (NBS-LRR) proteins, which recognize specific pests and pathogens. Transgenic methods can be used to stack multiple R genes from resistant landraces or wild relatives into susceptible varieties. This has been successfully deployed to confer resistance to pathogens including late blight in potatoes (Ghislain *et al.*, 2019) and rust in wheat (Luo *et al.*, 2021). There have been some successes deploying R genes for resistance to insects. For example, transgenic expression of *Mi-1.2*, an NBS-LRR protein from wild tomato in susceptible commercial cultivars, conferred resistance to potato aphids, *Macrosiphum euphorbiae* (Rossi *et al.*, 1998; Vos *et al.*, 1998). One limitation, however, is that NBS-LRR *R* genes can be highly specific to biotypes, and thus, when *Mi-1.2* was transferred to eggplant, it could not confer resistance to eggplant-feeding biotypes of the same species (Goggin *et al.*, 2006).

An alternative strategy for engineering genetic resistance is to remove genes that confer susceptibility to pathogens (S genes). Genome editing technologies, such as those derived from bacterial CRISPR systems, have been successfully applied in a wide range of crops and can be used to eliminate the accumulation of specific gene products either by deleting the gene or by introducing mis-sense mutations into the gene of interest (Gao, 2021). For example, the production of rice plants with targeted mutations in the cytochrome P450 gene *CYP71A* that catalyses conversion of tryptamine to serotonin resulted in insect-resistant plants, which lacked serotonin but accumulated increased levels of salicylic acid (Lu *et al.*, 2018). In several global jurisdictions, gene-edited crops can reach market with fewer regulatory

hurdles than GM crops (Waltz, 2018). This may make genome editing approaches more attractive for the development of new-generation insect-resistant crops than plants with transgene stacks. However, there is not yet global consensus on regulation: the European Court of Justice decided that, according to the text of Directive 2001/18/EC, genome-edited products should be regulated as GM (Court of Justice of the European Union, 2018a, b), although a recent scientific opinion from the European Food Safety Authority concluded that some genome editing techniques pose no more hazards than conventional plant breeding (Naegeli et al., 2020).

RNA interference for pest control

A different approach has leveraged RNA interference (RNAi) mechanisms to provide plants with molecules capable of down-regulating essential genes in the insects that feed on them.

RNAi is a regulatory mechanism present in many eukaryotes that uses double-stranded RNA (dsRNA) to control the stability of mRNA (Figure 1). Since the discovery of the mechanism in the 1990s, the expression of engineered small interfering RNAs (siRNAs) has become a widely used approach for investigating gene function (Hannon, 2002). The first applications of RNAi technology to agricultural pest control were published over a decade ago (Baum et al., 2007; Mao et al., 2007). The most challenging part of this approach is to enable efficient uptake of dsRNA by the insect. Two options for the production and delivery of dsRNAs have been demonstrated. The first is the transgenic expression of dsRNAs from the crop genome, termed host-induced gene silencing (HIGS, Figure 1a). In this approach, insects feeding on the crop will consume the dsRNA. In the second approach, dsRNAs are produced at high concentrations using a heterologous expression system and, following purification, are applied to insect-infested crops as a foliar spray. This approach is termed spray-induced gene silencing (SIGS, Figure 1b). In both approaches, in target species, the target genes will be silenced (Figure 1c) (Christiaens et al., 2020a).

Two studies published in 2007 provided proof-of-concept for the efficacy of RNAi-based insect pest control. Mao et al. (2007) described a strategy to control the lepidopteran pest cotton bollworm, Helicoverpa armigera, by engineering cotton plants to express dsRNAs targeting an insect gene encoding a cytochrome P450 that detoxifies the toxic plant metabolite, gossypol. Meanwhile, Baum et al. (2007) identified several target genes in western corn rootworms, Diabrotica virgifera virgifera, and Colorado potato beetles, Leptinotarsa decemlineata, of which RNAi-induced silencing caused high mortality. Subsequent examples include the production of transgenic maize plants expressing a dsRNA targeting Snf7, an essential vacuolar sorting gene (Bolognesi et al., 2012). Recently, tomato plants expressing a dsRNA targeting a gene encoding a phenolic glucoside malonyltransferase, which detoxifies phenolic glycosides, showed complete resistance to the tobacco whitefly, Bemisia tabaci. Interestingly, the target gene was, itself, identified as being of plant origin, acquired by the insect in a horizontal gene transfer event (Xia et al., 2021).

Several studies have also inserted dsRNA expression cassettes into the chloroplast genome, a cellular compartment that lacks RNAi machinery. This strategy enabled transplastomic potato plants to be protected from herbivory by the Colorado potato beetle (Zhang et al., 2015) with subsequent studies showing the length of dsRNAs are a key factor influencing the strength of the

insecticidal RNAi effect (He et al., 2020). Chloroplast-expressed dsRNAs were also effective against the tobacco hornworm, Manduca sexta (Burke et al., 2019) and tobacco whitefly (Dong et al., 2020).

After more than a decade of research and development, RNAi-based pest control products have advanced sufficiently to reach the market. A HIGS strategy for protection against western corn rootworm by Bayer Crop Science (formerly Monsanto) has been employed in MON87411 maize (Mat Jalaluddin et al., 2019). In general, the use of dsRNA provides several benefits over conventional insecticides, including the ability to control species specificity by targeting gene regions that vary between species. Other advantages include the rapid degradation of RNA into non-toxic compounds and the lack of toxicity to vertebrates and other non-target species. However, many challenges remain. The inherent lability of RNA, while ensuring that dsRNAs do not persist in the environment, is problematic in harsh environmental conditions and limits opportunities for SIGS approaches (Bramlett et al., 2020). Also, while some pests rapidly take up dsRNA resulting in high mortality rates, in other species low dsRNA uptake and nuclease degradation lead to inefficient results (Christiaens et al., 2020b; Shaffer, 2020). Success is also dependent on whether sufficient levels of dsRNA accumulate in the tissues on which the insects feed. Ongoing research is addressing dsRNA stability and uptake by the development of novel spray formulations, many utilizing nanomaterials (Christiaens et al., 2020b). Finally, while rapid increases in sequence availability improve the ability to design species-specific dsRNAs, concerns remain about adverse effects on non-target organisms (Rodrigues and Petrick, 2020) and significant questions remain about how insects may evolve resistance (Khajuria et al., 2018; Shaffer, 2020). Such concerns inform both regulatory and public deliberation on these approaches and may contribute to delaying or limiting their deployment in some world regions.

Genetic methods for controlling insect populations

The use of genetic insect control methods dates to the first half of the twentieth century when impressive results were achieved by releasing radiation-sterilized primary screwworms, Cochliomyia hominivorax (Scott et al., 2017). In this approach, known as the sterile insect technique (SIT), sterile males compete with the wild population to mate with females, which are then unable to produce viable offspring. However, SIT can be difficult as the fitness of irradiated males is generally compromised. In addition, it poses operational challenges including the need for the males to be separated prior to release to avoid crop damage by females and a risk that large numbers of non-sterile insects may be unintentionally released from rearing facilities.

To overcome some of these issues, a strategy known as the release of insects carrying a dominant lethal trait (RIDL) was proposed. This typically involves the rearing and release of insects carrying a repressible dominant lethal transgene. To enable the rearing of such populations, sex-specific conditional dominant lethality is employed. For example, the lethal gene is controlled using genetic elements that enable sex-specific expression to be repressed by a specific diet component unavailable outside of the laboratory. This allows female insects to be selectively eliminated before release by withdrawing the repressor. A RIDL system was developed for Drosophila melanogaster using tetracycline-repressible transcriptional trans-activators under the control of
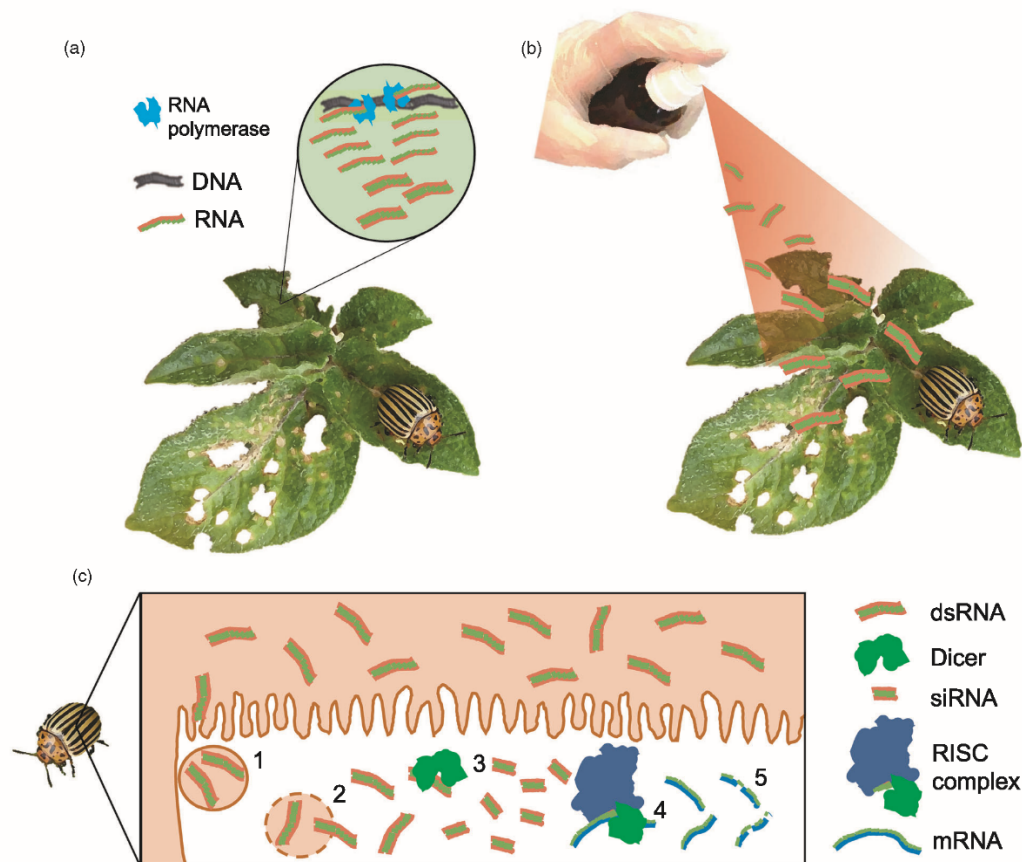
Figure 1 Methods for RNA interference (RNAi)-mediated insect pest control. (a) In host-induced gene silencing (HIGS), double-stranded RNAs (dsRNA) are expressed from transgenes in the crop plant. (b) In spray-induced gene silencing (SIGS), dsRNA is produced in a heterologous system and applied to the crop as spray before being consumed by the insect. (c) When insects feed on the plant, the dsRNA induces RNAi in the target species. Following uptake of dsRNAs into the insect gut epithelium cells by endocytosis (1) the dsRNAs are released, (2) short interfering RNA (siRNA) are generated by the Dicer complex (3) and the RNA-induced silencing complex (RISC) mediates cleavage of target mRNAs with complementary to the siRNA's leading strand (4). Finally, cleaved mRNAs are degraded by the nonsense-mediated decay pathway (5).

female-specific promoters (Thomas *et al.*, 2000). Subsequently, a conserved sex determination mechanism based on alternative splicing (Figure 2a and b) was used as the basis for engineering female-specific tetracycline-repressible lethality in Mediterranean fruit flies, *Ceratitis capitata* (Fu *et al.*, 2007), pink bollworms, *Pectinophora gossypiella* (Jin *et al.*, 2013), and diamondback moths, *Plutella xylostella* (Jin *et al.*, 2013). This has subsequently been marketed as Friendly™ technology by Oxitec Ltd. aimed at controlling insect vectors of human diseases as well as crop pests. Field-cage studies with diamondback moths have demonstrated effectiveness in population suppression (Leftwich *et al.*, 2014) and delays in the spread of insecticide resistance (Harvey-Samuel *et al.*, 2015). Further, in open-field trials, dispersal, persistence and field survival rates of the released insects were shown to be similar to the wild type (Shelton *et al.*, 2020).

More recently, gene drives have been proposed for facilitating the introduction of desirable traits into wild populations. Gene drives spread a desired allele into the population by enabling higher-than-Mendelian rates of inheritance. This approach can be employed for either population suppression or the modification of specific genes, for example, reversion of insecticide resistance alleles (Champer *et al.*, 2016) (Figure 2a and d). A successful application of gene drives was the development of a maternal effect dominant embryonic arrest (*Medea*) in *Drosophila suzukii*, a highly invasive crop pest. This consisted of a miRNA expressed during oogenesis in Medea-bearing mothers (toxin) that prevents the synthesis of a protein essential for embryogenesis together with a miRNA-resistant copy of the target gene (antidote) expressed in Medea-bearing embryos (Figure 2c; Buchman *et al.*, 2018).

As molecular tools for targeted mutagenesis have become available, several different strategies for the construction and deployment of synthetic gene drives have been proposed (Esvelt *et al.*, 2014; Hammond *et al.*, 2016; Sinkins and
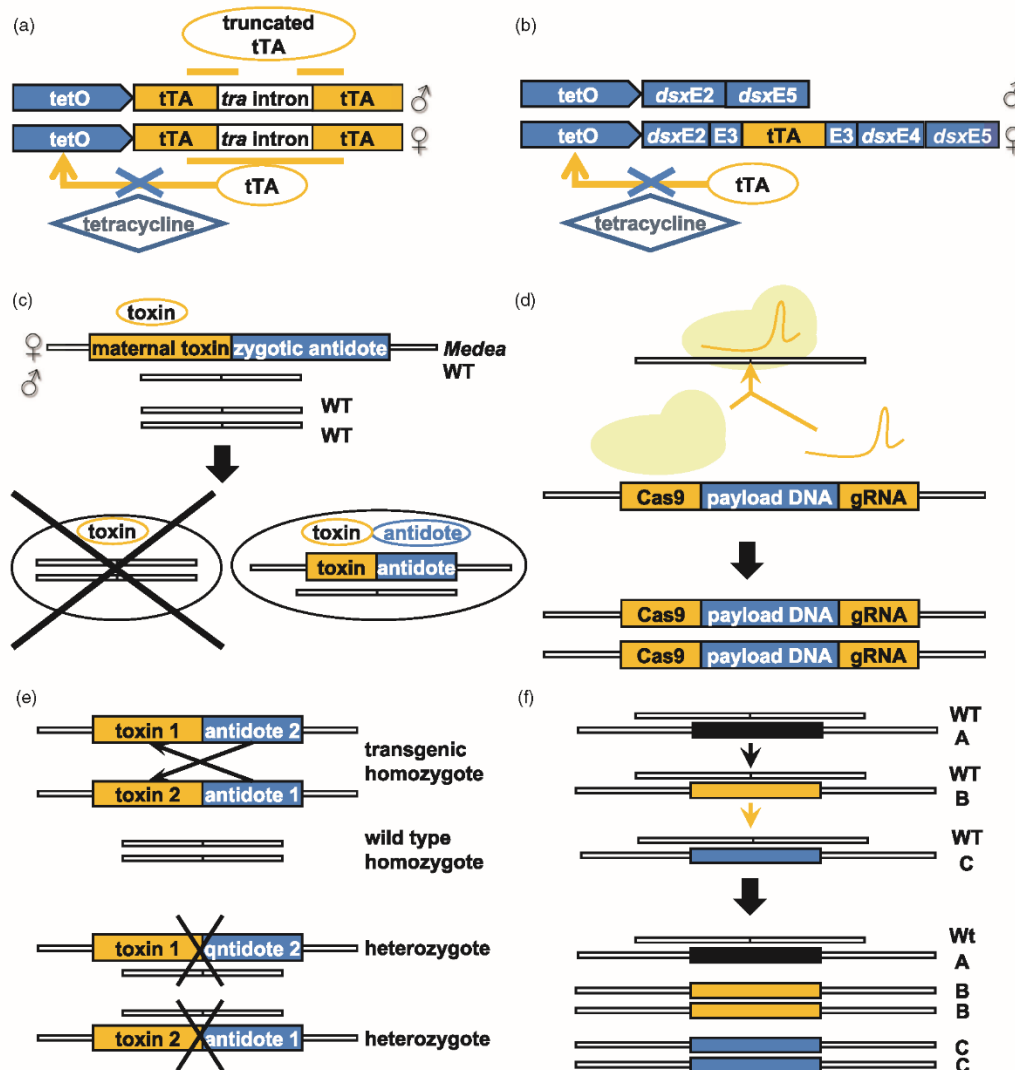
Figure 2 Strategies for genetic control of insect populations. (a and b): Release of insects carrying a female-specific dominant lethal trait (RIDL). Expression of the transcription factor (tTA) is lethal and is controlled by the tetracycline-repressible promoter (tetO) allowing transcription to be repressed with tetracycline. Female-specific expression is conferred by (a) the inclusion of the *tra* (*transformer*) intron that is only spliced in females or (b) by placing the *tTA* gene within the female-specific exon of the *dsx* (*doublesex*) gene. (c) Deployment of the maternal effect dominant embryonic arrest (*Medea*) gene drive facilitates expression of the maternal toxin during oogenesis in *Medea*-bearing mothers. This is transmitted to all progeny, but *Medea*-bearing embryos are rescued by expression of an antidote during embryogenesis. (d) In homing-based gene drives, a transgene cassette is integrated at the locus of interest. The transgene encodes the Cas9/sgRNA genes to induce double-stranded breaks and triggers homology-directed repair in the equivalent locus. This ensures homozygosity of the transgene in any progeny and, thus, inheritance by all descendants. The use of underdominance or heterozygote inferiority results in a self-limiting gene drive (e). In this case, heterozygotes have lower fitness than parental homozygotes. Homozygotes carrying two transgenic alleles survive because the toxin encoded by each allele is neutralized by the antidote encoded by the other allele. The spread of an underdominance gene drive requires high introduction rate and can be stopped by the release of wild type insects. In daisy-chain gene drives (f) the drive and the elements they drive are located at independently segregating loci. In this example, A drives B, B drives C; A is not driven and declines. WT = wild type.

Gould, 2006; Windbichler *et al.*, 2011). CRISPR-gene drives have been tested in *D. melanogaster* (Gantz *et al.*, 2015) as well as in two species of *Anopheles* mosquitoes, vectors of the malaria parasite, suppressing of reproduction of *A. gambiae* (Hammond *et al.*, 2016) and blocking parasite development in *A. stephensi* (Gantz *et al.*, 2015). Symbiotic

30 Rubén Mateos Fernández *et al.*

associations of insects with microorganisms can also be exploited for suppression of pest populations and for gene drives (Panagiotis and Bourtzis, 2007). For example, a so-called incompatible insect technique (IIT), based on cytoplasmic incompatibility, induced by *Wolbachia* was used to control laboratory populations of the Mediterranean fruit fly (Zabalou *et al.*, 2004).

Opinions on the application of genetic methods for pest insect control vary (Zhang *et al.*, 2020). While SIT programmes using irradiated insects have previously faced little resistance, the

Organism	Reference	Pathway
YEASTS — *Saccharomyces cerevisiae*	Moto et al., 2003	E10,Z12-16:Acid (supplemented) →(*Bmpg*FAR) **E10,Z12-16:OH** (T)
	Hagström et al., 2013	16:CoA →(*Ase*Δ11) Z11-16:CoA →(*Ase*FAR) **Z11-16:OH** → **Z11-16:Ald** (T)
Yarrowia lipolytica	Holkenbrink et al., 2020	↑14:CoA →(*Atr*Δ11) Z9-14:CoA →(*Har*FAR) **Z9-14:OH** →(*Sc*ATF1) **Z9-14:OAc**
		↑16:CoA →(*Atr*Δ11) Z11-16:CoA →(*Har*FAR) **Z11-16:OH** → **Z11-16:Ald** (T)
PLANTS — *Nicotiana tabacum* stable	Nešněrová et al., 2004	16:CoA →(*Tni*Δ11) Z11-16:CoA → → Z11–16:Me → **Z11-16:OAc** (T)
Nicotiana benthamiana transient	Ding et al., 2014	14:CoA →(*Ave*Δ11) E11-14:CoA →(*Har*FAR_KKYR) **E11-14:OH** →(*Ea*DACT) **E11-14:OAc** (T*)
		14:CoA →(*Ave*Δ11) Z11-14:CoA →(*Har*FAR_KKYR) **Z11-14:OH** →(*Ea*DACT) **Z11-14:OAc** (T*)
		16:CoA →(*Atr*Δ11) Z11-16:CoA →(*Har*FAR_KKYR) **Z11-16:OH** →(*Ea*DACT) **Z11-16:OAc** (T*)
Nicotiana benthamiana stable / *Nicotiana tabacum* stable	Xia et al., 2020	14:ACP →(*Cpa*FATB) 14:CoA →(*Ave*Δ11) Z11-14:CoA → **Z11-14:OH**
		14:ACP →(*Cpa*FATB) 14:CoA →(*Cpa*E11) E11-14:CoA → **E11-14:OH**
		16:ACP →(*Cpu*FATB) 16:CoA →(*Atr*Δ11) Z11-16:CoA → **Z11-16:OH**
Camelina sativa stable	Ortiz et al., 2020	→(uFATB) 16:CoA →(uΔ11) Z11-16:CoA → **Z11-16:OH** → **Z11-16:OAc** (T); **Z11-16:OH** (T); → **Z11-16:Ald** (T)
Nicotiana benthamiana stable	Mateos-Fernández et al., 2021	16:CoA →(*Atr*Δ11) Z11-16:CoA →(*Har*FAR) **Z11-16:OH** →(*Ea*DACT) **Z11-16:OAc**; **Z11-16:OH** (T); → **Z11-16:Ald**

Figure 3 Strategies for the biosynthesis of lepidopteran sex pheromones. Blue arrows represent synthesis by a heterologous enzyme; black arrows represent chemical synthesis; purple arrows represent synthesis by an endogenous enzyme. Metabolites in red text are known to act as sex pheromones. (T) indicates experimental assays have shown that the molecule affected the behaviour of moths and (T*) indicates that the behaviour assay was conducted with a chemically synthesized molecule, even if also produced via biosynthesis. *BmpgFAR* = *Bombyx mori pheromone gland fatty-acyl reductase*; *AseΔ11* = *Agrotis segetum* Δ11 fatty-acyl desaturase; *AseFAR* = *Agrotis segetum* fatty-acyl reductase; *AtrΔ11* = *Amyelois transitella* Δ11 fatty-acyl desaturase; *HarFAR* = *Helicoverpa armigera* fatty-acyl reductase; *ScATF1* = *Saccharomyces cerevisiae* alcohol acetyl transferase; *Trichoplusia ni* Δ11 fatty-acyl desaturase; *AveΔ11* = *Argyrotaenia velutinana* Δ11 fatty-acyl desaturase; *HarFAR_KKYR* = *Helicoverpa armigera* fatty-acyl reductase with C-terminal endoplasmic reticulum retention signal; *EaDACT* = *Euonymus alatus* acetyltransferase; *CpaFATB* *Cuphea palustris* 14:ACP fatty acid thioesterase; *CpuFATB* = *Cuphea pulcherrima* fatty acid thioesterase; *CpaE11* = *Choristoneura parallela* E11 desaturase; FATB = unspecified acyl carrier protein thioesterase; uΔ11 = unspecified Δ11 fatty-acyl desaturase.

release of genetically modified insects has encountered criticisms (Baltzegar *et al.*, 2018). Concerns have been raised about the inherent pervasiveness and potentially irreversibility of gene drives, raising questions of proportionality (Callaway, 2018). Support for the use of gene drives has been found to be higher when used to control non-native pest species, or if they include a mechanism to limit drive spread (Jones *et al.*, 2019). Consequently, it is possible that the development of self-limiting gene drive systems, for example underdominance (Dhole *et al.*, 2018) or daisy-chain drives (Noble *et al.*, 2019) (Figure 2e and f), may provide options for wider deployment of these technologies in the future, particularly if directed towards invasive and non-native pests.

Biomanufacturing pest control products

As noted above, several natural products, particularly plant specialized metabolites, have been used as agents for insect pest control. While this is a viable option for abundant chemicals for which extraction from the original plant source is economically viable and for those that are easily produced via synthetic chemistry, the use of many bioactive organic products is limited by the inability to affordably scale up production. Biomanufacturing, accelerated by the application of synthetic biology approaches to metabolic engineering, is an emerging technology providing the potential for the large-scale production of complex molecules with little or no chemical waste. Direct or foliar application of biomanufactured molecules, either purified from their production organisms or used as semi-processed formulations, may encounter fewer regulatory barriers than engineered crops.

To date, the most significant advances have been made using microbial organisms as chassis for biomanufacturing natural products for health and industry (Yang *et al.*, 2020), including known insect repellents nootkatone (Guo *et al.*, 2018) and cembratrienol (Zhang *et al.*, 2021). However, plants have also been envisioned as platforms for bioproduction of insecticidal compounds. For example, the biosynthesis pathway of pyrethric acid, the monoterpene acyl moiety of the widely used pyrethrin insecticides, has been transferred to *Nicotiana benthamiana* (Xu *et al.*, 2019). More excitingly, bioproduction has also been proposed as a potential solution for manufacturing novel classes of insect-controlling chemicals including insect sex pheromones. These, being highly species-specific, provide an attractive alternative to broad-spectrum pesticides. Further, pheromones are typically volatile and emitted in minute quantities into the environment rather than being applied to the crop itself. Crucially, they are likely to remain effective against pesticide-resistant insect populations; evolution of pheromone resistance is considered unlikely due to strong selection against losing the ability to find a mate (Rizvi *et al.*, 2021). While several pheromones are easy to

produce by chemical synthesis and have already reached market, the chemical synthesis of many other insect sex pheromones remains challenging or expensive, mainly due to their complex molecular structures and requirement for multiple stereoselective steps. Thus, production costs can range from several hundred to several thousand dollars per kilogram, a cost only affordable for the protection of high-value agricultural products such as speciality fruits (Petkevicius *et al.*, 2020). Even when affordable chemical synthesis is possible, biomanufacturing may represent a more sustainable method of production, requiring renewable feedstocks and producing little or no hazardous waste.

Lepidopteran sex pheromones, mainly fatty alcohols and their corresponding aldehyde and acetate derivatives, are some of the best-studied pheromones due to the economic impact as well as their relatively simple chemical formulation. Biosynthesis of bioactive lepidopteran sex pheromone and chemically modifiable precursors has been explored in several biological chassis (Figure 3). Hagström *et al.*, (2013) demonstrated production of the fatty alcohol components of moth sex pheromones in *Saccharomyces cerevisiae* expressing insect fatty-acyl desaturases and reductases. Another yeast, the oleaginous *Yarrowia lipolytica*, was additionally engineered to improve the yield of moth sex pheromones by down-regulating fatty alcohol degradation and storage lipids besides expressing pheromone synthesis enzymes (Holkenbrink *et al.*, 2020). Alternative approaches based on a combination of biological and chemical synthesis, such as a dried formulation of yeast biomass that is processed into desaturated fatty alcohols, have also been explored and patented (Konrad *et al.*, 2017). Recently, BioPhero, a spin-out from the Technical University of Denmark, demonstrated large-scale production of field-tested moth pheromones in yeast (Petkevicius *et al.*, 2020).

Plants are also being used to trial the production of insect sex pheromones due to their high biomass and ability to produce complex molecules. The first example of plant production of insect sex pheromones described a transgenic tobacco line producing moth sex pheromone precursors (Nešněrová *et al.*, 2004). Subsequent examples demonstrated the production of precursors in *Nicotiana spp.* (Xia *et al.*, 2020) and in false flax, *Camelina sativa*, where products accumulated in seeds (Ortiz *et al.*, 2020). In 2014, several fatty alcohols and their corresponding aldehyde and acetate forms were produced via transient expression (agroinfiltration) of *N. benthamiana* leaves, providing a biologically active pheromone blend (Ding *et al.*, 2014).

Pheromone production in plants also provides the opportunity of direct dispensation from the living production platform, negating the need for extraction and packaging into man-made traps or dispensers. While living biodispensers would not be useful for attract and kill strategies where the pheromone and an insecticide are combined within a trap, they could be used in

mating disruption strategies in which the aim is to impede the ability of males to locate a female mate. In 2020, live plant dispensers of chemical signals were included in a shortlist of emerging products of bioengineering (Kemp *et al.*, 2020) and, recently, transgenic *N. benthamiana* plants transformed with a three-gene pathway resulted in the production of high levels of the *(Z)*-11-hexadecen-1-ol (Z11-16OH) and *(Z)*-11-hexadecenyl acetate (Z11-16OAc) components of moth pheromones (Mateos-Fernández *et al.*, 2021). Although pheromone production was shown to negatively influence plant growth and only a small fraction of the pheromones were released to the environment in volatile forms, this first report of a living biodispenser could pave the way for future iterations.

As discussed above, transgenic plants expressing the insect alarm pheromones *(E)*-β-farnesene and *(E)*-β-caryophyllene showed decreased levels of insect infestation. While work to date has aimed at engineering these pathways into crop plants, these compounds might also be targets for biomanufacturing, enabling their inclusion in sophisticated chemical blends. Of further interest is the ability to produce blends that include or co-emit plant-based compounds known to play roles in insect communication. Some plant endogenous volatiles have been described to act synergistically with insect sex pheromones to increase their attractiveness (Bruce and Pickett, 2011; Gregg *et al.*, 2018). Several terpenoid and aromatic compounds exert this effect towards Lepidoptera (von Arx *et al.*, 2012), while some green leaf volatiles (C6 fatty acid derivatives) emitted as a consequence of phytophagy is active towards a broad range of species (Dickens *et al.*, 1993). Future insect sex pheromones strategies could consider including such compounds in novel chemical blends to optimize their effects. Further, such blends might be produced by co-expressing the desired biosynthetic pathways within the same production chassis. This approach could include herbivore-induced plant volatiles (HIPVs) to attract predators and parasitoids of herbivore pests (Nishida, 2014; Wei and Kang, 2011).

Harnessing biocontrol

Biological pest control methods are now a crucial component of integrated pest management strategies. Natural predators, parasitoids, competitors and pathogens are all employed to control insect infestations. However, while progress has been made at improving biocontrol agents using artificial selection (Lirakis and Magalhães, 2019) including boosting thermotolerance of entomopathogenic fungus *Metarhizium anisopliae* (de Crecy *et al.*, 2009) and selecting for truncated wings in predaceous ladybird beetles to prolong residence on aphid-infested host plants (Lommen *et al.*, 2019), to date, little has been done to exploit their full potential. Despite numerous experimental efforts and advances, aside from a few recombinant *Bt* strains, genetically engineered biocontrol agents have not been widely commercialized (Karabörklü *et al.*, 2018). However, the application of emerging genetic and genomic approaches to biocontrol agents could become an integral part of developing efficient biocontrol strategies (Leung *et al.*, 2020).

Entomopathogenic agents, including fungi, bacteria, viruses and nematodes, represent the majority of biocontrol agents on the market (Lacey *et al.*, 2015). Biotechnology provides the opportunity to engineering these species to improve their efficacy. For example, transgenic approaches have been used to increase the efficacy of entomopathogenic fungi following

overexpression of virulence factors, toxins and proteins that disrupt the homeostasis of physiological processes (Fan *et al.*, 2012; St. Leger *et al.*, 1996; Wang and St Leger, 2007). Additionally, fungi, bacteria and viruses have been engineered to produce insect-specific dsRNAs (Al Baki *et al.*, 2020; Bao *et al.*, 2016; Mysore *et al.*, 2019), and baculoviruses have been used as an effective expression and delivery system for insecticidal proteins and hold promise for implementation of RNAi (Harrison and Bonning, 2000; Kroemer *et al.*, 2015). In the future, genetic engineering might also be applied to improve the resistance of entomopathogenic agents to abiotic stresses to modulate their host range or their sensitivity to chemical pesticides and fungicides (Bielza *et al.*, 2020). However, to achieve this, a better understanding of virulence factors (Gao *et al.*, 2020; Semenova *et al.*, 2020), fitness (Mou *et al.*, 2020) and host–pathogen interactions (Hussain, 2018; Yang *et al.*, 2014a) is required.

Species currently known to negatively impact pest populations are also a useful source of molecules that could be leveraged using the transgenic and biomanufacturing technologies described in previous sections. Besides the well-known *Bt* toxins, toxins from bacterial symbionts of entomopathogenic nematodes *Photorhabdus luminescens* and *Xenorhabdus nematophilus* (Ffrench-Constant and Bowen, 2000) and from soil-dwelling bacteria *Pseudomonas chlororaphis* (Schellenberger *et al.*, 2016), as well as many other natural peptides (Harrison and Bonning, 2010; Paul and Das, 2021), have been proposed as potential insecticides. These have been shown to be effective following oral ingestion by insects either alone or following fusion to carrier proteins (Yang *et al.*, 2014b). The use of specific bioactive molecules may also avoid the potential ecological effects of widespread release of entomopathogens.

Conclusions and outlook

The ability to engineer organisms has steadily increased in the first decades of the 21st century, driven both by the availability of genome engineering tools and by the application of engineering approaches (synthetic biology) to biotechnology that has been instrumental in enabling scalable biomanufacturing of natural products (Lorenzo *et al.*, 2018). Interestingly, and with similarities to crop varieties produced by radiation, the release of a population of irradiated insects encountered little resistance in the 20th century. However, while genetically modified insect populations show potential and populations of engineered diamondback moths, pink bollworms and, most recently, *Aedes aegypti* mosquitoes, have all been released in non-contained trials in the United States, engineered populations, particularly using gene drives, seem less likely to have an easy route to market (Baltzegar *et al.*, 2018).

In recent years, concerns about the ecological impacts of broad-spectrum pesticides have increased, leading to bans and a growing interest in alternative methods of pest control (Butler, 2018). Evidence suggests that insect-resistant crops have significantly reduced the use of pesticides (Ahmed *et al.*, 2019; Knox *et al.*, 2006; Wilson *et al.*, 2018). However, the appearance of resistant populations has caused concern and is likely to influence the strategies used to develop new generations of insect-resistant crops. Further, even where resistant populations have not emerged, the widespread adoption of insect-resistant GM crops has had unforeseen consequences allowing pests other than the initial target species to flourish. For example, the planting of Bt cotton successfully reduced damage from bollworms and leaf-

Biotechnologies for insect pest management

feeding insect infestations, but sap feeders including whitefly, leafhoppers, aphids and thrips emerged as new dominant causes of crop loss (Shera *et al.*, 2020). Examples such as this highlight the difficulties of pest management.

With limitations on broad-spectrum chemicals, methods such as pheromones and RNAi, both capable of superb species specificity, may be increasingly valued. While pheromones have been in use for some decades, products available for agricultural pest control have been limited to those able to be chemically synthesized at low cost. Recent advances in synthetic biology and metabolic engineering are rapidly expanding the diversity of complex molecules that can be produced at scale providing new opportunities for pheromone production. This is exemplified by the recent emergence of pheromone biotechnology companies such as BioPhero and Provivi. With many nations outlining strategies to develop their bioeconomies, innovation in biomanufacturing that will increase the feasibility of commercial scale production looks set to increase (Kuckertz, 2020). Further, the application of synthetic biology to plant metabolic engineering provides the opportunity for novel deployment strategies such as living biodispensers (Kemp *et al.*, 2020).

However, while biotechnology may provide multiple options for novel methods of pest control, many products will require regulatory systems that, for some products and in some regions, may not yet be in place. Additionally, they will require the support of growers and consumers for which open dialogues, including the potential of new technologies to contribute to social progress, will be beneficial (Bauer and Bogner, 2020).

Acknowledgements

All authors gratefully acknowledge the European Research Area Cofund Action 'ERACoBioTech' for the support of SUSPHIRE (Sustainable Production of Pheromones for Insect Pest Control in Agriculture), which received funding from the Horizon 2020 research and innovation programme under grant agreement No. 722361. ŠB, KG, MP and MJ acknowledge national funding from the Slovenian Ministry of Education, Science and Sport, the support of the Slovenian Research Agency's research core funding grant P4-0165 and research project grant Z4-706. KK and NP acknowledge the support of the UK Biotechnology and Biological Sciences Research Council (BBSRC) Core Strategic Programme Grant (Genomes to Food Security) BB/CSP1720/1 and grant BB/R021554/1. EJ, RG and DO acknowledge the support of grant PCI2018-092893 and the FPU programme of the Spanish MINECO. RG acknowledges an FPI grant from the Generalitat Valenciana. IG, JG and AN acknowledge the support of the Deutsche Forschungsgemeinschaft (DFG).

Conflict of interest

All authors agree to publication of the manuscript. The authors report no commercial or proprietary interest in any product or concept discussed in this article.

Author contributions

NJP, DO, AN, SB and KG were involved in conceptualization and supervision. RMF, MP, IG, MJ, SB, KK, EMG, JG, AN and NJP drafted the text. All authors contributed to revising and editing the text.

References

Ahmed, A.U., Hoddinott, J.F., Islam, K.S., Khan, A.S.M.M.R., Abedin, N. and Hossain, N.Z. (2019) *Impacts of Bt brinjal (Eggplant) technology in Bangladesh.* International Food Policy Research Institute. https://pdf.usaid.gov/pdf_docs/PA00TZ7Z.pdf.

Al Baki, A., Jung, J.K. and Kim, Y. (2020) Alteration of insulin signaling to control insect pest by using transformed bacteria expressing dsRNA. *Pest Manag. Sci.* **76**, 1020–1030.

Alexandratos, N. (2012) World agriculture towards 2030/2050 The 2012 revision. *SA Work. Pap.* **12**, 146.

Alquézar, B., Volpe, H.X.L., Magnani, R.F., de Miranda, M.P., Santos, M.A., Wulff, N.A., Bento, J.M.S. *et al.* (2017) β-caryophyllene emitted from a transgenic Arabidopsis or chemical dispenser repels *Diaphorina citri*, vector of Candidatus Liberibacters. *Sci. Rep.* **7**(1):5639. https://doi.org/10.1038/s41598-017-06119-w

Alquézar, B., Volpe, H.X.L., Magnani, R.F., de Miranda, M.P., Santos, M.A., Marques, V.V. *et al.* (2021) Engineered orange ectopically expressing the arabidopsis β-caryophyllene synthase is not attractive to *Diaphorina citri*, the vector of the bacterial pathogen associated to huanglongbing. *Front. Plant Sci.* **12**, 200.

von Arx, M., Schmidt-Büsser, D. and Guerin, P.M. (2012) Plant volatiles enhance behavioral responses of grapevine moth males, lobesia botrana to sex pheromone. *J. Chem. Ecol.* **38**, 222–225.

Baltzegar, J., Cavin Barnes, J., Elsensohn, J.E., Gutzmann, N., Jones, M.S., King, S. and Sudweeks, J. (2018) Anticipating complexity in the deployment of gene drive insects in agriculture. *J. Responsible Innov.* **5**, S81–S97.

Bao, W., Cao, B., Zhang, Y. and Wuriyanghan, H. (2016) Silencing of Mythimna separata chitinase genes via oral delivery of in planta-expressed RNAi effectors from a recombinant plant virus. *Biotechnol. Lett.* **38**, 1961–1966.

Bauer, A. and Bogner, A. (2020) Let's (not) talk about synthetic biology: Framing an emerging technology in public and stakeholder dialogues. *Public Underst. Sci.* **29**, 492–507.

Baum, J.A., Bogaert, T., Clinton, W., Heck, G.R., Feldmann, P., Ilagan, O. *et al.* (2007) Control of coleopteran insect pests through RNA interference. *Nat. Biotechnol.* **25**, 1322–1326.

Beale, M.H., Birkett, M.A., Bruce, T.J.A., Chamberlain, K., Field, L.M., Huttly, A.K., Martin, J.L. *et al.* Aphid alarm pheromone produced by transgenic plants affects aphid and parasitoid behavior. *Proc. Natl. Acad. Sci. USA*, **103**, 10509–10513.

Benelli, G., Canale, A., Toniolo, C., Higuchi, A., Murugan, K., Pavela, R. and Nicoletti, M. (2017) Neem (*Azadirachta indica*): Towards the ideal insecticide? *Nat. Prod. Res.* **31**, 369–386.

Bielza, P., Balanza, V., Cifuentes, D. and Mendoza, J.E. (2020) Challenges facing arthropod biological control: identifying traits for genetic improvement of predators in protected crops. *Pest Manag. Sci.* **76**, 3517–3526.

Bolognesi, R., Ramaseshadri, P., Anderson, J., Bachman, P., Clinton, W., Flannagan, R., Ilagan, O. *et al.* Characterizing the mechanism of action of double-stranded RNA activity against western corn rootworm (*Diabrotica virgifera virgifera* LeConte). *PLoS ONE*, **7**, 47534.

Bowers, W.S., Nault, L.R., Webb, R.E. and Dutky, S.R. (1972) Aphid alarm pheromone: Isolation, identification, synthesis. *Science*, **177**, 1121–1122.

Bramlett, M., Plaetinck, G. and Maienfisch, P. (2020) RNA-based biocontrols—a new paradigm in crop protection. *Engineering*, **6**, 522–527.

Bravo, A. and Soberón, M. (2008) How to cope with insect resistance to Bt toxins? *Trends Biotechnol.* **26**, 573–579.

Bruce, T.J.A., Aradottir, G.I., Smart, L.E., Martin, J.L., Caulfield, J.C., Doherty, A., Sparks, C.A. *et al.* (2015) The first crop plant genetically engineered to release an insect pheromone for defence. *Sci. Rep.* **5**, 11183.

Bruce, T.J. and Pickett, J.A. (2011) Perception of plant volatile blends by herbivorous insects–finding the right mix. *Phytochemistry*, **72**, 1605–1611.

Buchman, A., Marshall, J.M., Ostrovski, D., Yang, T. and Akbari, O.S. (2018) Synthetically engineered Medea gene drive system in the worldwide crop pest *Drosophila suzukii*. *Proc. Natl. Acad. Sci. USA*, **115**, 4725–4730.

Burke, W.G., Kaplanoglu, E., Kolotilin, I., Menassa, R. and Donly, C. (2019) RNA Interference in the tobacco hornworm, *Manduca sexta*, using plastid-encoded long double-stranded RNA. *Front Plant Sci.*, **10**, 313.

34 Rubén Mateos Fernández *et al.*

Butler, D. (2018) Scientists hail European ban on bee-harming pesticides. *Nature*. https://doi.org/10.1038/d41586-018-04987-4

Callaway, E. (2018) UN treaty agrees to limit gene drives but rejects a moratorium. *Nature*. https://doi.org/10.1038/d41586-018-07600-w

Carrière, Y., Crickmore, N. and Tabashnik, B.E. (2015) Optimizing pyramided transgenic Bt crops for sustainable pest management. *Nat. Biotechnol.* **33**, 161–168.

Castañera, P., Farinós, G.P., Ortego, F. and Andow, D.A. (2016) Sixteen years of Bt maize in the EU hotspot: why has resistance not evolved? *PLoS ONE*, **11**, 1–13.

Champer, J., Buchman, A. and Akbari, O.S. (2016) Cheating evolution: Engineering gene drives to manipulate the fate of wild populations. *Nat. Rev. Genet*, **17**, 146–159.

Christiaens, O., Petek, M., Smagghe, G. and Taning, C.N.T. (2020b) The use of nanocarriers to improve the efficiency of RNAi-Based pesticides in agriculture. In *Nanopesticides - From Research and Development to Mechanisms of Action and Sustainable Use in Agriculture*, (Fraceto, L. F., De Castro, V. L. S., Grillo, R., Ávila, D., Oliveira, H. C. and Lima, R., eds), pp. 49–68. Cham: Springer Nature. https://doi.org/10.1007/978-3-030-44873-8

Christiaens, O., Whyard, S., Vélez, A.M. and Smagghe, G. (2020a) Double-stranded RNA technology to control insect pests: current status and challenges. *Front. Plant Sci.* **11**, 1–10.

Constable, F. and Bertaccini, A. (2017) Worldwide distribution and identification of grapevine yellows diseases. In *Grapevine Yellows Diseases and Their Phytoplasma Agents*, (Dermastia, M., Bertaccini, A., Constable, F. and Mehle, N., eds), pp. 17–46. Cham: Springer.

Court of Justice of the European Union (2018a) *Press Release No 04/18. Advocate General's Opinion in Case C-528/16. According to Advocate General Bobek, organisms obtained by mutagenesis are, in principle, exempted from the obligations in the Genetically Modified Organisms Directive*. https://curia.europa.eu/jcms/upload/docs/application/pdf/2018-01/cp180004en.pdf.

Court of Justice of the European Union (2018b) *Press Release No 111/18. Judgment in Case C-528/16. Organisms obtained by mutagenesis are GMOs and are, in principle, subject to the obligations laid down by the GMO Directive*. https://curia.europa.eu/jcms/upload/docs/application/pdf/2018-07/cp180111en.pdf.

de Crecy, E., Jaronski, S., Lyons, B., Lyons, T. and Keyhani, N. (2009) Directed evolution of a filamentous fungus for thermotolerance. *BMC Biotechnol.* **9**, 74.

Culliney, T.W. (2014) Crop losses to arthropods. In *Integrated Pest Management: Pesticide Problems*, Vol. **3** (Pimentel, D., and Peshin, R., eds), pp. 201–225. Dordrecht, Netherlands: Springer.

Deutsch, C.A., Tewksbury, J.J., Tigchelaar, M., Battisti, D.S., Merrill, S.C., Huey, R.B. and Naylor, R.L. (2018) Increase in crop losses to insect pests in a warming climate. *Science*, **361**, 916–919.

Dhole, S., Vella, M.R., Lloyd, A.L. and Gould, F. (2018) Invasion and migration of spatially self-limiting gene drives: A comparative analysis. *Evol. Appl.*, **11**, 794–808.

Dickens, J.C., Smith, J.W. and Light, D.M. (1993) Green leaf volatiles enhance sex attractant pheromone of the tobacco budworm, *Heliothis virescens* (Lep.: Noctuidae). *Chemoecology*, **4**, 175–177.

Ding, B.J., Hofvander, P., Wang, H.L., Durrett, T.P., Stymne, S. and Löfstedt, C. (2014) A plant factory for moth pheromone production. *Nat. Commun.*, **5**, 1–7.

Dong, Y., Yang, Y., Wang, Z., Wu, M., Fu, J., Guo, J., Chang, L. *et al.* (2020) Inaccessibility to double-stranded RNAs in plastids restricts RNA interference in *Bemisia tabaci* (whitefly). *Pest Manag. Sci.*, **76**, 3168–3176.

Duan, X., Li, X., Xue, Q., Abo-Ei-Saad, M., Xu, D. and Wu, R. (1996) Transgenic rice plants harboring an introduced potato proteinase inhibitor II gene are insect resistant. *Nat. Biotechnol.* **14**, 494–498.

El-Sayed, A.M. (2021) *The Pherobase: Database of Pheromones and Semiochemicals*. https://www.pherobase.com.

Esvelt, K.M., Smidler, A.L., Catteruccia, F. and Church, G.M. (2014) Concerning RNA-guided gene drives for the alteration of wild populations. *Elife*, **3**, 1–21.

Fan, Y., Borovsky, D., Hawkings, C., Ortiz-Urquiza, A. and Keyhani, N.O. (2012) Exploiting host molecules to augment mycoinsecticide virulence. *Nat. Biotechnol.* **30**, 35–37.

Ffrench-Constant, R.H. and Bowen, D.J. (2000) Novel insecticidal toxins from nematode-symbiotic bacteria. *Cell. Mol. Life Sci.* **57**, 828–833.

Fiebig, M., Poehling, H.-M. and Borgemeister, C. (2004) Barley yellow dwarf virus, wheat, and Sitobion avenae: a case of trilateral interactions. *Entomol. Exp. Appl.*, **110**, 11–21.

Fu, G., Condon, K.C., Epton, M.J., Gong, P., Jin, L., Condon, G.C. *et al.* (2007) Female-specific insect lethality engineered using alternative splicing. *Nat. Biotechnol.* **25**, 353–357.

Gantz, V.M., Jasinskiene, N., Tatarenkova, O., Fazekas, A., Macias, V.M., Bier, E. and James, A.A. (2015) Highly efficient Cas9-mediated gene drive for population modification of the malaria vector mosquito *Anopheles stephensi*. *Proc. Natl. Acad. Sci. U. S. A*, **112**, E6736–E6743.

Gao, B.J., Mou, Y.N., Tong, S.M., Ying, S.H. and Feng, M.G. (2020) Subtilisin-like Pr1 proteases marking the evolution of pathogenicity in a wide-spectrum insect-pathogenic fungus. *Virulence*, **11**, 365–380.

Gao, C. (2021) Genome engineering for crop improvement and future agriculture. *Cell*, **184**, 1621–1635.

Ghislain, M., Byarugaba, A.A., Magembe, E., Njoroge, A., Rivera, C., Román, M.L., Tovar, J.C. *et al.* (2019) Stacking three late blight resistance genes from wild species directly into African highland potato varieties confers complete field resistance to local blight races. *Plant Biotechnol. J.* **17**, 1119–1129.

Goggin, F.L., Jia, L., Shah, G., Hebert, S., Williamson, V.M. and Ullman, D.E. (2006) Heterologous expression of the Mi-1.2 gene from tomato confers resistance against nematodes but not aphids in eggplant. *Mol. Plant-Microbe Interact.* **19**, 383–388.

Gregg, P.C., Del Socorro, A.P. and Landolt, P.J. (2018) Advances in attract-and-kill for agricultural pests: beyond pheromones. *Annu. Rev. Entomol.* **7**, 453–470.

Guo, X., Sun, J., Li, D. and Lu, W. (2018) Heterologous biosynthesis of (+)-nootkatone in unconventional yeast *Yarrowia lipolytica*. *Biochem. Eng. J.* **137**, 125–131.

Gutensohn, M., Nguyen, T.T.H., McMahon, R.D., Kaplan, I., Pichersky, E. and Dudareva, N. (2014) Metabolic engineering of monoterpene biosynthesis in tomato fruits via introduction of the non-canonical substrate neryl diphosphate. *Metab. Eng.* **24**, 107–116.

Hagström, Å.K., Wang, H.L., Liénard, M.A., Lassance, J.M., Johansson, T. and Löfstedt, C. (2013) A moth pheromone brewery: production of (Z)-11-hexadecenol by heterologous co-expression of two biosynthetic genes from a noctuid moth in a yeast cell factory. *Microb. Cell Fact.* **12**, 125.

Hammond, A., Galizi, R., Kyrou, K., Simoni, A., Siniscalchi, C., Katsanos, D. *et al.* (2016) A CRISPR-Cas9 gene drive system targeting female reproduction in the malaria mosquito vector *Anopheles gambiae*. *Nat. Biotechnol.* **34**, 78–83.

Hannon, G.J. (2002) RNA interference. *Nature*, **418**, 244–251.

Harrison, R.L. and Bonning, B.C. (2000) Use of scorpion neurotoxins to improve the insecticidal activity of Rachiplusia ou multicapsid nucleopolyhedrovirus. *Biol. Control.* **17**, 191–201.

Harrison, R.L. and Bonning, B.C. (2010) Proteases as insecticidal agents. *Toxins (Basel)*, **2**, 935–953.

Harvey-Samuel, T., Morrison, N.I., Walker, A.S., Marubbi, T., Yao, J., Collins, H.L. *et al.* (2015) Pest control and resistance management through release of insects carrying a male-selecting transgene. *BMC Biol.* **13**, 1–15.

He, W., Xu, W., Xu, L., Fu, K., Guo, W., Bock, R. and Zhang, J. (2020) Length-dependent accumulation of double-stranded RNAs in plastids affects RNA interference efficiency in the Colorado potato beetle. *J. Exp. Bot.* **71**, 2670–2677.

Hilder, V.A., Gatehouse, A.M.R., Sheerman, S.E., Barker, R.F. and Boulter, D. (1987) A novel mechanism of insect resistance engineered into tobacco. *Nature*, **330**, 160–163.

Holkenbrink, C., Ding, B.J., Wang, H.L., Dam, M.I., Petkevicius, K., Kildegaard, K.R. *et al.* (2020) Production of moth sex pheromones for pest control by yeast fermentation. *Metab. Eng.* **62**, 312–321.

Hughes, M.F., Beck, B.D., Chen, Y., Lewis, A.S. and Thomas, D.J. (2011) Arsenic exposure and toxicology: a historical perspective. *Toxicol. Sci*, **123**, 305–332.

Hussain, A. (2018) Reprogramming the virulence: insect defense molecules navigating the epigenetic landscape of metarhizium robertsii. *Virulence*, **9**, 447–449.

International service for the acquisition of agri-biotech applications (ISAAA). (2018). *Brief 54: global status of commercialized biotech/GM crops.* Ithaca, NY: ISAAA. https://www.isaaa.org/resources/publications/briefs/54/

Jin, L., Walker, A.S., Fu, G., Harvey-Samuel, T., Dafa'Aalla, T. and Miles, A. *et al.* (2013) Engineered female-specific lethality for control of pest lepidoptera. *ACS Synth. Biol,* **2**, 160–166.

Jones, M.S., Delborne, J.A., Elsensohn, J., Mitchell, P.D. and Brown, Z.S. (2019) Does the U.S. Public support using gene drives in agriculture? And what do they want to know? *Sci. Adv,* **5**, eaau8462.

Karabörklü, S., Azizoglu, U. and Azizoglu, Z.B. (2018) Recombinant entomopathogenic agents: a review of biotechnological approaches to pest insect control. *World J. Microbiol. Biotechnol,* **34**, 1–12.

Kemp, L., Adam, L., Boehm, C.R., Breitling, R., Casagrande, R., Dando, M., Djikeng, A. *et al.* (2020) Bioengineering horizon scan 2020. *Elife,* **9**, 1–20.

Khajuria, C., Ivashuta, S., Wiggins, E., Flagel, L., Moar, W., Pleau, M., Miller, K. *et al.* (2018) Development and characterization of the first dsRNA-resistant insect population from western corn rootworm, *Diabrotica virgifera virgifera* LeConte. *PLoS ONE,* **13**, 1–19.

Knox, O.G.G., Constable, G.A., Pyke, B. and Gupta, V.V.S.R. (2006) Environmental impact of conventional and Bt insecticidal cotton expressing one and two Cry genes in Australia. *Aust. J. Agric. Res,* **57**, 501–509.

Konrad, O., Micah, S., Vu, B., Keith, W. and Effendi, L. (2017) *Semi-biosynthetic production of fatty alcohols and fatty aldehydes.* Patent No. WO2017214133A2.

Kroemer, J.A., Bonning, B.C. and Harrison, R.L. (2015) Expression, delivery and function of insecticidal proteins expressed by recombinant baculoviruses. *Viruses,* **7**, 422–455.

Kuckertz, A. (2020) Bioeconomy transformation strategies worldwide require stronger focus on entrepreneurship. *Sustain,* **12**, 2911.

Lacey, L.A., Grzywacz, D., Shapiro-Ilan, D.I., Frutos, R., Brownbridge, M. and Goettel, M.S. (2015) Insect pathogens as biological control agents: Back to the future. *J. Invertebr. Pathol.* **132**, 1–41.

Leftwich, P.T., Koukidou, M., Rempoulakis, P., Gong, H.-F., Zacharopoulou, A., Fu, G., Chapman, T. *et al.* (2014) Genetic elimination of field-cage populations of Mediterranean fruit flies. *Proc. R. Soc. B Biol. Sci.,* **281**, 20141372

Leung, K., Ras, E., Ferguson, K.B., Ariëns, S., Babendreier, D., Bijma, P., Bourtzis, K. *et al.* (2020) Next-generation biological control: the need for integrating genetics and genomics. *Biol. Rev.* **95**, 1838–1854.

Lirakis, M. and Magalhães, S. (2019) Does experimental evolution produce better biological control agents? A critical review of the evidence. *Entomol. Exp. Appl.* **167**, 584–597.

Lommen, S.T.E., Koops, K.G., Cornelder, B.A., de Jong, P.W. and Brakefield, P.M. (2019) Genetics and selective breeding of variation in wing truncation in a flightless aphid control agent. *Entomol. Exp. Appl,* **167**, 636–645.

Lorenzo, V., Prather, K.L.J., Chen, G.-Q., O'Day, E., Kameke, C., Oyarzún, D.A., Hosta-Rigau, L. *et al.* (2018) The power of synthetic biology for bioproduction, remediation and pollution control. *EMBO Rep.* **19**, e45658.

Lu, H.P., Luo, T., Fu, H.W., Wang, L., Tan, Y.Y., Huang, J.Z. *et al.* (2018) Resistance of rice to insect pests mediated by suppression of serotonin biosynthesis. *Nat. Plants,* **4**, 338–344.

Luo, M., Xie, L., Chakraborty, S., Wang, A., Matny, O., Jugovich, M. *et al.* (2021) A five-transgene cassette confers broad-spectrum resistance to a fungal rust pathogen in wheat. *Nat. Biotechnol,* **39**, 561–566.

Mao, Y.B., Cai, W.J., Wang, J.W., Hong, G.J., Tao, X.Y., Wang, L.J. *et al.* (2007) Silencing a cotton bollworm P450 monooxygenase gene by plant-mediated RNAi impairs larval tolerance of gossypol. *Nat. Biotechnol.* **25**, 1307–1313.

Maqbool, S.B., Riazuddin, S., Loc, N.T., Gatehouse, A.M.R., Gatehouse, J.A. and Christou, P. (2001) Expression of multiple insecticidal genes confers broad resistance against a range of different rice pests. *Mol. Breed,* **7**, 85–93.

Mat Jalaluddin, N.S., Othman, R.Y. and Harikrishna, J.A. (2019) Global trends in research and commercialization of exogenous and endogenous RNAi technologies for crops. *Crit. Rev. Biotechnol.,* **39**, 67–78.

Mateos-Fernández, R., Moreno-Giménez, E., Gianoglio, S., Quijano-Rubio, A., Gavaldá-García, J., Estellés, L. *et al.* (2021) Production of volatile moth sex pheromones in transgenic *Nicotiana benthamiana* plants. *bioRxiv.* https://doi.org/10.1101/2021.03.31.437903

Mihale, M.J., Deng, A.L., Selemani, H.O., Mugisha-Kamatenesi, M., Kidukuli, A.W. and Ogendo, J.O. (2009) Use of indigenous knowledge in the management of field and storage pests around Lake Victoria basin in Tanzania. *African J. Environ. Sci. Technol.,* **3**, 251–259.

Moto, K., Yoshiga, T., Yamamoto, M., Takahashi, S., Okano, K., Ando, T., Nakata, T. and *et al.* (2003) Pheromone gland-specific fatty-acyl reductase of the silk moth, *Bombyx mori. Proc. Natl. Acad. Sci. USA,* **100**, 9156–9161.

Mou, Y.N., Gao, B.J., Ren, K., Tong, S.M., Ying, S.H. and Feng, M.G. (2020) P-type Na+/K+ ATPases essential and nonessential for cellular homeostasis and insect pathogenicity of *Beauveria bassiana. Virulence,* **11**, 1415–1431.

Mysore, K., Hapairai, L.K., Wei, N., Realey, J.S., Scheel, N.D., Severson, D.W. and Duman-Scheel, M. (2019) Preparation and use of a yeast shRNA delivery system for gene silencing in mosquito larvae. *Methods Mol. Biol.* **1858**, 213–231.

Naegeli, H., Bresson, J.L., Dalmay, T., Dewhurst, I.C., Epstein, M.M., Firbank, L.G. *et al.* (2020) Applicability of the EFSA Opinion on site-directed nucleases type 3 for the safety assessment of plants developed using site-directed nucleases type 1 and 2 and oligonucleotide-directed mutagenesis. *EFSA J.* **18**, 6299.

Nešněrová, P., Šebek, P., Macek, T. and Svatoš, A. (2004) First semi-synthetic preparation of sex pheromones. *Green Chem.* **6**, 305–307.

Nishida, R. (2014) Chemical ecology of insect–plant interactions: ecological significance of plant secondary metabolites. *Biosci. Biotechnol. Biochem.* **78**, 1–13.

Noble, C., Min, J., Olejarz, J., Buchthal, J., Chavez, A., Smidler, A.L. *et al.* (2019) Daisy-chain gene drives for the alteration of local populations. *Proc. Natl. Acad. Sci. U. S. A,* **116**, 8275–8282.

Oerke, E.C. and Dehne, H.W. (2004) Safeguarding production - Losses in major crops and the role of crop protection. *Crop Prot.* **23**, 275–285.

Ortiz, R., Geleta, M., Gustafsson, C., Lager, I., Hofvander, P., Löfstedt, C. *et al.* (2020) Oil crops for the future. *Curr. Opin. Plant Biol.,* **56**, 181–189.

Outchkourov, N.S., Rogelj, B., Strukelj, B. and Jongsma, M.A. (2003) Expression of sea anemone equistatin in potato. effects of plant proteases on heterologous protein production. *Plant Physiol.* **133**, 379–390.

Palma, L., Muñoz, D., Berry, C., Murillo, J., Caballero, P. and Caballero, P. (2014) Bacillus thuringiensis toxins: an overview of their biocidal activity. *Toxins (Basel),* **6**, 3296–3325.

Panagiotis, I. and Bourtzis, K. (2007) Insect symbionts and applications: The paradigm of cytoplasmic incompatibility-inducing Wolbachia. *Bull. Entomol. Res.* **37**, 125–138.

Paul, S. and Das, S. (2021) Natural insecticidal proteins, the promising bio-control compounds for future crop protection. *Nucleus,* **64**, 7–20.

Pavela, R. (2016) History, presence and perspective of using plant extracts as commercial botanical insecticides and farm products for protection against insects - A review. *Plant Prot. Sci.* **52**, 229–241.

Pellé, S. and Reber, B. (2015) Responsible innovation in the light of moral responsibility. *J. Chain Netw. Sci.* **15**, 107–117.

Petkevicius, K., Löfstedt, C. and Borodina, I. (2020) Insect sex pheromone production in yeasts and plants. *Curr. Opin. Biotechnol.* **65**, 259–267.

Rizvi, S.A.H., George, J., Reddy, G.V.P., Zeng, X. and Guerrero, A. (2021) Latest developments in insect sex pheromone research and its application in agricultural pest management. *Insects,* **12**, 484.

Rodrigues, T.B. and Petrick, J.S. (2020) Safety considerations for humans and other vertebrates regarding agricultural uses of externally applied RNA molecules. *Front. Plant Sci.* **11**, 1–12.

Rossi, M., Goggin, F.L., Milligan, S.B., Kaloshian, I., Ullman, D.E. and Williamson, V.M. (1998) The nematode resistance gene Mi of tomato confers resistance against the potato aphid. *Proc. Natl. Acad. Sci. USA,* **95**, 9750–9754.

Sayer, J., Margules, C. and McNeely, J.A. (2021) People and biodiversity in the 21st century. *Ambio,* **50**, 970–975.

Schellenberger, U., Oral, J., Rosen, B.A., Wei, J.-Z., Zhu, G., Xie, W., McDonald, M.J. *et al.* (2016) A selective insecticidal protein from Pseudomonas for controlling corn rootworms. *Science,* **354**, 634–637.

Scott, M.J., Concha, C., Welch, J.B., Phillips, P.L. and Skoda, S.R. (2017) Review of research advances in the screwworm eradication program over the past 25 years. *Entomol. Exp. Appl.* **164**, 226–236.

Semenova, T.A., Dunaevsky, Y.E., Beljakova, G.A. and Belozersky, M.A. (2020) Extracellular peptidases of insect-associated fungi and their possible use in biological control programs and as pathogenicity markers. *Fungal Biol.* **124**, 65–72.

36 Rubén Mateos Fernández *et al.*

Shaffer, L. (2020) RNA-based pesticides aim to get around resistance problems. *Proc. Natl. Acad. Sci. USA*, **117**, 32823–32826.

Shelton, A.M., Long, S.J., Walker, A.S., Bolton, M., Collins, H.L., Revuelta, L., Johnson, L.M. and *et al.* (2020) First field release of a genetically engineered, self-limiting agricultural pest insect: evaluating its potential for future crop protection. *Front. Bioeng. Biotechnol.* **7**, 1–15.

Shera, P.S., Kumar, V. and Jindal, V. (2020) Sucking pests of cotton. In *Sucking Pests of Crops*, (Omkar, ed), pp. 249–284. Singapore: Springer.

Sinkins, S.P. and Gould, F. (2006) Gene drive systems for insect disease vectors. *Nat. Rev. Genet*, **7**, 427–435.

Šmid, I., Gruden, K., Buh Gašparič, M., Koruza, K., Petek, M., Pohleven, J. *et al.* (2013) Inhibition of the growth of Colorado potato beetle larvae by macrocypins, protease inhibitors from the parasol mushroom. *J. Agric. Food Chem.* **61**, 12499–12509.

St. Leger, R.J., Joshi, L., Bidochka, M.J. and Roberts, D.W. (1996) Construction of an improved mycoinsecticide overexpressing a toxic protease. *Proc. Natl. Acad. Sci. USA*, **93**, 6349–6354.

Stoger, E., Williams, S., Christou, P., Down, R.E. and Gatehouse, J.A. (1999) Expression of the insecticidal lectin from snowdrop (Galanthus nivalis agglutinin; GNA) in transgenic wheat plants: Effects on predation by the grain aphid *Sitobion avenae. Mol. Breed*, **5**, 65–73.

Sun, Y., Huang, X., Ning, Y., Jing, W., Bruce, T.J.A., Qi, F. *et al.* (2017) TPS46, a rice terpene synthase conferring natural resistance to bird cherry-oat aphid, *Rhopalosiphum padi* (Linnaeus). *Front. Plant Sci.* **08**, 110.

Tabashnik, B.E. and Carrière, Y. (2017) Surge in insect resistance to transgenic crops and prospects for sustainability. *Nat. Biotechnol.* **35**, 926–935.

Thomas, D.D., Donnelly, C.A., Wood, R.J. and Alphey, L.S. (2000) Insect population control using a dominant, repressible, lethal genetic system. *Science*, **287**, 2474–2476.

Vos, P., Simons, G., Jesse, T., Wijbrandi, J., Heinen, L., Hogers, R. *et al.* (1998) The tomato Mi-1 gene confers resistance to both root-knot nematodes and potato aphids. *Nat. Biotechnol.* **16**, 1365–1369.

Waltz, E. (2018) With a free pass, CRISPR-edited plants reach market in record time. *Nat. Biotechnol.* **36**, 6–7.

Wang, C. and St Leger, R.J. (2007) A scorpion neurotoxin increases the potency of a fungal insecticide. *Nat. Biotechnol*, **25**, 1455–1456.

Wang, Z., Zhang, K., Sun, X., Tang, K. and Zhang, J. (2005) Enhancement of resistance to aphids by introducing the snowdrop lectin gene gna into maize plants. *J. Biosci.* **30**, 627–638.

Wei, J. and Kang, L. (2011) Roles of (Z)-3-hexenol in plant-insect interactions. *Plant Signal. Behav.* **6**, 369–371.

Wilson, L.J., Whitehouse, M.E.A. and Herron, G.A. (2018) The management of insect pests in Australian cotton: An evolving story. *Annu. Rev. Entomol.* **63**, 215–237.

Windbichler, N., Menichelli, M., Papathanos, P.A., Thyme, S.B., Li, H., Ulge, U.Y., Hovde, B.T. *et al.* (2011) A synthetic homing endonuclease-based gene drive system in the human malaria mosquito. *Nature*, **473**, 212–215.

Xia, J., Guo, Z., Yang, Z., Han, H., Wang, S., Xu, H. *et al.* (2021) Whitefly hijacks a plant detoxification gene that neutralizes plant toxins. *Cell*, **184**, 1693–1705.e17.

Xia, Y.H., Ding, B.J., Wang, H.L., Hofvander, P., Jarl-Sunesson, C. and Löfstedt, C. (2020) Production of moth sex pheromone precursors in Nicotiana spp.: a worthwhile new approach to pest control. *J. Pest Sci.* **93**, 1333–1346.

Xu, H., Li, W., Schilmiller, A.L., van Eekelen, H., de Vos, R.C.H., Jongsma, M.A. and Pichersky, E. (2019) Pyrethric acid of natural pyrethrin insecticide: complete pathway elucidation and reconstitution in Nicotiana benthamiana. *New Phytol.* **223**, 751–765.

Yang, D., Park, S.Y., Park, Y.S., Eun, H. and Lee, S.Y. (2020) Metabolic engineering of *Escherichia coli* for natural product biosynthesis. *Trends Biotechnol.* **38**, 745–765.

Yang, L., Keyhani, N.O., Tang, G., Tian, C., Lu, R., Wang, X., Pei, Y. and *et al.* (2014a) Expression of a toll signaling regulator serpin in a mycoinsecticide for increased virulence. *Appl. Environ. Microbiol.* **80**, 4531–4539.

Yang, S., Pyati, P., Fitches, E. and Gatehouse, J.A. (2014b) A recombinant fusion protein containing a spider toxin specific for the insect voltage-gated sodium ion channel shows oral toxicity towards insects of different orders. *Insect Biochem. Mol. Biol.* **47**, 1–11.

Yu, X., Zhang, Y., Ma, Y., Zu, Z., Wang, G. and Xia, L. (2013) Expression of an (E)-β-farnesene synthase gene from Asian peppermint in tobacco affected aphid infestation. *Crop J.* **1**, 50–60.

Zabalou, S., Riegler, M., Theodorakopoulou, M., Stauffer, C., Savakis, C. and Bourtzis, K. (2004) Wolbachia-induced cytoplasmic incompatibility as a means for insect pest population control. *Proc. Natl. Acad. Sci. USA*, **101**, 15042–15045.

Zhang, D., Hussain, A., Manghwar, H., Xie, K., Xie, S., Zhao, S. *et al.* (2020) Genome editing with the CRISPR-Cas system: an art, ethics and global regulatory perspective. *Plant Biotechnol. J.* **18**, 1651–1669.

Zhang, J., Khan, S.A., Hasse, C., Ruf, S., Heckel, D.G. and Bock, R. (2015) Pest control. Full crop protection from an insect pest by expression of long double-stranded RNAs in plastids. *Science*, **347**, 991–994.

Zhang, Y., Bian, S., Liu, X., Fang, N., Wang, C., Liu, Y. *et al.* (2021) Synthesis of cembratriene-ol and cembratriene-diol in yeast via the MVA pathway. *Microb. Cell Fact.* **20**, 29.

Zhao, J.Z., Cao, J., Li, Y., Collins, H.L., Roush, R.T., Earle, E.D. and Shelton, A.M. (2003) Transgenic plants expressing two Bacillus thuringiensis toxins delay insect resistance evolution. *Nat. Biotechnol.* **21**, 1493–1497.

2.2 Production of Volatile Moth Sex Pheromones in Transgenic *Nicotiana benthamiana* Plants

Rubén Mateos-Fernández, Elena Moreno-Giménez, Silvia Gianoglio, Alfredo Quijano-Rubio, Jose Gavaldá-García, Lucía Estellés, Alba Rubert, José Luis Rambla, Marta Vazquez-Vilar, Estefanía Huet, Asunción Fernández-del-Carmen, Ana Espinoza-Ruiz, Mojca Juteršek, Sandra Vacas, Ismael Navarro, Vicente Navarro-Llopis, Jaime Primo, and Diego Orzáez

This article describes the development of transgenic *N. benthamiana* plants with constitutive expression of three transgenes, resulting in the production of three moth sex pheromone compounds: (*Z*)-11-hexadecenol, (*Z*)-11-hexadecenal, and (*Z*)-11-hexadecenyl acetate. The first generation of plants had a severe dwarf phenotype in homozygous high-producing lines. Analysis of transgene expression also revealed truncation of the acetyltransferase transgene, resulting in a non-functional enzyme and low levels of (*Z*)-11-hexadecenyl acetate production. Therefore, a new generation of plants was created, with alleviated growth penalty and improved production of all three pheromone compounds. This work is the first to report a stable transgenic plant line producing three different sex pheromone compounds, which were also emitted from the plant tissue. However, the release was much lower than needed for the plants to act as biological dispensers. Apart from low volatility, growth penalty was exposed as one of the main obstacles for moth pheromone production in plants.

The PhD candidate contributed to this work with transgene expression quantification, which also revealed truncation of the acetyltransferase transgene in the first generation of transgenic plants. Based on the results, a new generation of plants with a new insertion event was prepared.

Research Article

Production of Volatile Moth Sex Pheromones in Transgenic *Nicotiana benthamiana* Plants

Rubén Mateos-Fernández [iD],[1] **Elena Moreno-Giménez,**[1] **Silvia Gianoglio** [iD],[1]
Alfredo Quijano-Rubio [iD],[1] **Jose Gavaldá-García** [iD],[1] **Lucía Estellés** [iD],[1] **Alba Rubert,**[1]
José Luis Rambla,[1,2] **Marta Vazquez-Vilar** [iD],[1] **Estefanía Huet,**[1]
Asunción Fernández-del-Carmen,[1] **Ana Espinosa-Ruiz,**[1] **Mojca Juteršek,**[3,4] **Sandra Vacas,**[5]
Ismael Navarro,[6] **Vicente Navarro-Llopis,**[5] **Jaime Primo** [iD],[5] **and Diego Orzáez** [iD][1]

[1]*Institute for Plant Molecular and Cell Biology (IBMCP), Consejo Superior de Investigaciones Científicas (CSIC) - Universidad Politécnica de Valencia (UPV), Valencia, Spain*
[2]*Jaume I University, Castellon de la Plana, Spain*
[3]*Department of Biotechnology and Systems Biology, National Institute of Biology, Ljubljana, Slovenia*
[4]*Jožef Stefan International Postgraduate School, Ljubljana, Slovenia*
[5]*Centro de Ecología Química Agrícola, Instituto Agroforestal del Mediterráneo, Universitat Politècnica de València, Valencia, Spain*
[6]*Ecología Y Protección Agrícola SL, Valencia, Spain*

Correspondence should be addressed to Diego Orzáez; dorzaez@ibmcp.upv.es

Rubén Mateos-Fernández and Elena Moreno-Giménez contributed equally to this work.

Plant-based bioproduction of insect sex pheromones has been proposed as an innovative strategy to increase the sustainability of pest control in agriculture. Here, we describe the engineering of transgenic plants producing *(Z)*-11-hexadecenol (Z11-16OH) and *(Z)*-11-hexadecenyl acetate (Z11-16OAc), two main volatile components in many Lepidoptera sex pheromone blends. We assembled multigene DNA constructs encoding the pheromone biosynthetic pathway and stably transformed them into *Nicotiana benthamiana* plants. The constructs contained the *Amyelois transitella AtrΔ11* desaturase gene, the *Helicoverpa armigera* fatty acyl reductase *HarFAR* gene, and the *Euonymus alatus* diacylglycerol acetyltransferase *EaDAct* gene in different configurations. All the pheromone-producing plants showed dwarf phenotypes, the severity of which correlated with pheromone levels. All but one of the recovered lines produced high levels of Z11-16OH, but very low levels of Z11-16OAc, probably as a result of recurrent truncations at the level of the *EaDAct* gene. Only one plant line (SxPv1.2) was recovered that harboured an intact pheromone pathway and which produced moderate levels of Z11-16OAc (11.8 μg g^{-1} FW) and high levels of Z11-16OH (111.4 μg g^{-1}). Z11-16OAc production was accompanied in SxPv1.2 by a partial recovery of the dwarf phenotype. SxPv1.2 was used to estimate the rates of volatile pheromone release, which resulted in 8.48 ng g^{-1} FW per day for Z11-16OH and 9.44 ng g^{-1} FW per day for Z11-16OAc. Our results suggest that pheromone release acts as a limiting factor in pheromone biodispenser strategies and establish a roadmap for biotechnological improvements.

1. Introduction

Insect pheromones are a sustainable alternative to broad-spectrum pesticides in pest control. Different pheromone-based pest management approaches can be employed to contain herbivore populations, thus limiting damage to food, feed, industrial crops, and stored goods. These approaches include multiple strategies, such as (i) attract-and-kill strategies, in which pheromones are used to lure insects into mass traps; (ii) push-pull strategies, in which different stimuli are

used to divert herbivores from crops to alternative hosts; and (iii) mating disruption techniques in which mating is prevented or delayed by providing males with misleading pheromone cues [1–4]. Broad-spectrum pesticides cause severe toxicity not only towards the targeted insect population but also towards predatory insects resulting in substantial ecological imbalances [5]. On the contrary, insect sex pheromones usually produced by females to attract males over long distances are highly species-specific and minimize environmental toxicity. Furthermore, pheromone-based pest control approaches are effective against pesticide-resistant insect populations and prevent the emergence of genetic pesticide resistance.

The global insect pheromone market was worth 1.9 billion USD in 2017, with projections reaching over 6 billion USD by 2025 [6]. Despite their biological potential and their value to farmers and the environment, their use suffers from some limitations: the chemical synthesis of insect sex pheromones can often be costly and complex and generate polluting by-products, which hamper their sustainability [7, 8]. The cost of chemically synthesized pheromones ranges from 500 to thousands USD kg^{-1}, making this solution profitable only for very high-value end products [9]. To make pheromone production more sustainable, engineered biological systems can be designed to function as pheromone biofactories from which the molecule(s) of interest can be purified to formulate conventional traps [10]. Ideally, live biodispensers can be envisioned, which directly release pheromones into the environment in an autonomous, self-sustained manner [11].

Around 160,000 lepidopteran species and 700 lepidopteran pheromones are known [12–14]. Many of these moths are relevant for agriculture and rely heavily on pheromones for mating. Lepidopteran sex pheromones have been the focus of many attempts at biotechnological production, because of their relatively simple chemical composition and their economic relevance. Sex pheromones emitted by female moths are composed of a discrete blend of volatile compounds, mostly C10-C18 straight chain primary alcohols, aldehydes, or acetates derived from palmitic and stearic acids [15]. Although hundreds of species share the same pheromone compounds, the components of the pheromone blend and their relative abundance constitute highly precise, species-specific cues for mating. The biosynthesis of many moth pheromones shares three fundamental steps, which follow fatty acid biosynthesis. Fatty acid desaturases (FADs) introduce double bonds at specific positions in the carbon chain (the most common in Lepidoptera are $\Delta 9$ and $\Delta 11$). Fatty acyl reductases (FARs) produce fatty alcohols, with different substrate specificities (some accept only a limited range of substrates, while others are more promiscuous). Finally, aldehydes and acetates can be obtained, respectively, by oxidation and esterification of these fatty alcohols. In addition, other important modifications can occur before specification of terminal functional groups, especially chain elongation or shortening which, coupled with the desaturation steps, determine the structure of the carbon backbone [15]. The biosynthesis of the acetate esters is thought to be performed by acetyltransferases, although no insect acetyl-

transferases have been identified which work on fatty alcohols [9]. Acetyltransferases from other sources, like plants and yeasts, have nonetheless been discovered, which work efficiently on insect pheromone alcohols [16].

Plants represent an alluring platform to produce moth sex pheromones: the scalability and relatively low costs and infrastructure requirements of plant biofactories make this system versatile and sustainable. In plants, photosynthesis provides the precursors to start fatty acid biosynthesis in the chloroplast. In a pioneering study, Nešněrová et al. [17], took advantage for the first time of the plant fatty acid pool to produce lepidopteran pheromone precursors in plants. Later, in the most extensive screening of candidate genes so far, Ding et al. [18] identified the most effective among 50 different gene combinations to produce moth pheromones by transient expression in *N. benthamiana*. Subsequently, Xia et al. [19] established stably transformed *N. benthamiana* and *N. tabacum* lines expressing precursors for the synthesis of a wide range of moth pheromones. However, to date, no stable transgenic plants have been reported producing the actual volatile pheromone components.

In this work, we aimed to test the ability of *N. benthamiana* plants to act as constitutive moth pheromone biofactories. *Nicotiana* species (*N. tabacum* and *N. benthamiana*) are ideal chassis for metabolic engineering, due to their large leaf biomass (especially for plastid-derived products) and amenability to genetic manipulation, both through stable transformation and agroinfiltration. For stable pheromone production, we selected three of the genes identified by Ding et al. [18], namely, the *Amyelois transitella AtrΔ11* desaturase, the *Helicoverpa armigera* reductase *HarFAR*, and the plant diacylglycerol acetyltransferase *EaDAct* from the bush *Euonymus alatus*. The products of this pathway, *(Z)*-11-hexadecenol (Z11-16OH) and its ester *(Z)*-11-hexadecenyl acetate (Z11-16OAc), are components of the specific pheromone blends of almost 300 lepidopteran species [13]. The generation of transgenic pheromone-producing plants (originally named as "Sexy Plants", SxP) turned out to be severely hampered by a strong growth penalty putatively imposed by the pheromone biosynthetic pathway. In the first round of attempts, only *N. benthamiana* plants accumulating the fatty alcohol were recovered, with all primary transformants showing dwarf phenotypes to different degrees. These transgenic lines were later shown to carry a truncated version of the *EaDAct* gene. This discovery led to the generation of new transformants, with new strategies aimed at ensuring the integrity of the construct that finally yielded a single transgenic line accumulating both the alcohol and the acetate components at relatively high levels, while maintaining acceptable levels of fertility and biomass production. This single line allowed us to gain insights into the challenges associated with fatty-acid derived pheromone production in plants, such as yield-associated growth penalties, changes in volatile profile, and compound volatility.

2. Results

2.1. Assembly of the Metabolic Pathway. To assess plant-based production of the target moth sex pheromone

compounds (Z11-16OH and Z11-16OAc), a T-DNA construct encoding the three biosynthetic genes, each under the control of the constitutive CaMV35S promoter, was agroinfiltrated in plant leaves after being mixed in a 1 : 1 ratio with an *Agrobacterium* culture carrying the P19 silencing suppressor [20] (Figure 1(a)). The total volatile organic compound (VOC) composition was analyzed at 5 days postinfiltration by gas chromatography/mass spectrometry (GC/MS). GC peaks corresponding to the pheromone compounds Z11-16OH and Z11-16OAc were detected in samples transformed with all three enzymes, but not with P19 alone (Figure 1(b)). Moreover, both substances were among the most predominant compounds in the leaf volatile profile, indicating that the transgenes were expressed at high levels. Interestingly, a small peak identified as *(Z)*-11-hexadecenal (Z11-16Ald) was also detected in the agroinfiltrated samples, likely due to the endogenous activity of alcohol oxidases, as previously suggested by Hagström et al. [21]. This aldehyde is itself a component of the pheromone blends of around 200 lepidopteran species [13]. Based on these results, a multigene construct (GB1491) for stable transformation of *N. benthamiana* plants was assembled. This construct comprised the three constitutively expressed enzymes, the kanamycin resistance gene *NptII*, and the visual selection marker *DsRed* (Figure 1(c)). Plants resulting from this transformation were denoted as the first version of the pheromone-producing plant (SxPv1.0).

2.2. SxPv1.0 Stable Transformants. The transformation of *N. benthamiana* with the GB1491 construct resulted in the selection of 11 kanamycin-resistant shoots, which also showed red fluorescence resulting from the expression of *DsRed* (T_0 generation SxPv1.0 plants). These shoots were further grown and rooted, and leaf samples were collected at the early flowering stage to assess pheromone production. As observed in Figure 1(d), several T_0 plants presented detectable levels of all three pheromone compounds in variable amounts. The relative abundance of all three pheromone compounds was consistent in each plant, despite Z11-16OAc levels being much lower than expected in all cases compared to transient pheromone expression. Furthermore, although phenotypic evaluation of *N. benthamiana* T_0 lines is generally cumbersome due to the influence of *in vitro* culture, severe growth penalties were observed in these plants, and only 5 out of 11 plants (SxPv1.0_4, 5, 7, 8, and 9) survived long enough to produce seeds.

To further understand the phenotypic effects of pheromone production, the progeny of plants SxPv1.0_4, SxPv1.0_5, and SxPv1.0_7 was analyzed up to the T_3 generation and the plant size and pheromone production levels were recorded for each individual. In the T_1 generation, growth penalties were also observed in most descendants for all three lines, generally associated with high pheromone production (Figures 2(a) and 2(b), A). Several plants could not be phenotyped, as they died soon after germination. Those producing enough seeds were brought to T_2, where a similar trend was also observed (Figure 2(b), B). A few T_2 plants clearly separated from the rest in terms of high Z11-16OH production, which was again associated with small size and reduced fertility. Neither T_1 nor T_2 plants showed signs of recovery in Z11-16OAc levels, although

the corresponding GC/MS peak remained detectable and above the wild type (WT) baseline (not shown). At this stage, we decided to reevaluate the integrity of the T-DNA in T_2 plants, finding that DNA rearrangements had occurred in all three lines in the *EaDAct* coding sequence, resulting in a truncated gene. Rearrangements and truncations of the T-DNA are not uncommon events in stable plant transformation [22, 23]. Interestingly, at least two independent truncation events could be inferred from PCR analysis of gDNA and cDNA samples. In SxPv1.0_7_4 plants, the presence of *a* ~700 bp insertion of a DNA fragment of plasmid origin could be identified at the 3′ end of the *EaDAct* coding sequence. In contrast, the same 700 bp genomic PCR fragment could not be recovered from the offspring of SxPv1.0_4_2, SxPv1.0_5_1, and SxPv1.0_5_2 plants, which nevertheless also had a truncated ORF, as evidenced by PCR analysis of cDNA samples (Figure S2). Despite the detection of a T-DNA truncation, the analysis of the SxPv1.0 offspring was continued up to T_3 (Figure 2(b), C), where a sharp separation between low and high producers was consolidated. Interestingly, the offspring from the SxPv1.0_5_1_7 homozygous line (100% kanamycin resistant) comprised only high producer plants, whereas heterozygous lines as SxPv1.0_4_2_2 or SxPv1.0_7_4_3 segregated in high and low producers, these correlating with small and large sized individuals, respectively. This observation strongly indicates a drastic effect of transgene copy number on both growth and pheromone production.

2.3. New Stable Transgenic Versions SxPv1.1 and SxPv1.2. The presence of at least two independent truncation events affecting *EaDAct* prompted us to design new transformation strategies by placing a selection marker adjacent to the *EaDAct* gene, ensuring its integrity. Two new DNA constructs were assembled (SxPv1.1 and SxPv1.2) carrying *DsRed* and *NptII* at different relative positions of the T-DNA, as depicted in Figures 3(a) and 3(b). Five SxPv1.1 and eight SxPv1.2 kanamycin-resistant T_0 plants were recovered from each transformation, many of them showing detectable red fluorescence, but unfortunately all but one failed to produce detectable levels of pheromones. The only exception corresponded to plant SxPv1.2_4, which not only showed Z11-16OH and Z11-16Ald amounts comparable to the SxPv1.0 plants but also Z11-16OAc levels close to those measured in transient experiments (Figures 3(c) and 3(d)). SxPv1.2_4 presented premature flowering, a feature that is not unusual in T_0*N. benthamiana* plants and produced viable seeds, giving us the opportunity to further investigate the phenotype of stable Z11-16OAc producers.

For a deeper understanding of the effect of fatty-acid-derived pheromone production in plant homeostasis, a comparative study between the progeny of the T_2 SxPv1.0_5_1_7 homozygous line and the T_0 SxPv1.2_4 line was performed. All analyzed SxPv1.2 T_1 plants (>50) were kanamycin resistant, indicating multiple copy insertions. The relative levels of all three pheromone compounds in leaves at two different developmental stages (young and adult) were recorded for twelve T_1 plants per genotype. Similarly, pheromone content in roots was also measured at the adult stage. Plant size was
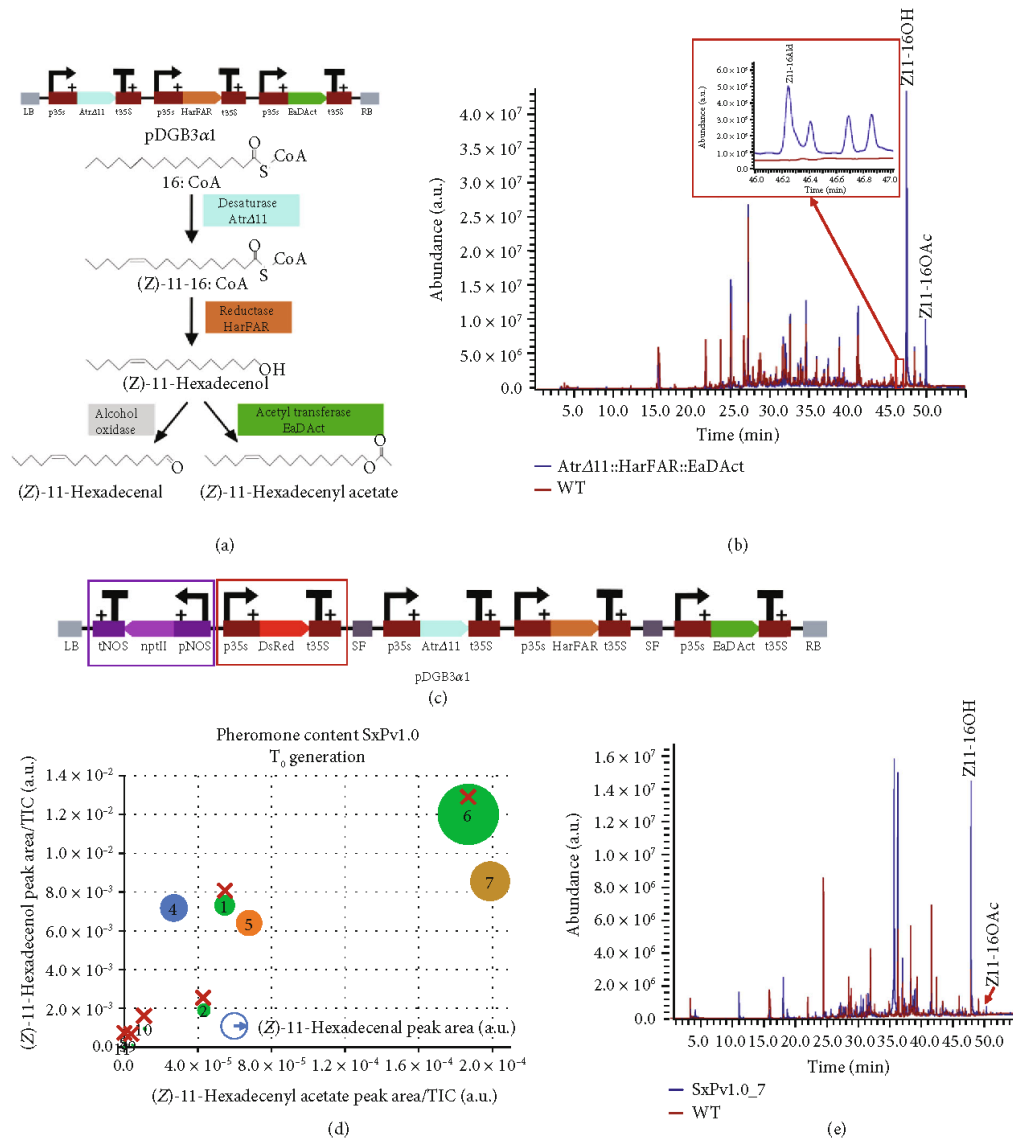
FIGURE 1: Stable and transient expression in *Nicotiana benthamiana* of the synthetic moth pheromone pathway. (a) Schematic view of the T-DNA construct used for transient expression, carrying the three transgenes *AtrΔ11*, *HarFAR*, and *EaDAct*, each under the control of the constitutive CaMV35s promoter and terminator, and the biosynthetic route of the moth pheromones. (b) GC/MS analysis of the volatile profile of *N. benthamiana* transiently expressing the transgenes (blue line) and a mock infiltrated plant with only P19 (red line). Peaks corresponding to the target insect pheromones are indicated with a label. Highlighted in red is the region of the (Z)-11-hexadecenal peak. (c) Schematic view of the T-DNA construct for the SxPv1.0 encoding the three transgenes and two selection markers. The two selection markers DsRed and NptII are highlighted in red and purple, respectively. (d) Pheromone content in SxPv1.0 T_0 plants (numbered from 1 to 11). The diameter of each dot corresponds to the (Z)-11-hexadecenal level of each sample. Plants marked with a red cross died before seeds could be collected. (e) Overlapped chromatograms showing the volatile profile of a representative SxPv1.0 T_0 plant (blue line) and a WT plant (red line).

recorded for all analyzed individuals. As expected, all transgenic plants produced detectable levels of both pheromones, but only in the case of SxPv1.2, Z11-16OAc and Z11-16OH

accumulated at similar levels. In all the SxPv1.2 samples, the higher Z11-16OAc accumulation seems to result in lower precursor alcohol levels, compared with equivalent SxPv1.0
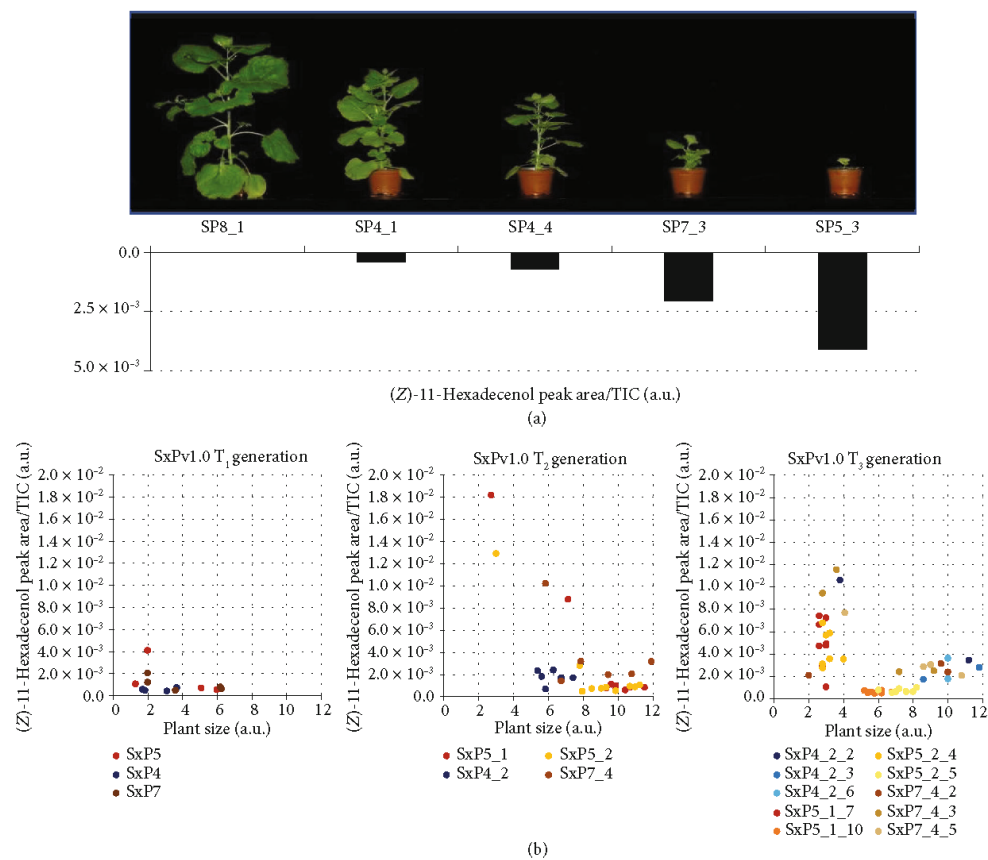
FIGURE 2: Growth penalty linked to pheromone production in SxPv1.0 plants. (a) Representative SxPv1.0 T_1 plants with their corresponding (Z)-11-hexadecenol levels. (b) Correlation between (Z)-11-hexadecenol content (arbitrary units, a.u.) and plant size (a.u.) in all three generations of SxPv1.0.

samples. Both insect pheromones are produced at higher levels in adult plant leaves (Figure 4(b)) when compared with young plant leaves (Figure 4(a)) and roots (Figure 4(c)). All pheromone-producing plants showed considerably reduced plant size; however, the growth penalty was significantly more pronounced in plants accumulating mainly Z11-16OH, whereas the conversion into the acetate form in SxPv1.2 seems to partially relieve the dwarf phenotype. Interestingly, both SxPv1.0 and SxPv1.2 plants showed similar morphology, with short petioles curved upwards and resulting in a compact "cabbage-like" characteristic shape (Figure 4(d)). Both SxP lines showed early senescence symptoms, with premature and progressive yellowing, which led, in the case of SxPv1.0, to the premature death of the plants soon after the fruits set.

2.4. The Plant Volatilome Is Affected by Pheromone Production. A nontargeted analysis of the plant volatile profiles was undertaken to understand the influence of the engi-

neered pheromone pathway on the volatilome. The analysis included leaf samples of 12 young and 12 adult plants from the progeny of SxPv1.0 5_1_7, SxPv1.2_4, and the wild type. The principal component analysis score plot based on the volatile profile showed clustering of the samples based on the different sample classes (Figure 5(a)). The first component accounted mainly for differences in leaf age, whereas the second principal component separated samples according to their genotype. Remarkably, SxPv1.2 samples have, according to both components, intermediate characteristics between the WT and SxPv1.0. The greater separation of SxPv1.0 and the WT probably reflects the more deleterious phenotypic effects experienced by lines accumulating higher Z11-16OH levels.

A clustered heatmap provides interesting visual information on the volatile leaf profiles of SxP plants (Figure 5(b)). The clustering reproduces with few exceptions the different classes, indicating that each genotype and each developmental stage produce a differential and characteristic blend of
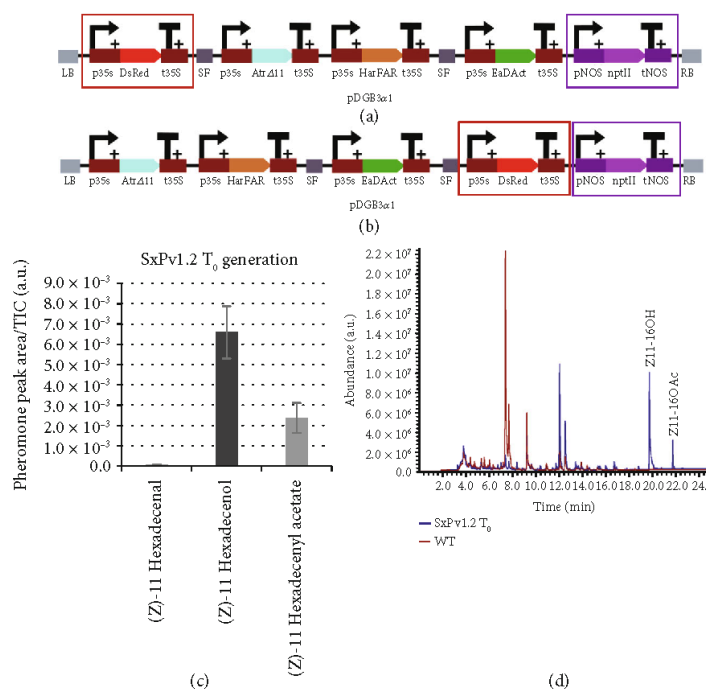
FIGURE 3: SxP version 1.1 and 1.2 stable plants. (a) Schematic representation of the T-DNA construct employed for stable transgenic SxPv1.1. The two selection markers *DsRed* and *NptII* are highlighted in red and purple, respectively. (b) Schematic representation of the T-DNA construct employed for stable transgenic v1.2. The two selection markers *DsRed* and *NptII* are highlighted in red and purple, respectively. (c) Pheromone content in the surviving SxPv1.2 T_0 plant. Error bars represent the average ± SE of 3 independent replicates. (d) Overlapped chromatograms showing the volatile profile of a SxPv1.2 T_0 plant (blue line) and a WT *Nicotiana benthamiana* (red line).

VOCs. In addition to the pheromone compounds themselves, which are clearly clustered in their respective groups, all SxP plants differentially accumulate other fatty-acid-derived volatile compounds (e.g., (*E*)-2-hexenal and 1-pentadecene), indicating a general activation of this metabolic pathway. Some compounds are characteristic of the adult stage, independently of the genotype. This is the case for some apocarotenoids, such as β-damascenone and β-damascone, and some phenylalanine-derived compounds, such as o-cymene and phenylacetaldehyde. Other VOCs, such as monoterpenoids (α-terpineol, linalool, limonene, and ocimenol), are markedly more abundant in WT than in SxP leaf tissues, with a gradient in which SxPv1.2 shows intermediate features between the wild type and the SxPv1.0 genotype. On the other hand, SxPv1.0 plants display a specific subset of volatile compounds (including the sesquiterpene cadalene) that accumulate at increasing levels at the adult stage. Z11-16Ald is detectable in both SxPv1.0 and SxPv1.2, although its levels are higher especially in leaves from adult SxPv1.0 plants, correlating with higher Z11-16OH production. In SxPv1.2 plants, in which Z11-16OH is partially converted to Z11-16OAc, Z11-16Ald is present at lower levels. Z11-16OAc is, instead, clearly restricted to SxPv1.2. The levels of all three pheromones increase with plant age.

2.5. Pheromone Identification and Determination of Its Biological Activity. Samples of Z11-16OH, Z11-16OAc, and Z11-16Ald were synthesized and characterized by GC/MS and nuclear magnetic resonance (NMR) to have analytical standards of the biosynthetic targets. Additionally, to provide unequivocal identification of the plant-made compound, hexane extracts of 120 g of SxPv1.2 leaves were purified by gravity column chromatography after solvent evaporation, and a 2 mg sample of the purest fractions of the biosynthesized alcohol (Z11-16OH) was also analyzed using NMR. The purity assigned by GC/MS was ca. 78% (Figure S3), and the data extracted from the main signals of both ^{1}H and ^{13}C NMR spectra were fully consistent with those obtained for the synthetic sample of Z11-16OH, confirming the structure and the *cis*-configuration of the double bond (Figures S4-S5). Further confirmation of the biological activity was provided by electrophysiological analysis. Hexane extracts of SxPv1.2 leaves were fractionated by column chromatography, and the fractions were analyzed by GC/MS. Those fractions that mainly contained Z11-16OH were gathered and employed in electroantennography (EAG) assays with *Sesamia nonagrioides* male moths. The plant-made pheromone was active, since the EAG probe registered significant antennal depolarizations when Z11-
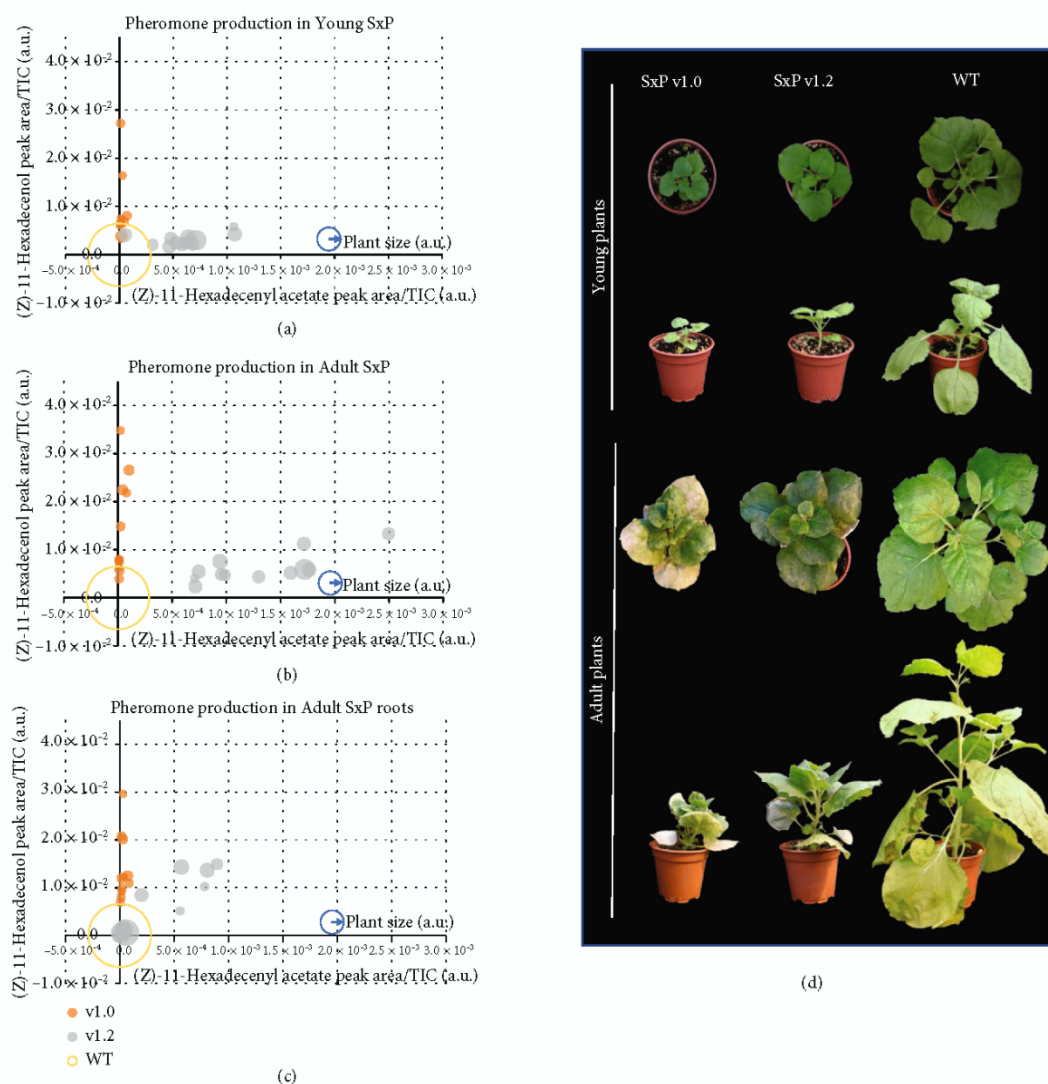
FIGURE 4: Comparative study between SxPv1.0 T_3 and SxPv1.2 T_1 plants. (a) Pheromone content in leaf samples from young plants of WT, SxPv1.0 and SxPv1.2 lines. (b) Pheromone content in leaf samples from adult plants of WT, SxPv1.0 and SxPv1.2 lines. (c) Pheromone content in root samples from adult plants of WT, SxPv1.0 and SxPv1.2 lines. The diameter of each dot corresponds to the plant size of each sample. Empty circles correspond to WT plants. (d) Comparative physiological development in SxPv1.0 5_1_7_X (T_3), SxPv1.2 4_X (T_1), and WT *Nicotiana benthamiana* plants at the young and adult stage. Pictures were taken from representative individuals at young (4 weeks after transplant) and adult (7 weeks after transplant) stages.

16OH reached the antennal preparations (Figure 6; retention time 15.89 min). An unidentified compound with a retention time of 15.54 min also elicited an intense response of the antennae but did correspond neither to Z11-16Ald nor to Z11-16OAc.

2.6. Quantification of Total Pheromone Content and Release. The total pheromone content and the rate of volatile emission were both quantified in SxPv1.2 plants. Solvent extraction was carried out in fresh leaves, as well as in leaves stored at -20°C and -80°C to evaluate the total content and the possible loss of pheromone under different storage conditions (Table 1). The Z11-16OH content in leaves was found to be in the range of $0.1 \, \mathrm{mg \, g^{-1}}$, (average $111.4 \pm 13.7 \, \mu\mathrm{g \, g^{-1}}$), whereas Z11-16OAc accumulated at lower levels (average $11.8 \pm 1.3 \, \mu\mathrm{g \, g^{-1}}$). Both pheromones were preserved in frozen leaves, although a part of Z11-16OH could be lost upon storage, although more
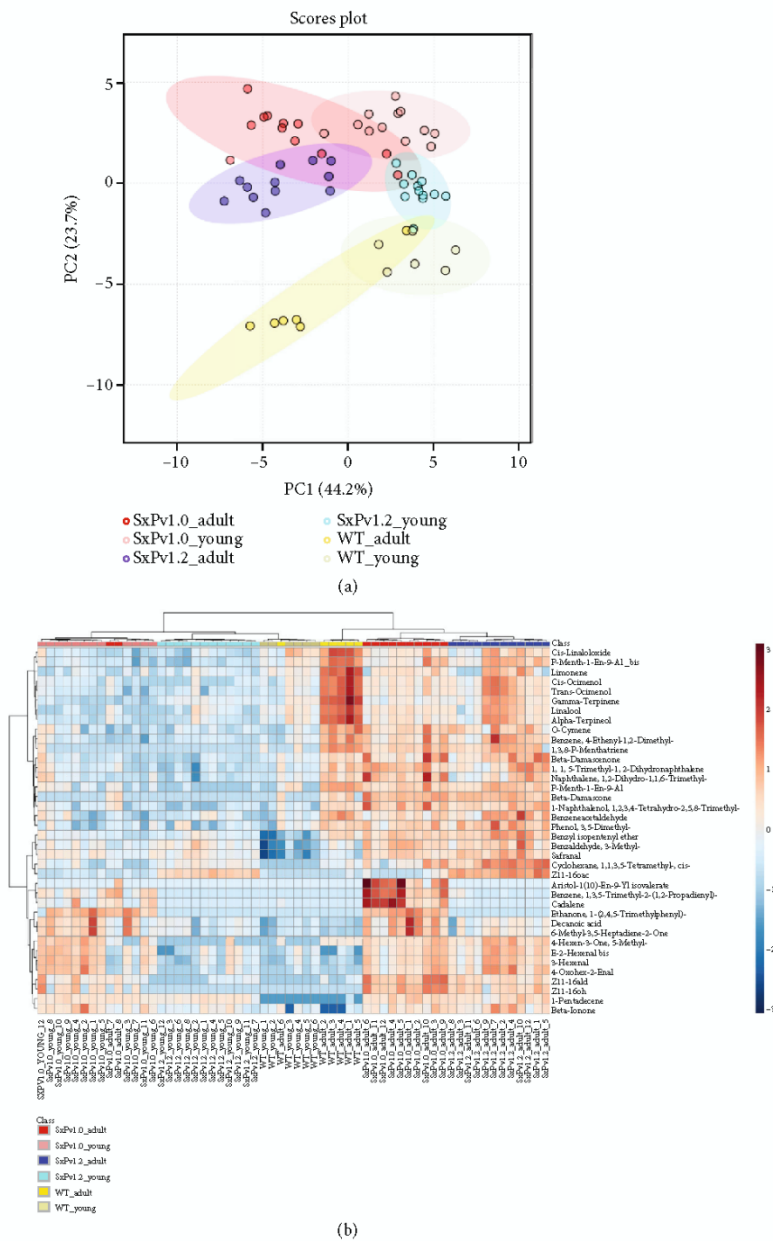
FIGURE 5: Untargeted analysis of the volatilome of SxPv1.0 and SxPv1.2 and of WT *N. benthamiana*. (a) Principal component analysis and (b) hierarchical clustering and heatmap representation (obtained using Ward's minimum variance method and Euclidean distance) of the composition of the volatilome of SxPv1.0, SxPv1.2, and wild-type *N. benthamiana* leaves. Twelve individuals for each SxP genotype and six WT plants were analyzed at two developmental stages, young (4 weeks old) and adult (7 weeks old).

data will be needed to ensure the actual effect of plant handling and storage temperature. Interestingly, the unbalanced ratio between the two main compounds was compensated when the rate at which pheromones are released to the environment was estimated. As shown in Table 2, an adult SxPv1.2 plant releases on average 79.3 $\pm$ 6.3 ng of Z11-16OH and 88.3 $\pm$ 11.5 ng of Z11-16OAc per day, as estimated in volatile collection experiments carried
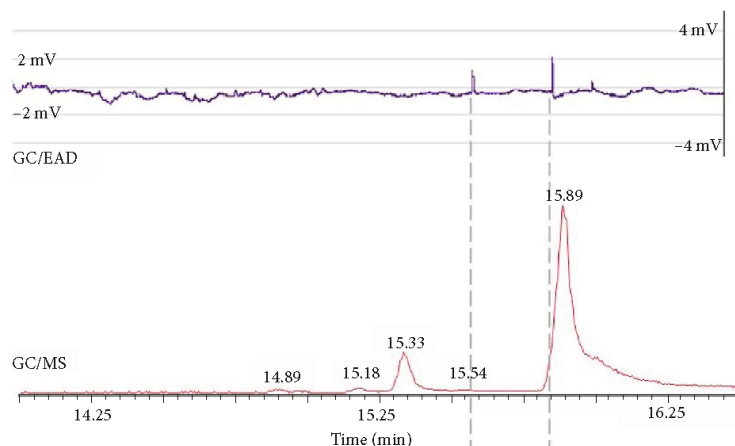
FIGURE 6: Electrophysiological activity. GC/MS chromatogram and EAD recording showing *Sesamia nonagrioides* male antenna response to the biosynthetic Z11-16OH (retention time = 15.89 min). Other compounds contained in the tested fraction were able to interact with the antennal receptors and triggered antennal responses (e.g., retention time 15.54). The GC-MS/EAD run was performed in a GC column ZB-5MS fused silica capillary column (30 m × 0.25 mm i.d.× 0.25 μm; Phenomenex Inc., Torrance, CA).

TABLE 1: Quantity (μg) of (Z)-11-hexadecenol (OH) and (Z)-11-hexadecenyl acetate (OAc) extracted from SxPv1.2 individuals by solvent extraction and GC/MS/MS quantification.

Plant	Material	μg OH/g plant	μg OAc/g plant
SxPv1.2 T$_1$-3	Fresh leaves	164,9	9,6
SxPv1.2 T$_1$-4	Fresh leaves	129,9	8,6
SxPv1.2 T$_1$-5	Frozen -20C	78,1	10,5
SxPv1.2 T$_1$-6	Frozen -20C	115,1	17,3
SxPv1.2 T$_1$-7	Frozen -80C	75,8	11,8
SxPv1.2 T$_1$-8	Frozen -80C	104,8	12,9
Mean ± se		111.4 ± 13.7	11.8 ± 1.3

out in dynamic conditions. Not unexpectedly, this indicates a much higher volatility of the acetylated moiety. In terms of pheromone release per biomass unit, both compounds are emitted at levels close to 0.01 μg day^{-1} g^{-1} (FW).

3. Discussion

This research was initiated as a Synthetic Biology project in the frame of the iGEM competition, where undergraduate students proposed the use of genetically engineered plants as dispensers of insect sex pheromones. The manufacturing of pheromones and their precursors employing biological factories, such as microbial bioreactors [21, 24] or plant biofactories [18, 19, 25] has become an intensively pursued objective, fuelled by the expected gains in sustainability. Beyond the general biofactory concept, our envisioned long-term approach consists of the design of plants that function as autonomous biodispensers of semiochemicals. A remarkable precedent of this concept was the engineering of wheat plants releasing the alarm pheromone *(E)-β*-farne-

sene as a protective strategy against aphid infestation [11]. Differently to the alarm pheromone concept, which was produced in the crop itself, the proposed biodispenser (originally named as "Sexy Plant", SxP) is based on the intercropping strategy, where a companion crop, rather than the main crop, is engineered to emit the sex pheromone into the environment. From here, two different strategies can be followed. In a mating disruption strategy [2, 26, 27], the dispensers release pheromones at relatively large quantities, impairing the male's ability to detect females and therefore disrupting the mating. Oppositely, in mass trapping or attract-and-kill strategies [28], dispensers release pheromones to attract males to traps. This later approach often requires lower pheromone levels to be released into the environment, but in turn requires higher semiochemical specificity (in terms of isomeric purity and exact ratios of the pheromone components), and also some associated equipment to trap and eventually kill the attracted insects.

The genetic engineering of *N. benthamiana* shown here was inspired by the seminal work of Ding et al. [18], where transient expression of various components of moth sex pheromone blends was achieved. Contrary to other insect pests, whose sex pheromones are made of a single, highly specific molecule, as with some mealybugs [29], lepidopteran sex pheromones are often made of more complex blends of fatty-acid derived compounds, many of them shared by several species. Species-specificity in these cases is provided by the precise ratio in the blend. For instance, Krokos et al. [30] tested the response of *Sesamia nonagrioides* (Lefèbvre) males to different blends of pheromone compounds, identifying a 90 : 10 : 5 blend of Z11-16OAc:Z11-16OH:Z11-16Ald as the most effective. This feature makes the genetic design of plant emitters for attract-and-kill strategies in moths extremely challenging, because ensuring the right proportions of the three compounds requires a tight control of

TABLE 2: Quantity (ng) of (Z)-11-hexadecenol (OH) and (Z)-11-hexadecenyl acetate (OAc) released by SxPv1.2 individuals obtained by volatile collection and GC/MS/MS quantification.

Plant	ng collected OH	ng OH/day	ng collected OAc	ng OAc/day
SxPv1.2 T_1-1	209,3	69,8	193,3	64,4
SxPv1.2 T_1-2	225,6	75,2	359,4	119,8
SxPv1.2 T_1-3	222,6	74,2	250,7	83,6
SxPv1.2 T_1-4	293,9	98,0	256,8	85,6
Mean ± se	237.8 ± 19.0	79.3 ± 6.3	265.0 ± 34.6	88.3 ± 11.5

several factors, from gene expression to enzymatic activity and differential release ratios. Conversely, mating disruption seems a more attainable objective in terms of heterologous pheromone production since, in many cases, the release of nonattractive incomplete mixtures can disrupt mating as effectively as the complete blend [31]. In this case, however, the main requirement imposed on a biological dispenser is to produce and release sufficient quantities of one or more compounds in the blend. Therefore, the main objective of this work was to understand the biological constraints accompanying the production and release of two of the most representative compounds of lepidopteran pheromone blends in *N. benthamiana* plants. We successfully generated a first generation of transgenic plants (SxPv1.0) producing mainly Z11-16OH. Homozygous SxPv1.0 lines maintained pheromone production up to the T_3 generation. It should also be noted that basal levels of Z11-16Ald and Z11-16OAc were detected in SxPv1.0, probably produced by endogenous enzymes, since no oxidase was included in this first version of the pathway, and the third enzyme of the route, *EaDAct*, was truncated. The disruption of the *EaDAct* gene in different transgenic lines may be explained by a tendency to recombine with plasmid DNA in the bacterial host. This seems to be the case based on the observation that a small fragment of plasmid origin was found interrupting the coding sequence in the truncated construct. In addition, the distal position of *EaDAct* with respect to the selection marker in SxPv1.0 could have made it more likely that rearrangements in this gene went unnoticed, as they did not affect regeneration on selective media. Although a relatively lower number of regenerants was obtained for SxPv1.1 and SxPv1.2 (8 and 5, respectively), compared to SxPv1.0 (11), this difference is most likely due to contingent factors such as chance, contamination, and even limited access to experimental facilities during the COVID-19 pandemic. The recovery of a single plant producing a blend of Z11-16OH and Z11-16OAc may have been aided by closely linking the previously truncated gene with selection markers to increase the probability of associating positive selection with an intact *EaDAct* gene. With the only exception of the above mentioned SxPv1.2 plant, all SxPv1.1 and SxPv1.2 recovered plants effectively integrated the intact construct but failed to produce measurable levels of pheromone compounds, probably due to silencing or positional effects. This seems to indicate that only certain levels/ratios of the two compounds are compatible with viable plant regeneration and biomass accumulation. Pheromone production in this new single line (now in the T_2 generation) is also very stable and maintains

remarkably homogeneous levels of production. The establishment of SxPv1.0 and SxPv1.2 stable plants has allowed us to study in detail the production levels of the different pheromone components, their relative abundance, and their volatility, together with an in-depth characterization of the accompanying phenotype.

As results of our analysis, two main bottlenecks were identified: the associated growth penalty and the poor release rates of the pheromones to the environment. As highlighted also by Reynolds et al. [32] and later by Xia et al. [19], one of the most significant downsides to the constitutive overexpression of medium-chain fatty acid biosynthesis pathways in plants is the associated developmental abnormalities. These may result from an imbalance caused by diverting metabolic resources from fatty acid metabolism towards the products of interest, and possibly from the toxicity of the end-products. Such toxic effects can hamper plant viability and result in a negative selection pressure against the genotypes with higher pheromone production levels. Interestingly, whereas Xia et al. [19] found strong deleterious effects associated with the production of *(E)*-11-tetradecenoic acid, the same authors regenerated normal plants that accumulated Z11-16CoA, the direct precursor of the volatile pheromones produced here. The fact that the simple addition of a desaturase activity leads to deleterious effects may indicate that Z11-16OH itself is responsible for the toxic effects observed when accumulated in leaves. Furthermore, this toxicity seems partially alleviated when a fraction of Z11-16OH is converted to Z11-16OAc, leading to higher biomass in the case of SxPv1.2.

Understanding the changes imposed on the leaf volatilome can shed light on the associated phenotypic changes and the possible imbalances produced by the introduction of the recombinant pheromone pathway. We show here that each SxP version has a distinctive volatile profile that differs from wild-type plants primarily by the presence of the pheromones themselves and a few related fatty-acid-derived compounds, which apparently result from endogenous enzyme activities operating on new-to-plant molecules. This seems to be the case for Z11-16Ald (itself a common component of moth pheromone blends) and also for the differential accumulation of other shorter chain fatty acid derivatives such as 1-pentadecene and hexenal. A close look at the clustered analysis shows that wild-type adult *N. benthamiana* tends to produce more monoterpenes (e.g., linalool) and phenolic VOCs (e.g., phenylalanine derivatives) than younger plants. However, this tendency is reduced in SxP plants in general and is even more severe in SxPv1.0 plants. The
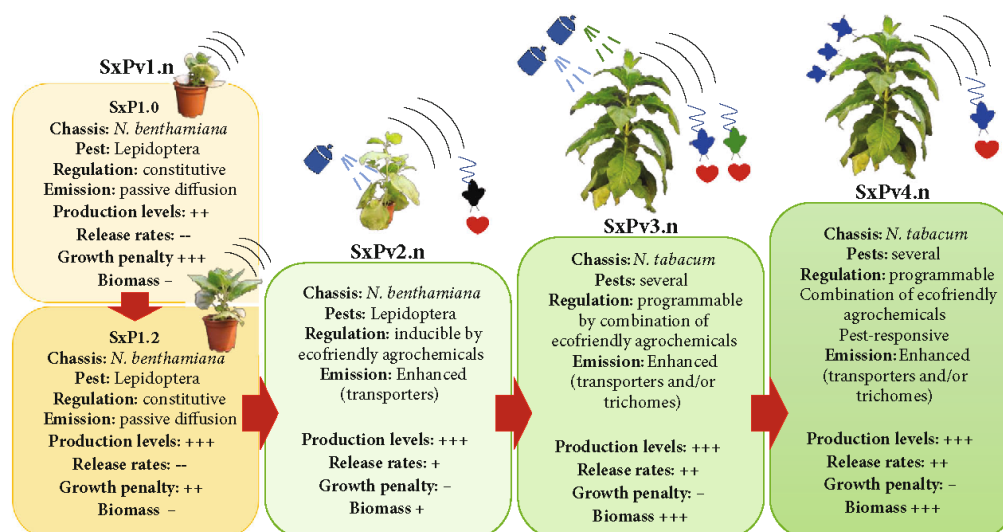
FIGURE 7: Roadmap for future SxP versions. The bottlenecks identified in SxPv1.n serve as guidance for future iterations in the development of pheromone biofactories. Key improvements in a second generation (SxPv2.n) should include inducible expression of the pheromone pathway to circumvent growth penalties, ideally triggered by environmentally friendly agrochemicals. Additionally, it should increase emission rates, e.g., by coexpressing carrier proteins. Progress towards a third generation (SxPv3.n) would require the transfer of SxPv2.n tools to a related chassis with higher biomass, probably N. tabacum. Other improvements would involve the ability to produce different pheromone "programs" in the same plant, each one triggered by different chemicals, and the selective accumulation of pheromones in glandular trichomes to facilitate their release. Ideally, subsequent iterations (SxPv4.n) should incorporate, among others, the ability to respond directly to the presence of the target pest, as well as additional improvements in the chassis itself that facilitate its use as biosafe emitters in the field (e.g., nonflowering).

observed downregulation of the normal volatile components in adult plants could reflect a reduced ability to set up a defence mechanisms. The fact that N. benthamiana is considered a generally immune-suppressed species [33, 34] could explain the premature senescence and the early collapse observed in many SxPv1.0 soon after flowering. The reasons behind the changes in the volatile profiles of the different plant lines may depend on a general reduction of plant fitness imposed by the expression of the heterologous pathway or may be due to specific changes affecting development and regulatory mechanisms. Insight into these imbalances may be fruitfully gained by transcriptomic analysis of the different genotypes. A strategy to alleviate deleterious effects would require disconnecting plant growth from pheromone production. This could be done by employing agronomically compatible inducible expression systems for the activation of the pathway, taking advantage of the increasing number of Synthetic Biology tools made available for plants and particularly for Nicotiana species [35–37]. Alternatively, the use of a different plant chassis displaying specialized structures, such as glandular trichomes to store potentially toxic pheromone compounds could be advantageous. Glandular trichomes serve as natural biofactories for VOC biosynthesis and release, e.g., in aromatic plant species [38]. A suggested roadmap showing the subsequent SxP version and the improvements they should incorporate in light of the problems encountered in SxPv1 is presented in Figure 7.

The quantification of pheromone tissue accumulation and environmental release in SxPv1.2 leads to interesting considerations. The maximum pheromone accumulation levels measured in SxPv1.2 reached $174.5\,\mu g\,g^{-1}$ FW (totalling both alcohol and acetate forms). This is about half of the levels of the precursors reported by Ding et al. [18] in transient experiments ($381\,\mu g\,g^{-1}$) or by Xia et al. [19] in stable plants ($335\,\mu g\,g^{-1}$) and may indicate a partial conversion into biologically active forms, or an upper limit for toxicity, especially in the case of Z11-16OH. However, only a small portion of the plant pheromone content can be detected in the environment after a 72 h incubation. Typically, mating disruption strategies require daily release rates between 20 and $500\,mg\,Ha^{-1}\,day^{-1}$ [1, 39]. Our data indicates that the maximum release rates per biomass unit are around $20\,\mu g$ $kg\,plant^{-1}\,day^{-1}$; therefore, it would require between 1,000 kg and 25,000 kg of pheromone-producing intercropping biomass per Ha for effective mate disruption. This is obviously not viable for dwarf SxPv1.2 plants, whose average fresh weight is 9.35 g (aerial parts), and it would be still challenging even if plant species with large biomasses are used as bioemitters. Therefore, it is concluded that the improvement in the release rates is an important objective to focus on. In leaves, VOCs are synthesized in mesophyll cells and release takes place through the stomata or cuticle [40]. Emission rates of endogenous VOCs are highly variable and depend on the chemical properties of each molecule. Furthermore,

volatility is temperature-dependent, with higher temperatures leading to a more rapid transition from the liquid to the gas phase ([41] and references therein). C16 fatty acid derivatives are indeed semivolatile compounds and, in the absence of specialized structures (like the glandular trichomes described above), active transport may play an important role in their release from mesophyll cells. Active transporters of the adenosine triphosphate-binding cassette (ABC) class are known to be required for the release of at least some volatile components of flower scent in petunia [42]. Pheromone-binding proteins (PBPs) play important roles in binding pheromones and bringing them in contact with receptor complexes in the antennae [43]. Interesting biotechnological approaches have shown that fusing odorant binding proteins with transit peptides allows them to efficiently cross lipid membranes, thus moving odorants to the desired compartments [44]. The use of engineered PBPs or transporters to facilitate pheromone release needs further exploration (Figure 7). The availability of a first version of a live pheromone biodispenser will facilitate the study of transporters and permeability intermediaries and serves as the basis for new design-build-test iterations towards the deployment of efficient SxPs as new components of integrated pest management strategies.

4. Materials and Methods

4.1. DNA Assembly and Cloning. The basic DNA elements (promoters, coding regions, and terminators) employed for the assembly of multigene constructs (level 0 parts) were designed, synthesised, and cloned using the GoldenBraid (GB) domestication strategy described by Sarrion-Perdigones et al. [45]. Once cloned into a pUPD2 vector, these new DNA elements were verified by enzymatic digestion and by sequencing. Transcriptional units (level 1 parts) were then assembled via multipartite BsaI restriction-ligation reactions from level 0 parts, while level > 1 modules were produced via binary BsaI or BsmBI restriction–ligation. All level ≥ 1 parts were confirmed by restriction enzyme analysis. All GB constructs created and/or employed in this study are reported in Table S1, and their sequences are publicly accessible at https://gbcloning.upv.es/search/features. All constructs were cloned using the *Escherichia coli* TOP 10 strain. Transformation was performed using the Mix & Go kit (Zymo Research) following the manufacturer's instructions. The final expression vectors were transformed into electrocompetent *Agrobacterium tumefaciens* GV3101 C58 or LBA4404 for transient or stable transformations, respectively.

4.2. Transient Expression Assays in Nicotiana benthamiana. *Agrobacterium tumefaciens* GV3101 cultures harbouring the constructs of interest were grown from glycerol stocks for 2 days to saturation, then refreshed by diluting them 1 : 1000 in LB liquid medium supplemented with the appropriate antibiotics. After being grown overnight, cells were pelleted and resuspended in agroinfiltration buffer (10 mM MES, pH 5.6, 10 mM $MgCl_2$ and 200 μM acetosyringone), incubated for 2 hours in the dark, and adjusted to an

OD_{600} of 0.1. Equal volumes of each culture were mixed when needed for coinfiltration. A P19 silencing suppressor was included in the mixes to reduce posttranscriptional gene silencing [20]. Agroinfiltration was carried out with a 1 mL needleless syringe through the abaxial surface of the three youngest fully expanded leaves of 4-5-week-old plants grown at 24°C (light)/20°C (darkness) with a 16 : 8 h light : darkness photoperiod. Samples were collected 5 days postinfiltration using a Ø 1.5-2 cm corkborer and snap frozen in liquid nitrogen.

4.3. Nicotiana benthamiana Stable Transformation. Stable transgenic lines were generated following the transformation protocol of Clemente [46], using *Agrobacterium tumefaciens* LBA4404 cultures with the corresponding plasmids. Briefly, leaves from 4-5-week-old *N. benthamiana* plants grown at 24°C (light)/20°C (darkness) with a 16 : 8 h light : darkness photoperiod were sterilized by washing in a 2.5% sodium hypochlorite solution for 15 minutes, then rinsed in 70% ethanol for 10 seconds and washed 3 times in sterile distilled water for 15 minutes. Leaf discs were then cut using a Ø 0.8-1.2 cm corkborer and transferred to a coculture medium (MS medium supplemented with vitamins, enriched with 1 mg L^{-1} 6-benzylaminopurine and 0.1 mg L^{-1} naphthalene acetic acid). After 24 h on this medium, discs were incubated for 15 minutes in an *Agrobacterium* culture grown overnight to OD_{600} of 0.2 in TY medium (10 g L^{-1} tryptone, 5 g L^{-1} yeast extract, and 10 g L^{-1} NaCl, pH = 5.6) supplemented with 2 mM $MgSO_4 \cdot 7H_2O$, 200 μM acetosyringone and the appropriate antibiotics. After incubation, discs were transferred back to the coculture medium and incubated for 48 h in the dark. Shoots were then induced by transferring to a MS medium supplemented with vitamins, 1 mg L^{-1} 6-benzylaminopurine, 0.1 mg L^{-1} naphthalene acetic acid, and 100 mg L^{-1} kanamycin for selection of transformants. After 2-3 weeks of growth with weekly transfers to fresh media, shoots developing from the calli were isolated and transferred to root-inducing medium (MS supplemented with vitamins and 100 mg L^{-1} kanamycin). All in vitro growth was performed in a growth chamber (16 : 8 h light : darkness photoperiod, 24°C, 60%–70% humidity, 250 μmol m^{-2} s^{-1}). Rooted shoots were finally transferred to soil and grown in a greenhouse at 24 : 20°C (light : darkness) with a 16 : 8 h light : darkness photoperiod.

4.4. Plant Growth and Sampling. Transgenic SxP seeds were placed in a germination medium (MS with vitamins 4.9 g L^{-1}, sucrose 30 g L^{-1}, Phytoagar 9 g L^{-1}, pH = 5.7) supplemented with 100 mg L^{-1} kanamycin for positive transgene selection. Control WT plants were obtained similarly by placing seeds in a non-selective germination medium. WT and kanamycin-resistant seedlings were transferred to the greenhouse a week after germination, where they were grown at 24 : 20°C (light : darkness) with a 16 : 8 h light : darkness photoperiod.

Samples for targeted VOC analysis were collected from the 2nd and 3rd youngest and fully expanded leaves of each plant at the early flowering stage. All samples were collected between 4 and 6 pm, frozen in liquid nitrogen immediately

after collection, and ground afterwards. Plant size was also estimated at this stage using a 1-10 scale. WT plants grown in parallel with each batch of transgenic plants were taken as a reference and given a score of 10.

For the comparative study of the SxPv1.0 and SxPv1.2 lines, seeds from SxPv1.0 5_1_7_X (T$_2$), SxPv1.2 4_X (T$_0$), and WT *N. benthamiana* plants were all sown simultaneously on selective and nonselective MS medium, then transferred to soil and grown in the conditions described above. Leaf samples and pictures were taken at 4 weeks and 7 weeks after transplant, which corresponds to the young and early flowering stages (hereafter, adults), respectively. Roots were collected at the adult stage. All samples were snap-frozen in liquid nitrogen and ground. All samples were analyzed according to the same GC/MS protocol, as described below.

4.5. VOC Analysis. 50 mg of frozen, ground leaf samples were weighed in a 10 mL headspace screw-cap vial and stabilized by adding 1 mL of 5 M CaCl$_2$ and 150 μL of 500 mM EDTA (pH = 7.5), after which they were sonicated for 5 minutes. Volatile compounds were captured by means of headspace solid phase microextraction (HS-SPME) with a 65 μm polydimethylsiloxane/divinylbenzene (PDMS/DVB) SPME fiber (Supelco, Bellefonte, PA, USA). Volatile extraction was performed automatically by means of a CombiPAL autosampler (CTC Analytics). Vials were first incubated at 80°C for 3 minutes with 500 rpm agitation. The fiber was then exposed to the headspace of the vial for 20 min under the same conditions of temperature and agitation. Desorption was performed at 250°C for 1 minute (splitless mode) in the injection port of a 6890 N gas chromatograph (Agilent Technologies). After desorption, the fiber was cleaned in a SPME fiber conditioning station (CTC Analytics) at 250°C for 5 min under a helium flow. Chromatography was performed on a DB5ms (60 m, 0.25 mm, 1 μm) capillary column (J&W) with helium as the carrier gas at a constant flow of 1.2 mL min^{-1}. For an initial identification of the pheromone peaks, oven programming conditions were 40°C for 2 min, with 5°C min^{-1} ramp until reaching 280°C, and a final hold at 280°C for 5 min. Once the target peaks were identified, the oven conditions were changed to an initial temperature of 160°C for 2 min, 7°C min^{-1} ramp until 280°C, and a final hold at 280°C for 6 minutes to reduce the overall running time without losing resolution of the desired compounds. Identification of compounds was performed by the comparison of both retention time and mass spectrum with pure standards (for pheromones) or by comparison between the mass spectrum for each compound with those of the NIST 2017 Mass Spectral library (Supplementary File 1). All pheromone values were divided by the total ion count (TIC) of the corresponding sample for normalization [47].

The quantification of pheromone compounds emitted by plants was carried out by volatile collection in dynamic conditions. Individual plants were placed inside 5 L glass reactors (25 cm high × 17.5 cm diameter flask) with a 10 cm open mouth and a ground glass flange to fit the cover with a clamp. The cover had a 29/32 neck on top to fit the head of a gas washing bottle and to connect a glass Pasteur pipette

downstream to trap effluents in 400 mg of Porapak-Q (Supelco Inc., Torrance, CA, USA) adsorbent. Samples were collected continuously for 72 h by using an ultrapurified-air stream, provided by an air compressor (Jun-air Intl. A/S, Norresundby, Denmark) coupled with an AZ 2020 air purifier system (Claind Srl, Lenno, Italy) to provide ultrapure air (amount of total hydrocarbons < 0.1 ppm). In front of each glass reactor, an ELL-FLOW digital flowmeter (Bronkhorst High-Tech BV, Ruurlo, The Netherlands) was fitted to provide an air push flow of 150 mL min^{-1} during sampling. Trapped volatiles were then extracted with 5 mL pentane (Chromasolv, Sigma-Aldrich, Madrid, Spain), and extracts were concentrated to 200 μL under a nitrogen stream. Twenty microliters of an internal standard solution (TFN, 100 μg/mL in hexane) was added to the resulting extract prior to the chromatographic analysis for pheromone quantification.

4.6. Statistical Analysis. For the untargeted volatilome analysis, data preprocessing was performed with Metalign [48]. Peak intensities were calculated for each compound for the SxP and WT samples and for blanks (mock CaCl$_2$+EDTA samples), and compounds were included in the analysis if the sample : blank ratio was ≥2 for at least one of the categories (SxPv1.0, SxPv1.2, or WT). The principal component analysis and hierarchical clustering were performed with MetaboAnalyst 5.0 (https://www.metaboanalyst.ca/). After generalized logarithm transformation, data scaling was performed by mean-centering and dividing by the square root of the standard deviation of each variable. Hierarchical clustering was done using Ward clustering algorithm and Euclidean distance measure. Plant size values were analyzed with the nonparametric Kruskal-Wallis test using the Past3 software to determine the significance of plant size differences.

4.7. Plant Solvent Extraction. The total quantity of pheromone compounds accumulated in each plant was extracted with toluene (TLN). Plant samples (ca. 3 g), mixed with fine washed sand (1 : 1, plant : sand, w/w), were manually ground with a mortar to aid in tissue breakdown and facilitate the extraction. The resulting material was then transferred to 50 mL centrifuge tubes with 10 mL TLN. The extraction process was assisted by magnetic agitation for 12 h and finally by ultrasound in a Sonorex ultrasonic bath (Bandelin electronic, Berlin, Germany) for 30 min. A 1 mL sample of the resulting extract was filtered through a PTFE syringe filter (0.25 μm). Two-hundred microliters of an internal standard solution (TFN, 100 μg/mL in hexane) was added to the sample prior to the chromatographic analysis for pheromone quantification.

4.8. Synthetic Pheromone Samples and Internal Standard Synthesis. A synthetic sample of 1 g of Z11-16OH was obtained following the method described by Zarbin et al. [49]. The sample was carefully purified by column chromatography using silica gel and a mixture of hexane : Et$_2$O (9 : 1 to 8 : 2) as an eluent. Evaporation of the solvent of the corresponding fraction generated a sample of 96% purity by GC-FID.

A standard acetylation of Z11-16OH was carried out using acetic anhydride (1.2 eq) and trimethylamine (1.3 eq) as a base in dichloromethane (DCM), generating the corresponding acetate in 95% yield, whose spectroscopical data was fully coincident with that described in the literature [49]. Oxidation with pyridinium chlorocromate of a 100 mg sample of Z11-16OH was carried out following the method described by Zakrzewski et al. [50] generating 62 mg (60%) of Z11-16Ald, whose spectroscopical data was fully coincident with that described in the literature [50].

Due to the abundance of compounds structurally related to the pheromone in the biological samples, a straight chain fluorinated hydrocarbon ester (heptyl 4,4,5,5,6,6,7,7,8,8,9,9,9-tridecafluorononanoate; TFN) was selected as the internal standard to improve both sensitivity and selectivity for MS/MS method optimization. TFN was synthesized as follows: to a solution of 4,4,5,5,6,6,7,7,8,8,9,9,9-tridecafluorononanoic acid (500 mg, 1.3 mmol) in DCM, oxalyl chloride was added. After 60 min of continuous stirring, the solvent was removed under vacuum. The residue was redissolved in dry DCM (15 mL) and 1-heptanol (0.26 mL, 1.5 mmol), followed by addition of triethyl amine (0.31 mL, 3 mmol) at room temperature, and the resultant solution was refluxed for 24 h. After this period, 15 mL of DCM was added and the solution was successively washed with HCl (1 M, 20 mL), NaHCO$_3$ (sat., 20 mL), and brine (15 mL) and dried with anhydrous MgSO$_4$. The solution was filtered, and the residue was purified by column chromatography (silica gel; eluent: 1% Et$_2$O/hexane) to yield heptyl 4,4,5,5,6,6,7,7,8,8,9,9,9-tridecafluorononanoate (281 mg, 45%), as a colorless oil of 95% of purity estimated by GC-FID. MS (70 eV, *m/z*): 393 (10%), 375 (40%), 373 (5%), 132 (10%), 98 (30%), 83 (15%), 70 (100%), 69 (70%), 57 (90%), and 56 (90%).

4.9. Plant Extract Preparation for Biosynthetic Pheromone Characterization. 120 g of a pool of 10 T$_1$ SxPv1.2 plants (whole aerial portion of the plant) were mixed with fine washed sand (1 : 1, plant : sand, *w/w*) and were manually ground with a mortar to aid tissue breakdown and facilitate the extraction. The resulting material was then transferred to a 1 L Erlenmeyer flask, and 400 mL of hexane were added. The extraction process was assisted by magnetic agitation for 12 h. After this time, the mixture was filtered, and the filtrated was concentrated in a rotary evaporator. The residue (ca. 2 g) was chromatographed in a gravity column (30 cm × 1.5 cm) using silica gel (50 g) as the stationary phase and a mixture of hexane : Et$_2$O (9 : 1) as the solvent. 60 fractions of ca. 3 mL were collected and analyzed by thin layer chromatography and GC/MS. Those fractions containing biosynthetic Z11-16OH were selected and those containing mainly biosynthetic Z11-16OH where mixed, and the solvent was rotary evaporated, generating 2 mg of material. The ^{1}H and ^{13}C NMR spectrum of the isolated biosynthetic Z11-16OH was recorded by a Bruker 600 Ultrashield Plus spectrometer (Bruker, Billerica, MA) at a frequency of 600 MHz, using CDCl$_3$ as the solvent and tetramethylsilane (TMS) as the internal standard.

4.10. Pheromone Quantification. The quantification of the pheromone compounds was carried out by gas chromatography coupled to mass spectrometry (GC/MS/MS) using a TSQ 8000 Evo triple quadrupole MS/MS instrument operating in SRM (selected reaction monitoring) mode using electron ionization (EI +), coupled with a Thermo Scientific TRACE 1300 gas chromatograph (GC). The GC was equipped with a ZB-5MS fused silica capillary column (30 m × 0.25 mm i.d.× 0.25 μm; Phenomenex Inc., Torrance, CA). The oven was held at 60°C for 1 min then was raised by 10°C min^{-1} up to 110°C, maintained for 5 min, raised by 10°C min^{-1} up to 150°C, maintained for 3 min and finally raised by 10°C min^{-1} up to 300°C held for 1 min. The carrier gas was helium at 1 mL min^{-1}. For each compound, pheromone components (Z11-16OH and Z11-16OAc), and the internal standard (TFN), the MS/MS method was optimized by selecting the precursor ion and the product ions that provided the most selective and sensitive determinations (Table S2).

The amount of pheromone and the corresponding chromatographic areas were connected by fitting a linear regression model, $y = a + bx$, where y is the ratio between pheromone and TFN areas and x is the amount of pheromone.

4.11. Plant Extract Fractionation for Electroantennography Assays. 10 g of T$_1$ SxPv1.2 plants (whole aerial portion of the plant) were mixed with fine washed sand (1 : 1, plant : sand, *w/w*) and were manually ground with a mortar to aid tissue breakdown and facilitate the extraction. The resulting material was then transferred to 50 mL centrifuge tubes with 40 mL TLN. The extraction process was assisted by magnetic agitation for 12 h and finally by ultrasounds in a Sonorex ultrasonic bath (Bandelin electronic, Berlin, Germany) for 60 min. After this time, the mixture was filtered off and the filtrated was concentrated in a rotary evaporator. The residue (ca. 0.2 g) was chromatographed in a gravity column (17 cm × 1 cm) using silica gel (15 g) as a stationary phase and a mixture hexane : Et$_2$O (9 : 1) as a solvent. Twenty-five fractions of ca. 2 mL were collected and analyzed by thin layer chromatography and GC-MS. Fractions 17-20 containing biosynthetic Z11-16OH were selected and combined for electroantennography assays.

4.12. Electroantennography Assays for Evaluating Moth Response to Biosynthetic Pheromone. Starter specimens of *Sesamia nonagrioides* (Lefèbvre) (Lepidoptera: Noctuidae) were collected from infested rice (*Oryza sativa*) plants in paddy fields located in Valencia (Spain). These were maintained on the stems until pupae were obtained and the progeny of the resulting adults was reared on an artificial diet [51]. Pupae were sexed using a stereomicroscope and males were kept separated from females in different chambers under an L16:D8 regime at 25 ± 2°C and 60% relative humidity.

The electrophysiological response of *S. nonagrioides* males to the biosynthetic Z11-16OH was tested by gas chromatography coupled to mass spectrometry and electroantennography detectors (GC/MS-EAD). For this purpose, 2-3-day-old males were individually placed into test tubes in an ice bath to excise their antenna. Between two and five terminal segments of the antenna were also

removed with a scalpel. The antenna was mounted between silver wire electrodes impregnated with conductive electrode gel (Spectra 360, Parker Laboratories, Inc., Fairfield, NJ, USA), to increase the electrical contact. A humidified and carbon-filtered airflow (50 mL/min) was directed continuously over the antenna preparation through a glass L-tube placed at less than 2 cm distance. The flow was delivered by a Syntech CS-55 stimulus controller (Ockenfels Syntech GmbH, Kirchzarten, Germany). A pore-sized opening in the elbow part of the L-tube allowed the introduction of the distal part of a fused-silica restrictor connected to the GC apparatus (Clarus 600 GC/MS, Perkin Elmer Inc., Wellesley, PA). The effluent of the GC column (ZB-5MS fused silica capillary column (30 m × 0.25 mm i.d.× 0.25 μm; Phenomenex Inc., Torrance, CA) was split 1:40 for simultaneous detection between the MS and the EAD apparatus. A Swafer S splitter (Perkin Elmer Inc., Wellesley, PA) was employed for this purpose. The GC-MS/EAD run was performed with the SxPv1.2 extract fraction containing the biosynthetic Z11-16OH obtained as described above. The GC oven temperature was programmed at 120°C for 2 min, then raised to 200°C at 10°C/min and finally from 200°C to 280°C (held for 10 min) at 5°C/min. The EAG responses were recorded with a Syntech IDAC 2 acquisition controller, and GC-EAD 32 (v. 4.3) software was employed for data recording and acquisition (Ockenfels Syntech GmbH, Kirchzarten, Germany).

Data Availability

All data is freely available upon request and will be deposited to the FAIRDOMHub database in the frame of the Era-CoBiotech SUSPHIRE project.

Additional Points

Current address of Alfredo Quijano-Rubio is: Institute for Protein Design, University of Washington, Seattle, WA, USA. Current address of José Gavalda-García is: Interuniversity Institute of Bioinformatics, Brussels, Belgium. Current address of Lucía Estellés is: CNAG-CRG, Centre for Genomic Regulation (CRG), The Barcelona Institute of Science and Technology, Baldiri Reixac 4, Barcelona 08028, Spain. Current address of Alba Rubert is: Vrije Universiteit, Amsterdam, The Netherlands.

Conflicts of Interest

Ismael Navarro is employed by the company Ecología y Protección Agrícola S.L. The remaining authors declare that the research was conducted in the absence of any commercial or financial relationships that could be construed as a potential conflict of interest.

Authors' Contributions

Rubén Mateos-Fernández and Elena Moreno-Giménez contributed equally to this work.

Acknowledgments

Supplementary Materials

Supplementary 1. Supplementary Data 1. Table S1: Golden-Braid Phytobricks created and used in this study. Table S2: optimized values of the MS/MS parameters for each target compound. Table S3: primers created and used in this study for testing the integrity of the EaDAct gene in SxPv1.0 plants. Figure S1: transient expression in Nicotiana benthamiana of the moth pheromone synthetic pathway. Figure S2: gel electrophoresis of the PCR results with gDNA and cDNA from SxPv1.0 T2 plants. Figure S3: GC/MS of biosynthetic Z11-16OH. Figure S4: ^{1}H NMR of biosynthetic Z11-16OH. Figure S5: ^{13}C NMR of biosynthetic Z11-16OH.

Supplementary 2. Supplementary File 1: data of principal component analysis and heatmap representation.

References

[1] C. Alfaro, V. Navarro-Llopis, and J. Primo, "Optimization of pheromone dispenser density for managing the rice striped stem borer, _Chilo suppressalis_ (Walker), by mating disruption," *Crop Protection*, vol. 28, no. 7, pp. 567–572, 2009.

[2] R. T. Carde and A. K. Minks, "Control of moth pests by mating disruption: successes and constraints," *Annual Review of Entomology*, vol. 40, no. 1, pp. 559–585, 1995.

[3] S. M. Cook, Z. R. Khan, and J. A. Pickett, "The use of push-pull strategies in integrated Pest management," *Annual Review of Entomology*, vol. 52, no. 1, pp. 375–400, 2007.

[4] P. C. Gregg, A. P. del Socorro, and P. J. Landolt, "Advances in attract-and-kill for agricultural pests: beyond pheromones," *Annual Review of Entomology*, vol. 63, no. 1, pp. 453–470, 2018.

[5] P. Witzgall, P. Kirsch, and A. Cork, "Sex pheromones and their impact on pest management," *Journal of Chemical Ecology*, vol. 36, no. 1, pp. 80–100, 2010.

[6] Agricultural Phermonone Market report FBI100071, "Fortune business insights," *Globalizations*, vol. 2021, 2021https://www.fortunebusinessinsights.com/industry-reports/agricultural-pheromones-market-100071.

[7]   K. Mori, "The synthesis of insect pheromones," in *Total Synthesis of Natural Products*, J. ApSimon, Ed., pp. 1979–1989, John Wiley & Sons Inc., Hoboken, 2007.

[8]   K. Mori, *Chemical Synthesis of Hormones, Pheromones and Other Bioregulators*, John Wiley & Sons Ltd., Hoboken, 2010.

[9]   K. Petkevicius, C. Löfstedt, and I. Borodina, "Insect sex pheromone production in yeasts and plants," *Current Opinion in Biotechnology*, vol. 65, pp. 259–267, 2020.

[10] C. Löfstedt and Y.-H. Xia, "Biological production of insect pheromones in cell and plant factories," in *Insect Pheromone Biochemistry and Molecular Biology*, G. J. Blomquist and R. G. Vogt, Eds., pp. 89–121, Academic Press, London, 2021.

[11] T. J. A. Bruce, G. I. Aradottir, L. E. Smart et al., "The first crop plant genetically engineered to release an insect pheromone for defence," *Scientific Reports*, vol. 5, no. 1, p. 11183, 2015.

[12] T. Ando, *List of Sex Pheromones*, Ando Laboratory, 2021, https://lepipheromone.sakura.ne.jp/lepi_phero_list_eng.html.

[13] A. M. El-Sayed, "The Pherobase: Database of Pheromones and Semiochemicals," 2021, https://www.pherobase.com/.

[14] E. J. V. Nieukerken, L. Kaila, I. J. Kitching et al., "Order Lepidoptera," in *Animal Biodiversity: An Outline of Higher-Level Classification and Survey of Taxonomic Richness*, Z.-Q. Zhang, Ed., pp. 212–221, Zootaxa, 2011.

[15] C. Löfstedt, N. Wahlberg, and J. G. Millar, "Evolutionary patterns of pheromone diversity in Lepidoptera," in *Pheromone Communication in Moths*, J. D. Allison and R. T. Cardé, Eds., pp. 43–78, University of California Press, Berkeley, 2016.

[16] B.-J. Ding, I. Lager, S. Bansal, T. P. Durrett, S. Stymne, and C. Löfstedt, "The yeast ATF1 acetyltransferase efficiently acetylates insect pheromone alcohols: implications for the biological production of moth pheromones," *Lipids*, vol. 51, no. 4, pp. 469–475, 2016.

[17] P. Nešněrová, P. Šebek, T. Macek, and A. Svatoš, "First semisynthetic preparation of sex pheromones," *Green Chemistry*, vol. 6, no. 7, pp. 305–307, 2004.

[18] B.-J. Ding, P. Hofvander, H. L. Wang, T. P. Durrett, S. Stymne, and C. Löfstedt, "A plant factory for moth pheromone production," *Nature Communications*, vol. 5, no. 1, p. 3353, 2014.

[19] Y.-H. Xia, B. J. Ding, H. L. Wang, P. Hofvander, C. Jarl-Sunesson, and C. Löfstedt, "Production of moth sex pheromone precursors in *Nicotiana* spp.: a worthwhile new approach to pest control," *Journal of Pest Science*, vol. 93, no. 4, pp. 1333–1346, 2020.

[20] N. Zheng, R. Xia, C. Yang et al., "Boosted expression of the SARS-CoV nucleocapsid protein in tobacco and its immunogenicity in mice," *Vaccine*, vol. 27, no. 36, pp. 5001–5007, 2009.

[21] Å. K. Hagström, H. L. Wang, M. A. Liénard, J. M. Lassance, T. Johansson, and C. Löfstedt, "A moth pheromone brewery: production of (*Z*)-11-hexadecenol by heterologous coexpression of two biosynthetic genes from a noctuid moth in a yeast cell factory," *Microbial Cell Factories*, vol. 12, no. 1, p. 125, 2013.

[22] J. G. Bartlett, M. Smedley, and W. Harwood, "Analysis of T-DNA/host-plant DNA junction sequences in single-copy transgenic barley lines," *Biology*, vol. 3, no. 1, pp. 39–55, 2014.

[23] A. Forsbach, D. Schubert, B. Lechtenberg, M. Gils, and R. Schmidt, "A comprehensive characterization of single-copy T-DNA insertions in the *Arabidopsis thaliana* genome," *Plant Molecular Biology*, vol. 52, no. 1, pp. 161–176, 2003.

[24] C. Holkenbrink, B. J. Ding, H. L. Wang et al., "Production of moth sex pheromones for pest control by yeast fermentation," *Metabolic Engineering*, vol. 62, pp. 312–321, 2020.

[25] R. Ortiz, M. Geleta, C. Gustafsson et al., "Oil crops for the future," *Current Opinion in Plant Biology*, vol. 56, pp. 181–189, 2020.

[26] L. L. Stelinski, L. J. Gut, and J. R. Miller, "An attempt to increase efficacy of moth mating disruption by co-releasing pheromones with kairomones and to understand possible underlying mechanisms of this technique," *Environmental Entomology*, vol. 42, no. 1, pp. 158–166, 2013.

[27] G. Benelli, A. Lucchi, D. Thomson, and C. Ioriatti, "Sex pheromone aerosol devices for mating disruption: challenges for a brighter future," *Insects*, vol. 10, no. 10, p. 308, 2019.

[28] M. S. Hossain, D. G. Williams, C. Mansfield, R. J. Bartelt, L. Callinan, and A. L. Il'ichev, "An attract-and-kill system to control *Carpophilus* spp. in Australian stone fruit orchards," *Entomologia Experimentalis et Applicata*, vol. 118, no. 1, pp. 11–19, 2006.

[29] Y. Zou and J. G. Millar, "Chemistry of the pheromones of mealybug and scale insects," *Natural Product Reports*, vol. 32, no. 7, pp. 1067–1113, 2015.

[30] F. D. Krokos, A. Ameline, J. Bau et al., "Comparative studies of female sex pheromone components and male response of the corn stalk borer *Sesamia nonagrioides* in three different populations," *Journal of Chemical Ecology*, vol. 28, no. 7, pp. 1463–1472, 2002.

[31] M. Evenden, "Mating disruption of moth pests in integrated pest management: a mechanistic approach," in *Pheromone Communication in Moths*, J. D. Allison and R. T. Cardé, Eds., pp. 365–394, University of California Press, Berkeley, 2016.

[32] K. B. Reynolds, M. C. Taylor, D. P. Cullerne et al., "A reconfigured Kennedy pathway which promotes efficient accumulation of medium-chain fatty acids in leaf oils," *Plant Biotechnology Journal*, vol. 15, no. 11, pp. 1397–1408, 2017.

[33] M. M. Goodin, D. Zaitlin, R. A. Naidu, and S. A. Lommel, "*Nicotiana benthamiana*: its history and future as a model for plant–pathogen interactions," *Molecular Plant-Microbe Interactions®*, vol. 21, no. 8, pp. 1015–1026, 2008.

[34] J. Bally, K. Nakasugi, F. Jia et al., "The extremophile *Nicotiana benthamiana* has traded viral defence for early vigour," *Nature Plants*, vol. 1, no. 11, p. 15165, 2015.

[35] J. M. Bernabé-Orts, A. Quijano-Rubio, M. Vazquez-Vilar et al., "A memory switch for plant synthetic biology based on the phage ϕC31 integration system," *Nucleic Acids Research*, vol. 48, no. 6, pp. 3379–3394, 2020.

[36] Y.-M. Cai, K. Kallam, H. Tidd, G. Gendarini, A. Salzman, and N. J. Patron, "Rational design of minimal synthetic promoters for plants," *Nucleic Acids Research*, vol. 48, no. 21, pp. 11845–11856, 2020.

[37] F. J. Molina-Hidalgo, M. Vazquez-Vilar, L. D'Andrea et al., "Engineering Metabolism in *Nicotiana* Species: A Promising Future," *Trends in Biotechnology*, vol. 39, no. 9, pp. 901–913, 2020.

[38] A. Huchelmann, M. Boutry, and C. Hachez, "Plant glandular trichomes: natural cell factories of high biotechnological interest," *Plant Physiology*, vol. 175, no. 1, pp. 6–22, 2017.

[39] A. Gavara, S. Vacas, I. Navarro, J. Primo, and V. Navarro-Llopis, "Airborne pheromone quantification in treated vineyards

with different mating disruption dispensers against *Lobesia botrana*," *Insects*, vol. 11, no. 5, p. 289, 2020.

[40] F. Loreto and J. P. Schnitzler, "Abiotic stresses and induced BVOCs," *Trends in Plant Science*, vol. 15, no. 3, pp. 154–166, 2010.

[41] A. O. Mofikoya, T. N. T. Bui, M. Kivimäenpää, J. K. Holopainen, S. J. Himanen, and J. D. Blande, "Foliar behaviour of biogenic semi-volatiles: potential applications in sustainable pest management," *Arthropod-Plant Interactions*, vol. 13, no. 2, pp. 193–212, 2019.

[42] F. Adebesin, J. R. Widhalm, B. Boachon et al., "Emission of volatile organic compounds from petunia flowers is facilitated by an ABC transporter," *Science*, vol. 356, no. 6345, pp. 1386–1388, 2017.

[43] J.-J. Zhou, "Odorant-binding proteins in insects," in *Vitamins & Hormones*, G. Litwack, Ed., pp. 241–272, Elsevier, 2010.

[44] F. Gonçalves, T. G. Castro, E. Nogueira et al., "OBP fused with cell-penetrating peptides promotes liposomal transduction," *Colloids and Surfaces B: Biointerfaces*, vol. 161, pp. 645–653, 2018.

[45] A. Sarrion-Perdigones, M. Vazquez-Vilar, J. Palaci et al., "GoldenBraid 2.0: a comprehensive DNA assembly framework for plant synthetic biology," *Plant Physiology*, vol. 162, no. 3, pp. 1618–1631, 2013.

[46] T. Clemente, "Nicotiana (Nicotiana tabaccum, Nicotiana benthamiana)," in *Agrobacterium Protocols*, K. Wang, Ed., pp. 143–154, Springer, 2006.

[47] Y. Wu and L. Li, "Sample normalization methods in quantitative metabolomics," *Journal of Chromatography A*, vol. 1430, pp. 80–95, 2016.

[48] A. Lommen, "MetAlign: interface-driven, versatile metabolomics tool for hyphenated full-scan mass spectrometry data preprocessing," *Analytical Chemistry*, vol. 81, no. 8, pp. 3079–3086, 2009.

[49] P. H. G. Zarbin, L. M. Lorini, B. G. Ambrogi, D. M. Vidal, and E. R. Lima, "Sex pheromone of *Lonomia obliqua*: daily rhythm of production, identification, and synthesis," *Journal of Chemical Ecology*, vol. 33, no. 3, pp. 555–565, 2007.

[50] J. Zakrzewski, J. Grodner, J. Bobbitt, and M. Karpińska, "Oxidation of unsaturated primary alcohols and ω-Haloalkanols with 4-Acetylamino-2,2,6,6-tetramethylpiperidine-1-oxoammonium tetrafluoroborate," *Synthesis*, vol. 2007, no. 16, pp. 2491–2494, 2007.

[51] M. Eizaguirre, C. López, L. Asín, and R. Albajes, "Thermoperiodism, photoperiodism and sensitive stage in the diapause induction of *Sesamia nonagrioides* (Lepidoptera: Noctuidae)," *Journal of Insect Physiology*, vol. 40, no. 2, pp. 113–119, 1994.

2.3 Transcriptional Deregulation of Stress-Growth Balance in *Nicotiana benthamiana* Biofactories Producing Insect Sex Pheromones

Mojca Juteršek, Marko Petek, Živa Ramšak, Elena Moreno-Giménez, Silvia Gianoglio, Rubén Mateos-Fernández, Diego Orzáez, Kristina Gruden, and Špela Baebler

This article describes the transcriptome-level analysis of transgenic *N. benthamiana* lines with high moth pheromone production levels. It builds on the results of the previous paper, which indicated that the dwarf phenotype is an obstacle for moth pheromone production in plants. Samples collected from both generations of transgenic plants, including lines with different production levels, were subjected to high-throughput transcriptome sequencing, followed by differential expression analysis and gene set enrichment analysis. The results indicate a stress-like transcriptional reprograming in high producers with dwarf phenotype, with decreased expression of genes involved in anabolic processes (photosynthesis, DNA, and protein synthesis) and increased expression of stress-related genes. Further analysis supported by knowledge networks indicate the interplay between jasmonic acid and gibberellic acid signalling as the most probable cause of stunted growth. We also linked the expression of genes related to secondary metabolism with the amounts of secondary metabolism-derived volatiles in high or low producers. Although we were not able to determine the mechanism behind the activation of defence-promoting jasmonic acid signalling, the involvement of gibberellic acid synthesis inhibition prompted by jasmonic acid signalling provides options for chassis improvement. Decoupling of the two signalling pathways by targeting the genes involved in the crosstalk could result in plants with favourable growth even in the presence of stress-triggering signals.

The PhD candidate is the first author of this publication. She contributed to the experimental planning and performed all the bioinformatic analyses of RNA-Seq data, including the differential expression and gene set enrichment analyses, functional annotation of the *N. benthamiana* genome, and network visualisation analysis. She wrote the manuscript and prepared most of the figures and tables.

Check for updates

Transcriptional deregulation of stress-growth balance in *Nicotiana benthamiana* biofactories producing insect sex pheromones

Mojca Juteršek[1,2]*, Marko Petek[1], Živa Ramšak[1],
Elena Moreno-Giménez[3], Silvia Gianoglio[3],
Rubén Mateos-Fernández[3], Diego Orzáez[3],
Kristina Gruden[1] and Špela Baebler[1]

[1]Department of Biotechnology and Systems Biology, National Institute of Biology,
Ljubljana, Slovenia, [2]Jožef Stefan International Postgraduate School, Ljubljana, Slovenia, [3]Institute
for Plant Molecular and Cell Biology (IBMCP), Consejo Superior de Investigaciones Científicas
(CSIC), Universidad Politécnica de Valencia (UPV), Valencia, Spain

Plant biofactories are a promising platform for sustainable production of high-value compounds, among which are insect sex pheromones, a green alternative to conventional insecticides in agriculture. Recently, we have constructed transgenic *Nicotiana benthamiana* plants ("Sexy Plants", SxP) that successfully produce a blend of moth (Lepidoptera) sex pheromone compounds (*Z*)-11-hexadecen-1-ol and (*Z*)-11-hexadecenyl acetate. However, efficient biosynthesis of sex pheromones resulted in growth and developmental penalty, diminishing the potential for commercial use of SxP in biomanufacturing. To gain insight into the underlying molecular responses, we analysed the whole-genome transcriptome and evaluated it in relation to growth and pheromone production in low- and high-producing transgenic plants of v1.0 and v1.2 SxP lines. In our study, high-producing SxPv1.2 plants accumulated the highest amounts of pheromones but still maintained better growth compared to v1.0 high producers. For an in-depth biological interpretation of the transcriptomic data, we have prepared a comprehensive functional *N. benthamiana* genome annotation as well as gene translations to *Arabidopsis thaliana*, enabling functional information transfer by using Arabidopsis knowledge networks. Differential gene expression analysis, contrasting pheromone producers to wild-type plants, revealed that while only a few genes were differentially regulated in low-producing plants, high-producing plants exhibited vast transcriptional reprogramming. They showed signs of stress-like response, manifested as downregulation of photosynthesis-related genes and significant differences in expression of hormonal signalling and secondary metabolism-related genes, the latter presumably leading to previously reported volatilome changes. Further network analyses confirmed stress-like response with activation of jasmonic acid and downregulation of gibberellic acid signalling, illuminating the possibility that the observed growth

penalty was not solely a consequence of a higher metabolic burden imposed upon constitutive expression of a heterologous biosynthetic pathway, but rather the result of signalling pathway perturbation. Our work presents an example of comprehensive transcriptomic analyses of disadvantageous stress signalling in *N. benthamiana* biofactory that could be applied to other bioproduction systems.

Introduction

Plant biofactories are emerging as a cost-effective, adaptable, fast, scalable, and sustainable platform for biomanufacturing of high value-added compounds, from small molecules to recombinant proteins (Schillberg et al., 2019; Huebbers and Buyel, 2021). Apart from metabolic engineering efforts aimed at improving production of endogenous plant metabolites with applications in health, nutrition, and agriculture (Lu et al., 2016; Mora-Vásquez et al., 2022), the new plant breeding technologies and advancements in synthetic biology are offering a possibility for utilising well-established and robust plant hosts for the production of various non-endogenous compounds (Tschofen et al., 2016; Owen et al., 2017). *Nicotiana benthamiana* has proven to be a versatile chassis with an extensive toolbox that enables rapid development of transgenic plants as well as mass production of desired products, either with transient or with stable transgenic expression systems (Bally et al., 2018; Molina-Hidalgo et al., 2021). Recently reported achievements include the synthesis of taxol intermediates (Li et al., 2019) and production of SARS-CoV-2-related proteins (Diego-Martin et al., 2020), as well as the first approved plant-produced vaccine (Ward et al., 2021).

One group of small molecules whose production has been envisioned and tested in plants are insect sex pheromones (Petkevicius et al., 2020), chemical signals emitted into the air by a member of a species to attract individuals of the same species for mating. They can be used for agricultural insect pest control and have important advantages over conventional broad-spectrum insecticides, such as species specificity, efficiency at lower concentrations, non-toxicity, rapid degradation, and lower odds of resistance (Rizvi et al., 2021). Upon reaching cost-effective yields, pheromone-producing plants could be used for manufacturing in greenhouses or even as living biodispensers grown in fields (Mateos Fernández et al., 2022). So far, most progress has been made in the production of moth (Lepidoptera) pheromones—fatty alcohols, aldehydes, and acetates, whose biosynthetic pathways have been deciphered in many species (reviewed in Petkevicius et al., 2020; Mateos-Fernández et al., 2022).
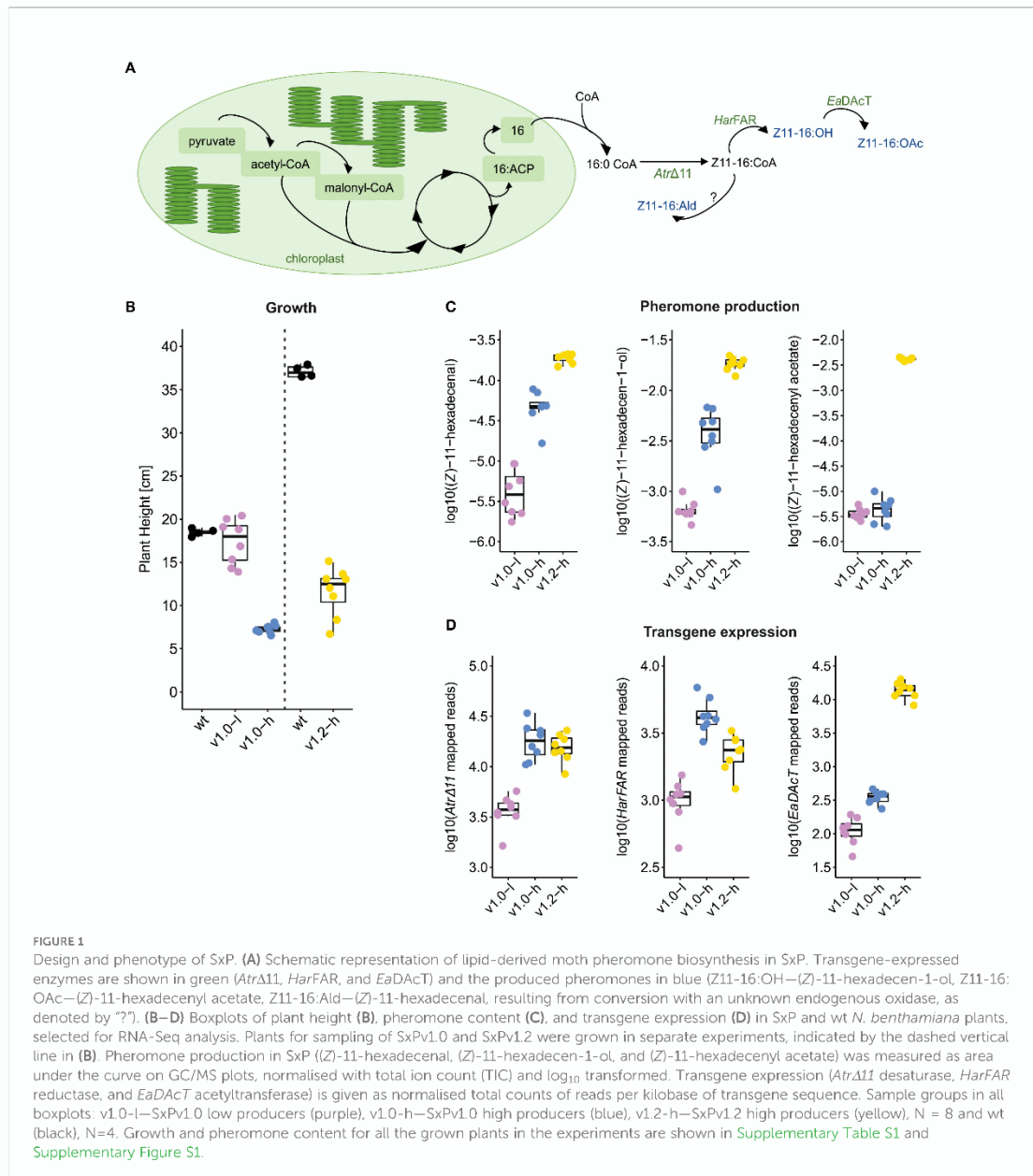
Recently, we reported the successful constitutive production of (*Z*)-11-hexadecen-1-ol and (*Z*)-11-hexadecenyl acetate in stable transgenic *N. benthamiana* plants ("Sexy Plants", SxP), reaching 111.4 and 11.8 μg of product per gram of fresh weight, respectively (Mateos-Fernández et al., 2021). The biosynthesis of insect pheromones is accomplished through a constitutive expression of three genes encoding the *Atr*Δ11 desaturase, the *Har*FAR reductase, and the *Ea*DAcT acetyltransferase (Figure 1A). Two transgenic lines were generated: SxPv1.0 contained a truncated *EaDAcT* transgene and therefore produced much lower amounts of (*Z*)-11-hexadecenyl acetate compared with SxPv1.2 plants with a full-length functional *EaDAcT* transgene. Both lines also produced detectable amounts of (*Z*)-11-hexadecenal, presumably as a result of endogenous oxidation of the produced (*Z*)-11-hexadecenyl-CoA. Efficient biosynthesis of sex pheromones resulted in yield-related growth and developmental penalty, diminishing the potential for commercial use of SxP in biomanufacturing (Mateos-Fernández et al., 2021).

Although growth defects associated with constitutive production of specialised metabolites or proteins have been reported in transgenic plants before (e.g., Lu et al., 2017), there is still a lack of insight into the underlying molecular changes, especially at the whole-genome level. To elucidate the perturbations in the SxP production system, we performed RNA-Seq of wild-type and pheromone-producing *N. benthamiana* plants. Differential expression analysis revealed extensive transcriptional reprogramming in high producers with a stress-like signature. In addition, we found a possible activation of the jasmonic acid signalling, leading to suppression of gibberellic acid signalling, which is a known switch between plant growth and stress responses.

Materials and methods

Plant growth conditions and sampling

We selected non-transgenic wild-type (wt) and transgenic SxP *N. benthamiana* seeds from two lines of v1.0 low producers

FIGURE 1

Design and phenotype of SxP. **(A)** Schematic representation of lipid-derived moth pheromone biosynthesis in SxP. Transgene-expressed enzymes are shown in green (*Atr*Δ11, *Har*FAR, and *Ea*DAcT) and the produced pheromones in blue (Z11-16:OH—(*Z*)-11-hexadecen-1-ol, Z11-16: OAc—(*Z*)-11-hexadecenyl acetate, Z11-16:Ald—(*Z*)-11-hexadecenal, resulting from conversion with an unknown endogenous oxidase, as denoted by "?"). **(B–D)** Boxplots of plant height **(B)**, pheromone content **(C)**, and transgene expression **(D)** in SxP and wt *N. benthamiana* plants, selected for RNA-Seq analysis. Plants for sampling of SxPv1.0 and SxPv1.2 were grown in separate experiments, indicated by the dashed vertical line in **(B)**. Pheromone production in SxP ((*Z*)-11-hexadecenal, (*Z*)-11-hexadecen-1-ol, and (*Z*)-11-hexadecenyl acetate) was measured as area under the curve on GC/MS plots, normalised with total ion count (TIC) and $\log_{10}$ transformed. Transgene expression (*Atr*Δ*11* desaturase, *HarFAR* reductase, and *EaDAcT* acetyltransferase) is given as normalised total counts of reads per kilobase of transgene sequence. Sample groups in all boxplots: v1.0-l—SxPv1.0 low producers (purple), v1.0-h—SxPv1.0 high producers (blue), v1.2-h—SxPv1.2 high producers (yellow), N = 8 and wt (black), N=4. Growth and pheromone content for all the grown plants in the experiments are shown in Supplementary Table S1 and Supplementary Figure S1.

(v1.0-low1, v1.0-low2), two lines of v1.0 high producers (v1.0-high1, v1.0-high2), and two lines of v1.2 high producers (v1.2-high1, v1.2-high2; for details on all lines see Supplementary Table S1 and Mateos-Fernández et al., 2021). SxPv1.0 plants have a truncated *EaDAcT* gene, probably due to an unwanted rearrangement of T-DNA that occurred during the transformation process. Due to the severity of the truncation

and the very low production of the acetylated product, the gene product is believed to be non-functional (Mateos-Fernández et al., 2021). Seed germination and plant growth were done as previously described (Mateos-Fernández et al., 2021). Two separate experiments were conducted, where four T_3 SxPv1.0 lines (two high-producing and two low-producing lines) were grown together with wt plants in the first, and two T_2 SxPv1.2

lines were grown together with wt plants in the second experiment. Plant height was measured before leaf sampling for pheromone analysis and RNA isolation. Samples were collected from the second and third youngest fully expanded leaves of each plant at the early flowering stage after 35 days of growing in soil, except for high-producing SxPv1.0 lines, which were sampled after 54 days in soil due to their slower development. All samples were frozen in liquid nitrogen immediately after collection and ground afterwards.

Pheromone analysis

Targeted analysis of pheromone production was performed as previously described (Mateos-Fernández et al., 2021). In short, 50 mg of frozen, ground leaf tissue was weighed in a 10-ml headspace screw-cap vial and stabilised by adding 1 ml of 5 M $CaCl_2$ and 150 µl of 500 mM EDTA (pH = 7.5), after which it was sonicated for 5 min. Volatile compounds were captured by headspace solid phase microextraction (HS-SPME). Vials were first incubated at 80°C for 3 min with agitation at 500 rpm. The fibre was then exposed to the headspace of the vial for 20 min under the same conditions of temperature and agitation. Desorption was performed at 250°C for 1 min (splitless mode). Oven conditions started with an initial temperature of 160°C for 2 min, a 7°C min^{-1} ramp until 280°C, and a final hold at 280°C for 6 min. Identification of compounds was performed by the comparison of both retention time and mass spectrum with pure standards (for pheromones) or by comparison between the mass spectrum for each compound with those of the NIST 2017 Mass Spectral Library. Quantification was performed based on measured areas under the curve for pheromone peaks, divided by the total ion count (TIC) of the corresponding sample.

RNA-Seq and differential expression analysis

Four plant samples per line were selected for RNA isolation and RNA-Seq analysis. RNA was extracted with the GeneJET Plant RNA Purification Mini Kit (Thermo Fisher Scientific, Waltham, MA, USA). Cleaned RNA was DNase treated and quality checked with Bioanalyzer (Agilent, Santa Clara, CA, USA). Preparation of a strand-specific transcriptome library and sequencing on the Illumina HiSeq platform with 150-bp paired-end reads were done by Novogene. Quality control of the reads was performed with FastQC (Andrews, 2010), and quality reports were merged into the final report with MultiQC (Ewels et al., 2016). Mapping with parameters mismatch cost 2, insertion cost 3, deletion cost 3, length fraction 0.9, and similarity fraction 0.9 and read summarisation (counting uniquely mapped paired reads as one) were done in CLC Genomics Workbench 21.0.5 to the *N.*

benthamiana reference genome, kindly provided by the *Nicotiana benthamiana* Sequencing Consortium (scaffolding v3.5, annotation v3, downloaded from https://www.nbenth.com/ on 15.12.2021). Differential expression analysis was performed in R, using R packages edgeR and limma (Law et al., 2018) with TMM normalisation. Genes with expression levels below a defined threshold were filtered out before normalisation using the filterByExpr function (min.count = 50 and min.total.count = 100). Experiments with SxPv1.0 and v1.2 plants were analysed separately, contrasting high-producing lines and low-producing lines to wt plants grown for each of the two experiments. Based on quality control (Supplementary Presentation S1), three samples (v1.0-wt-1, v1.0-high1-4, and v1.0-high2-4) were excluded from further analyses. Tables with total read counts as well as differential expression analysis results with log_2 fold change (logFC) and adjusted p-values (pAdj) are deposited at GEO along with raw sequencing reads (series accession GSE192369) and are also available as a supplement to this manuscript (Supplementary Data Sheet S1). Transgene expression was determined by mapping Illumina reads to the coding sequences of all three transgenes (see Mateos-Fernández et al. (2021) for description of gene constructs and their sequences) with CLC Genomics Workbench 21.0.5. The obtained total counts were multiplied by the calculated sample TMM normalisation factors to correct for library sizes and divided by gene lengths to obtain normalised counts per kilobase of sequence.

Functional annotation

Automated functional annotation of gene models from *N. benthamiana* genome v3.5 with MapMan ontology (Thimm et al., 2004) was performed with two versions of the Mercator software: 3.6 (Lohse et al., 2014) and 4v2.0 (Schwacke et al., 2019), mapping to MapMan v.3 and MapMan4 Ontology, respectively. MapMan v.3 ontology was used for generating MapMan mapping and GSEA gene set files using custom Perl scripts. Protein sequences were also submitted to InterProScan using interproscan-5.50-84.0 for annotation with Pfam and InterPro protein families (Jones et al., 2014). For translation between *Arabidopsis thaliana* (ath; Araport 11, Cheng et al., 2017) and *N. benthamiana* (nbe; v3.5) proteins, reciprocal best BLAST (RBB) matches from both directions were determined (ath *vs.* nbe and nbe *vs.* ath). If the match between a particular ath and nbe protein sequence was present in both unfiltered BLAST output result files (from both directions) and if E-value $\leq 10^{-20}$ for both directions, the match between the species was kept.

Gene set enrichment analysis

For Gene Set Enrichment Analysis, we used GSEA 4.2.1 software (Subramanian et al., 2005). RNA-Seq counts were

2.3. Transcriptional Deregulation of Stress-Growth Balance in Nicotiana benthamiana Biofactories Producing Insect Sex Pheromones

53

filtered, TMM-normalised (using edgeR package), and transformed to logCPM ($\log_{10}$ counts per million). We excluded samples v1.0-wt-1, v1.0-high1-4, and v1.0-high2-4 from GSEA, as explained above. MapMan v.3 BINs were used as gene sets and GSEA was run as previously described (Ramšak et al., 2021).

Differential VOC abundance

Statistical analysis of non-targeted volatilome data from Mateos-Fernández et al. (2021) was done by comparing $\log_{10}$-transformed peak areas measured in arbitrary units (a.u.) and statistical testing with Kruskal–Wallis one-way analysis of variance combined with the pairwise Wilcoxon rank-sum test.

Visualisation of differentially expressed genes in MapMan and knowledge networks

Differentially expressed genes were visualised in the context of biological pathways and processes in MapMan v3.6.0 using the custom mapping file generated with Mercator 3.6. Differential network visualisations were performed using DiNAR (Zagorščak et al., 2018) utilising two embedded prior knowledge networks: Plant Immune Signalling network and *A. thaliana* Comprehensive Knowledge Network (Ramšak et al., 2018). To translate *N. benthamiana* v3.5 gene models to both *A. thaliana* and *Solanum tuberosum* gene nodes in either of the two networks, we used RBB translation of *N. benthamiana* genes to *A. thaliana* (see above). Since for many gene IDs there was more than one identified homolog, we used a prioritisation script (available at https://github.com/NIB-SI/DiNAR/tree/master/IDprioritization) for choosing the most interesting homolog based on the logFC and pAdj values in our differential expression dataset. Its outputs, used as inputs for DiNAR, are available in Supplementary Data Sheet S2.

Results

SxP are transgenic *N. benthamiana* moth sex pheromone biofactories (Figure 1A) with a growth penalty phenotype. To improve their potential as living biodispensers, we were interested in deciphering the underlying molecular changes associated with high production and identifying potential targets for growth optimisation. Therefore, we performed RNA-Seq on leaf samples from high- and low-producing SxP lines of v1.0 and v1.2 as well as wt *N. benthamiana* and analysed them in relation to growth and pheromone content data.

High-producing SxPv1.2 plants accumulate the highest amounts of pheromones but still maintain better growth compared to v1.0 high producers

Similar to our previous study (Mateos-Fernández et al., 2021), the sampled SxP lines showed different extents of growth penalty (Figure 1B; Supplementary Figure S1). SxPv1.0 low producers (v1.0-l) had little to no growth penalty, with plant heights at sampling time not differing significantly from wt plants (Figure 1B). High producers of v1.0 (v1.0-h) showed the most severe growth penalty with the lowest heights and the biggest developmental delay as they reached the same stage (determined by the number of fully developed leaves) as wt and low-producing plants 19 days later. SxPv1.2 (v1.2-h) plants reached the same developmental stage as wt plants at the time of sampling but were still significantly smaller compared to wt plants. The differences in heights of wt plants grown along each of the SxP versions (Figure 1B) could be attributed to different seasons when the experiments were performed (Supplementary Table S1); therefore, comparisons were made for each experiment separately.

SxPv1.2 high producers accumulated the highest amounts of all three pheromone compounds (Figure 1C; Supplementary Figure S1). The highest production of (*Z*)-11-hexadecenyl acetate in SxPv1.2 is in accordance with their genetic background, as they contain a functional and full-length acetyltransferase gene (*EaDAcT*), while SxPv1.0 do not. The truncated *EaDAcT* transcript in SxPv1.0 also seemed to be less stable, as the read counts were substantially lower in v1.0 compared to v1.2 (Figure 1D). SxPv1.2 accumulated (*Z*)-11-hexadecen-1-ol at higher levels compared to v1.0 high producers as well, which differs from the results of our first study (Mateos-Fernández et al., 2021), where the (*Z*)-11-hexadecen-1-ol accumulation was lower in SxPv1.2. This could be attributed to the fact that in the previous work, first-generation v1.2 plants were used, while in this study, we sampled and analysed their progeny. Despite the much higher production of (*Z*)-11-hexadecenyl acetate in SxPv1.2, the pool of the precursor (*Z*)-11-hexadecen-1-ol did not seem to be affected, supporting the need for the improvement of the rate-limiting acetyltransferase step (Kallam et al., 2022).

High producers clearly show more severe penalty than low producers, indicating that a certain pheromone production level needs to be reached to trigger growth impairment. However, the extent of growth penalty in high producers cannot be unambiguously linked to the amount of accumulated pheromones, as demonstrated by absence of correlation between plant height and the amount of accumulated pheromones within each high-producing group (Supplementary Figure S2), as well as the fact that v1.2 high producers with higher accumulation of all three compounds

grow better than v1.0 high producers. This indicates that, besides direct toxicity of produced compounds and/or metabolic limitations, other mechanisms might underlie the observed growth limitation.

Moth pheromone production rate is reflected in the extent of transcriptional changes

To explore the possible underlying molecular changes causing growth penalty in pheromone-producing lines, we analysed the transcriptomes of SxP and wt plants. Gene expression in all three groups (v1.0-l, v1.0-h, and v1.2-h) was contrasted against the respective wt group for each of the SxP versions. Out of 57,221 genes defined in the *N. benthamiana* v3.5 genome, 31,114 genes were expressed above the threshold in either of the two sampling experiments and were considered for differential expression testing, which gave 9,707 differentially expressed genes ($|logFC| > 1$, pAdj < 0.05) in at least one of the three comparisons (Figure 2A).

The results pointed towards a weak transcriptional response in SxPv1.0 low producers, as we identified only four differentially expressed genes. Nevertheless, the differential expression of genes in each of the low-producing lines in contrast to wt separately resulted in seven differentially expressed genes in v1.0-low1 and 350 differentially expressed genes in the v1.0-low2 line (Figure 2B). This difference is a result of the fact that the gene expression profiles of the low1 line were more similar to wt than the low2 line (Supplementary Figure S3). Transcriptomic results coincide with pheromone production, as v1.0-low2 accumulated higher levels of (Z)-11-hexadecenal

compared to v1.0-low1 (Supplementary Figure S1). This indicates a stronger transcriptional response in low producers with higher accumulation of hexadecenal and therefore the potential of a dose-dependent transcriptional response to pheromone production, at least at lower production values.

Transcriptional reprogramming is considerably more extensive in high producers of both v1.0 and v1.2 with 7,734 and 6,584 differentially expressed genes, respectively, out of which 4,613 were differentially expressed in both versions (Figure 2A). Transcriptional profiles of high producers of both SxP versions show higher similarity between lines than low producers do (Supplementary Figure S3), which might be a consequence of more homogenous pheromone accumulation within each version (Supplementary Figure S1). Therefore, we decided to proceed with expression analyses in high producers with samples grouped into SxPv1.0 and SxPv1.2 high producers and not into separate lines.

Moth pheromone biosynthesis triggers stress-like transcriptional response in high producers

For biological interpretation of the transcriptome data, we generated different *N. benthamiana* gene annotations: MapMan BINs and descriptions according to v.3 and 4 of the ontology, InterPro and Pfam IDs, and closest *A. thaliana* gene matches as determined by the reciprocal best BLAST (RBB) approach. Out of 57,221 genes, we got MapMan ontology annotations (assignment to any BIN, except for BIN 35 "not assigned") for 32,467 genes with the v.3 and for 25,610 genes with the version 4 of the ontology (Supplementary Data Sheet S3). MapMan ontology

FIGURE 2
Transcriptional reprogramming is specific for high-producing SxP. Venn diagrams of differentially expressed genes when contrasting **(A)** samples from pheromone producing plants (v1.0-l, v1.0-h, and v1.2-h with N = 8, 6, and 8, respectively) to wt *N. benthamiana* plants or **(B)** samples from the two individual lines of low pheromone-producing plants (v1.0-low1, v1.0-low2, both N = 4) to wt plants. Numbers on the top correspond to upregulated genes and numbers in italic on the bottom to downregulated genes ($|logFC| > 1$, pAdj < 0.05).

annotation was used to construct a MapMan mapping file and a GSEA gene set file, which can be used as direct inputs in both applications (Supplementary Data Sheet S4, Supplementary Data Sheet S5), providing a valuable resource for *N. benthamiana* transcriptomic analyses in various applications.

Pathway analysis of gene expression changes in v1.0 and v1.2 high producers revealed transcriptional reprogramming towards stress responses. Gene sets (MapMan BINs) related to photosynthesis, DNA synthesis, protein synthesis, lipid synthesis, and cell wall metabolism were enriched with downregulated genes, while gene sets related to secondary metabolism, hormone metabolism, stress, protein degradation, lipid degradation, and some families of transcription factors showed enrichment with upregulated genes (Figure 3; Supplementary Data Sheet S6). Although the directionality of response was parallel between the v1.0 and v1.2 producers, some processes did show potentially important differences in magnitude of the response (Figure 3; Supplementary Data Sheet S6).

Despite of the small number of differentially expressed genes in v1.0 low producers, some pathway changes detected by GSEA, such as enrichment of gene sets related to DNA synthesis and protein synthesis with downregulated genes and of gene sets related to secondary and hormone metabolism with upregulated genes, showed the same pattern as in high producers (Figure 3A). Furthermore, starch degradation as well as MADS-box and AUX/IAA transcription factor families were enriched with upregulated genes in low producers but not in high producers (Supplementary Data Sheet S6).

SxP high producers show significant differences in expression of secondary metabolism-related genes, leading to volatilome changes

Functional analyses revealed differences in the extent of transcriptional reprogramming of secondary metabolism-related genes between the two SxP versions, with broader and more intense changes in v1.0 high producers compared to v1.2 high producers (Figure 3; Supplementary Data Sheet S1), especially in the phenylpropanoid pathway. Homologs of *PAL*, *C4H*, and *4CL* (descriptions and identifiers for all gene short names used in the manuscript are listed in Supplementary Table S2), all directing carbon flow towards various branches of phenylpropanoid metabolism, have stronger upregulation in v1.0 high producers (Figure 4). To connect these transcriptome changes with metabolite abundance, we have reanalysed previously published volatilome datasets (Mateos-Fernández et al., 2021, Supplementary Table S3). Activation of phenylpropanoid biosynthesis on the transcriptomic level correlates with the increase in 3-methylbenzaldehyde abundance in the volatilome of SxP (Figure 4A). Higher production of phenylpropanoids through activation of their biosynthesis might therefore also result in increased abundance

of phenylpropanoid-derived volatile organic compounds. SxP high producers also produced more green leaf volatiles, oxylipin-derived compounds resulting from the activity of 13-lipoxygenases (13-LOX), whose gene expression was strongly activated in SxP high producers (Figure 4B).

High pheromone production prompts significant reprogramming of hormonal signalling

Other pheromone production-related changes evident from transcriptomic data were considerable shifts in expression of hormone metabolism and signalling genes in high producers (Figure 5B). Abscisic acid (ABA)-related BINs were enriched in both low and high producers (Figure 3A; Supplementary Data Sheet S6), with several differentially expressed genes in high producers (Supplementary Table S4), indicating activation of ABA signalling. Specifically, ABA receptor subfamilies PYL1/2-like and PYL8/9-like were downregulated and upregulated in high producers, respectively (Supplementary Table S4). PYL8/9-like upregulation could indicate higher sensitivity of SxP high producers to growth-inhibiting effects of ABA, since the *pyl8a*, *pyl8b*, and *pyl8c* mutants are insensitive to ABA for growth and development inhibition in shoots (Pizzio et al., 2022). Downstream ABA signalling was activated as well, as evidenced by upregulation of genes with homology to ABA-responsive *ABF2* and *ABF3* transcription factors.

Interestingly, jasmonic acid (JA) biosynthesis and signalling showed a stronger pattern of upregulation in v1.0 compared to v1.2, as was also determined by GSEA (Supplementary Data Sheet S6). Gibberellic acid (GA) biosynthesis-related genes showed a distinct pattern of regulation, with strong downregulation of *GA20ox*, encoding a key enzyme in GA biosynthesis, and upregulation of *GA2ox*, *GA3ox*, and *GID1* expression (Figure 5A). *GA2ox* homologs with homology to *GA2ox1* and *GA2ox2* had higher expression, while those with homology to *GA2ox9* had lower expression in high-producing SxP. Since GA is a known stimulator of growth in general, deregulation of its biosynthesis and signalling, promoted by JA upregulation, might be a plausible explanation behind the dwarf phenotype of high-producing SxP (Figure 5C).
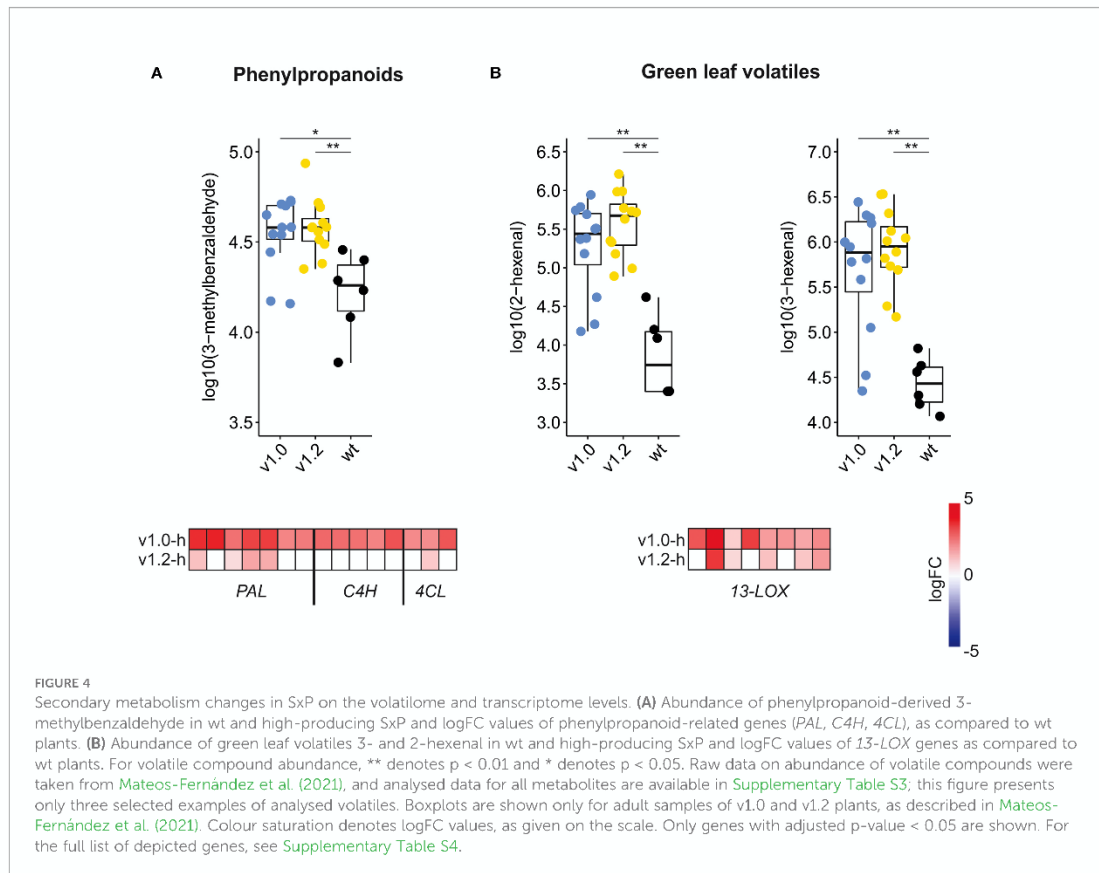
Jasmonic acid signalling shows consistent upregulation with a stronger response in v1.0 compared to v1.2 high producers

Following the results of pathway analyses, which pointed to an orchestrated transcriptional reprogramming of hormonal signalling networks in high-producing SxP, we decided to use knowledge networks of plant gene interactions to further explore

FIGURE 3

Functional analysis of differentially expressed genes in SxP. **(A)** Gene set enrichment analysis of SxP presented as a heatmap. Gene sets (MapMan BINs) enriched with downregulated genes are shown in blue and gene sets enriched with upregulated genes are shown in red. Contrasting was done for each of the transgenic groups (v1.0-l, v1.0-h, v1.2-h) against wt plants. The colour intensity follows the portion of genes in each gene set that contributed to the enrichment score, as given on the scale at the bottom right of the heatmap. Only selected gene sets with q-value <0.01 are shown, manually grouped into functional clusters given in the figure. A full list of enriched gene sets and gene sets depicted in this figure is presented in Supplementary Data Sheet S6. **(B)** MapMan visualisation of metabolism-related differentially expressed genes in SxPv1.0 (top) or SxPv1.2 (bottom) high producers. Only genes with |logFC| > 1 and pAdj < 0.05 in at least one of the comparisons are displayed. Colour intensities correspond to logFC values (red for positive and blue for negative values) and are given on the scale.

active signalling connections and hubs. For that, we have generated homology-based translations of 33,372 *N. benthamiana* genes to *A. thaliana* genes (Supplementary Data Sheet S3), enabling usage of differential network analysis with DiNAR (Zagoršćak et al., 2018). We visualised differentially expressed genes in the context of two embedded knowledge networks—the Plant Immune Signalling network (PIS) and the *Arabidopsis thaliana* Comprehensive Knowledge Network (CKN) (Ramšak et al., 2018). In the PIS network, which

encompasses ethylene (ET), salicylic acid (SA), and JA signalling, the latter showed the most consistent upregulation of all biosynthesis genes, as well as activation of downstream signalling (Figure 6A; Supplementary Data Sheet S2). Activation of JA signalling was evident also in CKN with the *MYC2* node and its first neighbours showing transcriptional upregulation (Figure 6B). The transcriptionally regulated genes included JA biosynthesis genes (*13-LOX*, *AOC*, *4CLL5*, *CYP74A*), biotic stress-related genes (*HEL*, *CHI-B*), and JA signalling genes

FIGURE 4
Secondary metabolism changes in SxP on the volatilome and transcriptome levels. **(A)** Abundance of phenylpropanoid-derived 3-methylbenzaldehyde in wt and high-producing SxP and logFC values of phenylpropanoid-related genes (*PAL, C4H, 4CL*), as compared to wt plants. **(B)** Abundance of green leaf volatiles 3- and 2-hexenal in wt and high-producing SxP and logFC values of *13-LOX* genes as compared to wt plants. For volatile compound abundance, ** denotes p < 0.01 and * denotes p < 0.05. Raw data on abundance of volatile compounds were taken from Mateos-Fernández et al. (2021), and analysed data for all metabolites are available in Supplementary Table S3; this figure presents only three selected examples of analysed volatiles. Boxplots are shown only for adult samples of v1.0 and v1.2 plants, as described in Mateos-Fernández et al. (2021). Colour saturation denotes logFC values, as given on the scale. Only genes with adjusted p-value < 0.05 are shown. For the full list of depicted genes, see Supplementary Table S4.

(*TIFY6B*, *TIFY10A*, *TIFY10B*) upregulated in both v1.0 and v1.2 high producers, with a more prominent activation in v1.0. Active edges in the PIS network also indicate possible interactions between JA signalling and ET (through *EIN3*), as well as SA (through *WRKY70* and *MYB73*) and auxin (AUX) (through *WRKY57*) signalling (Figure 6A). *WRKY57* was previously indicated as a defence-enhancing transcriptional regulator involved in the core JA-mediated stress-growth regulatory model in *A. thaliana* (Zhang et al., 2020).

Discussion

Sustainable production of insect sex pheromones in plant biofactories is currently an emerging topic in plant biotechnology (Xia et al., 2021; Mateos Fernández et al., 2022; Xia et al., 2022). Sexy Plant, a transgenic *N. benthamiana* moth pheromone biofactory, is a bioproduction platform with a constitutive expression of an entire moth sex pheromone biosynthetic pathway, producing and emitting the desired final products (Mateos-Fernández et al., 2021). Induced growth penalty,

coinciding with high pheromone production, was recognized as one of the important obstacles in SxP development (Mateos-Fernández et al., 2021). Engineered plants with constitutive transgene expression are often reported to exhibit different deleterious growth and development-related phenotypes, described for production of Pr55^{gag} protein (Scotti et al., 2015), anthocyanins (Fresquet-Corrales et al., 2017), betalain (Polturak et al., 2016), patchoulol (Wu et al., 2006), and squalene (Wu et al., 2012), among others. In astaxanthin-producing tobacco, introduction of inducible, instead of constitutive, production abolished the oxidative stress response and resolved growth penalty (Agrawal et al., 2022), suggesting that change in redox potential was the underlying cause of growth penalty. To gain comprehensive insight into bioproduction-induced growth restrictions in SxP, we have analysed whole-genome transcriptome of transgenic lines with different pheromone production and growth phenotypes.

The transcriptional changes in SxP indicated that the growth penalty was not solely a consequence of a higher metabolic burden imposed by the transgene expression but rather the result of signalling pathways perturbation. The new *N.*

FIGURE 5

Changes in expression of hormone biosynthesis and signalling genes in SxP high producers. **(A)** Expression of GA-related genes. Colour saturation denotes logFC values, as given on the scale. Only genes with adjusted p-value < 0.05 in at least one group are shown. For the full list of depicted genes, see Supplementary Table S4. **(B)** Directionality of hormonal regulation, as summarised from results of differential expression analysis and GSEA (Supplementary Data Sheet S1, Supplementary Data Sheet S6). − denotes general downregulation, + denotes general upregulation, and +/- denotes changes in both directions. **(C)** Schematic representation of the proposed JA-GA interplay behind SxP growth penalty (created with BioRender.com).

benthamiana functional annotations and translations to *A. thaliana* helped us to deduce that vast transcriptomic reprogramming in high producers of both SxP versions might be related to stress or development-induced hormonal changes. We therefore focused on hormonal deregulation as a possible explanation for the growth phenotype. Although several genes related to different plant hormones were differentially regulated (Figure 5B), network analyses identified JA to be most consistently and strongly activated both on the level of its biosynthesis and on downstream signalling, evidenced by the activation of the key transcriptional regulator *MYC2* (Figure 6). JA is a major regulator of plant growth, defence, and development, whose elevated levels enhance the plant's defences but also lead to reduced growth (Attaran et al., 2014; Huang et al., 2017; Savchenko et al., 2019). It also activates biosynthesis of different plant secondary metabolites (Baebler

et al., 2002; Wasternack and Strnad, 2019), which was observed for the phenylpropanoid pathway in SxP high producers on both the transcriptional and metabolic levels, the latter detected in their volatilome profiles (Figure 4).

Interestingly, the *de novo* lipid biosynthesis pathway was transcriptionally downregulated (Figure 3A), potentially as a direct response to the increased consumption of C16 fatty acids and by that acetyl-CoA due to pheromone biosynthesis, limiting the availability of acetyl-CoA for other anabolic processes. It is known that *Atr*Δ11 desaturase has a high transformation rate (Ding et al., 2014), supporting the hypothesis of a strong drain imposed on the lipid biosynthesis by pheromone production. Activation of *LOX-13* with concurrent downregulation of fatty acid biosynthesis could limit biosynthesis of other lipid compounds, while providing enough precursors for biosynthesis of stress-related JA and green leaf volatiles.

FIGURE 6

Differentially expressed genes in SxP high producers visualised in knowledge networks. **(A)** Visualisation in the Plant Immune Signalling network with differential expression data for v1.0 high producers (v1.0-h). **(B)** Visualisation of the *MYC2* node and its first neighbours in the Comprehensive Knowledge Network. Differential expression in v1.0 high producers is shown on top and in v1.2 high producers on the bottom. In both networks, only genes with adjusted p-values < 0.05 are shown. When two genes connected with an edge had expression values supported by adjusted p-values < 0.05, the corresponding edge is as shown in darker grey. Colouring and size of nodes denote logFC values, as given on the scale on the right side of the figure. Edges describing the reactions between two nodes are directed and represent activation (full line, unilateral arrows), inhibition (full line), or binding (dashed line, bilateral arrows). Full gene descriptions and identifiers are presented in Supplementary Table S2.

JA-GA interplay is often predicted to be the main regulator of growth-defence trade-offs (Yang et al., 2012) and has been studied in different plant species, including the *Nicotiana* genus. Previous work of Machado et al. (2017) supports the crucial role of hormonal cross talk as a suppressor of growth and carbohydrate accumulation in *Nicotiana attenuata*. In their experimental system, the JA-GA cross talk seems to be responsible for stunted growth, presumably through downregulation of plant photosynthetic capacity as a direct consequence of reduced GA activity. SxP high producers show a distinct regulatory pattern of GA-related genes, namely, strong downregulation of *GA20ox* and upregulation of *GA3ox, GA2ox,* and *GID1* (Figure 5), resembling previously described changes in *N. attenuata* mutants with increased JA levels (Heinrich et al., 2013). Similar regulation of GA biosynthesis genes by JA was recently also shown in tomato, with MYC2 inhibiting *GA20ox* and activating *GA2ox* expression (Panda et al., 2022). Based on this evidence, we propose activation of JA signalling with the coordinate GA suppression as a probable molecular mechanism behind pheromone production-induced growth penalty in SxP (Figure 5C). As evidenced by deregulation in signalling of other plant hormones (Figures 5, 6), e.g., ABA, there is a possibility of a wider cross talk leading to the final growth phenotype.

Despite the clear pattern of JA-related stress signalling upregulation in SxP, repeatedly seen for two different SxP versions in two separate experiments, and appearing as a plausible molecular perturbation orchestrating the growth arrest, we found limited evidence for the triggering mechanisms. It seems that the transcriptional changes and consequential growth penalty cannot be arising from sex pheromone toxicity or metabolic drainage alone, as this would imply stronger JA deregulation and growth arrest in SxPv1.2 compared to SxPv1.0, which was not the case. There was also no correlation between the measured plant heights and levels of any of the three pheromone compounds within each version of high producers (Supplementary Figure S2). Since the versions differ in functionality of the acetyltransferase gene, the changed metabolic flow through the pheromone biosynthetic pathway and consequently the feeding endogenous metabolic pathways might alleviate the stress-inducing potential of pheromone production in SxPv1.2. More severe growth penalty in SxPv1.0 might also be exacerbated by the production of a truncated

and non-functional *Ea*DAcT, potentially burdening the protein turnover machinery independently of the pheromone production levels. The differences in the extent of the transcriptional programming between SxPv1.0 and SxPv1.2 could also be just a consequence of positional effects or other factors, since the plants of SxPv1.0 and SxPv1.2 were grown at different times.

The nature of the stress-inducing mechanisms behind pheromone production in general therefore remains to be elucidated. Insect sex pheromones could be a trigger of JA stress response when produced *in planta*, acting as herbivore-associated molecular patterns (Bruce, 2015), with the example of plant defence activation in response to volicitin, a fatty acid–amino acid conjugate present in insect oral secretions (Truitt et al., 2004). However, following this hypothesis, we should expect a stronger response in higher-producing SxPv1.2, which was not the case. Determining the stress-triggering events would require an alternative experimental approach as adult plants with constitutive transgene expression and pheromone production probably represent an already well-established defensive state. To better understand the events prompting the transition from the normal to stressed state and its major regulatory players (Wang and Zhang, 2021), sampling after production initiation in a well-regulated and non-leaky inducible expression system (e.g. Garcia-Perez et al., 2022; Kallam et al., 2022) could give more conclusive insights.

Most work related to the growth-stress dependence has been done in relation to biotic (Brown and Rant, 2013; Ning et al., 2017; da Silva et al., 2019) and abiotic stressors (Bechtold and Field, 2018). Apart from research dedicated to discerning the growth penalty in plants with modified phenylpropanoid and lignin biosynthesis (Reem et al., 2018; Ha et al., 2021; Panda et al., 2021), no major steps have been taken toward understanding molecular mechanisms underlying fitness costs associated with metabolic engineering and/or transgene expression. Results from the analysis of transcriptional reprogramming in SxP support the possible key role of the JA-GA interplay in the insect sex pheromone production-induced growth penalty. In this case, efforts for improving both productivity and growth of SxP biofactories might benefit not only from approaches aiming to optimise metabolic fluxes but also from targeting stress signalling networks. Proof-of-concept work on mutant *A. thaliana* with uncoupled JA and GA signalling has proven that normal plant growth is attainable even in the presence of stress-inducing signals (Campos et al., 2016; Guo et al., 2018) or that severe growth retardation in stress-tolerant plants overexpressing stress-inducible genes can be overcome by co-expressing growth-enhancing genes (Kudo et al., 2019). Targeting orthologous genes in *N. benthamiana* is thus a promising option for establishing a more robust bioproduction chassis. Additionally, controlled regulation of hormonal pathways might even be desired in plants engineered for production of specialised secondary metabolites, for which precursor biosynthesis is hormonally activated (Lu et al., 2016). Considering the goal of developing SxP as living biodispensers in

fields, future research should also include assessment of stress-growth signalling interplay in multifactorial settings including different environmental conditions (Kliebenstein, 2016).

Taken together, our work presents an example of comprehensive transcriptomic analyses of yield-reducing stress signalling in plant biomanufacturing that could be applied to other production systems and could in the future contribute to more robust insect pheromone bioproduction without unwanted growth traits.

Data availability statement

The data presented in the study are deposited in the Gene Expression Omnibus (GEO, https://www.ncbi.nlm.nih.gov/geo/) repository, accession numbers GSE192369, GSE191269 and GSE192368.

Author contributions

MJ, MP, KG, DO, and ŠB conceived and designed the experiments. MJ, MP, ŽR, EM-G, SG, and RM-F performed the experiments and analysed results. MJ and ŠB drafted the manuscript. All authors contributed to the article and approved the submitted version.

Funding

Acknowledgments

Conflict of interest

The authors declare that the research was conducted in the absence of any commercial or financial relationships that could be construed as a potential conflict of interest.

Publisher's note

All claims expressed in this article are solely those of the authors and do not necessarily represent those of their affiliated organizations, or those of the publisher, the editors and the reviewers. Any product that may be evaluated in this article, or claim that may be made by its manufacturer, is not guaranteed or endorsed by the publisher.

Supplementary material

The Supplementary Material for this article can be found online at: https://www.frontiersin.org/articles/10.3389/fpls.2022.941338/full#supplementary-material

References

Agrawal, S., Karcher, D., Ruf, S., Erban, A., Hertle, A. P., Kopka, J., et al. (2022). Riboswitch-mediated inducible expression of an astaxanthin biosynthetic operon in plastids. *Plant Physiol.* 188, 637–652. doi: 10.1093/plphys/kiab428

Andrews, S. (2010) *FastQC: A quality control tool for high throughput sequence data.* Available at: https://www.bioinformatics.babraham.ac.uk/projects/fastqc/.

Attaran, E., Major, I. T., Cruz, J. A., Rosa, B. A., Koo, A. J. K., Chen, J., et al. (2014). Temporal dynamics of growth and photosynthesis suppression in response to jasmonate signaling. *Plant Physiol.* 165, 1302–1314. doi: 10.1104/pp.114.239004

Baebler, Š., Camloh, M., Kovač, M., Ravnikar, M., and Žel, J. (2002). Jasmonic acid stimulates taxane production in cell suspension culture of yew (*Taxus x media*). *Planta Med.* 68, 475–476. doi: 10.1055/S-2002-32083

Bally, J., Jung, H., Mortimer, C., Naim, F., Philips, J. G., Hellens, R., et al. (2018). The rise and rise of *Nicotiana benthamiana*: A plant for all reasons. *Annu. Rev. Phytopathol.* 56, 405–426. doi: 10.1146/annurev-phyto-080417-050141

Bechtold, U., and Field, B. (2018). Molecular mechanisms controlling plant growth during abiotic stress. *J. Exp. Bot.* 69, 2753–2758. doi: 10.1093/jxb/ery157

Brown, J. K. M., and Rant, J. C. (2013). Fitness costs and trade-offs of disease resistance and their consequences for breeding arable crops. *Plant Pathol.* 62, 83–95. doi: 10.1111/PPA.12163

Bruce, T. J. A. (2015). Interplay between insects and plants: dynamic and complex interactions that have coevolved over millions of years but act in milliseconds. *J. Exp. Bot.* 66, 455–465. doi: 10.1093/jxb/eru391

Campos, M. L., Yoshida, Y., Major, I. T., de Oliveira Ferreira, D., Weraduwage, S. M., Froehlich, J. E., et al. (2016). Rewiring of jasmonate and phytochrome B signalling uncouples plant growth-defense tradeoffs. *Nat. Commun.* 7, 12570. doi: 10.1038/ncomms12570

Cheng, C.-Y., Krishnakumar, V., Chan, A. P., Thibaud-Nissen, F., Schobel, S., and Town, C.D (2017). Araport11: A complete reannotation of the *Arabidopsis thaliana* reference genome.*Plant J.* 89, 789–804. doi: 10.1111/tpj.13415

da Silva, A. C., de Freitas Lima, M., Eloy, N. B., Thiebaut, F., Montessoro, P., Hemerly, A. S., et al. (2019). The yin and yang in plant breeding: the trade-off between plant growth yield and tolerance to stresses. *Biotechnol. Res. Innov.* 3, 73–79. doi: 10.1016/j.biori.2020.02.001

Diego-Martin, B., González, B., Vazquez-Vilar, M., Selma, S., Mateos-Fernández, R., Gianoglio, S., et al. (2020). Pilot production of SARS-CoV-2 related proteins in plants: A proof of concept for rapid repurposing of indoor farms into biomanufacturing facilities. *Front. Plant Sci.* 11, 612781. doi: 10.3389/fpls.2020.612781

Ding, B.-J., Hofvander, P., Wang, H.-L., Durrett, T. P., Stymne, S., and Löfstedt, C. (2014). A plant factory for moth pheromone production. *Nat. Commun.* 5, 3353. doi: 10.1038/ncomms4353

Ewels, P., Magnusson, M., Lundin, S., and Käller, M. (2016). MultiQC: summarize analysis results for multiple tools and samples in a single report. *Bioinformatics* 32, 3047–3048. doi: 10.1093/bioinformatics/btw354

Fresquet-Corrales, S., Roque, E., Sarrión-Perdigones, A., Rochina, M., López-Gresa, M. P., Díaz-Mula, H. M., et al. (2017). Metabolic engineering to simultaneously activate anthocyanin and proanthocyanidin biosynthetic pathways in *Nicotiana spp*. *PloS One* 12, e0184839. doi: 10.1371/journal.pone.0184839

Garcia-Perez, E., Diego-Martin, B., Quijano-Rubio, A., Moreno-Giménez, E., Selma, S., Orzaez, D., et al. (2022). A copper switch for inducing CRISPR/Cas9-based transcriptional activation tightly regulates gene expression in *Nicotiana benthamiana*. *BMC Biotechnol.* 22, 12. doi: 10.1186/s12896-022-00741-x

Guo, Q., Major, I. T., and Howe, G. A. (2018). Resolution of growth–defense conflict: mechanistic insights from jasmonate signaling. *Curr. Opin. Plant Biol.* 44, 72–81. doi: 10.1016/j.pbi.2018.02.009

Ha, C. M., Rao, X., Saxena, G., and Dixon, R. A. (2021). Growth defense trade-offs and yield loss in plants with engineered cell walls. *New Phytologist* 231, 60–74. doi: 10.1111/nph.17383

Heinrich, M., Hettenhausen, C., Lange, T., Wünsche, H., Fang, J., Baldwin, I. T., et al. (2013). High levels of jasmonic acid antagonize the biosynthesis of gibberellins and inhibit the growth of *Nicotiana attenuata* stems. *Plant J.* 73, 591–606. doi: 10.1111/tpj.12058

Huang, H., Liu, B., Liu, L., and Song, S. (2017). Jasmonate action in plant growth and development. *J. Exp. Bot.* 68, 1349–1359. doi: 10.1093/jxb/erw495

Huebbers, J. W., and Buyel, J. F. (2021). On the verge of the market - plant factories for the automated and standardized production of biopharmaceuticals. *Biotechnol. Adv.* 46, 107681. doi: 10.1016/j.biotechadv.2020.107681

Jones, P., Binns, D., Chang, H.-Y., Fraser, M., Li, W., McAnulla, C., et al. (2014). InterProScan5: genome-scale protein function classification. *Bioinformatics* 30, 1236–1240. doi: 10.1093/bioinformatics/btu031

Kallam, K., Moreno-Giménez, E., Mateos-Fernández, R., Tansley, C., Gianoglio, S., Orzaez, D., et al. (2022). Tunable control of insect pheromone biosynthesis in *Nicotiana benthamiana*. bioRxiv. doi: 10.1101/2022.06.15.496242

Kliebenstein, D. J. (2016). False idolatry of the mythical growth versus immunity tradeoff in molecular systems plant pathology. *Physiol. Mol. Plant Pathol.* 95, 55–59. doi: 10.1016/j.pmpp.2016.02.004

Kudo, M., Kidokoro, S., Yoshida, T., Mizoi, J., Kojima, M., Takebayashi, Y., et al. (2019). A gene-stacking approach to overcome the trade-off between drought stress tolerance and growth in arabidopsis. *Plant J.* 97, 240–256. doi: 10.1111/tpj.14110

Law, C. W., Alhamdoosh, M., Su, S., Dong, X., Tian, L., Smyth, G. K., et al. (2018). RNA-Seq analysis is easy as 1-2-3 with limma, glimma and edgeR. *F1000Research* 5, 1408. doi: 10.12688/f1000research.9005.3

Li, J., Mutanda, I., Wang, K., Yang, L., Wang, J., and Wang, Y. (2019). Chloroplastic metabolic engineering coupled with isoprenoid pool enhancement for committed taxanes biosynthesis in *Nicotiana benthamiana*. *Nat. Commun.* 10, 4850. doi: 10.1038/s41467-019-12879-y

Lohse, M., Nagel, A., Herter, T., May, P., Schroda, M., Zrenner, R., et al. (2014). Mercator: A fast and simple web server for genome scale functional annotation of plant sequence data. *Plant Cell Environ.* 37, 1250–1258. doi: 10.1111/pce.12231

Lu, Y., Stegemann, S., Agrawal, S., Karcher, D., Ruf, S., and Bock, R. (2017). Horizontal transfer of a synthetic metabolic pathway between plant species. *Curr. Biol.* 27, 3034–3041. doi: 10.1016/j.cub.2017.08.044

Lu, X., Tang, K., and Li, P. (2016). Plant metabolic engineering strategies for the production of pharmaceutical terpenoids. *Front. Plant Sci.* 7, 1647. doi: 10.3389/fpls.2016.01647

Machado, R. A. R., Baldwin, I. T., and Erb, M. (2017). Herbivory-induced jasmonates constrain plant sugar accumulation and growth by antagonizing gibberellin signaling and not by promoting secondary metabolite production. *New Phytol.* 215, 803–812. doi: 10.1111/nph.14597

Mateos-Fernández, R., Moreno-Giménez, E., Gianoglio, S., Quijano-Rubio, A., Gavaldá-García, J., Estellés, L., et al. (2021). Production of volatile moth sex pheromones in transgenic *Nicotiana benthamiana* plants. *BioDesign Res.* 2021, 9891082. doi: 10.34133/2021/9891082

Mateos Fernández, R., Petek, M., Gerasymenko, I., Juteršek, M., Baebler, Š., Kallam, K., et al. (2022). Insect pest management in the age of synthetic biology. *Plant Biotechnol. J.* 20, 25–36. doi: 10.1111/pbi.13685

Molina-Hidalgo, F. J., Vazquez-Vilar, M., D'Andrea, L., Demurtas, O. C., Fraser, P., Giuliano, G., et al. (2021). Engineering metabolism in *Nicotiana* species: A promising future. *Trends Biotechnol.* 39, 901–913. doi: 10.1016/j.tibtech.2020.11.012

Mora-Vásquez, S., Wells-Abascal, G. G., Espinosa-Leal, C., Cardineau, G. A., and García-Lara, S. (2022). Application of metabolic engineering to enhance the content of alkaloids in medicinal plants. *Metab. Eng. Commun.* 14, e00194. doi: 10.1016/J.MEC.2022.E00194

Ning, Y., Liu, W., and Wang, G.-L. (2017). Balancing immunity and yield in crop plants. *Trends Plant Sci.* 22, 1069–1079. doi: 10.1016/j.tplants.2017.09.010

Owen, C., Patron, N. J., Huang, A., and Osbourn, A. (2017). Harnessing plant metabolic diversity. *Curr. Opin. Chem. Biol.* 40, 24–30. doi: 10.1016/j.cbpa.2017.04.015

Panda, S., Jozwiak, A., Sonawane, P. D., Szymanski, J., Kazachkova, Y., Vainer, A., et al. (2022). Steroidal alkaloids defence metabolism and plant growth are modulated by the joint action of gibberellin and jasmonate signalling. *New Phytol.* 233, 1220–1237. doi: 10.1111/NPH.17845

Panda, S., Kazachkova, Y., and Aharoni, A. (2021). Catch-22 in specialized metabolism: balancing defense and growth. *J. Exp. Bot.* 72, 6027–6041. doi: 10.1093/jxb/erab348

Petkevicius, K., Löfstedt, C., and Borodina, I. (2020). Insect sex pheromone production in yeasts and plants. *Curr. Opin. Biotechnol.* 65, 259–267. doi: 10.1016/j.copbio.2020.07.011

Pizzio, G. A., Mayordomo, C., Lozano-Juste, J., Garcia-Carpintero, V., Vazquez-Vilar, M., Nebauer, S. G., et al. (2022). PYL1- and PYL8-like ABA receptors of *Nicotiana benthamiana* play a key role in ABA response in seed and vegetative tissue. *Cells* 11, 795. doi: 10.3390/cells11050795

Polturak, G., Breitel, D., Grossman, N., Sarrion-Perdigones, A., Weithorn, E., Pliner, M., et al. (2016). Elucidation of the first committed step in betalain biosynthesis enables the heterologous engineering of betalain pigments in plants. *New Phytol.* 210, 269–283. doi: 10.1111/nph.13796

Ramšak, Ž., Coll, A., Stare, T., Tzfadia, O., Baebler, Š., Van de Peer, Y., et al. (2018). Network modeling unravels mechanisms of crosstalk between ethylene and salicylate signaling in potato. *Plant Physiol.* 178, 488–499. doi: 10.1104/pp.18.00450

Ramšak, Ž., Petek, M., and Baebler, Š. (2021). "RNA Sequencing analyses for deciphering potato molecular responses," in *Solanum tuberosum. Methods in molecular biology.* Eds. D. Dobnik, K. Gruden, Ž. Ramšak and A. Coll (New York, NY: Humana), 57–94.

Reem, N. T., Chen, H.-Y., Hur, M., Zhao, X., Wurtele, E. S., Li, X., et al. (2018). Comprehensive transcriptome analyses correlated with untargeted metabolome reveal differentially expressed pathways in response to cell wall alterations. *Plant Mol. Biol.* 96, 509–529. doi: 10.1007/s11103-018-0714-0

Rizvi, S. A. H., George, J., Reddy, G. V. P., Zeng, X., and Guerrero, A. (2021). Latest developments in insect sex pheromone research and its application in agricultural pest management. *Insects* 12, 484. doi: 10.3390/insects12060484

Savchenko, T. V., Rolletschek, H., and Dehesh, K. (2019). Jasmonates-mediated rewiring of central metabolism regulates adaptive responses. *Plant Cell Physiol.* 60, 2613–2620. doi: 10.1093/pcp/pcz181

Schillberg, S., Raven, N., Spiegel, H., Rasche, S., and Buntru, M. (2019). Critical analysis of the commercial potential of plants for the production of recombinant proteins. *Front. Plant Sci.* 10, 720. doi: 10.3389/fpls.2019.00720

Schwacke, R., Ponce-Soto, G. Y., Krause, K., Bolger, A. M., Arsova, B., Hallab, A., et al. (2019). MapMan4: A refined protein classification and annotation framework applicable to multi-omics data analysis. *Mol. Plant* 12, 879–892. doi: 10.1016/j.molp.2019.01.003

Scotti, N., Sannino, L., Idoine, A., Hamman, P., De Stradis, A., Giorio, P., et al. (2015). The HIV-1 Pr55^{gag} polyprotein binds to plastidial membranes and leads to severe impairment of chloroplast biogenesis and seedling lethality in transplastomic tobacco plants. *Transgenic Res.* 24, 319–331. doi: 10.1007/s11248-014-9845-5

Subramanian, A., Tamayo, P., Mootha, V. K., Mukherjee, S., Ebert, B. L., Gillette, M. A., et al. (2005). Gene set enrichment analysis: a knowledge-based approach for interpreting genome-wide expression profiles. *Proc. Natl. Acad. Sci.* 102, 15545–15550. doi: 10.1073/pnas.0506580102

Thimm, O., Bläsing, O., Gibon, Y., Nagel, A., Meyer, S., Krüger, P., et al. (2004). MAPMAN: A user-driven tool to display genomics data sets onto diagrams of metabolic pathways and other biological processes. *Plant J.* 37, 914–939. doi: 10.1111/j.1365-313X.2004.02016.x

Truitt, C. L., Wei, H.-X., and Paré, P. W. (2004). A plasma membrane protein from *Zea mays* binds with the herbivore elicitor volicitin. *Plant Cell* 16, 523–532. doi: 10.1105/TPC.017723

Tschofen, M., Knopp, D., Hood, E., and Stöger, E. (2016). Plant molecular farming: much more than medicines. *Annu. Rev. Anal. Chem.* 9, 271–294. doi: 10.1146/annurev-anchem-071015-041706

Wang, T., and Zhang, X. (2021). Genome-wide dynamic network analysis reveals the potential genes for MeJA-induced growth-to-defense transition. *BMC Plant Biol.* 21, 450. doi: 10.1186/s12870-021-03185-1

Ward, B. J., Gobeil, P., Séguin, A., Atkins, J., Boulay, I., Charbonneau, P.-Y., et al. (2021). Phase 1 randomized trial of a plant-derived virus-like particle vaccine for COVID-19. *Nat. Med.* 27, 1071–1078. doi: 10.1038/s41591-021-01370-1

Wasternack, C., and Strnad, M. (2019). Jasmonates are signals in the biosynthesis of secondary metabolites - pathways, transcription factors and applied aspects - a brief review. *N. Biotechnol.* 48, 1–11. doi: 10.1016/j.nbt.2017.09.007

Wu, S., Jiang, Z., Kempinski, C., Nybo, S. E., Husodo, S., Williams, R., et al. (2012). Engineering triterpene metabolism in tobacco. *Planta* 236, 867–877. doi: 10.1007/s00425-012-1680-4

Wu, S., Schalk, M., Clark, A., Miles, R. B., Coates, R., and Chappell, J. (2006). Redirection of cytosolic or plastidic isoprenoid precursors elevates terpene production in plants. *Nat. Biotechnol.* 24, 1441–1447. doi: 10.1038/nbt1251

Xia, Y.-H., Ding, B.-J., Dong, S.-L., Wang, H.-L., Hofvander, P., and Löfstedt, C. (2022). Release of moth pheromone compounds from *Nicotiana benthamiana* upon transient expression of heterologous biosynthetic genes. *BMC Biol.* 20, 80. doi: 10.1186/s12915-022-01281-8

Xia, Y.-H., Wang, H.-L., Ding, B.-J., Svensson, G. P., Jarl-Sunesson, C., Cahoon, E. B., et al. (2021). Green chemistry production of codlemone, the sex pheromone of the codling moth (*Cydia pomonella*), by metabolic engineering of the oilseed crop camelina (*Camelina sativa*). *J. Chem. Ecol.* 47, 950–967. doi: 10.1007/s10886-021-01316-4

Yang, D.-L., Yao, J., Mei, C.-S., Tong, X.-H., Zeng, L.-J., Li, Q., et al. (2012). Plant hormone jasmonate prioritizes defense over growth by interfering with gibberellin signaling cascade. *Proc. Natl. Acad. Sci. U. S. A.* 109, E1192–E1200. doi: 10.1073/pnas.1201616109

Zagorščak, M., Blejec, A., Ramšak, Ž., Petek, M., Stare, T., and Gruden, K. (2018). DiNAR: revealing hidden patterns of plant signalling dynamics using differential network analysis in R. *Plant Methods* 14, 78. doi: 10.1186/S13007-018-0345-0

Zhang, N., Zhao, B., Fan, Z., Yang, D., Guo, X., Wu, Q., et al. (2020). Systematic identification of genes associated with plant growth–defense tradeoffs under JA signaling in *Arabidopsis*. *Planta* 251, 43. doi: 10.1007/s00425-019-03335-8

2.4 Identification and Characterisation of *Planococcus citri cis-* and *trans-*Isoprenyl Diphosphate Synthase Genes, Supported by Short- and Long-Read Transcriptome Data

Mojca Juteršek, Iryna M. Gerasymenko, Marko Petek, Elisabeth Haumann, Sandra Vacas, Kalyani Kallam, Silvia Gianoglio, Vicente Navarro-Llopis, Ismael Navarro Fuertes, Nicola Patron, Diego Orzáez, Kristina Gruden, Heribert Warzecha, Špela Baebler

This manuscript describes the identification and *in vitro* testing of IDS candidates from the citrus mealybug, *P. citri*, aiming to discover enzymes capable of catalysing the formation of irregular polyprenyl diphosphates. The latter are the main building blocks of mealybug sex pheromones, which are important for mating and used as less toxic insecticides in pest management. To date, no IDSs with irregular coupling activity have been identified in insects. We generated short- and long-read transcriptomic data to obtain contiguous virgin and mated female-specific coding sequence information from *P. citri*. Short reads were *de novo* assembled and used together with full-length sequenced transcripts and genomic data to search for sequences similar to *cis-* or *trans-*IDSs. We found several coding sequences with fully or partially conserved IDS motifs. We determined their putative functions based on sequence similarity searches and performed phylogenetic analysis, which demonstrated several sequences to be paralogous, pointing to different duplication events in the Coccoidea phylogenetic group. We cloned and expressed 11 candidate sequences in *E. coli*, followed by *in vitro* testing of their short-chain IDS activity. Five of them produced regular polyprenyl diphosphates, of which one also produced two different irregular polyprenyl chains. Irregular activity was very low, and none of the two backbones matched the structure of planococcyl acetate, the sex pheromone of *P. citri*. Nevertheless, the identified IDS sequences represent an important platform to study regular and irregular terpenoid biosynthesis in mealybugs and provide candidates whose activity could be improved and adjusted through protein engineering to obtain robust enzymes for use in biotechnology.

The PhD candidate is the first co-author of the manuscript. She contributed by performing quality control analysis of the generated transcriptomic data, searches for sequences similar to IDSs, candidate sequence alignments and phylogenetic analyses. She wrote the manuscript draft and prepared most of the figures and tables.

1 **Identification and characterisation of *Planococcus citri cis*- and *trans*-**
2 **isoprenyl diphosphate synthase genes, supported by short- and long-read**
3 **transcriptome data**

4 Mojca Juteršek[1,2,#,*], Iryna M. Gerasymenko[3,4,#], Marko Petek[1], Elisabeth Haumann[3,4], Sandra

5 Vacas[5], Kalyani Kallam[6], Silvia Gianoglio[7], Vicente Navarro-Llopis[5], Ismael Navarro

6 Fuertes[8], Nicola Patron[6], Diego Orzáez[7], Kristina Gruden[1], Heribert Warzecha[3,4], Špela

7 Baebler[1]

8 [1] National Institute of Biology, Department of Biotechnology and Systems Biology, Večna

9 pot 111, SI-1000 Ljubljana, Slovenia

10 [2] Jožef Stefan International Postgraduate School, Jamova 39, SI-1000 Ljubljana, Slovenia

11 [3] Plant Biotechnology and Metabolic Engineering, Department of Biology, Technical

12 University of Darmstadt, Schnittspahnstrasse 4, 64287 Darmstadt, Germany

13 [4] Centre for Synthetic Biology, Technical University of Darmstadt, Schnittspahnstrasse 4,

14 64287 Darmstadt, Germany

15 [5] Instituto Agroforestal del Mediterráneo-CEQA, Universitat Politècnica de València.

16 Camino de Vera s/n, Valencia, Spain

17 [6] Engineering Biology, Earlham Institute, Norwich Research Park, Norwich, Norfolk, NR4

18 7UZ, UK

19 [7] Institute for Plant Molecular and Cell Biology (IBMCP), Consejo Superior de

20 Investigaciones Científicas (CSIC) - Universitat Politècnica de València (UPV), Valencia,

21 Spain

22 [8] Department of Organic Chemistry, University of Valencia, Burjassot, València, Spain

23

24 [#] These authors contributed equally to the work.

25 *Coresspondence to mojca.jutersek@nib.si

26

27

28   **Abstract**

29   Many insect species rely on diverse terpenoids for their development and interorganismal

30   interactions. However, little is known about terpenoid biosynthesis in insects. The

31   monoterpenoid sex pheromones of mealybugs and scale insects (Coccoidea) are particularly

32   enigmatic, with several species producing unique structures presumed to result from the

33   irregular coupling activity of unidentified isopentenyl diphosphate synthases (IDSs). Enzymes

34   capable of similar transformations have previously only been described from a few plant,

35   bacterial and archaeal species. To investigate if insect irregular monoterpenes can be

36   biosynthesised by similar enzymes, we performed a comprehensive search for IDS coding

37   sequences in the genome of *Planococcus citri*, a widespread agricultural pest. We

38   complemented the available *P. citri* genome data with newly generated short- and long-read

39   transcriptome data. The identified candidate genes had homology to both short- and long-chain

40   IDSs and some appeared to be paralogous, indicating gene duplications and consequent IDS

41   gene family expansion in *P. citri*. We tested the activity of eleven candidate gene products,

42   confirming *in vitro* regular activity for five enzymes, one of which (*trans*IDS5) also produced

43   the irregular prenyl diphosphates, maconelliyl and lavandulyl diphosphate. Targeted

44   mutagenesis of selected aspartates and a lysine in the active site of *trans*IDS5 uncovered their

45   importance for chain-length preference and irregular coupling. This work provides an

46   important foundation for deciphering terpenoid biosynthesis in mealybugs, as well as a

47   potential source of enzymes for the biotechnological production of sustainable insect pest

48   management products.

49   **Keywords**

50   *Planococcus citri*, isopentenyl diphosphate synthase, transcriptome assembly, Iso-Seq,

51   irregular coupling, maconellily diphosphate, lavadulyl diphosphate, planococcyl diphosphate,

52   insect sex pheromones

53

54   ## Introduction

55   Terpenoids are a large class of metabolites produced by organisms in every branch of life. In

56   insects, terpenoids have important roles in development (e.g., juvenile and moulting hormones)

57   and as semiochemicals in intra- as well as interspecific interactions (e.g., sex, aggregating,

58   alarm, dispersal, maturation, anti-aphrodisiac or trail pheromones, and defence compounds)

59   (Tillman et al., 1999; Beran et al., 2019). Of special interest are the terpenoid sex pheromones

60   produced by some mealybug and scale insect species (order Hemiptera, Superfamily

61   Coccoidea). Sex pheromones are species-specific, volatile, long-range attractants. In

62   Coccoidea, they are produced by females to facilitate male navigation during mating and are

63   thus emitted by virgin females, with cessation of production after mating (Zou and Millar,

64   2015). The majority of mealybug (Family Pseudococcidae) and armoured scale insect (Family

65   Diaspididae) sex pheromones identified to date are irregular terpenoid compounds, mostly

66   esterified mono- or sesquiterpenoid alcohols and carboxylic acids (Zou and Millar, 2015;

67   Franco et al., 2022). Chemically synthesised mealybug and scale insect pheromones have been

68   successfully used for pest control, providing a sustainable measure in climate

69   change-challenged agriculture (Vacas et al., 2010; Zou et al., 2013; Zou and Millar, 2015;

70   Lucchi et al., 2019; Daane et al., 2021). Although an extensive body of research has been

71   dedicated to the identification and study of mealybug and scale insect sex pheromones, the

72   biosynthesis of their irregular backbone remains elusive.

73   The first step of terpenoid biosynthesis is catalysed by isoprenyl diphosphate synthases (IDSs

74   or prenyltransferases), which couple the C5 terpene building blocks, isopentenyl diphosphate

75   (IPP) and dimethylallyl diphosphate (DMAPP) into C10 (geranyl diphosphate, GPP), C15

76   (farnesyl diphosphate, FPP), C20 (geranylgeranyl diphosphate, GGPP) and longer prenyl

77   diphosphate precursor chains by sequential condensation steps (Nagel et al., 2019). The prenyl

78   diphosphate chains are then transformed into terpenoid compounds through the activity of

79   terpene synthases (TPSs).

80   IDSs can be classified as either *cis-* or *trans-*, depending on the stereochemistry of the double

81   bond in the reaction product. The two classes are evolutionarily and structurally distinct.

82   *Trans*-IDSs adopt an α-fold and contain two conserved aspartate-rich motifs known as FARM

83   (first aspartate rich motif) and SARM (second aspartate rich motif), which mainly occur as

84   "DDxx(x)D". *Cis*-IDSs, however, lack distinct conserved motifs and adopt the ζ-fold (Nagel

85   et al., 2019). Aspartate-rich motifs in *trans*-IDSs coordinate the Mg^{2+} ions important for

86   generation of the carbocation in the allylic substrate (DMAPP, GPP, FPP or other), which can

87   be attacked by IPP to form the new carbon-carbon (C-C) bond in the alkylation reaction. The

88   coupling step catalysed by IDSs can be also classified based on the orientation of the alkylation

89   reaction. Most IDS enzymes catalyse the formation of regular 1'-4 (head-to-tail) C-C bond

90   between the allylic substrate and IPP, while irregular head-to-middle reactions have been

91   described for some *cis*- and *trans*-IDS enzymes, coupling two DMAPP units or DMAPP with

92   an allylic substrate, forming branched or cyclic polyprenyl chains (Kobayashi and Kuzuyama,

93   2018). To date, only a few enzymes with irregular coupling activity have been identified from

94   plants (Rivera et al., 2001; Demissie et al., 2013), bacteria (Ozaki et al., 2014), and archaea

95   (Ogawa et al., 2016).

96   *Planococcus citri* (Risso, 1813), the citrus mealybug, is a small sucking insect. It is a

97   widespread pest of numerous crops and ornamental plants, causing serious damage and

98   economic losses (Watson, 2023). Its sex pheromone, planococcyl acetate, has an cyclobutane

99   backbone, presumably resulting from irregular IDS coupling. It has been successfully

100 chemically synthesised and deployed in integrated pest management via trap-based

101 management strategies, which require only milligram quantities (Bierl-Leonhardt et al., 1981;

102 Wolk et al., 1986; Dunkelblum et al., 2002; Passaro and Webster, 2004). Alternative

103 management strategies, such as mating disruption, demand larger quantities and, therefore,

104 require low-cost, scalable production methods (Zou and Millar, 2015). Biotechnological

105 production of sex pheromones has been demonstrated recently for lepidopteran pheromones

106 (Mateos-Fernández et al., 2021; Petkevicius et al., 2022) and biotechnological synthesis has

107 been proposed as a sustainable route for large-scale, low-cost pheromone production. However,

108 these methods require knowledge of the biosynthetic pathways.

109 To that end, we performed a comprehensive search of the *P. citri* genome, supported by newly

110 generated short- and long-read sequence datasets of *P. citri* females, to identify candidate

111 *cis*- and *trans*-IDSs. Eleven of the identified IDS sequences were tested for regular and

112 irregular coupling activity, with a focus on the production of short-chain backbones. We

113 confirmed regular coupling activity for five *trans*-IDS candidate enzymes, one of which also

114 produced smaller amounts of the irregular lavandulyl and maconelliyl diphosphates. Our work

115 contributes to understanding of mealybug terpenoid biosynthesis providing a foundation for its

116 biotechnological exploitation.

Results

Planococcus citri short- and long-read transcriptome resource

To complement the available *P. citri* genomic sequence data (*Pcitri*.v1 genome assembly) we generated short and long transcriptome reads by performing RNA-Seq and Iso-Seq. Short Illumina reads from virgin and mated *P. citri* females generated in this study were *de novo* assembled on its own (Figure 1a), and together with other available *P. citri* short-read sequence data, including reads from *P. citri* males (Figure 1b). Virgin and mated female-specific transcriptomic data was generated to obtain information on possible pheromone synthesis-related changes in gene expression. Both assemblies were combined, resulting in 389,962 unique sequences (Figure 1c). After the merge with the long-read transcriptome (Figure 1d), the full consolidated set contained 440,881 unique transcript sequences (Figure 1e), with an average length of 1,356 nucleotides and N50 of 2,908 nucleotides (Table S1). On average, around 80 % of short reads from each sample mapped back to *de novo* transcriptome assembly (Table S2). To retain as much variability as possible, we did not do any further assembly thinning and the presented dataset is, therefore, redundant. Approximately 53 % of the transcripts mapped to the *Pcitri*.v1 genome, with a third of them mapping to the annotated *Pcitri*.v1 gene models. Completeness assessment with BUSCO found 98.7 % complete BUSCOs for the consolidated transcriptome, the majority of which were duplicated (Figure S1). Transcript IDs with their InterPro annotations, information on mapping to *Pcitri*.v1 genome and virgin versus mated female differential expression values are available in Table S3a, as well as on FAIRDOMHub along with a fasta file with all sequences from the consolidated transcriptome (see Data Availability Statement).

140
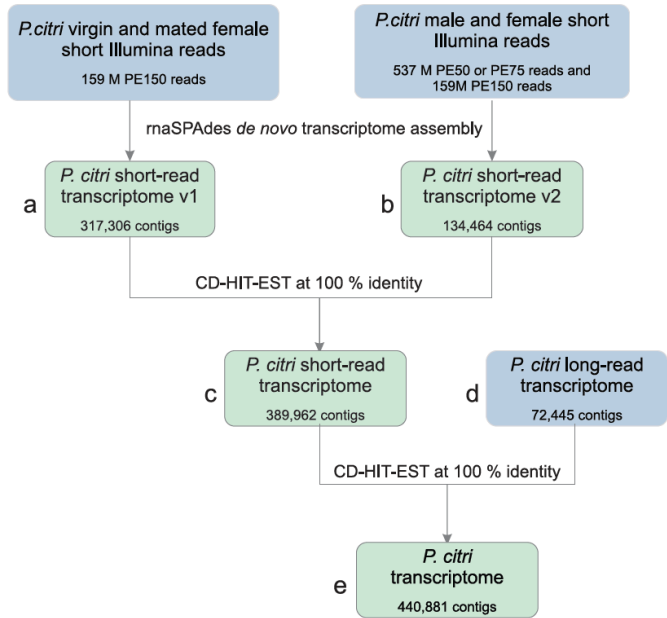
Figure 1: Construction of *P. citri* transcriptome resource. Diagram of consolidation steps taken to combine the short-read (a, b, merged into c) and long-read (d) *P. citri* transcriptome resources into a comprehensive dataset of all assembled and sequenced putative *P. citri* transcripts (e). Raw sequencing data are in blue boxes.

145

Due to the elusive nature of terpenoid biosynthesis in insects, it has been hypothesised that the origin of some terpenoids (or their precursors), might not be the insects themselves, but rather endosymbiotic bacteria or even plant food (Beran and Petschenka, 2022). For a comprehensive analysis of the biosynthetic capacity for terpenoids found in *P. citri*, our transcriptomic resource, therefore, contains transcripts of all taxonomic origins, as we elected not to exclude non-insect reads. Taxonomic analyses revealed that out of 207,753 protein sequences determined from the consolidated transcriptome, 26 % were unclassified, with the majority of classified sequences assigned to insects (Figure S2). 2,641 sequences were assigned to bacteria, 1,010 of which correlated best with sequences from *Candidatus* Moranella endobia, a secondary endosymbiont of *P. citri*. The acquired data also includes 2,364 viral, 1,629 plant, and 4,299 fungal sequences. Of the plant sequences, most were assigned to potato (*Solanum tuberosum*), probably originating from the *P. citri* food source. Of the fungal sequences, most were assigned to *Wallemia mellicola*, a cosmopolitan fungus with air-disseminated spores (Jančič et al., 2015).

Identification of putative IDS coding sequences

160

161   To find sequences with homology to *cis-* and *trans-*IDS enzymes, we searched *Pcitri*.v1

162   genome assembly as well as the *P. citri* consolidated transcriptome (Figure 1e) for sequences

163   with assigned InterPro family annotations IPR001441, and IPR036424 (for *cis*-IDS sequences)

164   or IPR000092 (for *trans*-IDS sequences). On the *Pcitri*.v1 genome assembly we also performed

165   MAST motif search. All extracted sequences (Table S4a and b) were collapsed into clusters

166   based on their sequence similarity. This resulted in a final number of 30 putative IDS sequences

167   (Table S4c). Newly acquired transcript sequence information provided alternative primary

168   sequences to matching *Pcitri*.v1 gene models for seven IDS sequences (Figure 2, Figure S3).

169   For five of them (*cis*IDS1, *trans*IDS4, *trans*IDS5, *trans*IDS11, and *trans*IDS12) we were able

170   to confirm the sequences predicted by the transcriptome data with amplification (Figure 2).

171   Eight of the identified IDS sequences most likely originated from other species: *trans*IDS14

172   has only one mismatch to a FPPS from potato, while *trans*IDS15, *cis*IDS7, and *cis*IDS10 have

173   100 % identity to different IDS sequences from the fungus *Wallemia mellicola*, respectively

174   (Table S4c). *Trans*IDS6, *trans*IDS7, *cis*IDS4, and *cis*IDS6 have homology to insect IDS

175   sequences. However, as determined by phylogenetic analysis (Supplementary Figures S4, S5,

176   S6, and S7), these grouped with homologous sequences from Chalcidoidea wasps

177   (Hymenoptera). Additionally, one sequence can be assigned to a *P. citri* symbiont: *cis*IDS8 is

178   identical to a protein annotated as a UPPS (undecaprenyl diphosphate synthase) from

179   *Candidatus* Moranella endobia.

180
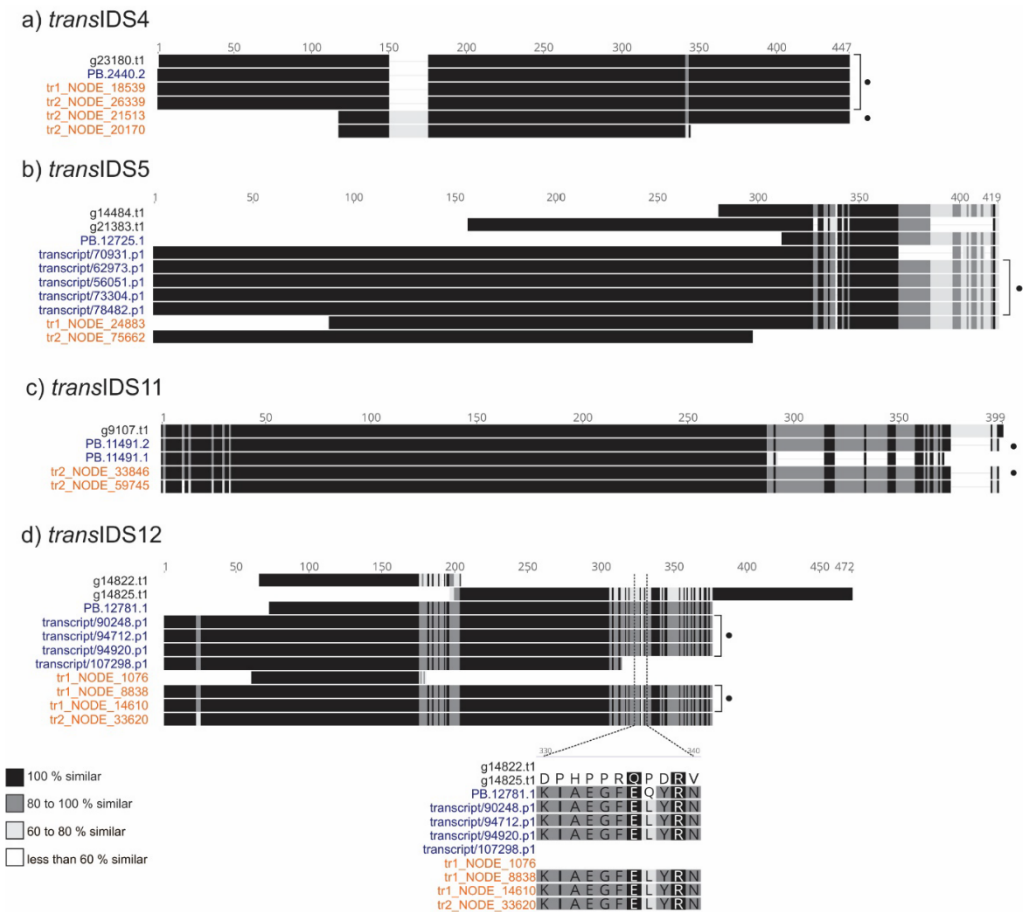
Figure 2: Identification and confirmation of IDS coding sequences predicted by transcriptome data. Multiple sequence alignments for clusters of overlapping transcripts and gene models for candidate sequences *trans*IDS4 (a), *trans*IDS5 (b), *trans*IDS11 (c), and *trans*IDS12 (d). Each cluster includes translated coding sequences obtained from *Pcitri*.v1 gene models (in black text), long-read transcripts (in blue text), and transcripts *de novo* assembled from short reads (in orange text). All sequences are available in Table S4. Sequences confirmed with amplification from cDNA and Sanger sequencing are marked with black dots. Colour-coded sequence similarity is given in the legend in the bottom left. The translated amplicon of *cis*IDS1 has Leu (L327) instead of His at position 327 (H327), the latter predicted in the gene model, while the transcripts all have L327 (not shown in Figure). Two different amplicons were obtained in the case of *trans*IDS4 (a), one identical to the gene model and one with N-terminal truncation and an insertion of 25 amino acids. For *trans*IDS5 (b), the gene model was missing 283 amino acids at the N-terminus. For *trans*IDS11 (c), we amplified a sequence with a frame-shift close to the C-terminus resulting in a 21 amino acids long C-terminus truncation. In the case of *trans*IDS12 (d), two variations of the same full-length sequence were amplified, differing in a single amino acid position: L328 versus Q328. The alignment around the L328 versus Q328 variation is shown below the full length alignments. The structure of the amplified sequence of *trans*IDS12 differed significantly from the annotated gene models. Multiple sequence alignment was done in MEGAX using the MUSCLE algorithm and visualised with Geneious software.

199   ***In silico* analysis reveals diverse putative functions of candidate *P. citri* IDSs**

200   We further analysed the sequence features and phylogeny of identified *P. citri* IDS sequences,

201   which suggested their potential functions (Table 1). Two candidate sequences (*trans*IDS2,

202   *trans*IDS4) are similar to decaprenyl diphosphate synthases (DPPSs), long-chain IDSs that

203   catalyse the formation of the ubiquinone prenyl sidechain, important in aerobic cellular

204   respiration. The functional DPPS enzyme forms a heterodimer of subunits 1 and 2, of which

205   subunit 1 has a higher sequence homology to IDSs, while subunit 2 acts as a regulatory subunit

206   (Zhang and Li, 2013; Song and Li, 2022). TransIDS2 is similar to sequences of DPPS

207   subunit 1, while *trans*IDS4 lacks the D-rich motifs and is similar to sequences of DPPS

208   subunit 2 (Table 1, Supplementary Figure S4, Supplementary Figure S8).

209   *Trans*IDS3 and *trans*IDS5 have high similarity to FPPSs (Table 1, Supplementary Figure S5).

210   Additionally, there are seven sequences (*trans*IDS8, *trans*IDS9, *trans*IDS10, *trans*IDS11,

211   *trans*IDS12, *trans*IDS13, *trans*IDS18) with similarity to FPPS-like sequences from other

212   Coccoidea species (Supplementary Figure S9). All seven of them have a canonical FARM

213   (DDxxD), but not SARM (Table 1). Phylogenetically, the FPPS-like sequences are separated

214   from the mealybug FPPS sequences with low sequence similarity between the two groups

215   (Supplementary Figure S9). Similar diversification pattern of IDS genes within Coccomorpha

216   has been indicated previously (Rebholz et al., 2023). *Trans*IDS3 and *trans*IDS5, as well as

217   *trans*IDS12 and *trans*IDS13 also have high pairwise sequence similarity (78 % and 75 %,

218   respectively), indicating a possibility of more recent duplication events.

219   *Trans*IDS16 is similar to geranylgeranyl pyrophosphate synthases (GGPPS), catalysing the

220   formation of the diterpenoid precursor (Supplementary Figure S10). Sequences of *trans*IDS1,

221   *trans*IDS19, and *trans*IDS20 do not have canonical D-rich motifs. Additionally, *trans*IDS1 is

222   similar to E3 ubiquitin protein ligases, while we could not find any similarity matches for

223   *trans*IDS19 and *trans*IDS20. *Trans*IDS17 is similar to otubain-like ubiquitin thioesterases

224   (Supplementary Figure S11) and includes a DDxxD motif aligning with FARM, as do all other

225   otubain-like orthologs identified from mealybugs and included in the phylogenetic analysis

226   (Supplementary Figure S11).

227   Out of the *cis*-IDS candidates, *cis*IDS1, *cis*IDS2, *cis*IDS3, and *cis*IDS5 are homologous to the

228   catalytic subunit of heterodimeric dehydrodolichyl diphosphate synthase (DHPPS)

229   (Supplementary Figure S6, Supplementary Figure S12), involved in the biosynthesis of

230   dolichol phosphate, the lipid carrier of glycosyl units used for N-glycosylation in eukaryotes.

231   Candidates *cis*IDS2, *cis*IDS3, and *cis*IDS5 have some closer orthologs within the Coccoidea,

232   however they are very distant to other DHPPS sequences and even *cis*IDS1 (Supplementary

233   Figure S12). On the other hand, *cis*IDS9 has highest similarity to sequences of the DHPPS

234   regulatory subunit (Supplementary Figure S7).

235   **Table 1: *P. citri cis*- and *trans*-IDS candidates.** For each candidate sequence, its putative function,

236   differential expression values (logFC), contrasting samples from virgin to mated females, and results of

237   *in vitro* regular (R) and irregular (I) C10 or C15 coupling activity tests of the proteins expressed in *E.*

238   *coli* are given. For *trans*-IDS candidates, amino acids positioned at the first and second D-rich motif

239   (FARM, SARM) according to the multiple sequence alignment are given as well. LogFC (log2-fold

240   changes) values were obtained by averaging logFC values for all sequences in the sequence cluster of

241   each candidate (Table S4c) and are coloured in red and green (for up- and downregulated expression,

242   respectively) if the differential expression was statistically significant (pAdj > 0.05) for at least one of

243   the sequences in each cluster. "/" – activity test not performed. Asterisk denotes the sequence originating

244   from *Candidatus* Moranella endobia.

245

Candidate	FARM	SARM	Putative function	logFC	R	I
*trans*IDS2	DDVID	DDLLD	DPPS subunit 1	0.18	Y	N
*trans*IDS3	DDIID	DDYLD	FPPS	1.20	Y	N
*trans*IDS4	/	/	DPPS subunit 2	0.32	N	N
*trans*IDS5	DDIMD	DDYLD	FPPS	0.22	Y	Y
*trans*IDS8	DDILD	NDYND	FPPS-like	-1.26	/	/
*trans*IDS9	DDIFD	NDYND	FPPS-like	3.11	/	/
*trans*IDS10	DDAID	KDQND	FPPS-like	0.93	N	N
*trans*IDS11	DDALD	NDYYD	FPPS-like	1.61	Y	N
*trans*IDS12	DDIAD	KLYND	FPPS-like	5.49	N	N
*trans*IDS13	DDVVD	KIFND	FPPS-like	-1.22	/	/
*trans*IDS16	DDIQD	DDYCN	GGPPS	0.08	N	N
*trans*IDS17	DDFHD	/	ubiquitin thioesterase	-0.13	Y	N
*trans*IDS18	DDALD	NDYYD	FPPS-like	-0.38	/	/
*cis*IDS1	/	/	DHPPS	0.07	N	N
*cis*IDS2	/	/	DHPPS-like	1.90	/	/
*cis*IDS3	/	/	DHPPS-like	0.09	/	/
*cis*IDS5	/	/	DHPPS-like	0.04	/	/
*cis*IDS8*	/	/	UPPS	NA	N	N
*cis*IDS9	/	/	DHPPS regulatory subunit	0.15	/	/

246

247   **Regular IDS activity was shown for five and irregular activity for one *P. citri* candidate**

248   With the aim of identifying enzymes involved in the synthesis of the irregular C10 sex

249   pheromone, we tested the activity of *P. citri* IDS candidates for producing short polyprenyl

250   chains. We selected 11 *P. citri* candidate sequences with homology to *trans*- or *cis*-IDSs for

251   which the full sequence was confirmed with long-read transcriptome sequencing (Table 1,

252   Table S4c). Two of these sequences (*trans*IDS3 and *trans*IDS10) were synthesised according

253   to long-read sequencing data, and nine sequences (*trans*IDS2, *trans*IDS4, *trans*IDS5,

254   *trans*IDS11, *trans*IDS12, *trans*IDS16, *trans*IDS17, *cis*IDS1, and *cis*IDS8) were amplified from

255   *P. citri* cDNA (Table S4c). All sequences were expressed in *E. coli* and purified recombinant

256   proteins were tested *in vitro* to identify regular and irregular IDS catalytic activity forming C10

257   or C15 backbones.

258   Five *trans*-IDS-like proteins (*trans*IDS2, *trans*IDS3, *trans*IDS5, *trans*IDS11, *trans*IDS17)

259   displayed regular activity (Table 1, Figure 3a). The products of *trans*IDS2, *trans*IDS5,

260   *trans*IDS11, and *trans*IDS17 were identified as geranyl and farnesyl diphosphates based on

261   chromatographic behaviour and mass spectra of diphosphates and their dephosphorylated

262   alcohol derivatives (Figure 3b, Figures S13-S19). Candidate *trans*IDS3 had an unusual pattern

263   of regular products. It formed two isomers of C10 prenyl diphosphate, geranyl and *iso*-geranyl

264   diphosphates, that were further elongated to two C15 isomers: farnesyl and *iso*-farnesyl

265   diphosphate (Figure 3b). Specific activities of *trans*IDS5 were significantly higher than those

266   of the other enzymes, with *trans*IDS3 also exhibiting a relatively high activity for production

267   of C10 prenyl diphosphates (Figure 3a, Table S5). Both *trans*IDS3 and *trans*IDS5 sequences

268   were expressed in *P. citri* females with *trans*IDS3 also differentially expressed between virgin

269   and mated females with higher expression in virgin females (Table 1, Supplementary Table

270   S4c).

271   Moreover, candidate *trans*IDS5 also had a low level of irregular IDS activity, if supplied with

272   DMAPP only (Figure 3b). The enzyme produced two compounds, which were identified as

273   lavandulyl (LPP) and maconelliyl diphosphate (MPP), based on GC-MS spectra of their

274   dephosphorylated derivatives (Figure S20).

275

276
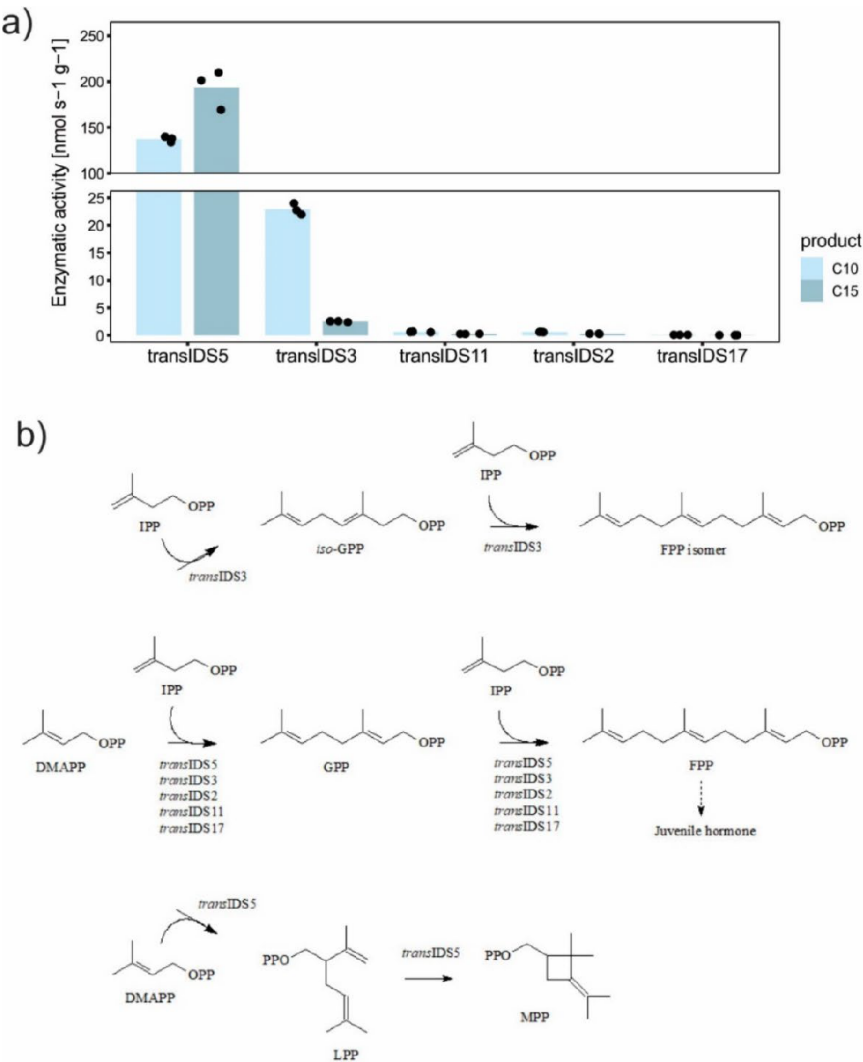
Figure 3: *In vitro* **activity of** *P. citri* **IDS sequences expressed in** *E. coli.* Measured enzymatic activity for production of C10 and C15 prenyl diphosphates (a) and schematic representation of confirmed coupling reactions performed by *P. citri trans*-IDS candidates (b). *Trans*IDS5, *trans*ID11, *trans*IDS2, and *trans*IDS17 produced C10 geranyl diphosphate (GPP) and C15 farnesyl pyrophosphate (FPP); *trans*IDS3 produced C10 GPP and *cis*-isogeranyl diphosphate and two C15 FPP isomers. (a) Activity for production of C10 prenyl diphosphates (light blue bars) and activity for production of C15 prenyl diphosphates (dark blue bars). Height of the bars represents the mean of three separate measurements, plotted as block dots. Raw data is available in Table S5. Note the y-axis break due to much higher activity of *trans*IDS5. We did not detect any C10 or C15 products with other tested candidates (Table 1). In (b), dimethylallyl diphosphate (DMAPP) can be joined to its isomer isopentenyl diphosphate (IPP) to form regular terpenes geranyl and iso-geranyl diphosphates (GPP and iso-GPP) and isomers of farnesyl diphosphate (FPP). Alternatively, two DMAPP units can be assembled into irregular lavandulyl diphosphate (LPP) and maconelliyl diphosphate (MPP). FPP is a precursor for juvenile hormone biosynthesis as denoted by the dashed arrow.

291   To assess the activities of candidate proteins *in vivo* in the eukaryotic cell environment, the
292   candidate IDS sequences were transiently expressed in the plant heterologous expression model
293   *Nicotiana benthamiana*. HPLC-MS analysis of leaf extracts did not reveal irregular terpene
294   diphosphates. Similarly, no production of volatile organic compounds derived from irregular
295   monoterpenoids was detected by GC-MS in agroinfiltrated *N. benthamiana* leaves. Regular
296   activity of candidate proteins could not be assessed in this system due to the presence of native
297   plant regular monoterpenes.

298   **Mutagenesis of *trans*IDS5 active site revealed functional importance of active site residues**
299   **for its enzymatic activity**

300   We further set to identify the amino acid residues important for the irregular coupling activity
301   of *trans*IDS5 by performing mutagenesis. It was suggested that replacement of the first
302   aspartate (D) in SARM with asparagine (N) played an important role in the evolution of
303   irregular coupling activity (Liu et al., 2012). However, in *trans*IDS5, analogous mutation
304   (D308N) caused a complete loss of irregular activity. The same was observed after the
305   exchange of two other aspartate residues in SARM (D309N and D312N), and the first aspartate
306   in FARM (D166N).

307   Moreover, the regular activity of aspartate mutants was affected to different degrees
308   (Figure 4a). The regular activity of D166N mutant was significantly diminished, although the
309   ratio between C10 GPP and C15 FPP was similar to the wild-type (wt) *trans*IDS5 (Figure 4a).
310   D308N and D312N substitutions had impact on the regular product length. Both mutants
311   performed the initial coupling of IPP and DMAPP to C10 chains at levels comparable to the
312   wt enzyme, but the addition of the second IPP to form the C15 chain was hampered compared
313   to the wt (Figure 4a). The regular activity was completely abolished after the D309N exchange
314   (Figure 4a).

315

316
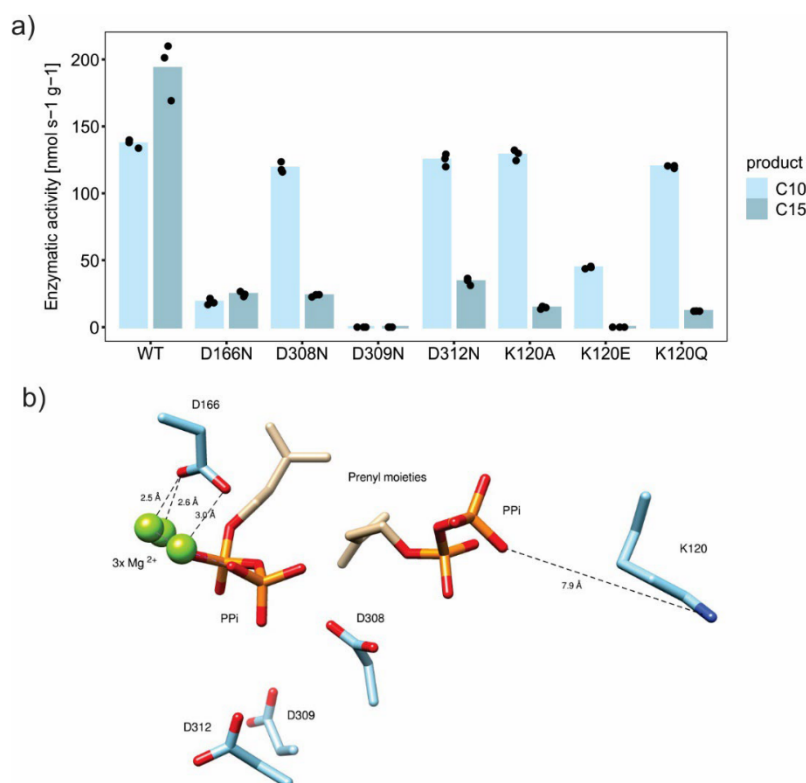
317

Figure 4: Mutagenesis of *trans*IDS5 active site residues. (a) Activity of *trans*IDS5 and its mutants
expressed in *E. coli*. Activity for production of C10 geranyl diphosphate (GPP, light blue bars) and
activity for production of C15 farnesyl diphosphate (FPP, dark blue bars) are plotted. Height of the bars
represents the mean of three separate measurements, plotted as black dots. Raw data is available in
Table S5. (b) Mutated aminoacids and their position in the active site, based on a computational model
of active centre of *trans*IDS5 with two bound substrate molecules showing the aspartate of the first
(D166) and the second (D308, D309, D312) aspartate-rich motifs and lysine 120 (K120). Oxygen atoms
in aspartate side chains and in pyrophosphate moieties (PPi) of the substrates are shown in red; the
nitrogen atom of lysine side chain is highlighted in blue.

327   To find additional residues important for the catalytic activity of *trans*IDS5, we build a

328   computational model of its 3D structure (Figure 4b). We identified a positively charged lysine

329   (K) residue in position 120 located at a comparatively short distance from the negatively

330   charged diphosphate moiety of the substrate (Figure 4b). We exchanged this residue with

331   alanine (K120A), polar uncharged glutamine (K120Q), and negatively charged glutamate

332   (K120E). All three substitutions resulted in the loss of irregular coupling activity, as well as in

333   the diminished elongation of GPP (C10) to FPP (C15). As expected, the K120E exchange,

334   introducing negative charge in the active site, had the most inhibiting effect, precluding FPP

335   formation entirely (Figure 4a).

14

336 **Heteromeric associations did not change IDS activity**

337 In most cases, *trans-* and *cis-*IDSs are active in the form of homodimers (Gao et al., 2012).

338 However, some IDSs form heterodimers with non-catalytic subunits, which modulate or

339 stimulate their activity (Burke et al., 1999; Tholl et al., 2004; Qu et al., 2015; Yin et al., 2017;

340 Zhou et al., 2017; Emi et al., 2019; Dong et al., 2023). To determine if irregular coupling might

341 depend on the presence of other subunits, we tested *P. citri* IDS candidates in combinations

342 with potential interactors (Table S6). In the *P. citri* genome, we identified homologs of the

343 DPPS and DHPPS regulatory subunits (*trans*IDS4 and *cis*IDS9, respectively) and both were

344 combined with all IDS-like candidates in irregular activity assays (Table S6). In addition, we

345 examined two *P. citri* non-IDS-like proteins for their IDS-modifying activities: the protein

346 product of g23689.t1, annotated as a pheromone-binding protein (PBP) and highly expressed

347 in virgin females (Table S3b), and g36424.t1, identified as a *P. citri* homolog of isopentenyl

348 diphosphate isomerase (IDI), an enzyme catalysing the reversible isomerisation of IPP to

349 DMAPP (Table S6). Addition of *P. citri*-IDI to the reaction with IDS candidates supported

350 formation of regular products, if either IPP or DMAPP only were added to the reaction.

351 However, none of the tested putative regulatory subunits altered or spurred irregular coupling

352 activity of IDS candidates.

353 We also tested the hypothesis that heterodimeric complexes consisting of two IDS subunits are

354 required for irregular coupling. Activity assays with DMAPP as the only substrate were carried

355 out with pairwise combinations of *P. citri* IDS candidate proteins with each other as well as

356 with IDS proteins forming irregular prenyl diphosphates (Table S6). The latter allows for

357 detection of terpene synthase (TPS) activities of *P. citri* IDS candidates, converting the prenyl

358 diphosphate substrates into corresponding prenyl alcohols. Combined assays did not reveal any

359 changes to the enzymatic activities of IDS candidates, which also did not demonstrate TPS

360 activity on the tested irregular prenyl diphosphates.

361

362 **Discussion**

363   Sustainable insect pest management, supported by state-of-the-art knowledge and technology,

364   is an integral part of sustainable food production in a changing climate, in which the

365   geographical ranges of many insect species are expected to widen (Schneider et al., 2022).

366   However, the use of biotechnology and genetic solutions depend on detailed information about

367   gene function. In this work, we present the results of a comprehensive search for candidate

368   genes coding for isopentenyl diphosphate synthase (IDS) activity from the citrus mealybug, *P.*

369   *citri*. The identification of these genes has the potential to enable either biological production

370   of *P. citri* sex pheromones or gene silencing approaches, both of which provide novel options

371   for pest management (reviewed in Mateos Fernández et al., 2022).

372   Functional genomics of many insect species is hindered by the lack of well-annotated, high-

373   quality genome sequences (Li et al., 2019; Hotaling et al., 2021). To improve the available

374   genetic resources for *P. citri,* we complemented the existing genome data with short- and

375   long-read transcriptome data (Figure 1). The transcriptomic dataset enabled us to predict and

376   amplify alternative transcript sequences (Figure 2, Figure S3). In addition, we found a novel

377   coding sequence (*trans*IDS5). Using all resources, we were able to identify 18 candidate *P. citri*

378   IDS sequences. Among these were putative DHPPS, FPPS, FPPS-like, GGPPS, DPPS and

379   DPPS-like coding sequences, as well as an ubiquitin thioesterase-like sequence with a D-rich

380   motif (Table 1).

381   However, inferring function from sequence analyses alone is inconclusive for IDSs, as even

382   small changes can alter substrate and chain-length specificity (Wallrapp et al., 2013). To test

383   the activity of IDS candidates, we focused on the detection of C10 and C15 coupling products.

384   We, therefore, did not confirm if the predicted DHPPS, GGPPS and DPPS had longer

385   chain-producing activities. *Trans*IDS16, a predicted GGPPS did not produce any C10 or C15

386   products. Similarly, neither of the two tested *cis*-IDS-like proteins produced detectable levels

387   of regular or irregular C10 or C15 backbones, as both were predicted to be long-chain IDSs,

388   namely DHPPS (*cis*IDS1) and UPPS (*cis*IDS8) (Table 1). Interestingly, *trans*IDS2, a predicted

389   long-chain IDS (DPPS catalytic subunit), produced low amounts of FPP and GPP. This might

390   be attributed to functional promiscuity *in vitro*, producing polyprenyl chains of different

391   lengths, as reported for other IDS enzymes (Lackus et al., 2019). Additionally, *trans*IDS17,

392   which was not homologous to IDS sequences but rather to otubain-like ubiquitin thioesterases,

393   was able to produce regular C10 and C15 backbones, albeit at the lowest rate of all candidates.

394   It remains unknown if otubain-like sequences from other mealybug species have IDS activity,

395   and whether this activity has a biological function.

396   The two putative FPPS sequences (*trans*IDS3 and *trans*IDS5) both displayed regular coupling

397   activity resulting in C10 and C15 units. Our enzymatic activity and gene expression results

398   indicate that *trans*IDS5 might be the major source of C15 terpenes in *P. citri*, while the C10

399   could be mainly composed of *trans*IDS5 and possibly also *trans*IDS3 products. The highest

400   specific activity was measured for *trans*IDS5, also producing low amounts of irregular prenyl

401   diphosphates, LPP and MPP (Figure 3b), which have not been reported in *P. citri*. The

402   2-methylbutanoated versions of both compounds have been identified as the sex pheromone of

403   *Maconellicoccus hirsutus*, the pink hibiscus mealybug (Zhang et al., 2004). Esterified

404   lavandulol compounds act as sex pheromones also in some other *Planococcus*, *Pseudococcus*

405   and *Dysmicoccus* species (Zou and Millar, 2015). However, the irregular coupling activity of

406   *trans*IDS5 only takes place in the absence of IPP and might, therefore, be unlikely to occur

407   *in vivo* where the presence of IPP is expected. Although we did not find conclusive evidence

408   for the role *trans*IDS5 in the biosynthesis of the *P. citri* sex pheromone, we propose that it is

409   the main source of regular sesquiterpenes in *P. citri*, possibly including the juvenile hormone

410   (Figure 3b). Using structure-informed mutagenesis, we additionally demonstrated the

411   importance of K120, D166, D308, D309, and D312 for the irregular coupling mechanism

412   observed for *trans*IDS5 *in vitro* (Figure 4a).

413   Terpenoids are known for their extensive evolutionary divergence, with many instances of

414   lineage-specific pathways and, therefore, metabolites. Despite the occurrence of many

415   common and unique terpenoids in animals, terpenoid diversification is better understood in

416   plants and microbes (Beran et al., 2019; Tholl et al., 2023). In plants, terpenoid diversity is

417   mainly determined by the activity of TPSs, which have high evolutionary divergence and

418   functional plasticity (Karunanithi and Zerbe, 2019). However, sequences with homology to

419   plant and microbial TPSs have not been identified in insect genomes. Instead, numerous

420   instances of IDS gene-family expansion have been observed, with frequent gene duplications

421   resulting in functional redundancy or neofunctionalization (Gilg et al., 2009; Beran et al., 2016;

422   Lancaster et al., 2018, 2019; Darragh et al., 2021; Rebholz et al., 2023). Among the *P. citri*

423   IDS sequences, we observed expansions of FPPS-like sequences and DHPPS-like sequences

424   (Figure S9, Figure S12). The former extends the previously reported FPPS-like diversification

425   within the Coccomorpha (Rebholz et al., 2023). Three FPPS-like sequences were successfully

426   cloned and tested (*trans*IDS10, *trans*IDS11, and *trans*IDS12), however, only one candidate

427 (*trans*IDS11) exhibited IDS activity, producing low amounts of GPP and FPP. Interestingly,

428 while we were not able to confirm GPPS or FPPS activity for *trans*IDS12, its expression was

429 observed to be strongly upregulated in virgin compared to mated *P. citri* females, which was

430 also true for *trans*IDS9, *trans*IDS10, and *trans*IDS11 (Table 1). This differential expression

431 suggests a possible role in mating or reproduction and needs further investigation.

432 Despite detecting two irregular prenyl diphosphate products, none of the IDS-like candidates

433 that we tested displayed coupling activity leading to *cis*-planococcyl diphosphate under our

434 experimental conditions. *In vitro* functional characterization of IDS enzymes can be unreliable,

435 as activity can depend on many factors, including the formation of heteromers (Zhang and Li,

436 2013). To that end, we tested for modulating activity of several potential interactors but did not

437 detect any changes in the activity of *P. citri* IDS candidates.

438 The model of irregular terpenoid biosynthesis via a genome-encoded IDS has been challenged.

439 Alternative hypotheses include the possibility that insects sequester plant-derived compounds

440 or utilise products of their endosymbionts' metabolism. Many studies reveal a straightforward

441 strategy of modification and accumulation of plant defence compounds (Beran and Petschenka,

442 2022), but, in some cases, the derivatives of plant secondary metabolites are also used in sexual

443 communication. For example, fragments of plant pyrrolizidine alkaloids and phenylpropanoid

444 metabolites are reported to make danaine butterfly males more attractive to the co-specific

445 females (Nishida et al., 1991). However, the presence of irregular monoterpene structures has

446 not been reported for known *P. citri* host plants which makes the sequestration hypothesis

447 improbable. Like other insects feeding on nutritionally unbalanced plant sap, mealybugs rely

448 on obligate endosymbiotic bacteria as a source of amino acids and vitamins (Husnik et al.,

449 2013). *P. citri* is a part of a nested tripartite endosymbiotic system, where the insect harbours

450 the   Betaproteobacteria   *Candidatus*   Tremblaya   princeps,   which   contains   the

451 Gammaproteobacteria *Candidatus* Moranella endobia (McCutcheon and Dohlen, 2011; López-

452 Madrigal et al., 2013). Although we were unable to identify any short-chain IDS-coding

453 sequences within the genomes of *P. citri* endosymbionts, we cloned and tested one IDS

454 sequence, a putative UPPS, from *Candidatus* Moranella endobia (*cis*IDS8). However, this did

455 not produce any regular or irregular short prenyl chains. Moreover, genetic crosses between

456 *P. citri* and *Planococcus minor* - the latter producing a branched lavandulol-type

457 monoterpene - indicate that the enzyme responsible for the formation of the irregular terpene

458 skeleton is encoded in the insect nuclear genome and is present at a single locus (Tabata, 2022).

459   The structure of the sex pheromone is also not inherited maternally (Tabata, 2022), as would
460   be expected if synthesis requires the transfer of egg-transmitted endosymbionts.

461   Another possibility is that the mealybug sex pheromones are biosynthesised via a different
462   catalytic mechanism, executed by a different, and as yet unidentified, class of enzymes. Novel
463   terpene synthases have been described, expanding on the canonical models of terpene
464   biosynthesis (Rudolf and Chang, 2020). A recent example is the elucidation of the iridoid
465   pheromone found in the pea aphid, *Acyrthosiphon pisum*. Biosynthesis of this molecule
466   proceeds through the same intermediates as in plants, however, it was shown to involve a set
467   of enzymes which lack homology to the plant counterparts (Köllner et al., 2022). The insect
468   enzymes were identified by transcriptomic analysis of the female hind legs, the site of
469   pheromone biosynthesis (Köllner et al., 2022). Targeted transcriptome analyses of pheromone
470   glands were also useful for determining the genes related to pheromone metabolism and
471   transport in Lepidoptera species (Vogel et al., 2010; Gu et al., 2013; Nuo et al., 2021; Yao et
472   al., 2021). At present, however, such approaches are not possible in *P. citri* as the site of the
473   pheromone gland remains unknown.

474   The identification of the *P. citri* IDS gene family provides an important foundation for
475   deciphering terpenoid biosynthesis in this species as well as other mealybugs. The candidate
476   FPPS and FPPS-like sequences with confirmed regular and irregular activity might also present
477   a starting point for protein engineering; mutations have been shown to increase or even spur
478   irregular coupling activity in IDSs (Chan et al., 2017; Gerasymenko et al., 2022).
479   Diversification of IDS sequences in Coccoidea is an intriguing genomic enigma for future
480   investigation, especially in relation to their capacity for species-specific irregular monoterpene
481   synthesis, a unique feature in this insect superfamily, which still remains elusive.

482

483   Methods

484   Insect rearing and sampling

485   The stock colony of *P. citri* was established in the insectary facilities at the Universitat

486   Politècnica de València (UPV, Valencia, Spain) using specimens from Servei de Sanitat

487   Vegetal of Generalitat Valenciana (GVA, Valencia, Spain). Mealybugs were reared on organic

488   green lemons, maintained in a rearing chamber, in the dark at 24 ± 2 °C, with $40-60$ % relative

489   humidity. Mated females were allowed to oviposit and, when ovisacs were laid, they were

490   gently transferred with an entomological needle to new lemons. To obtain samples of virgin

491   females, some lemons were separated from the main colony and were visually inspected every

492   3–4 days for the presence of male cocoons, which were manually removed with an

493   entomological needle to leave only virgin females. Mated females were sampled on the lemons

494   from the main stock colony after checking for the presence of ovisacs. The production of sex

495   pheromone was confirmed by collection of emitted volatiles from a group of 20–30 virgin

496   females by solid phase microextraction technique (SPME) (Vacas et al., 2017). The identity of

497   the sex pheromone was unequivocally confirmed by full coincidence of its mass spectra and

498   retention time with an analytical standard sample synthesised according to the method

499   described by Kukovinets et al., 2006.

500   RNA isolation

501   RNA was isolated from approximately 150 (cca. 100 mg) pooled virgin and mated *P. citri*

502   females separately, using TRIzol Reagent (Thermo Fisher Scientific, Waltham, MA, USA)

503   according to the manufacturer's instructions. RNA was isolated from four biological replicates,

504   resulting in eight RNA samples, four from pools of virgin females and four from pools of mated

505   females. RNA quality was assessed using the Quant-iT™ RNA Assay Kit (Thermo Fisher

506   Scientific, Waltham, MA, USA).

507   Short read Illumina RNA-Seq

508   Approximately 1 µg of isolated RNA from all eight RNA samples was purified to extract

509   polyadenylated mRNA using biotin beads, fragmented, and primed with random hexamers to

510   produce the first cDNA strand followed by second-strand synthesis to produce double-stranded

511   cDNA. Libraries were constructed at the Earlham Institute, UK, on a Sciclone G3 NGSx

512   workstation (PerkinElmer, Waltham, MA, USA) using the TruSeq RNA protocol v2 (Illumina

513   Part # 15026495 Rev.F) and sequenced on two lanes of a HiSeq 4000 (Illumina, San Diego,

514   CA, USA) generating 150 bp negative strand-specific paired-end reads. Illumina reads were

515   subjected to adapter trimming, read quality filtering, mapping and read summarization

516   (counting only uniquely mapped paired reads) in CLC Genomics Workbench 10.0.1 (Qiagen,

517   Hilden, Germany), with mapping parameters: mismatch cost 2, insertion cost 3, deletion cost

518   3, length fraction 0.9, similarity fraction 0.9. Reads were mapped to the *Pcitri*.v1 genome,

519   downloaded from the MealyBugBase (https://ensembl.mealybug.org/index.html). Differential

520   expression analysis was performed with R packages edgeR and limma (Law et al., 2018),

521   contrasting samples from virgin and mated *P. citri* females.

Long-read Iso-Seq transcriptome

523   Approximately 2 μg of RNA isolated from pooled virgin *P. citri* females was sent for PacBio

524   SMRT sequencing using the Iso-Seq protocol (National Genomics Infrastructure, Sweden).

525   High and low quality full-length transcript isoforms were mapped to the *Pcitri*.v1 genome

526   using minimap2 (Li, 2018). Based on the genome mapping, the isoforms were collapsed and

527   representative isoforms were filtered to exclude isoforms with 5' artefacts, all using scripts

528   from cDNA_cupcake Github repository (Tseng, 2022).

De novo short-read transcriptome assembly

530   Trimmed paired and orphan Illumina RNA-Seq reads were subjected to *de novo* transcriptome

531   assembly using rnaSPAdes v3.13.0 (Bushmanova et al., 2019). Two assemblies were created,

532   first, using the virgin and mated female *P. citri* paired-end short reads (2x150 nt) obtained in

533   this study, and second, combining them with paired-end reads of seven samples of *P. citri,*

534   kindly provided by Dr. Laura Ross at the University of Edinburgh (2x75 nt and 2x50 nt, see

535   Data Availability Statement). For the first assembly, default rnaSPAdes parameters were used,

536   whereas for the second assembly, adapter trimming and sequencing artefact removal was

537   additionally performed using BBTools' bbduk script (Bushnell, 2022), followed by SPAdes'

538   BayesHammer (Nikolenko et al., 2013) and BBTools' ecco, ecc (6 passes) and tadpole read

539   error correction scripts. Assembly was done using k-mer lengths 29 and 49.

Consolidation of sequence resources, annotation and quality control

541   The two Illumina short read assemblies (Figure 1a and b) were combined into a single set

542   (Figure 1c) by removing identical sequences with CD-HIT-EST v6.4 (Fu et al., 2012) using

543   100% sequence identity threshold. In a successive run, the combined short read transcriptome

544   and the Iso-Seq transcriptome (combining mapped and unmapped representative isoforms,

545   Figure 1d) were consolidated into a single set (Figure 1e), again using CD-HIT-EST at 100%

546   sequence identity threshold. The final consolidated transcriptome dataset as well as both

547   short- and long-read datasets were quality checked using rnaQUAST (Bushmanova et al.,

548   2016) and their completeness was assessed using BUSCO v5.4.3 (Manni et al., 2021) with

549   insecta_odb10 lineage dataset. The consolidated transcriptome set was mapped to the *Pcitri*.v1

550   genome using STARlong v2.7.5c (Dobin et al., 2013) and mapped transcripts were matched

551   with the gene models and scaffolds using matchAnnot (Skelly, 2015; version 20150611.02).

552   Transcripts were also subjected to ORF prediction and translation using Transdecoder v5.5.0

553   (Haas, 2023), followed by the annotation of the predicted protein sequences with PFAM and

554   InterPro (IPR) IDs using InterProScan v5.56-89.0 (Jones et al., 2014). The longest ORFs were

555   further used for taxonomic classification using mmseq2 taxonomy tool (Mirdita et al., 2021),

556   querying against the non-redundant NCBI protein database (downloaded on 19.07.2022).

557   Results of taxonomic classification were visualised with Pavian (Breitwieser and Salzberg,

558   2020). Illumina short reads were mapped back to both *de novo* assemblies as well as IsoSeq

559   transcriptome using STAR v2.7.5c (Dobin et al., 2013) with default parameters. Short read

560   mapping counts for all three datasets were used for differential transcript expression analysis

561   based on R packages edgeR and limma (Law et al., 2018).

562   Candidate selection

563   We queried the IPR annotations of *Pcitri*.v1 gene models and our consolidated transcriptome

564   dataset with IDS-related IPR IDs, namely IPR001441 (Decaprenyl diphosphate synthase-like

565   family), IPR036424 (Decaprenyl diphosphate synthase-like superfamily) and IPR000092

566   (Polyprenyl synthetase family), to identify homologs of *cis*- and *trans*-prenyltransferases.

567   Besides using the IPR search to determine *trans*-IDS homologs, we also conducted a motif

568   search using MAST v5.0.1 in MEME Suite (Bailey et al., 2015). Twenty-one sequences of

569   farnesyl pyrophosphate synthases (FPPS) from different organisms were used as an input for

570   MEME. The identified motifs were used as a query against the *Pcitri*.v1 proteins (Table S7).

571   Additionally, we also searched for *P. citri* isopentenyl diphosphate isomerase (IDI) homologs

572   by querying the *P. citri*.v1 protein sequences with *Nicotiana tabacum* IDI sequence (GenBank

573   accession NP_001313140) using blastp (Altschul et al., 1990).

574   All extracted sequences with homology to *cis*- and *trans*-IDSs longer than 100 amino acids

575   were subjected to CD-HIT with 100% sequence identity threshold to remove duplicates. They

576   were further grouped into clusters, using CD-HIT along with multiple sequence alignments

577   with MUSCLE (Edgar, 2004), and the sequence representing the most probable full-length

578   coding sequence was selected within each cluster.

579   For the phylogenetic analyses of candidate sequences, we first searched for similar sequences

580   using blastp against the non-redundant protein bases or tblastn against the transcriptome

581   shotgun assembly sequences (TSA). Additionally, we searched for homologs from

582   *Planococcus ficus* and *Pseudococcus longispinus* genome assemblies in the MealyBugBase

583   (https://ensembl.mealybug.org/index.html), and from *Maconellicoccus hirsutus* transcriptomic

584   resource (Kohli et al., 2021). Amino acid sequences were aligned using the MUSCLE

585   algorithm (Edgar, 2004) and used to construct maximum-likelihood phylogenetic trees with

586   LG model (Le and Gascuel, 2008) tested with the bootstrap method at 1000 replicates in

587   MEGA-X, version 10.0.5 (Kumar et al., 2018).

Candidate sequence amplification and expression in *E. coli*

589   The candidate sequences were amplified from the cDNA prepared with oligoT primer

590   (T15NNN) from total RNA isolated from virgin *P. citri* females using primers listed in

591   Table S8 and cloned into pMAL-c5X expression vector (New England Biolabs, Ipswich, MA,

592   USA) using *NcoI*/*Bam*HI sites. The proteins were expressed in BL21(DE3)pLysS *E. coli* cells.

593   The expression was induced by 0.5 mM IPTG and carried out at 30 °C overnight. The proteins

594   were purified on the amylose resin (New England Biolabs, Ipswich, MA, USA) and stored

595   at -20 °C in 25 % glycerol. The protein concentration was determined by the method of

596   Bradford (Bradford, 1976).

Enzyme activity assays

598   Isopentenyl, dimethylallyl, and geranyl diphosphate (IPP, DMAPP, and GPP) were purchased

599   as tri-ammonium salts from Echelon Biosciences (Salt Lake City, UT, USA). The compounds

600   were dissolved in the mixture of methanol:water (7:3) at the concentration of 1 mg/mL and

601   stored at -20 °C. The activity assays were carried out using 10–180 μg of protein in a total

602   volume of 100 μL in 35 mM HEPES buffer, pH 7.4, containing 10 mM $MgCl_2$ and 5 mM β-

603   mercaptoethanol at 30 °C for 30 or 60 min. Regular coupling activity was determined using

604   IPP and DMAPP as substrates, both at 100 μM, while the assays for irregular activity contained

605   200 μM of only DMAPP. The reaction was stopped by adding 100 μL of chloroform, and the

606   proteins were precipitated by vigorous shaking followed by centrifugation (10 min at 16,000

607   g). The water phase (injection volume 5 μL) was used for LC-MS analysis performed on an

608   1260 Infinity HPLC system coupled to a G6120B quadrupole mass spectrometry detector

609   (Agilent Technologies, Santa Clara, CA, USA). The separation was carried out on a Poroshell

610   120 EC-C18 (3.0 x 50 mm, 2.7 μm) column (Agilent Technologies, Santa Clara, CA, USA)

611   using the method described in (Nagel et al., 2012). The detection of C10 and C15 prenyl

612   diphosphates was performed in negative single ion mode; m/z 313 and 381, respectively. The

613   quantity of formed products was calculated based on peak areas using a calibration line built

614   for GPP.

615   For analysis of regular terpene alcohols, the reactions were carried out with 70–330 μg of

616   protein in a total volume of 400 μL in 35 mM HEPES buffer, pH 7.4, containing 10 mM $MgCl_2$,

617   5 mM β-mercaptoethanol, and substrates (1 mM IPP and 1 mM DMAPP) at 28 °C overnight.

618   For dephosphorylation of prenyl diphosphates, the reaction mixture was supplemented with 80

619   μL of 0.5 M glycine-NaOH buffer (pH 10.5) containing 5 mM $ZnSO_4$; 80 units of calf intestinal

620   alkaline phosphatase (Promega, Madison, WI, USA) were added and the mixture was incubated

621   at 37 °C for 1 h. The alcohols were extracted 3 times with 400 μL of methyl tert-butyl ether

622   (MTBE); the organic phase was evaporated to approximately 150 μL under compressed air

623   flow. GC-MS analysis was carried out using DB-5ms column (30 m x 0.250 mm x 0.25 μm;

624   Agilent Technologies, Santa Clara, CA, USA) with the following temperature gradient: 50 °C,

625   from 50 °C to 120 °C at 7 °C per min, 120 °C to 320 °C at 35 °C per min, hold 5 min. Carrier

626   gas (H_2) flow was set at 3 mL/min. Injection volume was 1 μL (PTV splitless injection, initial

627   injector temperature 60 °C, final injector temperature 250 °C, injector heating rate 50 °C/sec).

628

629   For identification of irregular products of *trans*IDS5, 1 mg of protein was incubated with 2 mg

630   of DMAPP tri-ammonium salt in 1.6 mL of 35 mM HEPES buffer, pH 7.4, containing 10 mM

631    $MgCl_2$, and 5 mM β-mercaptoethanol at 28 °C overnight. The products were dephosphorylated

632   and extracted as described above, and separated on ALUGRAM® Xtra SIL G/UV$_{254}$ TLC plates

633   (0.20 mm silica gel layer, Macharey-Nagel, Düren, Germany) using hexane:acetone (4:1)

634   mixture. Individual substances were extracted from silica gel with MTBE and analysed by GC-

635   MS using Cyclosil-B capillary column (30 m x 0.250 mm x 0.25 μm; Agilent Technologies,

636   Santa Clara, CA, USA) with the following temperature gradient: 50 °C for 3 min → from 50

637   °C to 120 °C at 2 °C per min → 120 °C to 230 °C at 10 °C per min. Helium was applied as the

638   carrier gas at a flow rate of 1 mL/min. Injection volume was 1 μL (1:100 split).

639

Candidate expression in *Nicotiana benthamiana*

640
641 Genetic constructs for candidate expression in plants were assembled with the Golden Braid
642 (GB) cloning system (Sarrion-Perdigones et al., 2011). Transcriptional units in alpha-level GB
643 vectors included IDS coding sequences fused with a C-terminal His-tag under control of the
644 35S CaMV promoter. Each candidate gene was tested in its native form and with the addition
645 of a modified chloroplast transit peptide (cTP) of ribulose bisphosphate carboxylase small
646 subunit from *Nicotiana sylvestris* (GenBank accession number XP_009794476.1). If a different
647 (e.g. mitochondrial) localization signal was predicted, it was removed before adding the cTP.
648 Transient expression in *N. benthamiana* leaves was carried out as described earlier
649 (Gerasymenko et al., 2019). For detection of irregular IDS activity, the plant material (200 mg)
650 was frozen in liquid nitrogen, ground and extracted with 80 % methanol (400 μL) by 30 min
651 incubation in the ice ultrasound bath. Supernatants after two centrifugation steps (10 min at
652 16,000 g) were analysed using 1260 Infinity HPLC system coupled to G6120B quadrupole
653 mass spectrometry detector (Agilent Technologies, Santa Clara, CA, USA). The separation was
654 carried out on Zorbax Extend-C18 (4.6 x 150 mm, 3.5 μm) column (Agilent Technologies,
655 Santa Clara, CA, USA) with mobile phase consisting of 5 mM ammonium bicarbonate in water
656 as solvent A and acetonitrile as solvent B applying the following gradient (% B): starting at 0,
657 0 to 8 within 2 min, holding 8 for 15 min, 8 to 64 within 3 min, 64 to 100 within 2 min, holding
658 100 for 4 min, 100 to 0 within 1 min, re-equilibrating at 0 for 12 min. The detection of C10 and
659 C15 prenyl diphosphates was performed in negative single ion mode; m/z 313 and 381,
660 respectively. For detection of volatile compounds, samples from agroinfiltrated leaves were
661 collected 5 dpi, snap-frozen in liquid nitrogen and analysed by GC-MS as described previously
662 (Mateos-Fernández et al., 2021).
663

Computational model and site-directed mutagenesis of *trans*IDS5

664
665 The 3-D model of *trans*IDS5 was built on the SWISS-MODEL homology-modelling server
666 (Waterhouse et al., 2018) using the crystal structure of *Saccharomyces cerevisiae*
667 geranylgeranyl pyrophosphate synthase in complex with magnesium and IPP (PDB DOI:
668 10.2210/pdb2E8U/pdb) as a template. For structure visualisation and analysis, UCSF Chimera
669 v.1.14 was applied (Pettersen et al., 2004). Mutations were introduced using the Q5-SDM kit
670 (New England Biolabs) with primers listed in Table S8.
671

695

696   Data and code availabilitys

697   Raw Illumina reads from *P. citri* virgin and mated females, along with results of the differential
698   expression analysis (as given in Table S3b as well), were deposited at GEO under accession
699   GSE179660. Raw Iso-Seq reads were deposited at SRA under accession SRR15093694.
700   *P. citri* short reads provided by the University of Edinburgh and used in the second *de novo*
701   transcriptome assembly are deposited at SRA under accession numbers SRR11260462,
702   SRR11260463, SRR11260468, SRR11260469, SRR11260470, and SRR11260471. *De novo*
703   transcriptome   assembly   FASTA   file   is   available   at   FAIRDOMHub

704   (https://fairdomhub.org/data_files/6316/content_blobs/17124/download), together with an

705   annotation file (https://fairdomhub.org/data_files/6317/content_blobs/17125/download), also

706   included in the Supplemental Files (Table S3a).

707

708   **Supplemental Files**

709   **Table S1:** Quality assessment of short- and long-read transcriptome data.

710   **Table S2:** Percent of short reads mapping to transcriptome sequences.

711   **Table S3:** Differential expression of *P. citri* genes between virgin and mated females.

712   **Table S4:** Selected IDS sequences.

713   **Table S5:** IDS activity measurements of *P. citri* candidates.

714   **Table S6:** Combined activity assays performed for detection of irregular IDS and terpene
715   synthase activities.

716   **Table S7:** Input and output of the MEME motif search for *P. citri* sequences containing *trans*-
717   IDS motifs.

718   **Table S8:** Primers used for amplification of IDS sequences from *P. citri* cDNA and for
719   introducing mutations into *trans*IDS5 sequence.

720   **Figure S1:** BUSCO assessment of transcriptome completeness.

721   **Figure S2:** Taxonomic classification of the *P. citri* transcriptome dataset.

722   **Figure S3:** Alignments of sequence resources for *trans*IDS10 and *trans*IDS13.

723   **Figure S4:** Phylogenetic tree of putative DPPS subunit 1 sequences from selected species with
724   *trans*IDS2 and *trans*IDS7.

725   **Figure S5:** Phylogenetic tree of putative FPPS sequences from selected species with
726   *trans*IDS3, *trans*IDS5, and *trans*IDS6.

727   **Figure S6:** Phylogenetic tree of putative DHPPS catalytic subunit sequences from selected
728   species with *cis*IDS1, and *cis*IDS4.

729   **Figure S7:** Phylogenetic tree of putative DHPPS regulatory subunit sequences from selected
730   species with *cis*IDS6, and *cis*IDS9.

731   **Figure S8:** Phylogenetic tree of putative DHPPS regulatory subunit sequences from selected

732   species with *cis*IDS6, and *cis*IDS9.

733   **Figure S9:** Phylogenetic tree of putative FPPS and FPPS-like sequences from Coccoidea

734   species.

735   **Figure S10:** Phylogenetic tree of putative GGPPS sequences from selected species with

736   *trans*IDS16.

737   **Figure S11:** Phylogenetic tree of putative otubain-like sequences from selected species with

738   *trans*IDS17.

739   **Figure S12:** Phylogenetic tree of putative DHPPS and DHPPS-like sequences from selected

740   Coccoidea species.

741   **Figure S13:** Identification of regular monoterpenes synthesised by *trans*-IDS enzymes from

742   *P. citri*.

743   **Figure S14:** EI mass spectra of geraniol generated by dephosphorylation of standard GPP (1A)

744   and products of *trans*IDS5 (1B) and *trans*IDS3 (1C).

745   **Figure S15:** EI mass spectra of geraniol generated by dephosphorylation of standard GPP (1A)

746   and products of *trans*IDS5 (1B) and *trans*IDS3 (1C).

747   **Figure S16:** Identification of regular sesquiterpenes synthesised by *trans*-IDS enzymes from

748   *P. citri*.

749   **Figure S17:** EI mass spectra of *trans*-farnesol generated by dephosphorylation of products of

750   FPPS from *Tanacetum cinerariifolium* known to produce *trans*-farnesyl diphosphate (4A) and

751   *trans*IDS5 (4B).

752   **Figure S18:** EI mass spectra of dephosphorylated products of *trans*IDS3, *trans*-farnesol (4C)

753   and farnesol isomer (5).

754   **Figure S19:** Identification of regular monoterpene diphosphates synthesised by *trans*-IDS

755   enzymes from *P. citri*.

756   **Figure S20:** Identification of irregular monoterpenes synthesised by *trans*IDS5.

Bibliography

757

758 Altschul, S. F., Gish, W., Miller, W., Myers, E. W., and Lipman, D. J. (1990). Basic Local
759 Alignment Search Tool. *J. Mol. Biol.* 215, 403–410. doi:10.1016/S0022-2836(05)80360-
760 2.

761 Bailey, T. L., Johnson, J., Grant, C. E., and Noble, W. S. (2015). The MEME Suite. *Nucleic*
762 *Acids Res.* 43, W39–W49. doi:10.1093/nar/gkv416.

763 Beran, F., Köllner, T. G., Gershenzon, J., and Tholl, D. (2019). Chemical convergence
764 between plants and insects: biosynthetic origins and functions of common secondary
765 metabolites. *New Phytol.* 223, 52–67. doi:10.1111/nph.15718.

766 Beran, F., and Petschenka, G. (2022). Sequestration of Plant Defense Compounds by Insects:
767 From Mechanisms to Insect-Plant Coevolution. *Annu. Rev. Entomol.* 67, 163–180.
768 doi:10.1146/annurev-ento-062821-062319.

769 Beran, F., Rahfeld, P., Luck, K., Nagel, R., Vogel, H., Wielsch, N., et al. (2016). Novel
770 family of terpene synthases evolved from trans-isoprenyl diphosphate synthases in a flea
771 beetle. *Proc. Natl. Acad. Sci. U. S. A.* 113, 2922–2927. doi:10.1073/pnas.1523468113.

772 Bierl-Leonhardt, B. A., Moreno, D. S., Schwarz, M., Fargerlund, J. A., and Plimmer, J. R.
773 (1981). Isolation, identification and synthesis of the sex pheromone of the citrus
774 mealybug, Planococcus citri (risso). *Tetrahedron Lett.* 22, 389–392. doi:10.1016/0040-
775 4039(81)80107-4.

776 Bradford, M. M. (1976). A rapid and sensitive method for the quantitation of microgram
777 quantitites of protein utilizing the principle of protein-dye binding. *Anal. Biochem.* 72,
778 248–254. doi:10.1016/0003-2697(76)90527-3.

779 Breitwieser, F. P., and Salzberg, S. L. (2020). Pavian: interactive analysis of metagenomics
780 data for microbiome studies and pathogen identification. 36, 1303–1304.
781 doi:10.1093/bib/bbx120.Kim.

782 Burke, C. C., Wildung, M. R., and Croteau, R. (1999). Geranyl diphosphate synthase:
783 Cloning, expression, and characterization of this prenyltransferase as a heterodimer.
784 *Proc. Natl. Acad. Sci. U. S. A.* 96, 13062–13067. doi:10.1073/pnas.96.23.13062.

785 Bushmanova, E., Antipov, D., Lapidus, A., and Prjibelski, A. D. (2019). RnaSPAdes: A de
786 novo transcriptome assembler and its application to RNA-Seq data. *Gigascience* 8, 1–

787   13. doi:10.1093/gigascience/giz100.

788   Bushmanova, E., Antipov, D., Lapidus, A., Suvorov, V., and Prjibelski, A. D. (2016).
789   RnaQUAST: A quality assessment tool for de novo transcriptome assemblies.
790   *Bioinformatics* 32, 2210–2212. doi:10.1093/bioinformatics/btw218.

791   Bushnell, B. (2022). BBMap. Available at: https://sourceforge.net/projects/bbmap/.

792   Chan, Y.-T., Ko, T.-P., Yao, S.-H., Chen, Y.-W., Lee, C.-C., and Wang, A. H.-J. (2017).
793   Crystal Structure and Potential Head-to-Middle Condensation Function of a Z,Z-
794   Farnesyl Diphosphate Synthase. *ACS Omega* 2, 930–936.
795   doi:10.1021/acsomega.6b00562.

796   Daane, K. M., Cooper, M. L., Mercer, N. H., Hogg, B. N., Yokota, G. Y., Haviland, D. R., et
797   al. (2021). Pheromone Deployment Strategies for Mating Disruption of a Vineyard
798   Mealybug. *Hortic. Entomol.* 114, 2439–2451. doi:10.1093/jee/toab198.

799   Darragh, K., Orteu, A., Black, D., Byers, K. J. R. P., Szczerbowski, D., Warren, I. A., et al.
800   (2021). A novel terpene synthase controls differences in anti-aphrodisiac pheromone
801   production between closely related Heliconius butterflies. *PLoS Biol.* 19, e3001022.
802   doi:10.1371/JOURNAL.PBIO.3001022.

803   Demissie, Z. A., Erland, L. A. E., Rheault, M. R., and Mahmoud, S. S. (2013). The
804   biosynthetic origin of irregular monoterpenes in lavandula: Isolation and biochemical
805   characterization of a novel cis-prenyl diphosphate synthase gene, lavandulyl diphosphate
806   synthase. *J. Biol. Chem.* 288, 6333–6341. doi:10.1074/jbc.M112.431171.

807   Dobin, A., Davis, C. A., Schlesinger, F., Drenkow, J., Zaleski, C., Jha, S., et al. (2013).
808   STAR: Ultrafast universal RNA-seq aligner. *Bioinformatics* 29, 15–21.
809   doi:10.1093/bioinformatics/bts635.

810   Dong, C., Zhang, M., Song, S., Wei, F., Qin, L., Fan, P., et al. (2023). A Small Subunit of
811   Geranylgeranyl Diphosphate Synthase Functions as an Active Regulator of Carotenoid
812   Synthesis in Nicotiana tabacum. *Int. J. Mol. Sci.* 24, 992. doi:10.3390/ijms24020992.

813   Dunkelblum, E., Zada, A., Gross, S., Fraistat, P., and Mendel, Z. (2002). Sex pheromone and
814   analogs of the citrus mealybug , Planococcus citri : synthesis and biological activity. 25,
815   1–9.

816   Edgar, R. C. (2004). MUSCLE: Multiple sequence alignment with high accuracy and high

817   throughput. *Nucleic Acids Res.* 32, 1792–1797. doi:10.1093/nar/gkh340.

818   Emi, K., Sompiyachoke, K., Okada, M., and Hemmi, H. (2019). A heteromeric cis-
819   prenyltransferase is responsible for the biosynthesis of glycosyl carrier lipids in
820   Methanosarcina mazei. *Biochem. Biophys. Res. Commun.* 520, 291–296.
821   doi:10.1016/j.bbrc.2019.09.143.

822   Franco, J. C., Cocco, A., Lucchi, A., Mendel, Z., Suma, P., Vacas, S., et al. (2022). Scientific
823   and technological developments in mating disruption of scale insects. *Entomol. Gen.* 42,
824   251–273. doi:10.1127/entomologia/2021/1220.

825   Fu, L., Niu, B., Zhu, Z., Wu, S., and Li, W. (2012). CD-HIT: Accelerated for clustering the
826   next-generation sequencing data. *Bioinformatics* 28, 3150–3152.
827   doi:10.1093/bioinformatics/bts565.

828   Gao, Y., Honzatko, R. B., and Peters, R. J. (2012). Terpenoid synthase structures: A so far
829   incomplete view of complex catalysis. *Nat. Prod. Rep.* 29, 1153–1175.
830   doi:10.1039/c2np20059g.

831   Gerasymenko, I., Sheludko, Y. V., Navarro Fuertes, I., Schmidts, V., Steinel, L., Haumann,
832   E., et al. (2022). Engineering of a Plant Isoprenyl Diphosphate Synthase for
833   Development of Irregular Coupling Activity. *ChemBioChem* 23, e202100465.
834   doi:10.1002/cbic.202100465.

835   Gerasymenko, I., Sheludko, Y., Fräbel, S., Staniek, A., and Warzecha, H. (2019).
836   Combinatorial biosynthesis of small molecules in plants: Engineering strategies and
837   tools. *Methods Enzymol.* 617, 413–442. doi:10.1016/BS.MIE.2018.12.005.

838   Gilg, A. B., Tittiger, C., and Blomquist, G. J. (2009). Unique animal prenyltransferase with
839   monoterpene synthase activity. *Naturwissenschaften* 96, 731–735. doi:10.1007/s00114-
840   009-0521-1.

841   Gu, S.-H., Wu, K.-M., Guo, Y.-Y., Pickett, J. A., Field, L. M., Zhou, J.-J., et al. (2013).
842   Identification of genes expressed in the sex pheromone gland of the black cutworm
843   Agrotis ipsilon with putative roles in sex pheromone biosynthesis and transport. *BMC*
844   *Genomics* 14, 636. doi:10.1186/1471-2164-14-636.

845   Haas, B. (2023). TransDecoder. Available at:
846   https://github.com/TransDecoder/TransDecoder.

847   Hotaling, S., Sproul, J. S., Heckenhauer, J., Powell, A., Larracuente, A. M., Pauls, S. U., et al.
848   (2021). GBE Long Reads Are Revolutionizing 20 Years of Insect Genome Sequencing.
849   *Genome Biol. Evol.* 13, evab138. doi:10.1093/gbe/evab138.

850   Husnik, F., Nikoh, N., Koga, R., Ross, L., Duncan, R. P., Fujie, M., et al. (2013). Horizontal
851   Gene Transfer from Diverse Bacteria to an Insect Genome Enables a Tripartite Nested
852   Mealybug Symbiosis. *Cell* 153, 1567–1578. doi:10.1016/j.cell.2013.05.040.

853   Jančič, S., Nguyen, H. D. T., Frisvad, J. C., Zalar, P., Schroers, H. J., Seifert, K. A., et al.
854   (2015). A Taxonomic Revision of the Wallemia sebi Species Complex. *PLoS One* 10,
855   e0125933. doi:10.1371/journal.pone.0125933.

856   Jones, P., Binns, D., Chang, H.-Y., Fraser, M., Li, W., McAnulla, C., et al. (2014).
857   InterProScan 5: Genome-scale protein function classification. *Bioinformatics* 30, 1236–
858   1240. doi:10.1093/bioinformatics/btu031.

859   Karunanithi, P. S., and Zerbe, P. (2019). Terpene Synthases as Metabolic Gatekeepers in the
860   Evolution of Plant Terpenoid Chemical Diversity. *Front. Plant Sci.* 10, 1166.
861   doi:10.3389/fpls.2019.01166.

862   Kobayashi, M., and Kuzuyama, T. (2018). Structural and Mechanistic Insight into Terpene
863   Synthases that Catalyze the Irregular Non-Head-to-Tail Coupling of Prenyl Substrates.
864   *ChemBioChem* 20, 29–33. doi:10.1002/cbic.201800510.

865   Kohli, S., Gulati, P., Narang, A., Maini, J., Shamsudheen, K. V., Pandey, R., et al. (2021).
866   Genome and transcriptome analysis of the mealybug Maconellicoccus hirsutus:
867   Correlation with its unique phenotypes. *Genomics* 113, 2483–2494.
868   doi:10.1016/j.ygeno.2021.05.014.

869   Köllner, T. G., David, A., Luck, K., Beran, F., Kunert, G., Zhou, J.-J., et al. (2022).
870   Biosynthesis of iridoid sex pheromones in aphids. *Proc. Natl. Acad. Sci. U. S. A.* 119,
871   e2211254119. doi:10.1073/pnas.2211254119.

872   Kukovinets, O. S., Zvereva, T. I., Kasradze, V. G., Galin, F. Z., Frolova, L. L., Kuchin, A.
873   V., et al. (2006). Novel synthesis of Planococcus citri pheromone. *Chem. Nat. Compd.*
874   42, 216–218. doi:10.1007/s10600-006-0082-x.

875   Kumar, S., Stecher, G., Li, M., Knyaz, C., and Tamura, K. (2018). MEGA X: Molecular
876   evolutionary genetics analysis across computing platforms. *Mol. Biol. Evol.* 35, 1547–

877   1549. doi:10.1093/molbev/msy096.

878   Lackus, N. D., Petersen, N. P., Nagel, R., Schmidt, A., Irmisch, S., Gershenzon, J., et al.
879   (2019). Identification and Characterization of trans -Isopentenyl Diphosphate Synthases
880   Involved in. *Molecules* 24, 2408. doi:10.3390/molecules24132408.

881   Lancaster, J., Khrimian, A., Young, S., Lehner, B., Luck, K., Wallingford, A., et al. (2018).
882   De novo formation of an aggregation pheromone precursor by an isoprenyl diphosphate
883   synthase-related terpene synthase in the harlequin bug. *Proc. Natl. Acad. Sci. U. S. A.*
884   115, E8634–E8641. doi:10.1073/pnas.1800008115.

885   Lancaster, J., Lehner, B., Khrimian, A., Muchlinski, A., Luck, K., Köllner, T. G., et al.
886   (2019). An IDS-Type Sesquiterpene Synthase Produces the Pheromone Precursor (Z)-α-
887   Bisabolene in Nezara viridula. *J. Chem. Ecol.* 45, 187–197. doi:10.1007/s10886-018-
888   1019-0.

889   Law, C. W., Alhamdoosh, M., Su, S., Dong, X., Tian, L., Smyth, G. K., et al. (2018). RNA-
890   seq analysis is easy as 1-2-3 with limma, Glimma and edgeR. *F1000Research* 5, 1408.
891   doi:10.12688/f1000research.9005.3.

892   Le, S. Q., and Gascuel, O. (2008). An Improved General Amino Acid Replacement Matrix.
893   *Mol. Biol. Evol.* 25, 1307–1320. doi:10.1093/molbev/msn067.

894   Li, F., Zhao, X., Li, M., He, K., Huang, C., Zhou, Y., et al. (2019). Insect genomes : progress
895   and challenges. *Insect Mol. Biol.* 28, 739–758. doi:10.1111/imb.12599.

896   Li, H. (2018). Minimap2: Pairwise alignment for nucleotide sequences. *Bioinformatics* 34,
897   3094–3100. doi:10.1093/bioinformatics/bty191.

898   Liu, P.-L., Wan, J.-N., Guo, Y.-P., Ge, S., and Rao, G.-Y. (2012). Adaptive evolution of the
899   chrysanthemyl diphosphate synthase gene involved in irregular monoterpene
900   metabolism. *BMC Evol. Biol.* 12, 214. doi:10.1186/1471-2148-12-214.

901   López-Madrigal, S., Latorre, A., Porcar, M., Moya, A., and Gil, R. (2013). Mealybugs nested
902   endosymbiosis : going into the ' matryoshka ' system in Planococcus citri in depth. *BMC*
903   *Microbiol.* 13, 74. doi:10.1186/1471-2180-13-74.

904   Lucchi, A., Suma, P., Ladurner, E., Iodice, A., Savino, F., Ricciardi, R., et al. (2019).
905   Managing the vine mealybug , Planococcus ficus , through pheromone-mediated mating
906   disruption. *Environ. Sci. Pollut. Res.* 26, 10708–10718.

907   Manni, M., Berkeley, M. R., Seppey, M., and Zdobnov, E. M. (2021). BUSCO: Assessing
908   Genomic Data Quality and Beyond. *Curr. Protoc.* 1, e323. doi:10.1002/cpz1.323.

909   Mateos-Fernández, R., Moreno-Giménez, E., Gianoglio, S., Quijano-Rubio, A., Gavaldá-
910   García, J., Estellés, L., et al. (2021). Production of Volatile Moth Sex Pheromones in
911   Transgenic Nicotiana benthamiana Plants. *BioDesign Res.* 2021, 9891082.
912   doi:10.34133/2021/9891082.

913   Mateos Fernández, R., Petek, M., Gerasymenko, I., Juteršek, M., Baebler, Š., Kallam, K., et
914   al. (2022). Insect pest management in the age of synthetic biology. *Plant Biotechnol. J.*
915   20, 25–36. doi:10.1111/pbi.13685.

916   McCutcheon, J. P., and Dohlen, C. D. Von (2011). An Interdependent Metabolic Patchwork
917   in the Nested Symbiosis of Mealybugs. *Curr. Biol.* 21, 1366–1372.
918   doi:10.1016/j.cub.2011.06.051.

919   Mirdita, M., Steinegger, M., Breitwieser, F., Söding, J., and Levy Karin, E. (2021). Fast and
920   sensitive taxonomic assignment to metagenomic contigs. *Bioinformatics* 37, 3029–3031.
921   doi:10.1093/bioinformatics/btab184.

922   Nagel, R., Gershenzon, J., and Schmidt, A. (2012). Nonradioactive assay for detecting
923   isoprenyl diphosphate synthase activity in crude plant extracts using liquid
924   chromatography coupled with tandem mass spectrometry. *Anal. Biochem.* 422, 33–38.
925   doi:10.1016/j.ab.2011.12.037.

926   Nagel, R., Schmidt, A., and Peters, R. J. (2019). Isoprenyl diphosphate synthases : the chain
927   length determining step in terpene biosynthesis. *Planta* 249, 9–20. doi:10.1007/s00425-
928   018-3052-1.

929   Nikolenko, S. I., Korobeynikov, A. I., and Alekseyev, M. A. (2013). BayesHammer :
930   Bayesian clustering for error correction in single-cell sequencing. *BMC Genomics* 14,
931   S7.

932   Nishida, R., Kim, C.-S., Fukami, H., and Irik, R. (1991). Ideamine N-Oxides: Pyrrolizidine
933   Alkaloids Sequestered by the Danaine Butterfly, Idea leuconoe. *Biosci. Biotechnol.*
934   *Biochem.* 55, 1787–1792. doi:10.1080/00021369.1991.10870842.

935   Nuo, S.-M., Yang, A.-J., Li, G.-C., Xiao, H.-Y., and Liu, N.-Y. (2021). Transcriptome
936   analysis identifies candidate genes in the biosynthetic pathway of sex pheromones from

937   a zygaenid moth , Achelura yunnanensis (Lepidoptera : Zygaenidae). *PeerJ* 9, e12641.
938   doi:10.7717/peerj.12641.

939   Ogawa, T., Emi, K., Koga, K., Yoshimura, T., and Hemmi, H. (2016). A cis-
940   prenyltransferase from Methanosarcina acetivorans catalyzes both head-to-tail and
941   nonhead-to-tail prenyl condensation. *FEBS J.* 283, 2369–2383. doi:10.1111/febs.13749.

942   Ozaki, T., Zhao, P., Shinada, T., Nishiyama, M., and Kuzuyama, T. (2014). Cyclolavandulyl
943   Skeleton Biosynthesis via Both Condensation and Cyclization Catalyzed by an
944   Unprecedented Member of the cis - Isoprenyl Diphosphate Synthase Superfamily. *J. Am.*
945   *Chem. Soc.* 136, 4837–4840.

946   Passaro, L. C., and Webster, F. X. (2004). Synthesis of the Female Sex Pheromone of the
947   citrus mealybug, Planococcus citri. *J. Agric. Food Chem.* 52, 2896–2899.
948   doi:10.1021/jf035301h.

949   Petkevicius, K., Wenning, L., Kildegaard, K. R., Sinkwitz, C., Smedegaard, R., Holkenbrink,
950   C., et al. (2022). Biosynthesis of insect sex pheromone precursors via engineered β-
951   oxidation in yeast. *FEMS Yeast Res.* 22, foac041. doi:10.1093/FEMSYR/FOAC041.

952   Pettersen, E. F., Goddard, T. D., Huang, C. C., Couch, G. S., Greenblatt, D. M., Meng, E. C.,
953   et al. (2004). UCSF Chimera - A visualization system for exploratory research and
954   analysis. *J. Comput. Chem.* 25, 1605–1612. doi:10.1002/jcc.20084.

955   Qu, Y., Chakrabarty, R., Tran, H. T., Kwon, E.-J. G., Kwon, M., Nguyen, T.-D., et al. (2015).
956   A lettuce (Lactuca sativa) homolog of human Nogo-B receptor interacts with cis-
957   prenyltransferase and is necessary for natural rubber biosynthesis. *J. Biol. Chem.* 290,
958   1898–1914. doi:10.1074/jbc.M114.616920.

959   Rebholz, Z., Lancaster, J., Larose, H., Khrimian, A., Luck, K., Sparks, M. E., et al. (2023).
960   Ancient origin and conserved gene function in terpene pheromone and defense evolution
961   of stink bugs and hemipteran insects. *Insect Biochem. Mol. Biol.* 152, 103879.
962   doi:10.1016/j.ibmb.2022.103879.

963   Rivera, S. B., Swedlund, B. D., King, G. J., Bell, R. N., Hussey, C. E., Shattuck-Eidens, D.
964   M., et al. (2001). Chrysanthemyl diphosphate synthase: isolation of the gene and
965   characterization of the recombinant non-head-to-tail monoterpene synthase from
966   Chrysanthemum cinerariaefolium. *Proc. Natl. Acad. Sci. U. S. A.* 98, 4373–4378.

967   doi:10.1073/pnas.071543598.

968   Rudolf, J. D., and Chang, C.-Y. (2020). Terpene synthases in disguise: enzymology,
969   structure, and opportunities of non-canonical terpene synthases. *Nat. Prod. Rep.* 37,
970   425–463. doi:10.1039/c9np00051h.

971   Sarrion-Perdigones, A., Falconi, E. E., Zandalinas, S. I., Juárez, P., Fernández-del-Carmen,
972   A., Granell, A., et al. (2011). GoldenBraid: An iterative cloning system for standardized
973   assembly of reusable genetic modules. *PLoS One* 6, e21622.
974   doi:10.1371/journal.pone.0021622.

975   Schneider, L., Rebetez, M., and Rasmann, S. (2022). The effect of climate change on
976   invasive crop pests across biomes. *Curr. Opin. Insect Sci.* 50, 100895.
977   doi:10.1016/j.cois.2022.100895.

978   Skelly, T. (2015). MatchAnnot. Available at: https://github.com/TomSkelly/MatchAnnot.

979   Song, X., and Li, Z.-X. (2022). Functional characterization of two different decaprenyl
980   diphosphate synthases in the vetch aphid Megoura viciae. *Arch. Insect Biochem.*
981   *Physiol.* 110, e21900. doi:10.1002/arch.21900.

982   Tabata, J. (2022). Genetic Basis Underlying Structural Shift of Monoterpenoid Pheromones
983   in Mealybugs. *J. Chem. Ecol.* 48, 546–553. doi:10.1007/s10886-021-01339-x.

984   Tholl, D., Kish, C. M., Orlova, I., Sherman, D., Gershenzon, J., Pichersky, E., et al. (2004).
985   Formation of monoterpenes in Antirrhinum majus and Clarkia breweri flowers involves
986   heterodimeric geranyl diphosphate synthases. *Plant Cell* 16, 977–992.
987   doi:10.1105/tpc.020156.

988   Tholl, D., Rebholz, Z., Morozov, A. V., and O'Maille, P. E. (2023). Terpene synthases and
989   pathways in animals: enzymology and structural evolution in the biosynthesis of volatile
990   infochemicals. *Nat. Prod. Rep.* 40, 766–793. doi:10.1039/d2np00076h.

991   Tillman, J. A., Seybold, S. J., Jurenka, R. A., and Blomquist, G. J. (1999). Insect pheromones
992   -an overview of biosynthesis and endocrine regulation. *Insect Biochem. Mol. Biol.* 29,
993   481–514. Available at: www.elsevier.com/locate/ibmb [Accessed May 30, 2023].

994   Tseng, E. (2022). cDNA_Cupcake. Available at:
995   https://github.com/Magdoll/cDNA_Cupcake.

996   Vacas, S., Alfaro, C., Navarro-llopis, V., and Primo, J. (2010). Mating disruption of

997   California red scale, Aonidiella aurantii Maskell (Homoptera : Diaspididae), using

998   biodegradable mesoporous pheromone dispensers. *Pest Manag. Sci.* 66, 745–751.

999   doi:10.1002/ps.1937.

1000   Vacas, S., Navarro, I., Seris, E., Ramos, C., Hernández, E., Navarro-Llopis, V., et al. (2017).

1001   Identification of the male-produced aggregation pheromone of the four-spotted coconut

1002   weevil, diocalandra frumenti. *J. Agric. Food Chem.* 65, 270–275.

1003   doi:10.1021/acs.jafc.6b04829.

1004   Vogel, H., Heidel, A. J., Heckel, D. G., and Groot, A. T. (2010). Transcriptome analysis of

1005   the sex pheromone gland of the noctuid moth Heliothis virescens. *BMC Genomics* 11,

1006   29. doi:10.1186/1471-2164-11-29.

1007   Wallrapp, F. H., Pan, J.-J., Ramamoorthy, G., Almonacid, D. E., Hillerich, B. S., Seidel, R.,

1008   et al. (2013). Prediction of function for the polyprenyl transferase subgroup in the

1009   isoprenoid synthase superfamily. *Proc. Natl. Acad. Sci.* 110, E1196–E1202.

1010   doi:10.1073/pnas.1300632110.

1011   Waterhouse, A., Bertoni, M., Bienert, S., Studer, G., Tauriello, G., Gumienny, R., et al.

1012   (2018). SWISS-MODEL: Homology modelling of protein structures and complexes.

1013   *Nucleic Acids Res.* 46, W296–W303. doi:10.1093/nar/gky427.

1014   Watson, G. (2023). CABI Compendum, Planococcus citri (citrus mealybug). Available at:

1015   https://www.cabidigitallibrary.org/doi/10.1079/cabicompendium.45082.

1016   Wolk, J. L., Goldschmidt, Z., and Dunkelblum, E. (1986). A short stereoselective synthesis of

1017   (+)-cis-planococcyl acetate, sex pheromone of the citrus mealybug Planococcus citri

1018   (Risso). *Synthesis (Stuttg)*. 1986, 347–348. doi:10.1055/S-1986-31613.

1019   Yao, S., Zhou, S., Li, X., Liu, X., Zhao, W., Wei, J., et al. (2021). Transcriptome Analysis of

1020   Ostrinia furnacalis Female Pheromone Gland: Esters Biosynthesis and Requirement for

1021   Mating Success. *Front. Endocrinol. (Lausanne)*. 12, 736906.

1022   doi:10.3389/fendo.2021.736906.

1023   Yin, J.-L., Wong, W.-S., Jang, I.-C., and Chua, N.-H. (2017). Co-expression of peppermint

1024   geranyl diphosphate synthase small subunit enhances monoterpene production in

1025   transgenic tobacco plants. *New Phytol.* 213, 1133–1144. doi:10.1111/nph.14280.

1026   Zhang, A., Amalin, D., Shirali, S., Serrano, M. S., Franqui, R. A., Oliver, J. E., et al. (2004).
1027   Sex pheromone of the pink hibiscus mealybug, Maconellicoccus hirsutus, contains an
1028   unusual cyclobutanoid monoterpene. *Proc Natl Acad Sci U S A* 101, 9601–9606.
1029   doi:10.1073/pnas.0401298101.

1030   Zhang, H., and Li, Z.-X. (2013). In vitro and in vivo characterization of a novel insect
1031   decaprenyl diphosphate synthase: A two-major step catalytic mechanism is proposed.
1032   *Biochem. Biophys. Res. Commun.* 442, 105–111. doi:10.1016/j.bbrc.2013.11.025.

1033   Zhou, F., Wang, C.-Y., Gutensohn, M., Jiang, L., Zhang, P., Zhang, D., et al. (2017). A
1034   recruiting protein of geranylgeranyl diphosphate synthase controls metabolic flux
1035   toward chlorophyll biosynthesis in rice. *Proc. Natl. Acad. Sci. U. S. A.* 114, 6866–6871.
1036   doi:10.1073/pnas.1705689114.

1037   Zou, Y., Chinta, S. P., and Millar, J. G. (2013). "Irregular Terpenoids as Mealybug and Scale
1038   Pheromones : Chemistry and Applications," in *Pest Management with Natural Products*,
1039   eds. J. J. Beck, J. R. Coats, S. O. Duke, and M. E. Koivunen (American Chemical
1040   Society), 125–143. doi:10.1021/bk-2013-1141.

1041   Zou, Y., and Millar, J. G. (2015). Chemistry of the pheromones of mealybug and scale
1042   insects. *Nat. Prod. Rep.* 32, 1067–1113. doi:10.1039/c4np00143e.

1043

1044

1045

2.5 Chloroplast Redox State Changes Mark Cell-to-Cell Signalling in the Hypersensitive Response

Tjaša Lukan, Anže Župani, Tjaša Mahkovec Povalej, Jacob O. Brunkard, Mirjam Kmeti, Mojca Juteršek, Špela Baebler, and Kristina Gruden

This article explores the spatiotemporal dynamics of chloroplast redox state changes and stromule formation in resistant potato plants with an elicited hypersensitive response to PVY infection. Additionally, it evaluated the role of salicylic acid in both phenomena. Using confocal microscopy and custom image analysis, we confirmed the presence of highly oxidized chloroplasts in the cells surrounding the cell death zone, with oxidization levels decreasing with increasing distances from the cell death zone. Furthermore, we discovered cells with moderately oxidized chloroplasts further away from the cell death zone. As the distant oxidized cells were not present in the salicylic-acid-depleted genotype, we proposed that they play a role in signalling for resistance. We also confirmed that stromule formation is salicylic-acid-dependent and spatiotemporally regulated in the hypersensitive response of potato to PVY. Blocking chloroplast redox state changes revealed genes with expression patterns that depend on the redox state. This work therefore provides important insight into the complex intra- and inter-cellular communication involved in programmed cell death and hypersensitive response-conferred resistance to PVY infection.

The PhD candidate contributed to this work by generating the GFP-tagged PVY infectious clone, which was used for tracking the viral spread in infected potato plants. She designed the genetic construct, performed molecular cloning, and characterised the resulting PVY-GFP infectious clone. She also wrote the methods section describing her work.

Chloroplast redox state changes mark cell-to-cell signaling in the hypersensitive response

Tjaša Lukan[1] (iD), Anže Županič[1] (iD), Tjaša Mahkovec Povalej[1] (iD), Jacob O. Brunkard[2] (iD), Mirjam Kmetič[1] (iD), Mojca Juteršek[1,3] (iD), Špela Baebler[1] (iD) and Kristina Gruden[1] (iD)

[1]National Institute of Biology, Večna pot 111, 1000, Ljubljana, Slovenia; [2]Laboratory of Genetics, University of Wisconsin – Madison, Madison, WI 53706, USA; [3]Jožef Stefan International Postgraduate School, Jamova 39, 1000, Ljubljana, Slovenia

Summary

- Hypersensitive response (HR)-conferred resistance is associated with induction of programmed cell death and pathogen spread restriction in its proximity. The exact role of chloroplastic reactive oxygen species and its link with salicylic acid (SA) signaling in HR remain unexplained.
- To unravel this, we performed a detailed spatiotemporal analysis of chloroplast redox response in palisade mesophyll and upper epidermis to potato virus Y (PVY) infection in a resistant potato genotype and its transgenic counterpart with impaired SA accumulation and compromised resistance.
- Besides the cells close to the cell death zone, we detected individual cells with oxidized chloroplasts further from the cell death zone. These are rare in SA-deficient plants, suggesting their role in signaling for resistance. We confirmed that chloroplast redox changes play important roles in signaling for resistance, as blocking chloroplast redox changes affected spatial responses at the transcriptional level.
- Through spatiotemporal study of stromule induction after PVY infection, we show that stromules are induced by cell death and also as a response to PVY multiplication at the front of infection. Overall induction of stromules is attenuated in SA-deficient plants.

Introduction

Plants have evolved a range of constitutive and inducible resistance mechanisms to respond to pathogen attack. The effector-triggered immunity (ETI) is mediated by intracellular resistance (R) proteins, which recognize pathogen-derived effectors (Jones & Dangl, 2006). Successful ETI often results in hypersensitive response (HR)-conferred resistance and is associated with the formation of localized programmed cell death (PCD) (Künstler *et al.*, 2016). This response involves salicylic acid (SA) biosynthesis in cytosol and production of reactive oxygen species (ROS) in chloroplasts and the apoplast (Lu & Yao, 2018; Balint-Kurti, 2019; Littlejohn *et al.*, 2021). Besides hosting the biosynthesis of SA and ROS, chloroplasts play a central role in plant immunity as integrators of environmental signals and transmitters of pro-defense signals (Serrano *et al.*, 2016; Kachroo *et al.*, 2021; Li & Kim, 2022). Stromules are stroma-filled tubules that extend from chloroplasts and are induced in several different processes, including HR (Caplan *et al.*, 2015). Stromules are putatively involved in retrograde signaling after pathogen invasion or light stress (Brunkard *et al.*, 2015; Caplan *et al.*, 2015) and in movement of chloroplasts within the cell (Kumar *et al.*, 2018).

It is established that SA is required for the restriction of pathogens during HR in various interactions, including plant–virus pathosystems (Mur *et al.*, 2008; Baebler *et al.*, 2014; Künstler *et al.*, 2016; Calil & Fontes, 2017). Several studies have also pointed to the essential role of apoplastic ROS, leading to redox state changes in the cytoplasm in HR-conferred virus resistance (Hernández *et al.*, 2016; Lukan *et al.*, 2020). It has been suggested that chloroplastic ROS are also involved in the signaling for and/or execution of HR cell death in incompatible interactions (Liu *et al.*, 2007; Zurbriggen *et al.*, 2009; Straus *et al.*, 2010; Ishiga *et al.*, 2012; Kim *et al.*, 2012; Xu *et al.*, 2019; Lukan *et al.*, 2020). Zurbriggen *et al.* (2009) suggested that ROS generated in chloroplasts during nonhost disease resistance are essential for the progress of PCD, but do not contribute to the induction of pathogenesis-related genes or other signaling components of the response, including SA signaling. On the other hand, Ochsenbein *et al.* (2006) found that chloroplastic singlet oxygen ($^1O_2$) can activate SA-mediated signaling, although SA is not required for $^1O_2$-mediated cell death (Ochsenbein *et al.*, 2006). Similarly, Straus *et al.* (2010) suggested that chloroplastic ROS acts as a flexible spatiotemporal integration point, leading to opposite SA signaling reactions in infected and surrounding tissue (Straus *et al.*, 2010). Moreover, recent evidence suggests that chloroplastic ROS might also be involved

in controlling plant immune responses by reprogramming transcription of genes involved in response to pathogen attack as one of the retrograde signals (Ochsenbein *et al.*, 2006; Lee *et al.*, 2007; Maruta *et al.*, 2012; Nomura *et al.*, 2012; Sewelam *et al.*, 2014; Pierella Karlusich *et al.*, 2017). For example, inducible silencing of chloroplastic *THYLAKOIDAL ASCORBATE PEROXIDASE* increased H_2O_2 production in chloroplasts, which activated SA biosynthesis and SA-inducible gene expression (Maruta *et al.*, 2012).

To decipher the consequence of events involving chloroplastic ROS in HR-conferred resistance, a detailed spatiotemporal analysis of the chloroplast redox state in response to pathogen infection is needed. Nondestructive real-time measurement of the redox state has been feasible since genetically encoded sensors became available, for example redox state-sensitive green fluorescent proteins (roGFP1 and roGFP2) in plants (Jiang *et al.*, 2006). Measurement of roGFP fluorescence intensity following excitation at two different excitation maxima permits an evaluation of the relative proportion of roGFP in a reduced or oxidized state. By adding the coding sequence for the RuBisCO small subunit transit peptide to the roGFP coding sequence, pt-roGFP was constructed for measuring changes of the redox state in chloroplasts (Stonebloom *et al.*, 2012). pt-roGFP also allows visualization of stromule formation and observation of redox state changes in stromules.

Potato virus Y (PVY), a member of the genus *Potyvirus*, is the most harmful virus of cultivated potatoes (Karasev & Gray, 2013) and is among the top 10 most economically important plant viruses overall (Quenouille *et al.*, 2013). In response to PVY, HR in potato cv. Rywal is manifested as the formation of necrotic lesions on inoculated leaves at 3 d post-inoculation (dpi) and the virus is restricted to the site of inoculation (Szajko *et al.*, 2008). We have shown previously that SA regulates HR-conferred resistance in a spatiotemporal manner, as for some genes involved in immune response the spatiotemporal regulation is completely lost in the SA-deficient line, whereas other genes show diverse spatiotemporal responses (Lukan *et al.*, 2020). We have also proposed the role of chloroplastic ROS as a signal orchestrating PCD (Lukan *et al.*, 2020). However, the potential role of chloroplastic ROS in viral arrest has not yet been deciphered.

Here, we developed a protocol for confocal imaging of pt-roGFP potato plants complemented by custom image analysis scripts to simultaneously interrogate the chloroplast redox state and stromule formation in proximity to the cell death zone in palisade mesophyll cells and upper epidermis with spatiotemporal resolution. To decipher the link between cell death, SA signaling, chloroplast redox state and stromule formation, we also analyzed the responses to PVY infection in the SA-depleted transgenic counterpart of pt-roGFP (pt-roGFP-NahG). We show that chloroplasts are strongly oxidized in the cells adjacent to the cell death zone. More intriguingly, we detected individual cells with chloroplasts in moderately oxidized redox state close to the cell death zone as well as further away from it. The presence of such cells was sparse in SA-deficient plants, supporting the hypothesis that these cells are involved in the signaling of HR-conferred resistance.

Materials and Methods

Generation of redox state sensor plants

Potato (*Solanum tuberosum* L.) transgenic lines pt-roGFP and pt-roGFP-NahG were prepared by introducing pt-roGFP2 encoding construct (Stonebloom *et al.*, 2012) into cv. Rywal, which is resistant to PVY infection following HR response, and NahG-Rywal with the SA accumulation reduced to < 10% of that in nontransgenic plants, thus rendering HR ineffective in blocking the viral spread (the depletion of SA renders NahG plants susceptible; Baebler *et al.*, 2014). pCAMBIA1304_pt-roGFP2 was electroporated into *Agrobacterium tumefaciens* LBA4404 (Eppendorf Electroporator 2510, Hamburg, Germany) at 2000 V following the manufacturer's protocol. The transformed bacteria were used for the transformation of cv. Rywal and NahG-Rywal stem internodes from *in vitro* plantlets as described elsewhere (Baebler *et al.*, 2014), with some modifications (Supporting Information Methods S1). Well-rooted hygromycin-resistant plants were subcultured to produce plantlets of the independently transformed lines. The selection of transgenic lines with strong and stable GFP fluorescence in chloroplasts was performed by confocal microscopy (see later). To confirm that the detected signal is specific for GFP emission, we used Rywal and NahG-Rywal plants as controls.

Transgenic lines were grown in stem node tissue culture. At 2 wk after node segmentation, they were transferred to soil in a growth chamber and kept under controlled environmental conditions as described previously (Baebler *et al.*, 2009).

Construction of PVY-N605(123)-GFP infectious clone

PVY-N605(123)-GFP was constructed by inserting GFP coding sequence between the coding sequences for viral proteins NIb and CP in the PVY-N605(123) infectious clone (Bukovinszki *et al.*, 2007) using a similar design as Rupar *et al.* (2015), allowing the GFP reporter to be excised from the polyprotein following translation.

The GFP coding sequence was amplified from plasmid p2GWF7 (Karimi *et al.*, 2002) using GFPF40 and GFPR40 primers (Methods S2) with Phusion polymerase (New England BioLabs, Ipswich, MA, USA) according to the provider's instructions. The primers were designed with overhangs enabling addition of the PVY-N605(123) annealing sequence and protease recognition site to the GFP sequence, making the amplicon serve as a megaprimer for restriction-free insertion with mutagenesis. The reaction was designed using the RF-Cloning online tool (Bond & Naus, 2012) and carried out using Phusion polymerase with a 1 : 20 molar ratio of PVY-N605(123) plasmid to GFP amplicon (megaprimer). After *Dpn*I digestion, the mutagenesis mixture was transformed into *E. coli* XL10-Gold Ultracompetent Cells following the manufacturer's instructions (Agilent Technologies, Santa Clara, CA, USA). The transformants were plated on LB-agar with ampicillin selection and grown overnight at 37°C. Grown colonies were screened with colony PCR using

CP-F and UnivR primers and KAPA2G Robust HotStart Kit (Agilent Technologies; Methods S2). Sanger sequencing of the selected clone confirmed the correct sequence of the PVY-coding part and correct in-frame insertion of the GFP coding sequence. Constructed PVY-N605(123)-GFP was coated onto gold microcarriers and used for *Nicotiana clevelandii* bombardment with a Helios® gene gun (Bio-Rad) according to Stare *et al.* (2020). Detailed PCR reaction conditions and cloning steps are given in Methods S2.

Virus inoculation

Two- to four-week-old potato plants in soil were inoculated with PVY$^{N-Wilga}$ (PVY^{N-Wi}; EF558545), PVY N605-GFP (Rupar *et al.*, 2015), PVY-N605(123)-GFP or mock.

For inoculation with PVY$^{N-Wilga}$, 6- to 8-wk-old PVY$^{N-Wilga}$-infected cv. Pentland plants from tissue cultures were used. For inoculation with PVY N605-GFP and PVY-N605(123)-GFP, upper noninoculated leaves of PVY N605-GFP- and PVY-N605 (123)-GFP-inoculated *Nicotiana clevelandii* at 3–4 dpi were used. Before inoculation, GFP fluorescence in the leaves used for inoculum was confirmed under confocal microscope. The tissue was ground in phosphate buffer supplemented with DIECA in a plant material : buffer ratio of 1 : 4. For mock inoculation (MOCK), noninfected *N. clevelandii* and cv. Pentland plants were used.

Inoculation was performed as described in Baebler *et al.* (2009). Briefly, the first three fully developed bottom leaves of potato plants were dusted with carborundum powder. Leaves were rubbed with the inoculum (*c.* 60 μl per leaf) which was removed after 10 min by rinsing with tap water.

Treatments with oxidant and reductant

The second and third leaves of 2- to 4-wk-old pt-roGFP and pt-roGFP-NahG potato transgenic lines were treated with an oxidant (200 mM solution of hydrogen peroxide, H_2O_2, adapted for potato from Jiang *et al.*, 2006), a reductant (200 mM solution of dithiothreitol (DTT) adapted for potato from Jiang *et al.*, 2006) or a control (bidistilled water, ddH_2O) by vacuum infiltration using a syringe. We followed the relative redox state in the chloroplasts 30 min after the treatment, to confirm that the redox state sensor roGFP2 is functional in the selected transgenic lines (Fig. S1; Tables S1, S2).

Treatments with ROS inhibitor

Uracil, a ROS inhibitor (Montaña *et al.*, 2009; Abdollahi & Ghahremani, 2011), was infiltrated into PVY-N605(123)-GFP-inoculated leaves of pt-roGFP L2 plants with 100 μM uracil (Sigma; U0750-25G in 224 μM NaOH diluted in ddH_2O; left side of the leaf) at 4 dpi. As a control, the right side of the leaf was inoculated with 224 μM NaOH diluted in ddH_2O. At 48 h post-treatment, the relative chloroplast redox state close to the lesion was determined to confirm functionality of chloroplastic ROS inhibitor in the selected transgenic line.

Confocal microscopy

A confocal microscope (Leica TCS LSI macroscope with Plan APO ×5 and ×20 objective; Leica Microsystems, Wetzlar, Germany) was used to detect emission of Chl or redox state-sensitive GFP (pt-roGFP2) for the selection of transgenic plants, stromule counting and redox state detection.

To select potato transgenic lines with strong and stable roGFP2 fluorescence (emission window 505–520 nm) in the chloroplasts, plants from tissue cultures were analyzed with a ×20 objective, zoom factor set to 3.00, frame average to 2 and z-stack size adjusted to 10 steps to cover at least 30 μm of the mesophyll after excitation with 488 nm laser.

For redox state detection experiments, confocal imaging was adapted from Jiang *et al.* (2006). The emission of roGFP2 was followed after excitation with 405 nm (detection of oxidized roGFP2) and 488 nm (detection of reduced roGFP2) laser in the window between 505 and 520 nm. The Chl fluorescence was excited with the 488 nm laser and the emission was measured in the window between 690 and 750 nm. The fluorescence was followed on the upper side of the leaf which was detached from the plant on the particular day post-inoculation or 30 min after the treatment with an oxidant or a reductant and immediately analyzed. Plants were imaged with a ×20 objective, zoom factor set to 3.00, and frame average to 2. Regions of interest (ROI) were scanned unidirectionally with a scan speed of 400 Hz. Fluorescence emissions were collected sequentially through three channels (roGFP2 fluorescence after excitation with 405 nm laser, roGFP2 fluorescence after excitation with 488 nm laser and Chl fluorescence). z-stack size was adjusted to 10 steps to cover at least 30 μm of the mesophyll. As the line between epidermal and mesophyll cells in potato leaf is not flat and epidermal cells often reach into the plane of mesophyll cells, epidermal chloroplasts were also analyzed in several images. ROI sizes and magnifications for individual experiments are specified in Tables S1 and S3. The images were processed using LEICA LAS X software (Leica Microsystems) to obtain maximum projections from z-stacks for each of two or three channels. On mock-inoculated and oxidant−/reductant-treated plants, ROIs were selected randomly on the leaf. On PVY$^{N-Wilga}$-inoculated plants, two consecutive ROIs were imaged adjacent to the lesion (ROI1, ROI2) and one ROI was imaged distant from the lesion (CTR) (Fig. 1a). See Table S1 for the number of analyzed plants, leaves, lesions and ROIs for each experiment for each treatment and time point. On PVY-N605(123)-GFP-inoculated plants, ROI1 was imaged adjacent to the lesion (ROI1) or on the front of the virus spread (ROIV) (Fig. 5; Table S1).

For stromule detection in relation to virus localization, two z-stacks were taken at the same position. One z-stack size was adjusted to 10 steps to cover at least 30 μm of the mesophyll (palisade tissue) and the second to cover the whole epidermis (*c.* 30 μm) and at least 30 μm of the mesophyll (palisade tissue) (see comments in Table S1).

For stromule counting experiments, the emission of roGFP2 was measured after excitation with a 488 nm laser in the window between 505 and 530 nm. Fluorescence emissions were collected
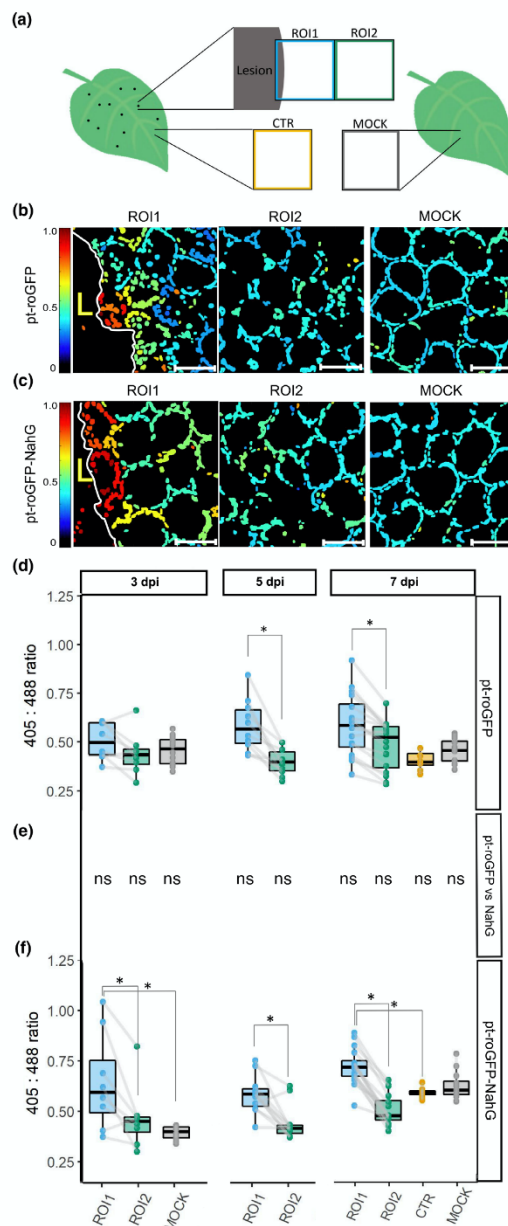
Fig. 1 Chloroplast redox state is spatially regulated around the cell death zone during potato virus Y (PVY)-induced hypersensitive response (HR). (a) After inoculating leaves with PVY, the chloroplast redox state was measured in transgenic sensor plants (pt-roGFP and salicylic acid (SA)-deficient pt-roGFP-NahG) with redox state-sensitive green fluorescent protein (roGFP) targeted to chloroplasts. The chloroplast redox state was measured in three regions: the area adjacent to the lesion (region of interest 1, ROI1), the area adjacent to ROI1 (ROI2), and an area distant from the lesion (control, CTR) on the same leaf. As a negative control, the chloroplast redox state was also measured in mock-inoculated plants (MOCK). To estimate the location of the lesion and determine the border between the cell death zone and normal tissue, the tissue was scanned in the channel for the background chloroplast fluorescence detection (the border of the lesion is marked with mesophyll cells with disorganized chloroplasts that moved away from the cell periphery) and brightfield (to detect dead tissue). In normal tissue, chloroplasts are well arranged between the vacuole and the cell wall, forming a ring in a circular shape of a mesophyll cell. (b, c) Visual presentation of the ratios of fluorescence intensities of roGFP after excitation with 405 and 488 nm laser (405 : 488 ratio, chloroplast redox state) presented on the rainbow scale for pt-roGFP L2 (b) and pt-roGFP-NahG L2 (c) in ROI1, ROI2 and MOCK (from left to right). Images are maximum projections from z-stacks processed with in-house MATLAB script. Higher ratios denote chloroplasts in a more oxidized state (red). Chloroplasts in the cells surrounding the cell death zone are highly oxidized, in contrast with more distant cells. Bar, 50 µm. (d, f) Chloroplast redox state in the earlier-mentioned leaf areas in pt-roGFP L2 (d) and pt-roGFP-NahG L2 (f) plants at 3, 5 or 7 d post-inoculation. Results are presented as boxplots with 405 : 488 ratios of each measured ROI shown as dots (Exp3NahG and Exp5NT in Supporting Information Table S1). Gray lines connect ROI1 and ROI2 pairs for each lesion. Asterisks denote statistically significant differences ($P < 0.05$) between the marked regions (ROI2, CTR or MOCK) and ROI1, determined by the mixed-effects model (ANOVA). Boundaries of the box, 25th and 75th percentiles; horizontal line, median; vertical line, all points except outliers. The experiment was performed three times independently on three transgenic lines (Redox Exp6NT in Fig. S1; Tables S1, S2; doi: 10.5281/zenodo.6417635). (e) Comparison of 405 : 488 ratios for marked regions (ROI1, ROI2, CTR and MOCK) between genotypes determined by the mixed-effects model (ANOVA). ns, not statistically significant. See Lukan et al. (2018, 2020) for the figures showing visual and microscopic lesion formation and reactive oxygen species (ROS) staining at different days post-inoculation (dpi).

average was set to 3 and the z-stack was adjusted to 12–15 steps (1.50–2.00 µm per step). Four consecutive ROIs were imaged adjacent to the lesion (ROI1–ROI4; Fig. S2). In Exp4NT, plants were imaged with ×5 and ×20 objectives, the frame average was set to 3 and the z-stack size was adjusted to 15 steps (0.8–1.0 µm per step). Two consecutive ROIs were imaged adjacent to the lesion (ROI1 and ROI2; Fig. 4a). In Exp6NTNahG, plants were imaged with a ×20 objective, the frame average was set to 3 and the z-stack size was adjusted to 15 steps to cover the whole epidermis and at least 50 µm of the mesophyll. Two consecutive ROIs were imaged adjacent to the lesion (ROI1 and ROI2; Fig. 4a). See Table S3 for zoom factor, digital zoom, optical zoom and the numbers of analyzed plants, leaves, lesions and ROIs for each experiment for each treatment and time point.

In the experiment with chloroplastic ROS inhibitor, two consecutive ROIs were imaged adjacent to the lesion (ROI1, ROI2) in PVY-N605(123)-GFP-inoculated plants on the left (inhibitor-infiltrated) and right (control-infiltrated) sides of the leaf with the

sequentially through two channels only (roGFP2 fluorescence after excitation with 488 nm laser and Chl fluorescence).

In stromule counting experiments, PVY N605-GFP-inoculated plants were imaged. In Exp3NT and Exp5NahG (Table S3), plants were imaged with a ×5 objective, the frame

same settings as in the redox state detection experiments (Fig. 6 a). See Table S4 for details.

Raw and analyzed imaging data were deposited at Zenodo (doi: 10.5281/zenodo.6417635).

Image analysis

For the detection of chloroplast redox state, maximum projections from z-stacks for each of three channels – Chl fluorescence, roGFP2 fluorescence after excitation with a 405 nm laser line, and GFP fluorescence after excitation with a 488 nm laser line – were, for each ROI, exported from Leica las X software as a tif file.

Image analysis was performed using an in-house Matlab script (MATLAB and Image Processing Toolbox Release 2019b). The images were analyzed with the following steps: import of tif files, conversion to grayscale, filtering out pixels of low intensity, conversion to binary format using spatial adaptive thresholding, a round or erosion and dilation to remove single pixel noise around the chloroplasts, followed by size-based segmentation of individual chloroplasts. The ratios of fluorescence intensities 405 : 488 were then calculated for each pixel belonging to the chloroplast masks obtained in the previous step. Results were calculated per image (normalized to the fraction of pixels belonging to chloroplasts) and per individual chloroplast in each image (see 405_488 in Table S1 for 405 : 488 ratios). The ratios present the relative redox state and were not normalized to ratios obtained by treatment with H_2O_2 and DTT, as oxidation of potato chloroplasts in close proximity to HR-PCD was stronger than oxidation with H_2O_2, which is most probably a result of the ineffective uptake of the solution into the potato cells.

In the next step, ROI1 and ROI2 were further divided into five regions (bins; Fig. S3a), depending on the distance from the lesion (bin 1 being closest and bin 5 furthest from the lesion). Again, the 405 : 488 ratios were determined for each pixel inside chloroplast masks, and then the first four bins were normalized to the 405 : 488 ratio in bin 5, which was set to 1 (Table S5).

For counting stromules, maximum projections from z-stacks for each of two channels (Chl and 488) were, for each ROI, exported from Leica las X software as a tif file. The stromules were counted manually on the 488 tif images, and the number of the chloroplasts was determined as described earlier. The number of stromules was normalized to the number of chloroplasts for the corresponding ROI (Table S3). Details of all the parameters used in the image analysis can be found in the analysis scripts, which are available on Github (https://github.com/NIB-SI/SensorPlantAnalysis).

Statistics

To determine which factors contributed most to the variability in measured 405 : 488 ratio values, we used a linear mixed effects model (LME):

$$F^{ijkno} = T_i + D_j + L_k + P_n + \text{LE}_{no} + e_{ijkno}$$

where F is the fluorescence (405 : 488 ratio) measured on day j after treatment/ROI i, on leaf o of plant n belonging to plant line

k; T_i is the mean (fixed) effect of treatment/ROI i; D_j is the mean (fixed) effect of time after treatment/viral infection j; L_k is the mean (fixed) effect of the specific plant line k; P_n is the (random) effect of plant n, assumed to be normally distributed with mean 0; LE_{no} is the (random) effect of the chosen leaf n on plant o, assumed to be normally distributed with mean 0; and e_{ijkno} is the residual error, assumed to be normally distributed with mean 0. If factors were not relevant for individual experiments (e.g. experiments run on a single line, or measured on a single day after treatment), they were removed from the mixed-effects model. The final LME model was fitted with maximum likelihood to model the 405 : 488 ratio as the dependent variable, treatment/ROI, dpi, transgenic line/genotype as fixed effects, and plant and leaf as random effects.

Statistical analysis was implemented as an R-based script, with significance calculation of the fixed factors performed using the 'anova' function (Satterthwaite's method) from the package LMERTEST (Kuznetsova et al., 2017) and post hoc pairwise comparisons within levels of significant fixed factors performed using the 'emmeans' function (Kendall–Roger method) available from the package EMMEANS (Lenth et al., 2021). The post hoc pairwise comparisons were performed between levels of individual fixed factors (e.g. between ROI1 and ROI2 after viral infection), with and without stratification by the other fixed factors. For instance, comparison between ROI1 and ROI2 after viral infection was performed for the whole experiment, as well as for the data available only for a single line, on a single day post-infection, and for all combinations between line and day post-infection (Table S2).

The results of the experiments with the ROS inhibitor were analyzed using a linear model with factors treatment, tissue sections and interaction between the two. Significance was calculated using the 'anova' and 'emmeans' function, as for the mixed model.

Frequency of ROI2 with individual cells with moderately oxidized chloroplasts was calculated with Fisher's exact test.

All scripts were deposited on Github (https://github.com/NIB-SI/SensorPlantAnalysis).

Spatial RT-qPCR expression analysis

Left and right sides of the first fully developed leaf of PVY-N605 (123)-GFP-inoculated pt-roGFP L2 transgenic plants were infiltrated with ROS inhibitor/control as described earlier. At 5 dpi, for each of the 12 lesions from four plants, two tissue sections were sampled: the lesion and its close proximity (A) and a 1 mm section adjacent to section A (B; Fig. 6b). As a control, tissue sections of the same size as the A and B sections together were sampled further from the lesions on both the inhibitor- and control-treated sides of the leaf (Fig. 6b). Lesions in which we did not detect viral RNA or with inaccurate sampling were excluded from the analysis. See Table S4 for the details.

Total RNA was extracted from the sampled A and B sections using 50 µl of TRizol reagent (Thermo Fisher Scientific, Waltham, MA, USA) combined with RNA purification on Zymo-Spin columns (Direct-zol RNA MicroPrep Kit; Zymo Research, Irvine, CA, USA) according to the manufacturer's protocols. To

elute RNA, 15 μl of prewarmed (80°C) DNase/RNase-free water was added to the Zymo-Spin columns and incubated at room temperature for 10 min before centrifugation at 16 000 g for 1 min. DNase-treated (0.5 μl DNase per μg RNA; Qiagen) total RNA was quality-controlled using 2100 Bioanalyzer and RNA 6000 Pico LabChip Kit (Agilent Technologies) and then reverse-transcribed using the High Capacity cDNA Reverse Transcription Kit (Thermo Fisher Scientific).

Samples were analyzed in the setup for quantitative PCR (qPCR) as previously described (Lukan *et al.*, 2020). The expression of 13 genes involved in different steps of immune signaling (Table S6 for a full list of genes) was analyzed and normalized to the expression of two validated reference genes, COX and elongation factor 1 (EF-1), as described previously (Petek *et al.*, 2014; see Lukan *et al.*, 2020 for primer and probe information). Additionally, CALS (Glucan synthase like 1/GSL1, Sotub07g019600.1.1.) gene expression was analyzed (forward primer: 5′-GAACACGAACTGGAGGATATTTTACC-3′, probe: FAM/TTGTCCTGGTGGTTCCAGAGTCGG-3′ Zen Iowa BlackTM FQ, reverse primer: 5′-GATTCCACGACCCACAA ACG-3′). In parallel with the gene expression of those genes, the relative quantity of PVY RNA was measured (Lukan *et al.*, 2020). The standard curve method was used for relative gene expression quantification using QuantGenius (http://quantgenius.nib.si; Baebler *et al.*, 2017).

Results

Chloroplast redox state is highly oxidized in the cells surrounding the cell death zone

Our previous studies of HR in potato–PVY interactions suggested the role of chloroplastic ROS as a signal orchestrating PCD (Lukan *et al.*, 2020). To further explore the role of chloroplastic ROS in PCD induction in a spatiotemporal manner, we constructed transgenic plants of cv. Rywal with redox state-sensitive GFP2 (roGFP2) targeted to chloroplasts (hereafter pt-roGFP plants). Measurement of roGFP2 emission following excitation at 405 and 488 nm in constructed transgenic plants permits an evaluation of the chloroplast relative redox state as the relative proportion of roGFP2 in an oxidized or reduced state (405 : 488 ratio) (Jiang *et al.*, 2006). Transgenic lines (pt-roGFP L2, L4 and L15) with strong and stable roGFP fluorescence in the chloroplasts were selected for further work (Table S1).

To determine if the chloroplast redox state is spatially and/or temporally regulated around the cell death zone, we measured the relative redox state in the palisade mesophyll chloroplasts of pt-roGFP plants in the areas adjacent to the lesion (ROI1) and adjacent to ROI1 (ROI2) at 3, 5, and 7 dpi with PVY, as well as in the area distant from the lesion (control, CTR) at 7 dpi (Fig. 1 a). Within the ROI1, chloroplasts in the cells surrounding the cell death zone were highly oxidized, in contrast to more distant cells (more distant from cell death zone within ROI1, in ROI2, and in CTR) (Fig. 1b,d; doi: 10.5281/zenodo.6417635). As a control of the normal physiological redox state in potato chloroplasts, we also measured the chloroplast redox state in mock-inoculated pt-roGFP plants at 3 and 7 dpi (Fig. 1a). The chloroplast redox state was highly uniform across all analyzed mock samples and comparable to the redox state of chloroplasts in cells distant to the cell death zone in PVY-infected plants (Fig. 1b,d; doi: 10.5281/zenodo.6417635).

We also imaged the epidermal cell layer in the majority of the analyzed areas but not in all, as a result of unevenness of the leaf cell layer distribution. We analyzed the redox state of their chloroplasts. In most cases, the chloroplasts in epidermal cells were in a similar redox state to chloroplasts in the underlying palisade mesophyll cells. Interestingly, in ROI1, chloroplasts in some of the epidermal cells were more reduced than those in mesophyll cells which we inspected in more detail in further experiments.

The measured variability of chloroplast redox state in ROI1 of the mesophyll cells was higher than in mock samples (Fig. 1d), as a result of the highly oxidized chloroplasts in cells of the PCD transition zone (Fig. 1b,d). To perform a more detailed spatiotemporal analysis of the redox state, we separated each ROI into five regions (bins), according to the distance from the cell death zone (Fig. S3a). The results show that the chloroplast redox state is indeed the most oxidized close to the cell death zone (bin 1) and is getting less oxidized with increasing distance from the cell death zone at different time points (Figs S3b, S4). In the most distant bin from the cell death zone (bin 5 of ROI1), the redox state stabilizes and remains comparable in all five bins of ROI2 (Fig. S3b).

Individual cells with moderately oxidized chloroplasts spread further away from the cell death zone

In cells at the border of the cell death zone, within ROI1, strongly oxidized chloroplasts often became more disorderly in their arrangement as they moved from the cell periphery towards the interior (Fig. 1b). These cells probably represent mesophyll cells that are in transition between normal cells and cells undergoing PCD, as supported by electron microscopy in our previous work (Lukan *et al.*, 2020). However, we also observed chloroplasts in a moderately oxidized redox state that were well arranged, following the shape of a normal mesophyll cell further from the cell death zone in ROI2 (Figs 2a, S5). Such cells, which we named signaling cells, were rarely observed in mock-inoculated plants (Fig. 1b).

SA-dependent presence of cells with oxidized chloroplasts further away from the cell death zone suggests their role in signal transmission in HR-conferred resistance

To study the link between SA signaling and chloroplast redox state in PCD and resistance, we also introduced roGFP2 in the SA-depleted transgenic counterpart NahG-Rywal (hereafter pt-roGFP-NahG plants). Potato genotype NahG-Rywal is a transgenic counterpart of cv. Rywal, depleted in the accumulation of SA (reduced to < 10% of native values). The depletion of SA renders NahG plants susceptible to PVY (catechol-independent; Baebler *et al.*, 2014), allowing the virus to spread throughout the plant (Baebler *et al.*, 2014). Transgenic lines (pt-roGFP-NahG
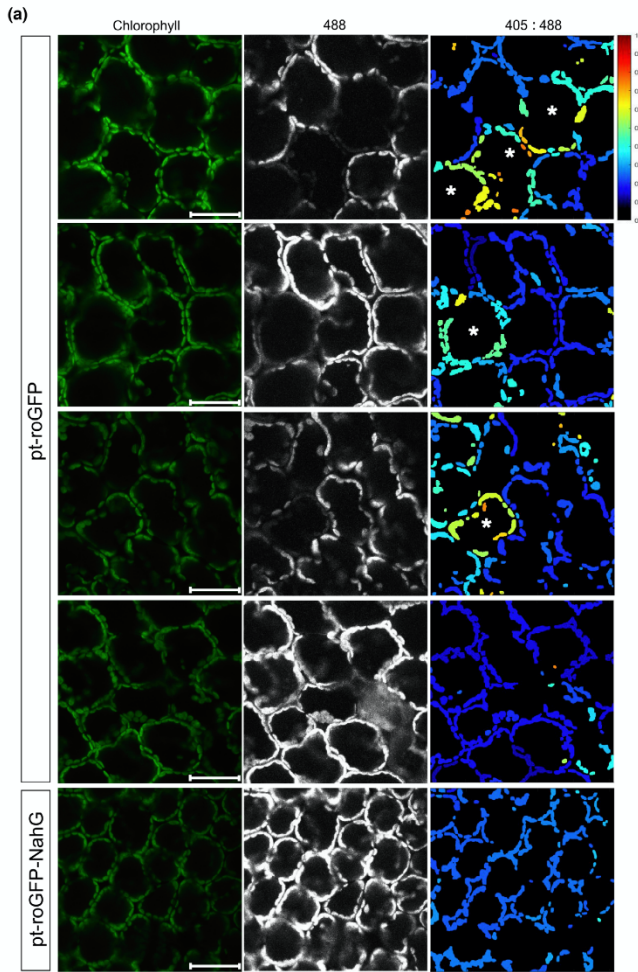
Fig. 2 Individual cells with moderately oxidized chloroplasts (asterisks) can be observed further from the cell death zone (region of interest 2, ROI2). (a) The first four panels present ROI2 in pt-roGFP2 plants with individual cells with moderately oxidized chloroplasts (signaling cells, first three panels) or with no signaling cells (fourth panel). The bottom panel presents ROI2 with no signaling cells in a salicylic acid (SA)-deficient pt-roGFP-NahG plant for comparison. Cells with oxidized chloroplasts further away from the cell death zone are marked with asterisks. Chlorophyll, Chl fluorescence; 488, roGFP fluorescence after excitation with 488 nm laser line showing reduced roGFP (brighter chloroplasts are more reduced); 405 : 488, relative redox state (405 : 488 ratio) presented on a rainbow scale. Higher ratios denote more oxidized chloroplasts (red). Bar, 50 μm. (b) Frequency of ROI2 with signaling cells for pt-roGFP (NT) and pt-roGFP-NahG (NahG). P-value comparing frequency of ROI2 with signaling cells between potato virus Y (PVY) and control treatments (PVY vs c) and between PVY treatments of each genotype (NT vs NahG) was calculated with Fisher's exact test. PVY, ROI2 of PVY-inoculated plants; control, combined MOCK and CTR inspected ROIs (Fig. 1a).

(b)

Genotype treatment		ROI2 No.		signaling	P-value	
		All	signaling	freq (%)	PVY vs c	NT vs NahG
NT	Control	121	4	3,3	0,0016	
	PVY	122	19	15,6		$< 10^{-5}$
NahG	Control	149	0	0,0	0,4772	
	PVY	136	1	0,7		

L2 and L7) with strong and stable GFP fluorescence in the chloroplasts were selected for further work. We next followed the chloroplast redox state after viral infection in different regions, close to or further away from the cell death zone at three time points. Similarly as in pt-roGFP plants (Fig. 1b), within the ROI1, chloroplasts in the cells surrounding the cell death zone were highly oxidized (Fig. 1c). This was further confirmed by image analysis, as the chloroplast redox state was more oxidized in ROI1 and was statistically significantly different from the chloroplast redox state in ROI2 at all analyzed time points

(Figs 1f, S1; Tables S1, S2). We conclude that the chloroplast redox state is precisely spatially regulated around the cell death zone in both pt-roGFP and SA-deficient pt-roGFP-NahG plants. Interestingly, however, the cells with moderately oxidized chloroplasts, further away from the cell death zone, were rarely observed in SA-deficient plants (Fig. 2; doi: 10.5281/zenodo.6417635). This result suggests that chloroplast oxidation distant from the cell death zone requires SA signaling, whereas chloroplast oxidation near the cell death zone occurs independently of SA signaling. As SA is required to prevent the viral spread, but not for the development of PCD (Lukan *et al.*, 2018, 2020), we hypothesize that chloroplast oxidation in distant cells participates in signaling for resistance, whereas chloroplast oxidation near the cell death zone is related to PCD.

Spatiotemporal regulation of stromule formation around the cell death zone is SA signaling-dependent

Although our experimental setup was focused on measuring the redox state in the mesophyll cells, because of the unevenness of the leaf cell layer distribution, we also imaged epidermal cells layer in the majority of investigated areas. Chloroplasts in epidermal cells were in a similar redox state as chloroplasts in underlying palisade mesophyll cells. Interestingly, we observed individual epidermal cells with highly reduced chloroplasts, often in the area between the cell death zone and signaling mesophyll cells (Fig. 3 a,b). In those cells, we were also able to observe clustering of chloroplasts and intensive connectivity via stromules (Fig. 3a,b). We confirmed that the clustering of chloroplasts is the result of their movement towards the nucleus (Video S1). Our observation that chloroplasts with stromules are highly reduced is in disagreement with the results of some other studies (Brunkard *et al.*, 2015; Caplan *et al.*, 2015; Barton *et al.*, 2018; Ding *et al.*, 2019). It is possible, however, that our findings are specific for cell-to-cell signaling in this particular plant–virus interaction, which was not yet studied in this aspect. Moreover, we observed the majority of chloroplasts with stromules in epidermal cells, which is in agreement with the literature showing that stromules are a characteristic cell-specific feature and are more frequently present in epidermal cells (reviewed in Natesan *et al.*, 2005).

We performed additional experiments to investigate these results further. In these experiments, we adjusted z-stack size to cover the whole epidermis and at least 50 μm of the mesophyll. We observed increased stromule formation frequency in epidermal chloroplasts after inoculation at all time points, which was even more pronounced in the cell death zone proximity in pt-roGFP plants (Fig. 4). When comparing the frequency of stromules between ROI1 and ROI2 in pt-roGFP plants, the difference was statistically significant at 4 and 5 dpi. By contrast, in pt-roGFP-NahG plants, the number of stromules was similar between ROI1 and ROI2 at all time points (Fig. 4d; Tables S3, S7). The frequency of stromules of PVY-inoculated plants was higher if compared with random regions on the leaf of mock-inoculated plants at all time points in pt-roGFP plants (Fig. 4d; Tables S3, S7). The induction of stromules was, however, less pronounced in pt-roGFP-NahG plants. We also compared the

frequency of stromules between genotypes, and the difference was statistically significant at 4 and 5 dpi for ROI1, but not for ROI2 (Fig. 4d). We thereby conclude that in PVY-induced HR in potato, stromule formation is spatiotemporally regulated around the cell death zone and is SA signaling-dependent.

Stromules are induced in immediate proximity to virus multiplication zone

To investigate why the stromule frequency is 5 dpi in pt-roGFP-NahG plants induced in both ROI1 and ROI2, whereas in pt-roGFP plants the induction was visible only in ROI1, we decided to expand our characterization of the spatiotemporal responses to PVY infection and check stromule frequency in ROI3 and ROI4 as well. We followed stromule formation in four consecutive regions adjacent to the cell death zone at different time points following inoculation in both genotypes (ROI1–ROI4; Fig. S2a,b, d). This experiment confirmed the previous results showing that stromule formation is differentially spatiotemporally regulated between genotypes. In pt-roGFP-NahG plants, induction of stromule frequency was, besides ROI2, higher also in ROI3, whereas in pt-roGFP plants, the induction was visible only in ROI1 (Figs 4, S2a,b,d; Tables S3, S7).

In our previous study, we reported that PVY accumulated in the cells on the border of the cell death zone in nontransgenic plants at all analyzed time points (most frequently at 4 dpi), but the virus did not spread beyond this zone. In NahG plants, however, we observed concentric virus spread to adjacent cells, such that PVY reached the outer borders of ROI2 within 6–7 dpi (Lukan *et al.*, 2018). The viral spread correlates with stromule frequency, which in pt-roGFP is statistically higher in ROI1 than in ROI2, ROI3, ROI4 or MOCK, while in pt-roGFP-NahG, both ROI1 and ROI2 have higher stromule frequency as compared with ROI3, ROI4 or MOCK (Figs 4d, S2a,b,d).

To confirm the relationship between stromule frequency and virus multiplication, we followed the cells on the border of the virus multiplication zone in pt-roGFP plants at 4 dpi and in pt-roGFP-NahG plants at 7 dpi using GFP-tagged PVY (Fig. 5a,c; Table S1). We collected two z-stacks in the same ROI, one covering the whole epidermis with at least 50 μm of the mesophyll and one only 50 μm of the mesophyll. In both genotypes, we observed epidermal chloroplasts with stromules in the cell adjacent to the cell with PVY-GFP accumulation (Fig. 5b,d). We therefore conclude that stromule formation was more pronounced in the cell adjacent to the infected cell, which could be a result of plant-mediated response to the presence of the virus or virus multiplication. Owing to a strong background in the 405 nm channel as a result of strong PVY-GFP fluorescence, an evaluation of the chloroplast relative redox state as the relative proportion of roGFP in an oxidized or reduced state (405 : 488 ratio) was not possible.

Blocking the chloroplastic redox changes affects the spatial response at the transcriptional level in HR

To further study the mechanism of this chloroplast redox state-dependent signaling and its downstream targets, we treated plants
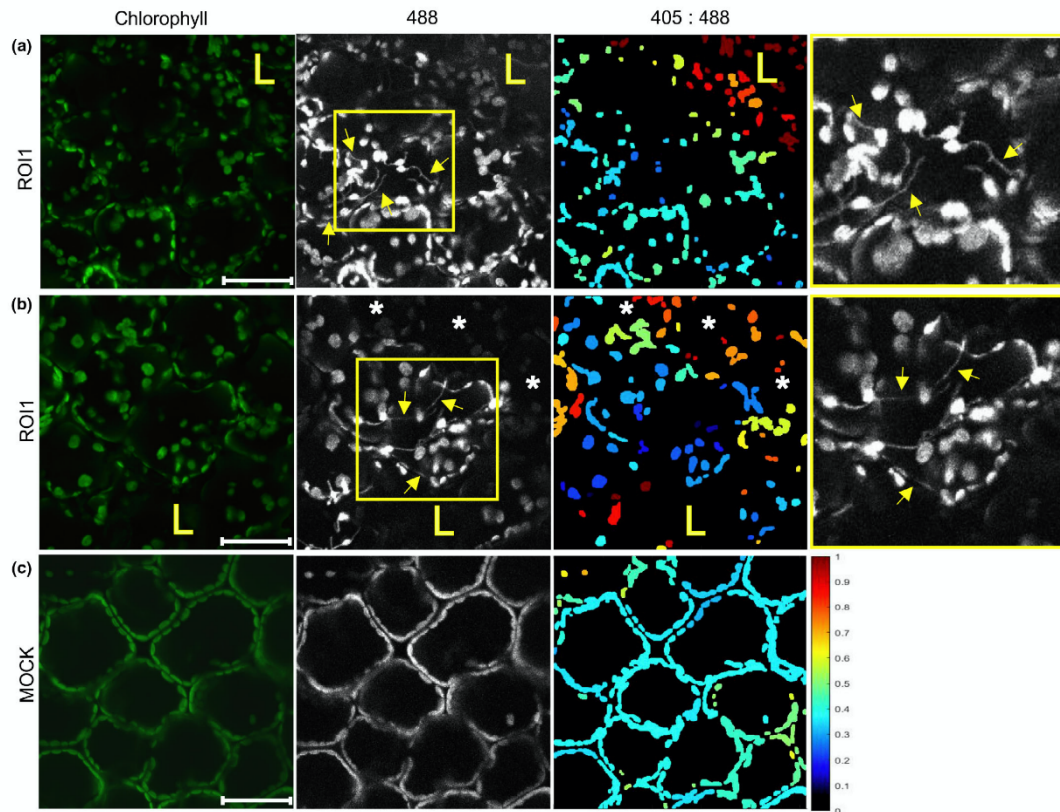
Fig. 3 Stromules are induced in cells adjacent to the hypersensitive response (HR) cell death zone. (a, b) Chloroplasts with stromules (arrows) in the cells on the border of the cell death zone in ROI1 (a) or in the cells between the cell death zone and the cells with oxidized chloroplasts in ROI1 (b) in leaf epidermis of potato virus Y (PVY)-inoculated pt-roGFP plants. A strongly reduced redox state is shown as a high signal in 488 channel, black or dark blue on 405 : 488 ratio images. Higher magnification of an area with stromules (boxed with yellow) is shown in the rightmost panel. (c) Epidermal chloroplasts in the mock-inoculated pt-roGFP plant for the comparison of redox state. Images were taken in PVY- and mock-inoculated pt-roGFP plants at 5 and 3 d post-inoculation, respectively. Stromules are marked with arrows. Cells with oxidized chloroplasts further away from the cell death zone are marked with asterisks. The cell death zone is marked with an 'L'. ROI1, region of interest adjacent to cell death zone (Fig. 1a); chlorophyll, Chl fluorescence; 488, roGFP fluorescence after excitation with 488 nm laser line showing reduced roGFP (brighter chloroplasts are more reduced); 405 : 488, relative redox state (405 : 488 ratio) presented on a rainbow scale. Higher ratios denote more oxidized chloroplasts (red). z-stack size was adjusted to 10–15 steps to cover at least 30 µm of the mesophyll. As the line between epidermal and mesophyll cells in potato leaf is not flat and epidermal cells often reach into the plane of mesophyll cells, in several images we were also able to observe epidermal chloroplasts. Bar, 50 µm.

with ROS scavenger uracil (Abdollahi & Ghahremani, 2011) and performed spatial transcriptomics in cell death zone proximity at 5 dpi (Fig. 6). The target genes were selected according to their involvement in redox potential homeostasis (*CAT1*, *PRX28*, *RBOHD*, *RBOHA*, *TRXH*), JA signaling (*13-LOX*, *9-LOX*, *ACX3*), ET signaling (*ERF1*), stability of R proteins (*HSP70*) and actuation of defense (*BGLU*, *PR1B*, *CALS*) and all showed spatial regulation following PVY inoculation (Lukan *et al.*, 2020). We show that induction of chloroplast oxidation around the site of viral foci was successfully blocked when treated with uracil (Fig. 6a). Genes show different spatial transcriptional

responses (Figs 6c, S6). *ERF1* was upregulated further from the cell death zone (section B) when ROS signaling was hampered compared with induction in the cell death zone (section A) in the control (Fig. 6; Tables S4, S6, S8, S9). *RBOHD* expression is, by contrast, higher in section A of inhibitor-treated plants, and *RBOHA*, *HSP70* and *CAT1* showed similar spatial regulation in the control and inhibitor-treated tissue. Interestingly, *TRXH* expression is lower if ROS is generated as its expression was higher in inhibitor-treated tissue in both the A and B zones. Therefore, ERF1, RBOHD and TRXH are downstream chloroplast redox state-dependent signaling for resistance.
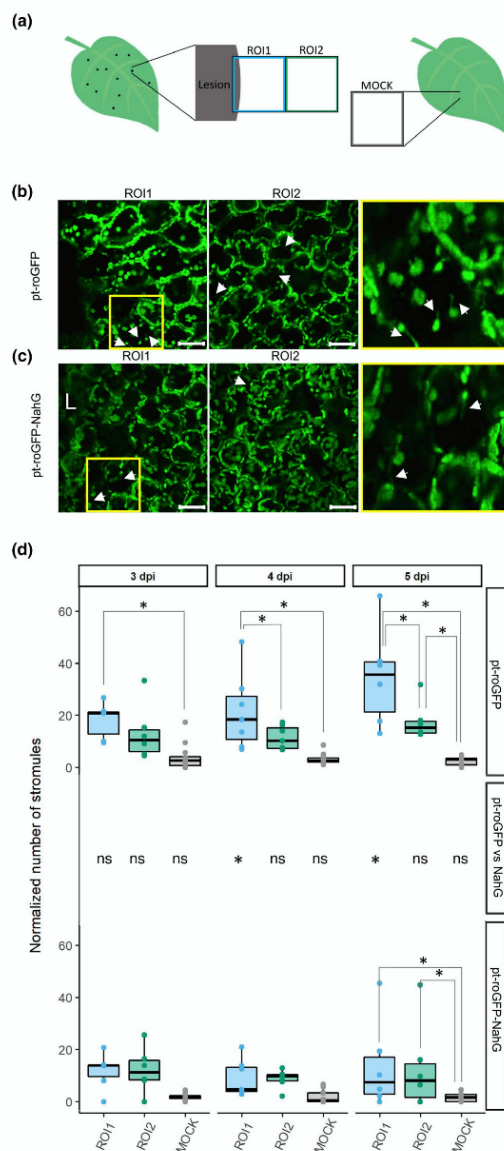
Fig. 4 Spatiotemporal regulation of stromule formation around the cell death zone is salicylic acid (SA) signaling-dependent. (a) Stromule formation was followed in redox state sensor plants after potato virus Y (PVY) inoculation. See Fig. 1 legend for the details. (b, c) Confocal image showing the difference in the number of stromules between region of interest 1 (ROI1, left) and ROI2 (right) in pt-roGFP (b) and pt-roGFP-NahG (c). After inoculation, we observed stromule formation, which was even more pronounced in the proximity of the cell death zone in pt-roGFP plants. Higher magnification of an area with stromules (boxed in yellow) is shown in the rightmost panel. Arrows show stromules. Bar, 50 μm. (d) Normalized number of stromules, calculated by dividing the number of stromules by the number of chloroplasts counted in the earlier-mentioned leaf areas in pt-roGFP L2 and pt-roGFP-NahG L2 transgenic lines at 3, 4 and 5 d post-inoculation (dpi) (Exp6NTNahG in Supporting Information Table S3). Results are presented as boxplots with normalized numbers of stromules for each ROI shown as dots (Stromules Exp6NTNahG in Table S3). Asterisks denote statistically significant differences ($P < 0.05$) between regions (shown on the boxplots connecting lines; see Stromules Exp6NTNahG in Table S7 for P-values) or between genotypes (pt-roGFP vs NahG, shown for each region for each day post-inoculation in the middle panel; see Stromules Exp6NTNahG in Table S7 for P-values), determined by the mixed-effects model (ANOVA). z-stack size was adjusted to 15 steps to cover the whole epidermis and at least 50 μm of the mesophyll. ns, not statistically significant. Boundaries of the box, 25th and 75th percentiles; horizontal line, median; vertical line, all points except outliers.

et al., 2017; Su *et al.*, 2018). Our results showing that the disordered chloroplasts in the cells adjacent to the cell death zone were strongly oxidized (Figs S3b,c (top panel), S4) are in agreement with and extend these previous conclusions. In addition, close to the border of the cell death zone (ROI1; Fig. S3b,c), as well as further away from the cell death zone (ROI2; Figs 2a, S5; Table S1), we observed the so-called signaling cells, individual mesophyll cells with moderately oxidized chloroplasts. These cells were sparse in SA-deficient plants with compromised resistance, which indicates their role in signal transmission in HR-conferred resistance. This is supported by the results of several studies showing that decreased chloroplastic ROS production leads to compromised resistance (Su *et al.*, 2018; Xu *et al.*, 2019; Schmidt *et al.*, 2020). Here we also show that chloroplastic redox changes are modulating spatial transcriptional response of immunity-related genes (Fig. 6). Indeed, the regulation of genes involved in ethylene signaling (ERF1) and redox state sensing (TRXH) was changed further away from the viral foci when oxidation of chloroplast was blocked, confirming the signaling role of chloroplastic redox changes in PVY-induced HR response (Fig. 6c). The chloroplast redox state has previously been studied during HR-PCD, triggered by N-mediated recognition of a fragment of the helicase domain of the TMV replicase (p50) with the HyPer2 H_2O_2 sensor (Caplan *et al.*, 2015). The authors detected higher concentrations of ROS in chloroplasts at 28 h post-agroinfiltration to express p50. As their approach causes even expression of p50 across all cells and does not track an actual virus infection, the spatial dynamics of redox state changes during HR and the effect on signaling could not be directly interrogated. Our study thus brings a new perspective to redox signaling during HR resistance.

Reactive oxygen species production in plant organelles triggers intracellular communication pathways that alter intercellular communication via plasmodesmata (PD) (Stonebloom *et al.*,

Discussion

Programmed cell death has been associated with increased chloroplastic ROS production (Wagner *et al.*, 2004; Liu *et al.*, 2007; Straus *et al.*, 2010). Generation of chloroplastic ROS was proposed as a signal orchestrating PCD, rather than only being a consequence of PCD (Zurbriggen *et al.*, 2010; Pierella Karlusich

2012). They showed that oxidized plastids resulted in decreased PD transport, whereas reduced plastids can facilitate PD transport. Thus, we could assume that the highly oxidized chloroplasts at the border of the cell death zone have PD closed to prevent the spread of the pathogen. Interestingly, the cells with high frequency of stromules that we observed in proximity to the cell death zone or to the cell in which we observed PVY-GFP accumulation had reduced chloroplasts (Fig. 5), meaning they could

have increased PD transport. This is in accordance with Caplan *et al.* (2015), who suggested that stromule function is HR-PCD signaling. However, their experimental approach with transient expression of HR-triggering proteins only focused on signaling for PCD while signaling for viral arrest was not studied. We additionally showed that the increase in stromule formation observed in SA-deficient plants in ROI2 (Fig. S2) was linked to the border of the virus multiplication zone (Fig. 5).
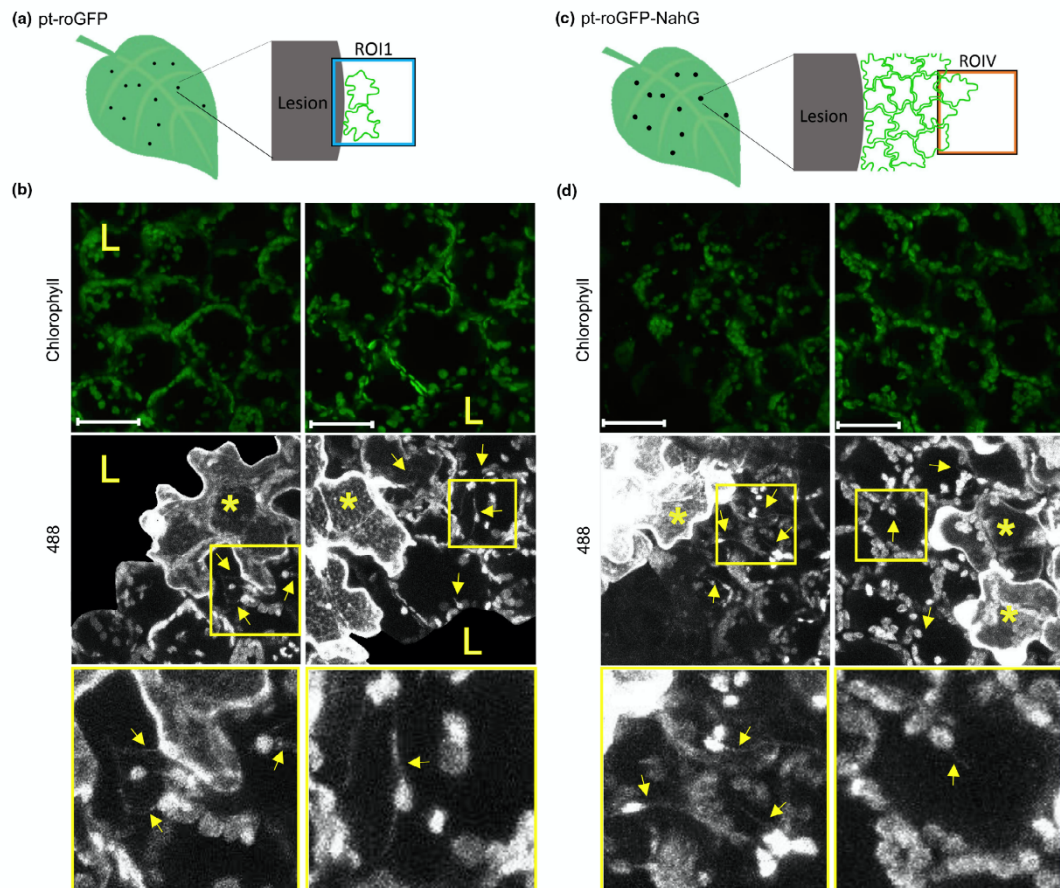
Fig. 5 Stromules are induced in immediate proximity to the virus multiplication zone. (a, c) Stromule formation was followed in pt-roGFP on the border of the cell death zone (ROI1) in the cells adjacent to the cell in which we observed potato virus Y-green fluorescent protein (PVY-GFP) accumulation at 4 d post-inoculation (dpi) (a) or in pt-roGFP-NahG on the border of the virus multiplication zone (ROIV) in the cells adjacent to the cell in which we observed PVY-GFP accumulation at 7 dpi (c). (b, d) 488, stromules (arrows) are induced adjacent to the cell in which we observed PVY-GFP accumulation (asterisks). Boxed areas show higher magnification of regions with stromules. Owing to high background signal in the cell death zone, as a result of virus-derived GFP fluorescence, GFP signal is not shown in the cell death zone in 488 images. Owing to a strong background in the 405 nm channel as a result of strong virus-derived GFP fluorescence, an evaluation of the chloroplast relative redox state as the relative proportion of roGFP in an oxidized or reduced state was not possible, and therefore 405 : 488 ratios are not presented. Left and right panels present different ROIs. Stromules are marked with arrows. Cells in which we observed PVY-GFP accumulation are marked with asterisks. The cell death zone is marked with an 'L'. ROI1, region of interest adjacent to cell death zone; ROIV, region of interest adjacent to the virus multiplication zone. Chlorophyll, Chl fluorescence; 488, roGFP fluorescence after excitation with 488 nm laser line showing reduced roGFP (brighter chloroplasts are more reduced). z-stack size was adjusted to 10 steps to cover the whole epidermis (c. 30 μm) and at least 30 μm of the mesophyll. Bar, 50 μm.
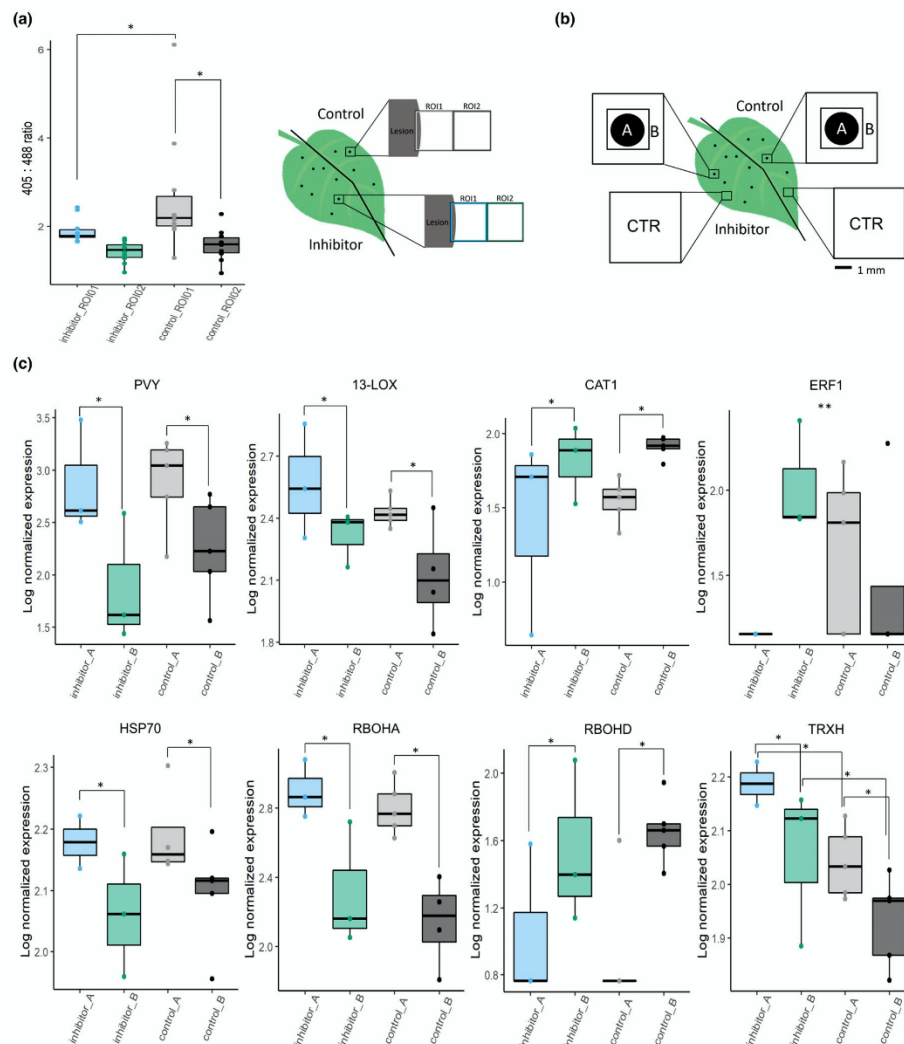
Fig. 6 Chloroplastic redox changes regulate spatial expression of selected genes. (a) Uracil is efficiently blocking chloroplastic reactive oxygen species (ROS) production near potato virus Y (PVY) infection lesions. Left and right sides of the PVY-green fluorescent protein (PVY-GFP)-inoculated leaves of pt-roGFP plants were infiltrated with chloroplastic ROS inhibitor and control at 4 d post-inoculation (dpi). At 48 h post-treatment, two consecutive regions of interest (ROIs) were imaged adjacent to the lesion (ROI1, ROI2) on the left (inhibitor-infiltrated) and right (control-infiltrated) sides of the leaf with the same settings as in redox state detection experiments using confocal microscopy. The relative chloroplast redox state was determined to confirm functionality of the chloroplastic ROS inhibitor in the selected transgenic line. (b) Schematic overview of sampling for transcriptomics. PVY-GFP-inoculated leaves of pt-roGFP L2 plants were infiltrated as described earlier. At 5 dpi, two tissue sections were sampled: lesion (section A) and a 1 mm section adjacent to section A (section B). As a control (CTR), tissue sections of the same size as the A and B sections together were sampled further away from the lesions on both the inhibitor- and control-treated sides of the leaf. (c) Viral RNA abundance (PVY) and expression profiles of seven genes (HSP70, heat shock protein 70; RBOHD, potato respiratory burst oxidase homolog D; RBOHA, potato respiratory burst oxidase homolog A; CAT1, catalase 1; 13-LOX, 13-lipoxygenase; ERF1, potato ethylene responsive transcription factor 1a; TRXH, thioredoxin H) are presented as boxplots with logarithmic normalized relative expression in sections A and B for chloroplastic ROS inhibitor-treated and control-treated lesions shown as dots. Abundance/expression is presented as a log_2 ratio between relative expression in each section and averaged relative expression in CTR sections. Significance for effects of treatment, tissue section and interaction between the two was tested using a linear model (ANOVA), and significant relationships are marked by an asterisk (*) in the figure for treatment and tissue section and two asterisks (**) for the interaction (Supporting Information Table S9). See Tables S4 and S6 for the details, number of analyzed lesions and P-values for all analyzed genes. Asterisks (* and **) denote statistically significant differences ($P < 0.05$). Boundaries of the box, 25th and 75th percentiles; horizontal line, median; vertical line, all points except outliers.

Maruta *et al.* (2012) suggested that the chloroplastic H_2O_2 and SA activate each other and that this positive feedback loop is involved in the plant immune response. By contrast, we found no major differences between the chloroplast redox state of SA-deficient pt-roGFP-NahG compared with pt-roGFP plants close to the lesion (Figs 1, S3). However, the frequency of previously mentioned signaling cells with moderately oxidized chloroplasts was lower in SA-depleted plants (Fig. 2). Additionally, we studied SA involvement in stromule formation. Previous studies showed that an oxidative environment induces stromule formation (Brunkard *et al.*, 2015; Caplan *et al.*, 2015; Barton *et al.*, 2018; Ding *et al.*, 2019). Indeed, in our study, the number of stromules was induced in lesion proximity. Interestingly, however, the frequency of stromules was statistically significantly higher in pt-roGFP than in SA-deficient pt-roGFP-NahG plants (Fig. 4), although the oxidative state of chloroplasts adjacent to the cell death zone was the same (Fig. 1). This is in agreement with results from Caplan *et al.* (2015), who showed that application of an SA analog induces stromules when HR is triggered by pathogen recognition. Therefore, we conclude that stromule induction does not depend solely on the redox state of chloroplasts in adjacent cells.

Our results collectively show that the increase in mesophyll chloroplast redox state is linked to PCD signaling, which is SA-independent, and also to signaling for HR-conferred resistance to the virus, which is SA-dependent. The later phenomenon is supported by the presence of mesophyll cells with moderately oxidized chloroplasts further away from the cell death zone which are linked to epidermal cells with reduced chloroplasts and high stromule connectivity and changes in transcriptional regulation, indicating intensive intracellular and cell-to-cell communication activity.

Competing interests

None declared.

Author contributions

KG and TL designed the research; TMP, MJ, MK and TL performed the research; AŽ, TMP and TL contributed new analytic/computational/imaging tools; TL, KG, AŽ, TMP, MK, JB and ŠB analyzed the data. TL, KG, AŽ, TMP, MJ, ŠB and JB contributed to the writing or revision of the article.

ORCID

Špela Baebler https://orcid.org/0000-0003-4776-7164
Jacob O. Brunkard https://orcid.org/0000-0001-6407-9393
Kristina Gruden https://orcid.org/0000-0001-5906-8569
Mojca Juteršek https://orcid.org/0000-0003-0183-2493
Mirjam Kmetič https://orcid.org/0000-0002-6729-4416
Tjaša Lukan https://orcid.org/0000-0002-6235-2816
Tjaša Mahkovec Povalej https://orcid.org/0000-0003-3706-2371
Anže Županič https://orcid.org/0000-0003-3303-9086

Data availability

Raw and analyzed imaging data were deposited at Zenodo and are openly available at doi: 10.5281/zenodo.6417635. Scripts were deposited at Github and are openly available at https://github.com/NIB-SI/SensorPlantAnalysis.

References

Abdollahi H, Ghahremani Z. 2011. The role of chloroplasts in the interaction between *Erwinia amylovora* and host plants. *Acta Horticulturae* 896: 215–222.

Baebler Š, Krečič-Stres H, Rotter A, Kogovšek P, Cankar K, Kok EJ, Gruden K, Kovač M, Žel J, Pompe-Novak M *et al.* 2009. PVY^{NTN} elicits a diverse gene expression response in different potato genotypes in the first 12 h after inoculation. *Molecular Plant Pathology* 10: 263–275.

Baebler Š, Svalina M, Petek M, Stare K, Rotter A, Pompe-Novak M, Gruden K. 2017. QUANTGENIUS: implementation of a decision support system for qPCR-based gene quantification. *BMC Bioinformatics* 18: 276.

Baebler Š, Witek K, Petek M, Stare K, Tušek-Žnidarič M, Pompe-Novak M, Renaut J, Szajko K, Strzelczyk-Zyta D, Marczewski W *et al.* 2014. Salicylic acid is an indispensable component of the *Ny-1* resistance-gene-mediated response against *Potato virus Y* infection in potato. *Journal of Experimental Botany* 65: 1095–1109.

Balint-Kurti P. 2019. The plant hypersensitive response: concepts, control and consequences. *Molecular Plant Pathology* 20: 1163–1178.

Barton KA, Wozny MR, Mathur N, Jaipargas EA, Mathur J. 2018. Chloroplast behaviour and interactions with other organelles in *Arabidopsis thaliana* pavement cells. *Journal of Cell Science* 131: jcs202275.

Bond SR, Naus CC. 2012. RF-Cloning.org: an online tool for the design of restriction-free cloning projects. *Nucleic Acids Research* 40: 209–213.

Brunkard JO, Runkel AM, Zambryski PC. 2015. Chloroplasts extend stromules independently and in response to internal redox signals. *Proceedings of the National Academy of Sciences, USA* 112: 10044–10049.

Bukovinszki Á, Götz R, Johansen E, Maiss E, Balázs E. 2007. The role of the coat protein region in symptom formation on *Physalis floridana* varies between PVY strains. *Virus Research* 127: 122–125.

Calil IP, Fontes EPB. 2017. Plant immunity against viruses: antiviral immune receptors in focus. *Annals of Botany* 119: 711–723.

Caplan JL, Kumar AS, Park E, Padmanabhan MS, Hoban K, Modla S, Czymmek K, Dinesh-Kumar SP. 2015. Chloroplast stromules function during innate immunity. *Developmental Cell* 34: 45–57.

Ding X, Jimenez-Gongora T, Krenz B, Lozano-Duran R. 2019. Chloroplast clustering around the nucleus is a general response to pathogen perception in *Nicotiana benthamiana*. *Molecular Plant Pathology* 20: 1298–1306.

Hernández JA, Gullner G, Clemente-Moreno MJ, Künstler A, Juhász C, Díaz-Vivancos P, Király L. 2016. Oxidative stress and antioxidative responses

in plant–virus interactions. *Physiological and Molecular Plant Pathology* 94: 134–148.

Ishiga Y, Ishiga T, Wangdi T, Mysore KS, Uppalapati SR. 2012. NTRC and chloroplast-generated reactive oxygen species regulate *Pseudomonas syringae* pv. tomato disease development in tomato and *Arabidopsis*. *Molecular Plant–Microbe Interactions* 25: 294–306.

Jiang K, Schwarzer C, Lally E, Zhang S, Ruzin S, Machen T, Remington SJ, Feldman L. 2006. Expression and characterization of a redox-sensing green fluorescent protein (reduction-oxidation-sensitive green fluorescent protein) in Arabidopsis. *Plant Physiology* 141: 397–403.

Jones JDG, Dangl JL. 2006. The plant immune system. *Nature* 444: 323–329.

Kachroo P, Burch-Smith TM, Grant M. 2021. An emerging role for chloroplasts in disease and defense. *Annual Review of Phytopathology* 59: 423–445.

Karasev AV, Gray SM. 2013. Continuous and emerging challenges of *Potato virus Y* in potato. *Annual Review of Phytopathology* 51: 571–586.

Karimi M, Inzé D, Depicker A. 2002. GATEWAY™ vectors for *Agrobacterium*-mediated plant transformation. *Trends in Plant Science* 7: 193–195.

Kim C, Meskauskiene R, Zhang S, Lee KP, Ashok ML, Blajecka K, Herrfurth C, Feussner I, Apela K. 2012. Chloroplasts of *Arabidopsis* are the source and a primary target of a plant-specific programmed cell death signaling pathway. *Plant Cell* 24: 3026–3039.

Kumar AS, Park E, Nedo A, Alqarni A, Ren L, Hoban K, Modla S, McDonald JH, Kambhamettu C, Dinesh-Kumar SP *et al.* 2018. Stromule extension along microtubules coordinated with actin-mediated anchoring guides perinuclear chloroplast movement during innate immunity. *eLife* 7: e23625.

Künstler A, Bacsó R, Gullner G, Hafez YM, Király L. 2016. Staying alive – is cell death dispensable for plant disease resistance during the hypersensitive response? *Physiological and Molecular Plant Pathology* 93: 75–84.

Kuznetsova A, Brockhoff PB, Christensen RHB. 2017. LMERTEST package: tests in linear mixed effects models. *Journal of Statistical Software* 82: 1–26.

Lee KP, Kim C, Landgraf F, Apel K. 2007. EXECUTER1- and EXECUTER2-dependent transfer of stress-related signals from the plastid to the nucleus of *Arabidopsis thaliana*. *Proceedings of the National Academy of Sciences, USA* 104: 10270–10275.

Lenth RV, Buerkner P, Herve M, Love J, Riebl H, Singmann H. 2021. *Package 'EMMEANS' estimated marginal means, aka least-squares means.* [WWW document] URL http://cran.r-project.org/package=emmeans [accessed 09 February 2021].

Li M, Kim C. 2022. Chloroplast ROS and stress signaling. *Plant Communications* 3: 100264.

Littlejohn GR, Breen S, Smirnoff N, Grant M. 2021. Chloroplast immunity illuminated. *New Phytologist* 229: 3088–3107.

Liu Y, Ren D, Pike S, Pallardy S, Gassmann W, Zhang S, Life B. 2007. Chloroplast-generated reactive oxygen species are involved in hypersensitive response-like cell death mediated by a mitogen-activated protein kinase cascade. *The Plant Journal* 51: 941–954.

Lu Y, Yao J. 2018. Chloroplasts at the crossroad of photosynthesis, pathogen infection and plant defense. *International Journal of Molecular Sciences* 19: 3900.

Lukan T, Baebler Š, Pompe-Novak M, Guček K, Zagorščak M, Coll A, Gruden K. 2018. Cell death is not sufficient for the restriction of potato virus Y spread in hypersensitive response-conferred resistance in potato. *Frontiers in Plant Science* 9: 1–12.

Lukan T, Pompe-Novak M, Baebler Š, Tušek-Žnidarič M, Kladnik A, Križnik M, Blejec A, Zagorščak M, Stare K, Dušak B *et al.* 2020. Precision transcriptomics of viral foci reveals the spatial regulation of immune-signaling genes and identifies *RBOHD* as an important player in the incompatible interaction between potato virus Y and potato. *The Plant Journal* 104: 645–661.

Maruta T, Noshi M, Tanouchi A, Tamoi M, Yabuta Y, Yoshimura K, Ishikawa T, Shigeoka S. 2012. H$_2$O$_2$-triggered retrograde signaling from chloroplasts to nucleus plays specific role in response to stress. *Journal of Biological Chemistry* 287: 11717–11729.

Montaña MP, Blasich N, Haggi E, García NA. 2009. Oxygen uptake in the vitamin B2-sensitized photo-oxidation of tyrosine and tryptophan in the presence of uracil: kinetics and mechanism. *Photochemistry and Photobiology* 85: 1097–1102.

Mur LAJ, Kenton P, Lloyd AJ, Ougham H, Prats E. 2008. The hypersensitive response; the centenary is upon us but how much do we know? *Journal of Experimental Botany* 59: 501–520.

Natesan SKA, Sullivan JA, Gray JC. 2005. Stromules: a characteristic cell-specific feature of plastid morphology. *Journal of Experimental Botany* 56: 787–797.

Nomura H, Komori T, Uemura S, Kanda Y, Shimotani K, Nakai K, Furuichi T, Takebayashi K, Sugimoto T, Sano S *et al.* 2012. Chloroplast-mediated activation of plant immune signalling in *Arabidopsis*. *Nature Communications* 3: 1–10.

Ochsenbein C, Przybyla D, Danon A, Landgraf F, Göbel C, Imboden A, Feussner I, Apel K. 2006. The role of EDS1 (enhanced disease susceptibility) during singlet oxygen-mediated stress responses of Arabidopsis. *The Plant Journal* 47: 445–456.

Petek M, Rotter A, Kogovšek P, Baebler Š, Mithöfer A, Gruden K. 2014. Potato virus Y infection hinders potato defence response and renders plants more vulnerable to Colorado potato beetle attack. *Molecular Ecology* 23: 5378–5391.

Pierella Karlusich JJ, Zurbriggen MD, Shahinnia F, Sonnewald S, Sonnewald U, Hosseini SA, Hajirezaei MR, Carrillo N. 2017. Chloroplast redox status modulates genome-wide plant responses during the non-host interaction of Tobacco with the hemibiotrophic bacterium *Xanthomonas campestris* pv. *vesicatoria*. *Frontiers in Plant Science* 8: 1158.

Quenouille J, Vassilakos N, Moury B. 2013. *Potato virus Y*: a major crop pathogen that has provided major insights into the evolution of viral pathogenicity. *Molecular Plant Pathology* 14: 439–452.

Rupar M, Faurez F, Tribodet M, Gutierrez-Aguirre I, Delaunay A, Glais L, Kriznik M, Dobnik D, Gruden K, Jacquot E *et al.* 2015. Fluorescently tagged *Potato virus Y*: a versatile tool for functional analysis of plant–virus interactions. *Molecular Plant–Microbe Interactions* 28: 739–750.

Schmidt A, Mächtel R, Ammon A, Engelsdorf T, Schmitz J, Maurino VG, Voll LM. 2020. Reactive oxygen species dosage in Arabidopsis chloroplasts can improve resistance towards *Colletotrichum higginsianum* by the induction of WRKY33. *New Phytologist* 226: 189–204.

Serrano I, Audran C, Rivas S. 2016. Chloroplasts at work during plant innate immunity. *Journal of Experimental Botany* 67: 3845–3854.

Sewelam N, Jaspert N, Van Der Kelen K, Tognetti VB, Schmitz J, Frerigmann H, Stahl E, Zeier J, Van Breusegem F, Maurino VG. 2014. Spatial H$_2$O$_2$ signaling specificity: H$_2$O$_2$ from chloroplasts and peroxisomes modulates the plant transcriptome differentially. *Molecular Plant* 7: 1191–1210.

Stare K, Coll A, Gutiérrez-Aguirre I, Tušek Žnidarič M, Ravnikar M, Kežar A, Kavčič L, Podobnik M, Gruden K. 2020. Generation and *in planta* functional analysis of potato virus Y mutants. *Bio-Protocol* 10: 1–19.

Stonebloom S, Brunkard JO, Cheung AC, Jiang K, Feldman L, Zambryski P. 2012. Redox states of plastids and mitochondria differentially regulate intercellular transport via plasmodesmata. *Plant Physiology* 158: 190–199.

Straus MR, Rietz S, Ver Loren Van Themaat E, Bartsch M, Parker JE. 2010. Salicylic acid antagonism of EDS1-driven cell death is important for immune and oxidative stress responses in Arabidopsis. *The Plant Journal* 62: 628–640.

Su J, Yang L, Zhu Q, Wu H, He Y, Liu Y, Xu J, Jiang D, Zhang S. 2018. Active photosynthetic inhibition mediated by MPK3/MPK6 is critical to effector-triggered immunity. *PLoS Biology* 16: e2004122.

Szajko K, Chrzanowska M, Witek K, Strzelczyk-Zyta D, Zagórska H, Gebhardt C, Hennig J, Marczewski W. 2008. The novel gene *Ny-1* on potato chromosome IX confers hypersensitive resistance to *Potato virus Y* and is an alternative to *Ry* genes in potato breeding for PVY resistance. *Theoretical and Applied Genetics* 116: 297–303.

Wagner D, Przybyla D, Op Den Camp R, Kim C, Landgraf F, Keun PL, Würsch M, Laloi C, Nater M, Hideg E *et al.* 2004. The genetic basis of singlet oxygen-induced stress response of *Arabidopsis thaliana*. *Science* 306: 1183–1185.

Xu Q, Tang C, Wang X, Sun S, Zhao J, Kang Z, Wang X. 2019. An effector protein of the wheat stripe rust fungus targets chloroplasts and suppresses chloroplast function. *Nature Communications* 10: 5571.

Zurbriggen MD, Carrillo N, Hajirezaei MR. 2010. ROS signaling in the hypersensitive response: when, where and what for? *Plant Signaling and Behavior* 5: 393–396.

Zurbriggen MD, Carrillo N, Tognetti VB, Melzer M, Peisker M, Hause B, Hajirezaei MR. 2009. Chloroplast-generated reactive oxygen species play a major

role in localized cell death during the non-host interaction between tobacco and *Xanthomonas campestris* pv. *vesicatoria*. *The Plant Journal* **60**: 962–973.

Supporting Information

Additional Supporting Information may be found online in the Supporting Information section at the end of the article.

Fig. S1 Relative chloroplast redox state after PVY and MOCK inoculation and H_2O_2 and DTT treatments.

Fig. S2 Stromule formation around the cell death zone is differentially spatiotemporally regulated between potato genotypes.

Fig. S3 Chloroplast redox state is highly oxidized around the cell death zone.

Fig. S4 Detailed spatial analysis of relative chloroplast redox state around the cell death zone.

Fig. S5 Individual cells with chloroplasts in oxidized redox state in ROI2 in PVY-inoculated redox state sensor plants.

Fig. S6 Impact of chloroplast inhibitor on transcriptional response.

Methods S1 Stable transformation.

Methods S2 Construction of PVY-N605(123)-GFP infectious clone.

Table S1 Sample information and 405 : 488 ratios for chloroplast redox detection experiments.

Table S2 Statistical evaluation of observed relative redox changes in different conditions in individual experiments.

Table S3 Sample information and normalized number of stromules for stromule counting experiments.

Table S4 Sample information and 405 : 488 ratios for chloroplast redox detection experiments with the inhibitor.

Table S5 405 : 488 ratios in five bins of ROI1 and ROI2.

Table S6 Chloroplast redox regulated spatial expression of selected genes.

Table S7 Statistical evaluation of stromule counts in different conditions in individual experiments.

Table S8 Statistical evaluation of observed relative redox changes after chIROS inhibitor and control treatment.

Table S9 Statistical analysis of the effects of chloroplastic ROS inhibitor (chIROS) and control treatment on expression of selected genes.

Video S1 Epidermal chloroplasts cluster around the nucleus in potato plants in response to PVY infection.

Please note: Wiley Blackwell are not responsible for the content or functionality of any Supporting Information supplied by the authors. Any queries (other than missing material) should be directed to the *New Phytologist* Central Office.

Chapter 3

Discussion

3.1 Biotechnological Production of Insect Sex Pheromones in Plants

Biotechnological production of chemical compounds is a sustainable alternative to chemical synthesis (Gavrilescu & Chisti, 2005). Besides bacterial and yeast fermentation, autotrophic organisms (cyanobacteria, algae, and plants) are emerging as bioproduction platforms because they use carbon dioxide as the major starting material and sunlight as the energy source (Barbosa, Janssen, Südfeld, D'Adamo, & Wijffels, 2023; Sethi, Kumari, & Dey, 2021; Sirirungruang, Markel, & Shih, 2022). Plants have been implemented mainly for the production of therapeutic recombinant proteins because they have some advantages over currently used systems, i.e., mostly *E. coli* and mammalian cell cultures. Plants are cheaper and easier to grow with established practices and infrastructure for large-scale production. Compared to *E. coli*, their glycosylation profile is closer to that of humans and compared to mammalian cells, they pose a much lower risk of contamination with human pathogens (Buyel, Twyman, & Fischer, 2017). In addition to molecular farming of pharmaceutical proteins, plants can be used to produce a plethora of small molecules, either by improving the production of endogenous plant metabolites or by introducing exogenous biosynthetic pathways (Mora-Vásquez, Wells-Abascal, Espinosa-Leal, Cardineau, & García-Lara, 2022; Tschofen, Knopp, Hood, & Stöger, 2016). For the production of pharmaceuticals or small compounds, *N. benthamiana* has emerged as a versatile host and serves as a plant chassis for most biotechnological applications (Bally et al., 2018; Molina-Hidalgo et al., 2021)

The development of plant biofactories, however, is still a long process with many scientific challenges. In this thesis we attempted to tackle two of them, namely the growth and developmental costs often associated with high yields of production, and the task of determining the biosynthetic pathways of target metabolites in non-model organisms. Our first system of interest was the production of insect sex pheromones in *N. benthamiana*. Transgenic lines producing high amounts of moth sex pheromones exhibit stunted growth and delayed or arrested development, making them unsuitable for large-scale production. We approached this problem by determining and comparing the transcriptional profiles of wild-type *N. benthamiana* and transgenic lines to identify the molecular perturbations underlying the observed growth penalty. Gene expression analysis of transgenic lines also revealed the incorrect insertion of one of the transgenes — a truncation, resulting in the expression of a non-functional enzyme. This initiated the construction of another version of plant lines with correct transgene insertions producing all target compounds.

Differential gene expression analysis of the high-producing *N. benthamiana* lines revealed a stress-like transcriptional response. This was further characterised using

knowledge networks, revealing activation of jasmonic acid signalling and downregulation of gibberellic acid signalling. Hardwired signalling interplay between stress-promoting jasmonic acid and growth-promoting gibberellic acid hormones has been previously implicated as the major signalling hub underlying the stress-growth balance in plants (Heinrich et al., 2013; D. L. Yang et al., 2012; Zhang, Zhao, & Zhu, 2020). Growth repression upon stress signal perception is common in plants and has been exposed as an important obstacle in breeding plant cultivars with both good growth performance and stress resilience. If the production of heterologous metabolites triggers a jasmonic-acid-conveyed stress response, growth repression can be uncoupled by manipulating genes involved in the crosstalk between the jasmonic acid and gibberellic acid signalling pathways, as has been achieved for some crop species (M. L. Campos et al., 2016; Guo, Major, & Howe, 2018).

From the transcriptomic data alone, we were unable to determine the exact perturbation that triggered the observed stress response. Besides general energy and metabolite shortages due to sex pheromone biosynthesis, one option could be the direct perturbation of jasmonic acid biosynthesis, as it is a fatty-acid-derived compound, as are moth sex pheromones. Another plausible option could be plant sensing of insect semiochemicals as a danger signal. However, the magnitude of stress signalling does not seem to be directly correlated to the amount of sex pheromone production, as would be expected if the underlying reason was one of the above mentioned. The second generation of plants with the correct insertion of all three genes produced higher amounts of all three pheromone compounds but had a less severe phenotype, correlating well with more moderate transcriptional responses. Further research with different experimental setups is needed to gain more insight into the pheromone-driven stress response in *N. benthamiana* and to find genetic targets that could improve *N. benthamiana* as a sex pheromone production chassis. Functional annotation of the *N. benthamiana* genome could contribute to the further development of its bioproduction. We have provided *in silico* annotations based on MapMan ontology (Thimm et al., 2004), which is useful for interpreting differential expression analysis. More complete *N. benthamiana* genomic data recently released should further facilitate the use and interpretation of transcriptomic data from this model species (Kurotani et al., 2023; Ranawaka et al., 2023; Vollheyde et al., 2023).

Besides addressing the stress-triggering effects of pheromone production, a solution could also be inducible expression of transgenes, enabling production only in already full-grown plants. With the tools of synthetic biology, scalable inducible systems can be developed, avoiding the onset of growth inhibition during the early stages of plant growth (Garcia-Perez et al., 2022; Vazquez-Vilar, Selma, & Orzaez, 2023). This approach is also of interest for developing plants as on-site producers and dispersers of insect sex pheromones. Although plant biodispensers could present a sustainable pest management tool, their use is currently unattainable in the EU, due to regulatory limitations.

Additionally, we aimed to identify the genes coding for enzymes catalysing the formation of the irregular terpenoid backbone of *P. citri* sex pheromone, which could be implemented for biotechnological production *in planta*. Biotechnological production would be an important development in the production of the otherwise hard-to-synthesize sex pheromones of these aggressive pests in agriculture and horticulture. To obtain reliable genome-level coding sequence information, we generated short- and long-read transcriptome data from *P. citri* virgin and mated females and used homology-based searches to identify candidate genes. We selected several sequences with homology to IDSs, which putatively catalyse the formation of the irregular polyprenyl backbones in Coccoidea sex pheromones. However, *in vitro* testing of candidates expressed in *E. coli* and *in vivo* testing in *N. benthamiana* did not show target activity. Most active candidates exhibited

only regular IDS activity, with one candidate also producing very low amounts of irregular polyprenyl chains.

There are several possibilities as to why we were unable to detect target activity. Apart from the possibility that the cyclobutane structure of the *P. citri* sex pheromones results from a different catalytic mechanism and is thus catalysed by an enzyme from a different family, our testing conditions might lack necessary factors, which are only present in native *P. citri* pheromone gland cells. Protein interactors or ionic or other cofactors might be needed for the irregular catalytic activity of the tested IDSs. *In vitro* characterisations of IDSs can be difficult, as presumably even subtle structural and electronic changes to the protein shift product and substrate specificity. For example, changes in IDS activity were detected after substitution of the divalent cations in the active site (Mg^{2+} for $Mn2^{+}$) (Jarstfer, Zhang & Poulter, 2002). Several IDSs also exhibit promiscuous activity when tested *in vitro*. The importance of expression systems and the testing environment has emerged in the testing of not only IDS enzymes but also enzymes involved in the biosynthesis of Lepidoptera pheromones (Xia et al., 2022). Besides characterisation difficulties, this also implies that the genes must be carefully selected and tested in the final bioproduction chassis to ensure target activity. If the identified enzyme does not exhibit the desired activity in its native state, protein engineering could be applied (Gerasymenko et al., 2022).

Identification of biosynthesis genes for insect sex pheromones could be difficult due to the nature of their evolutionary emergence and diversification. Moth sex pheromone biosynthesis genes (FADs, FARs) have a dynamic evolutionary history with numerous gene duplications, creating a broad protein space with many unique and novel functions (Buček et al., 2015; B. J. Ding, Carraher, & Löfstedt, 2016; Lassance et al., 2021; Liénard, Strandh, Hedenström, Johansson, & Löfstedt, 2008; Roelofs et al., 2002). Sex pheromone communication can also be an important driver for speciation. One possible example of such speciation is the European corn borer moth, in which an allelic variation in a single FAR gene results in pheromone blends with opposite ratios of isomers in two sympatric strains of the same species (Lassance et al., 2010). Due to the evolutionary dynamics of genes involved in insect sex pheromone biosynthesis and the lack of mechanistic understanding of the sequence-to-function relation, functional predictions based on homology to already characterised genes can be misleading (Wallrapp et al., 2013).

3.2 Implementation of a PVY Infectious Clone for Studies of Potato–PVY Interactions

We have successfully engineered a monopartite PVY infectious clone tagged with GFP. It enabled precise localisation of PVY infection and spread in the potato, facilitating spatiotemporal analysis of stromule formation in response to viral replication. The presented protocol for insertion of reporter proteins at desired target sites in the PVY genome enables the construction of engineered clones for different functional studies. We plan to construct a PVY infectious clone tagged with fluorescent proteins with different spectral properties to enable the simultaneous use of several fluorescent markers. For example, the chloroplast redox state reporter used in our work to follow reactive oxygen signalling during PVY infection is also based on GFP. Thus, we were unable to use the PVY-GFP clone concurrently, as it would be impossible to distinguish signal from the two reporter systems. Using the developed protocol, we therefore aim to construct a PVY clone tagged with the mTurquoise fluorescent protein, the spectra of which is well separated from the GFP spectra. This will enable a more detailed analysis of the redox response to PVY replication and spread.

We also want to pursue in-frame N- or C-terminal fusions of the fluorescent reporter coding sequence with the viral protein coding sequence. This design enables localization studies of the tagged viral proteins with confocal microscopy (Agbeci, Grangeon, Nelson, Zheng, & Laliberté, 2013; Dai, He, Bernards, & Wang, 2020). Viruses as intracellular parasites depend on hijacking the plant cellular machinery for their reproduction, movement, and encapsidation, all of which is counteracted by plant defence mechanisms. To perform these functions, viral proteins interact with plant proteins and are localized to different cellular compartments (Garcia-Ruiz, 2019). Confocal imaging of fluorescently tagged viral proteins enables localization studies, whereas their interacting proteins can be determined by co-immunoprecipitation by exploiting the fluorescent tag on the viral protein as an antigen. With this approach, we plan to characterise the functions of PVY proteins in viral replication and movement and their potato protein interactors, which are potentially important in the plant immune response to viral infection.

We also want to use the PVY-GFP clone to introduce point mutations or deletions in PVY genes to study their function. For previous work on mutants of PVY coat protein, the untagged PVY infectious clone was used and its spread was followed by quantitative polymerase chain reaction and transmission electron microscopy (Kežar et al., 2019). Use of the PVY-GFP clone will enable a more precise spatiotemporal analysis of the effects of specific mutations in the PVY proteins on their function in viral movement.

Chapter 4

Conclusions

To counteract the growing environmental burdens of agriculture, sustainability must be an important consideration in the development of improved practices and crops. With this dissertation, we aimed to advance the production of sustainable insecticides in plant biofactories and develop a versatile molecular tool for studying plant molecular responses to viral infections. The latter could generate knowledge on resistance genes applicable in breeding.

We contributed to the advancement of plant biofactories for the production of insect sex pheromones, which can be used as sustainable compounds for insect pest control. With the transcriptomic analysis of pheromone-producing transgenic plants with stunted growth, we detected extensive changes in gene expression, confirming our first hypothesis. Differential expression analysis further elucidated the regulatory perturbations leading to active growth arrest in high-producing plants with high production of pheromones, confirming our second hypothesis. We propose the interplay between stress-promoting jasmonic acid and growth-promoting gibberellic acid signalling as the putative regulatory hub governing the observed growth penalty. This insight provides a basis for the development of a robust chassis, in which the stress–growth balance can be decoupled to ensure acceptable growth of plant biofactories with a high production phenotype.

Another objective was to lay the foundation for the biotechnological production of mealybug sex pheromones with complex and unique chemical structures. We generated transcriptomic sequence data of the citrus mealybug with good integrity and contiguity, enabling accurate prediction of coding sequences and their amplification. Using the improved sequence data, we identified several candidate genes with homology IDSs, which putatively catalyse the synthesis of irregular monoterpene backbones of mealybug sex pheromones, confirming our third hypothesis. The identified sequences were cloned, expressed, and tested *in vitro,* resulting in several candidates with activity of interest, whose biotechnological applicability will be further studied. One of the candidates also produced irregular monoterpene backbones, albeit at very low levels.

We also generated a viral clone of PVY with an inserted sequence for GFP and confirmed its infectivity and spread in the potato plant. It was successfully used in a functional analysis of potato response to viral infection and therefore provides an important tool for further studies of interactions between the potato and PVY.

Appendix A

Supplementary Material of Included Publications

A.1 Supplementary Material for Publication 2.2

Supplementary material is available at https://spj.science.org/doi/10.34133/2021/9891082#supplementary-materials. Accessed: 17-July-2023

Mateos-Fernández, R., Moreno-Giménez, E., Gianoglio, S., Quijano-Rubio, A., Gavaldá-García, J., Estellés, L., … Orzáez, D. (2021). Production of Volatile Moth Sex Pheromones in Transgenic *Nicotiana benthamiana* Plants. *BioDesign Research*, *2021*, 9891082. https://doi.org/10.34133/2021/9891082

A.2 Supplementary Material for Publication 2.3

Supplementary material is available at https://www.frontiersin.org/articles/10.3389/fpls.2022.941338/full#supplementary-material. Accessed: 17-July-2023

Juteršek, M., Petek, M., Ramšak, Ž., Moreno-Giménez, E., Gianoglio, S., Mateos-Fernández, R., … Baebler, Š. (2022). Transcriptional deregulation of stress-growth balance in *Nicotiana benthamiana* biofactories producing insect sex pheromones. *Frontiers in Plant Science*, *13*, 941338. https://doi.org/10.3389/fpls.2022.941338

A.3 Supplementary Material for Publication 2.4

Supplementary material is available at https://www.biorxiv.org/content/10.1101/2023.06.09.544309v2.supplementary-material. Accessed: 17-July-2023

Juteršek, M., Gerasymenko, I. M., Petek, M., Haumann, E., González, S. V., Kallam, K., … Baebler, Š. (2023). Identification and characterisation of *Planococcus citri cis-* and

trans-isoprenyl diphosphate synthase genes, supported by short- and long-read transcriptome data. *BioRxiv.* https://doi.org/10.1101/2023.06.09.544309

A.4 Supplementary Material for Publication 2.5

Supplementary material is available at https://nph.onlinelibrary.wiley.com/doi/full/10.1111/nph.18425. Accessed: 17-July-2023

Lukan, T., Županič, A., Mahkovec Povalej, T., Brunkard, J. O., Kmetič, M., Juteršek, M., … Gruden, K. (2023). Chloroplast redox state changes mark cell-to-cell signaling in the hypersensitive response. *New Phytologist, 237*(2), 548–562. https://doi.org/10.1111/nph.18425

Appendix B

Permission for Reproduction of Included Publications

B.1 Permission for Reproduction of Publication 2.1

Review | 🔒 Open Access | (cc) (i)

Insect pest management in the age of synthetic biology

Rubén Mateos Fernández, Marko Petek, Iryna Gerasymenko, Mojca Juteršek, Špela Baebler, Kalyani Kallam, Elena Moreno Giménez, Janine Gondolf, Alfred Nordmann ... See all authors ⌄

First published: 20 August 2021 | https://doi.org/10.1111/pbi.13685 | Citations: 16

:≡ SECTIONS   🔴 PDF   🔧 TOOLS   < SHARE

Citation Statements beta (i)

Supporting	Mentioning	Contrasting
⊘ 0	⊘ 24	⊘ 0

Explore this article's citation statements on scite.ai

powered by **scite_**

🖼 Figures   🔗 References   ⧉ Related   ⓘ Information

Summary

Arthropod crop pests are responsible for 20% of global annual crop losses, a figure predicted to increase in a changing climate where the ranges of numerous species are projected to expand. At the same time, many insect species are beneficial, acting as pollinators and predators of pest species. For thousands of years, humans have used increasingly sophisticated chemical formulations to control insect pests but, as the scale of agriculture expanded to meet the needs of the global population, concerns about the negative impacts of agricultural practices on biodiversity have grown. While biological solutions, such as biological control agents and pheromones, have previously had relatively minor roles in pest management, biotechnology has opened the door to numerous new approaches for controlling insect pests. In this review, we look at how advances in synthetic biology and biotechnology are providing new options for pest control. We discuss emerging technologies for engineering resistant crops and insect populations and examine advances in biomanufacturing that are enabling the production of new products for pest control.

Metrics

Citations: 16

[Am] score | 26

Details

🔖 Check for updates

Introduction

It has been estimated that food production needs to increase by at least 50% over 2005 yields to meet the needs of the 2050 global population (Alexandratos, 2012). Improving crop yields and minimizing pre- and post-harvest losses are critical to achieving these goals. While

B.2 Permission for Reproduction of Publication 2.2

BioDesign Research
A SCIENCE PARTNER JOURNAL

Research Article

Production of Volatile Moth Sex Pheromones in Transgenic *Nicotiana benthamiana* Plants

Rubén Mateos-Fernández [ORCID],[1] Elena Moreno-Giménez,[1] Silvia Gianoglio [ORCID],[1]
Alfredo Quijano-Rubio [ORCID],[1] Jose Gavaldá-García [ORCID],[1] Lucía Estellés [ORCID],[1] Alba Rubert,[1]
José Luis Rambla,[1,2] Marta Vazquez-Vilar [ORCID],[1] Estefanía Huet,[1]
Asunción Fernández-del-Carmen,[1] Ana Espinosa-Ruiz,[1] Mojca Juteršek,[3,4] Sandra Vacas,[5]
Ismael Navarro,[6] Vicente Navarro-Llopis,[5] Jaime Primo [ORCID],[5] and Diego Orzáez [ORCID][1]

[1]Institute for Plant Molecular and Cell Biology (IBMCP), Consejo Superior de Investigaciones Científicas (CSIC) - Universidad
 Politécnica de Valencia (UPV), Valencia, Spain
[2]Jaume I University, Castellon de la Plana, Spain
[3]Department of Biotechnology and Systems Biology, National Institute of Biology, Ljubljana, Slovenia
[4]Jožef Stefan International Postgraduate School, Ljubljana, Slovenia
[5]Centro de Ecología Química Agrícola, Instituto Agroforestal del Mediterráneo, Universitat Politècnica de València, Valencia, Spain
[6]Ecología Y Protección Agrícola SL, Valencia, Spain

Correspondence should be addressed to Diego Orzáez; dorzaez@ibmcp.upv.es

Rubén Mateos-Fernández and Elena Moreno-Giménez contributed equally to this work.

Plant-based bioproduction of insect sex pheromones has been proposed as an innovative strategy to increase the sustainability of pest control in agriculture. Here, we describe the engineering of transgenic plants producing *(Z)*-11-hexadecenol (Z11-16OH) and *(Z)*-11-hexadecenyl acetate (Z11-16OAc), two main volatile components in many Lepidoptera sex pheromone blends. We assembled multigene DNA constructs encoding the pheromone biosynthetic pathway and stably transformed them into *Nicotiana benthamiana* plants. The constructs contained the *Amyelois transitella AtrΔ11* desaturase gene, the *Helicoverpa armigera* fatty acyl reductase *HarFAR* gene, and the *Euonymus alatus* diacylglycerol acetyltransferase *EaDAct* gene in different configurations. All the pheromone-producing plants showed dwarf phenotypes, the severity of which correlated with pheromone levels. All but one of the recovered lines produced high levels of Z11-16OH, but very low levels of Z11-16OAc, probably as a result of recurrent truncations at the level of the *EaDAct* gene. Only one plant line (SxPv1.2) was recovered that harboured an intact pheromone pathway and which produced moderate levels of Z11-16OAc (11.8 μg g^{-1} FW) and high levels of Z11-16OH (111.4 μg g^{-1}). Z11-16OAc production was accompanied in SxPv1.2 by a partial recovery of the dwarf phenotype. SxPv1.2 was used to estimate the rates of volatile pheromone release, which resulted in 8.48 ng g^{-1} FW per day for Z11-16OH and 9.44 ng g^{-1} FW per day for Z11-16OAc. Our results suggest that pheromone release acts as a limiting factor in pheromone biodispenser strategies and establish a roadmap for biotechnological improvements.

1. Introduction

Insect pheromones are a sustainable alternative to broad-spectrum pesticides in pest control. Different pheromone-based pest management approaches can be employed to contain herbivore populations, thus limiting damage to food, feed, industrial crops, and stored goods. These approaches include multiple strategies, such as (i) attract-and-kill strategies, in which pheromones are used to lure insects into mass traps; (ii) push-pull strategies, in which different stimuli are

B.3   Permission for Reproduction of Publication 2.3

Check for updates

Transcriptional deregulation of stress-growth balance in *Nicotiana benthamiana* biofactories producing insect sex pheromones

Mojca Juteršek[1,2]*, Marko Petek[1], Živa Ramšak[1],
Elena Moreno-Giménez[3], Silvia Gianoglio[3],
Rubén Mateos-Fernández[3], Diego Orzáez[3],
Kristina Gruden[1] and Špela Baebler[1]

[1]Department of Biotechnology and Systems Biology, National Institute of Biology,
Ljubljana, Slovenia, [2]Jožef Stefan International Postgraduate School, Ljubljana, Slovenia, [3]Institute
for Plant Molecular and Cell Biology (IBMCP), Consejo Superior de Investigaciones Científicas
(CSIC), Universidad Politécnica de Valencia (UPV), Valencia, Spain

Plant biofactories are a promising platform for sustainable production of high-value compounds, among which are insect sex pheromones, a green alternative to conventional insecticides in agriculture. Recently, we have constructed transgenic *Nicotiana benthamiana* plants ("Sexy Plants", SxP) that successfully produce a blend of moth (Lepidoptera) sex pheromone compounds (*Z*)-11-hexadecen-1-ol and (*Z*)-11-hexadecenyl acetate. However, efficient biosynthesis of sex pheromones resulted in growth and developmental penalty, diminishing the potential for commercial use of SxP in biomanufacturing. To gain insight into the underlying molecular responses, we analysed the whole-genome transcriptome and evaluated it in relation to growth and pheromone production in low- and high-producing transgenic plants of v1.0 and v1.2 SxP lines. In our study, high-producing SxPv1.2 plants accumulated the highest amounts of pheromones but still maintained better growth compared to v1.0 high producers. For an in-depth biological interpretation of the transcriptomic data, we have prepared a comprehensive functional *N. benthamiana* genome annotation as well as gene translations to *Arabidopsis thaliana*, enabling functional information transfer by using Arabidopsis knowledge networks. Differential gene expression analysis, contrasting pheromone producers to wild-type plants, revealed that while only a few genes were differentially regulated in low-producing plants, high-producing plants exhibited vast transcriptional reprogramming. They showed signs of stress-like response, manifested as downregulation of photosynthesis-related genes and significant differences in expression of hormonal signalling and secondary metabolism-related genes, the latter presumably leading to previously reported volatilome changes. Further network analyses confirmed stress-like response with activation of jasmonic acid and downregulation of gibberellic acid signalling, illuminating the possibility that the observed growth

B.4   Permission for Reproduction of Publication 2.4

Identification and characterisation of *Planococcus citri cis-* and *trans-*isoprenyl diphosphate synthase genes, supported by short- and long-read transcriptome data

Mojca Juteršek, Iryna M. Gerasymenko, Marko Petek, Elisabeth Haumann, Sandra Vacas, Kalyani Kallam, Silvia Gianoglio, Vicente Navarro-Llopis, Ismael Navarro Fuertes, Nicola Patron, Diego Orzáez, Kristina Gruden, Heribert Warzecha, Špela Baebler

doi: https://doi.org/10.1101/2023.06.09.544309

This article is a preprint and has not been certified by peer review [what does this mean?].

⊙ 0   ☑ 0   👥 0   ⚙ 0   🖳 0   🗐 0   🐦 10
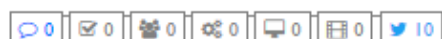
Abstract   Full Text   Info/History   Metrics   🗋 Preview PDF

Abstract

Many insect species rely on diverse terpenoids for their development and interorganismal interactions. However, little is known about terpenoid biosynthesis in insects. The monoterpenoid sex pheromones of mealybugs and scale insects (Coccoidea) are particularly enigmatic, with several species producing unique structures presumed to result from the irregular coupling activity of unidentified isopentenyl diphosphate synthases (IDSs). Enzymes capable of similar transformations have previously only been described from a few plant, bacterial and archaeal species. To investigate if insect irregular monoterpenes can be biosynthesised by similar enzymes, we performed a comprehensive search for IDS coding sequences in the genome of *Planococcus citri*, a widespread agricultural pest. We complemented the available *P. citri* genome data with newly generated short- and long-read transcriptome data. The identified candidate genes had homology to both short- and long-chain IDSs and some appeared to be paralogous, indicating gene duplications and consequent IDS gene family expansion in *P. citri*. We tested the activity of eleven candidate gene products, confirming *in vitro* regular activity for five enzymes, one of which (*trans*IDS5) also produced the irregular prenyl diphosphates, maconelliyl and lavandulyl diphosphate. Targeted mutagenesis of selected aspartates and a lysine in the active site of *trans*IDS5 uncovered their importance for chain-length preference and irregular coupling. This work provides an important foundation for deciphering terpenoid biosynthesis in mealybugs, as well as a potential source of enzymes for the biotechnological production of sustainable insect pest management products.

Competing Interest Statement

The authors have declared no competing interest.

B.5 Permission for Reproduction of Publication 2.5

Full paper | 🔒 Open Access | Ⓒ ⓘ ⓢ

Chloroplast redox state changes mark cell-to-cell signaling in the hypersensitive response

Tjaša Lukan ✉, Anže Županič, Tjaša Mahkovec Povalej, Jacob O. Brunkard, Mirjam Kmetič, Mojca Juteršek, Špela Baebler, Kristina Gruden

≡ SECTIONS   📄 PDF   🔧 TOOLS   < SHARE

Citation Statements beta ⓘ

Supporting	Mentioning	Contrasting
⊘ 0	⊘ 4	? 0

Explore this article's citation statements on scite.ai

powered by **scite_**

🖼 Figures | 🔗 References | ⚬ Related | ⓘ Information

Summary

- Hypersensitive response (HR)-conferred resistance is associated with induction of programmed cell death and pathogen spread restriction in its proximity. The exact role of chloroplastic reactive oxygen species and its link with salicylic acid (SA) signaling in HR remain unexplained.

- To unravel this, we performed a detailed spatiotemporal analysis of chloroplast redox response in palisade mesophyll and upper epidermis to potato virus Y (PVY) infection in a resistant potato genotype and its transgenic counterpart with impaired SA accumulation and compromised resistance.

- Besides the cells close to the cell death zone, we detected individual cells with oxidized chloroplasts further from the cell death zone. These are rare in SA-deficient plants, suggesting their role in signaling for resistance. We confirmed that chloroplast redox changes play important roles in signaling for resistance, as blocking chloroplast redox changes affected spatial responses at the transcriptional level.

- Through spatiotemporal study of stromule induction after PVY infection, we show that stromules are induced by cell death and also as a response to PVY multiplication at the front of infection. Overall induction of stromules is attenuated in SA-deficient plants.

Metrics

Citations: 6
Full text views: 1,472 ⓘ

Am score 19

Details

Ⓝ Check for updates

References

Abrahamian, P., Hammond, R. W., & Hammond, J. (2020). Plant Virus-Derived Vectors: Applications in Agricultural and Medical Biotechnology. *Annual Review of Virology*, *7*, 513–535. https://doi.org/10.1146/annurev-virology-010720-054958

Agbeci, M., Grangeon, R., Nelson, R. S., Zheng, H., & Laliberté, J. F. (2013). Contribution of Host Intracellular Transport Machineries to Intercellular Movement of Turnip Mosaic Virus. *PLoS Pathogens*, *9*(10), 1–15. https://doi.org/10.1371/journal.ppat.1003683

Baebler, Š., Coll, A., & Gruden, K. (2020). Plant Molecular Responses to Potato Virus Y: A Continuum of Outcomes from Sensitivity and Tolerance to Resistance. *Viruses*, *12*(2), 217. https://doi.org/10.3390/V12020217

Bailey-Serres, J., Parker, J. E., Ainsworth, E. A., Oldroyd, G. E. D., & Schroeder, J. I. (2019). Genetic strategies for improving crop yields. *Nature*, *575*(7781), 109–118. https://doi.org/10.1038/s41586-019-1679-0

Bally, J., Jung, H., Mortimer, C., Naim, F., Philips, J. G., Hellens, R., … Waterhouse, P. M. (2018). The Rise and Rise of Nicotiana benthamiana: A Plant for All Reasons. *Annual Review of Phytopathology*, *56*, 405–426. https://doi.org/10.1146/ANNUREV-PHYTO-080417-050141

Barbosa, M. J., Janssen, M., Südfeld, C., D'Adamo, S., & Wijffels, R. H. (2023). Hypes, hopes, and the way forward for microalgal biotechnology. *Trends in Biotechnology*, *41*(3), 452–471. https://doi.org/10.1016/j.tibtech.2022.12.017

Baulcombe, D. C., Chapman, S., & Santa Cruz, S. (1995). Jellyfish green fluorescent protein as a reporter for virus infections. *The Plant Journal*, *7*(6), 1045–1053. https://doi.org/10.1046/j.1365-313X.1995.07061045.x

Beck, J. J., Torto, B., & Vannette, R. L. (2017). Eavesdropping on Plant-Insect-Microbe Chemical Communications in Agricultural Ecology: A Virtual Issue on Semiochemicals. *Journal of Agricultural and Food Chemistry*, *65*(25), 5101–5103. https://doi.org/10.1021/acs.jafc.7b02741

Bedoya, L. C., Martínez, F., Orzáez, D., & Daròs, J. A. (2012). Visual tracking of plant virus infection and movement using a reporter MYB transcription factor that activates anthocyanin biosynthesis. *Plant Physiology*, *158*(3), 1130–1138. https://doi.org/10.1104/pp.111.192922

Beyene, G., Chauhan, R. D., & Taylor, N. J. (2017). A rapid virus-induced gene silencing (VIGS) method for assessing resistance and susceptibility to cassava mosaic disease. *Virology Journal*, *14*, 47. https://doi.org/10.1186/s12985-017-0716-6

Brewer, H. C., Hird, D. L., Bailey, A. M., Seal, S. E., & Foster, G. D. (2018). A guide to

the contained use of plant virus infectious clones. *Plant Biotechnology Journal, 16*(4), 832–843. https://doi.org/10.1111/pbi.12876

Buček, A., Weißflog, J., Matoušková, P., Jahn, U., Pichová, I., Svatoš, A., … Vogel, H. (2015). Evolution of moth sex pheromone composition by a single amino acid substitution in a fatty acid desaturase. *Proceedings of the National Academy of Sciences, 112*(41), 12586–12591. https://doi.org/10.1073/pnas.1514566112

Bukovinszki, Á., Götz, R., Johansen, E., Maiss, E., & Balázs, E. (2007). The role of the coat protein region in symptom formation on Physalis floridana varies between PVY strains. *Virus Research, 127*(1), 122–125. https://doi.org/10.1016/j.virusres.2007.03.023

Buyel, J. F., Twyman, R. M., & Fischer, R. (2017). Very-large-scale production of antibodies in plants: The biologization of manufacturing. *Biotechnology Advances, 35*(4), 458–465. https://doi.org/10.1016/j.biotechadv.2017.03.011

Cabaleiro, C., Pesqueira, A. M., & Segura, A. (2022). Planococcus ficus and the spread of grapevine leafroll disease in vineyards: a 30-year-long case study in north-West Spain. *European Journal of Plant Pathology, 163*(3), 733–747. https://doi.org/10.1007/s10658-022-02513-x

Campos, M. L., Yoshida, Y., Major, I. T., De Oliveira Ferreira, D., Weraduwage, S. M., Froehlich, J. E., … Howe, G. A. (2016). Rewiring of jasmonate and phytochrome B signalling uncouples plant growth-defense tradeoffs. *Nature Communications, 7*, 12570. https://doi.org/10.1038/ncomms12570

Carleton, R. D., Owens, E., Blaquière, H., Bourassa, S., Bowden, J. J., Candau, J.-N., … Johns, R. C. (2020). Tracking insect outbreaks: A case study of community-assisted moth monitoring using sex pheromone traps. *Facets, 5*(1), 91–104. https://doi.org/10.1139/FACETS-2019-0029

Cheng, D. J., Tian, Y. P., Geng, C., Guo, Y., Jia, M. A., & Li, X. D. (2020). Development and application of a full-length infectious clone of potato virus Y isolate belonging to SYR-I strain. *Virus Research, 276*, 197827. https://doi.org/10.1016/j.virusres.2019.197827

Chomnunti, P., Hongsanan, S., Aguirre-Hudson, B., Tian, Q., Peršoh, D., Dhami, M. K., … Hyde, K. D. (2014). The sooty moulds. *Fungal Diversity, 66*(1), 1–36. https://doi.org/10.1007/s13225-014-0278-5

Cody, W. B., & Scholthof, H. B. (2019). Plant Virus Vectors 3.0: Transitioning into Synthetic Genomics. *Annual Review of Phytopathology, 57*, 211–230. https://doi.org/10.1146/annurev-phyto-082718-100301

Cordero, T., Mohamed, M. A., López-Moya, J. J., & Daròs, J. A. (2017). A recombinant Potato virus Y infectious clone tagged with the Rosea1 visual marker (PVY-Ros1) facilitates the analysis of viral infectivity and allows the production of large amounts of anthocyanins in plants. *Frontiers in Microbiology, 8*, 611. https://doi.org/10.3389/fmicb.2017.00611

Dai, Z., He, R., Bernards, M. A., & Wang, A. (2020). The *cis*-expression of the coat protein of turnip mosaic virus is essential for viral intercellular movement in plants. *Molecular Plant Pathology, 21*(9), 1194–1211. https://doi.org/10.1111/mpp.12973

Dara, S. K. (2019). The New Integrated Pest Management Paradigm for the Modern Age.

Journal of Integrated Pest Management, *10*(1), 12. https://doi.org/10.1093/jipm/pmz010

Delgado-Baquerizo, M., Guerra, C. A., Cano-Díaz, C., Egidi, E., Wang, J.-T., Eisenhauer, N., … Maestre, F. T. (2020). The proportion of soil-borne pathogens increases with warming at the global scale. *Nature Climate Change*, *10*(6), 550–554. https://doi.org/10.1038/s41558-020-0759-3

Demissie, Z. A., Erland, L. A. E., Rheault, M. R., & Mahmoud, S. S. (2013). The biosynthetic origin of irregular monoterpenes in lavandula: Isolation and biochemical characterization of a novel *cis*-prenyl diphosphate synthase gene, lavandulyl diphosphate synthase. *The Journal of Biological Chemistry*, *288*(9), 6333–6341. https://doi.org/10.1074/jbc.M112.431171

Desaint, H., Aoun, N., Deslandes, L., Vailleau, F., Roux, F., & Berthomé, R. (2021). Fight hard or die trying: when plants face pathogens under heat stress. *New Phytologist*, *229*(2), 712–734. https://doi.org/10.1111/nph.16965

Deutsch, C. A., Tewksbury, J. J., Tigchelaar, M., Battisti, D. S., Merrill, S. C., Huey, R. B., & Naylor, R. L. (2018). Increase in crop losses to insect pests in a warming climate. *Science*, *361*(6405), 916–919. https://doi.org/10.1126/science.aat3466

Dhama, K., Natesan, S., Iqbal Yatoo, M., Patel, S. K., Tiwari, R., Saxena, S. K., & Harapan, H. (2020). Plant-based vaccines and antibodies to combat COVID-19: current status and prospects. *Human Vaccines and Immunotherapeutics*, *16*(12), 2913–2920. https://doi.org/10.1080/21645515.2020.1842034

Ding, B.-J., Hofvander, P., Wang, H.-L., Durrett, T. P., Stymne, S., & Löfstedt, C. (2014). A plant factory for moth pheromone production. *Nature Communications*, *5*, 3353. https://doi.org/10.1038/ncomms4353

Ding, B.-J., Lager, I., Bansal, S., Durrett, T. P., Stymne, S., & Löfstedt, C. (2016). The Yeast ATF1 Acetyltransferase Efficiently Acetylates Insect Pheromone Alcohols: Implications for the Biological Production of Moth Pheromones. *Lipids*, *51*(4), 469–475. https://doi.org/10.1007/s11745-016-4122-4

Ding, B. J., Carraher, C., & Löfstedt, C. (2016). Sequence variation determining stereochemistry of a δ11 desaturase active in moth sex pheromone biosynthesis. *Insect Biochemistry and Molecular Biology*, *74*, 68–75. https://doi.org/10.1016/j.ibmb.2016.05.002

Dong, O. X., & Ronald, P. C. (2019). Genetic engineering for disease resistance in plants: Recent progress and future perspectives. *Plant Physiology*, *180*(1), 26–38. https://doi.org/10.1104/pp.18.01224

Dubey, K. K., Luke, G. A., Knox, C., Kumar, P., Pletschke, B. I., Singh, P. K., & Shukla, P. (2018). Vaccine and antibody production in plants: Developments and computational tools. *Briefings in Functional Genomics*, *17*(5), 295–307. https://doi.org/10.1093/bfgp/ely020

Dunkelblum, E., Zada, A., Gross, S., Fraistat, P., & Mendel, Z. (2002). Sex pheromone and analogs of the citrus mealybug, *Planococcus citri*: synthesis and biological activity. *IOBC-WPRS Bullertins*, *25*.

Eckardt, N. A., Ainsworth, E. A., Bahuguna, R. N., Broadley, M. R., Busch, W., Carpita, N. C., … Zhang, X. (2023). Climate change challenges, plant science solutions. *Plant*

Cell, *35*(1), 24–66. https://doi.org/10.1093/plcell/koac303

European Commission. (2020). Chlorpyrifos & Chlorpyrifos-methyl. Retrieved from https://food.ec.europa.eu/plants/pesticides/approval-active-substances/renewal-approval/chlorpyrifos-chlorpyrifos-methyl_en

European Commission. (2022). Green Deal: pioneering proposals to restore Europe's nature by 2050 and halve pesticide use by 2030. Retrieved from https://ec.europa.eu/commission/presscorner/detail/en/ip_22_3746

Fakhfakh, H., Vilaine, F., Makni, M., & Robaglia, C. (1996). Cell-free cloning and biolistic inoculation of an infectious cDNA of potato virus Y. *Journal of General Virology*, *77*(3), 519–523. https://doi.org/10.1099/0022-1317-77-3-519

FAOSTAT. (2023). Pesticides Use. Retrieved from https://www.fao.org/faostat/en/#data/RP

Fontdevila Pareta, N., Khalili, M., Maachi, A., Rivarez, M. P. S., Rollin, J., Salavert, F., … Massart, S. (2023). Managing the deluge of newly discovered plant viruses and viroids: an optimized scientific and regulatory framework for their characterization and risk analysis. *Frontiers in Microbiology*, *14*, 1181562. https://doi.org/10.3389/fmicb.2023.1181562

Franco, J. C., Cocco, A., Lucchi, A., Mendel, Z., Suma, P., Vacas, S., … Navarro-Llopis, V. (2022). Scientific and technological developments in mating disruption of scale insects. *Entomologia Generalis*, *42*(2), 251–273. https://doi.org/10.1127/entomologia/2021/1220

Gaffney, J., Bing, J., Byrne, P. F., Cassman, K. G., Ciampitti, I., Delmer, D., … Warner, D. (2019). Science-based intensive agriculture: Sustainability, food security, and the role of technology. *Global Food Security*, *23*, 236–244. https://doi.org/10.1016/j.gfs.2019.08.003

Garcia-Perez, E., Diego-Martin, B., Quijano-Rubio, A., Moreno-Giménez, E., Selma, S., Orzaez, D., & Vazquez-Vilar, M. (2022). A copper switch for inducing CRISPR/Cas9-based transcriptional activation tightly regulates gene expression in *Nicotiana benthamiana*. *BMC Biotechnology*, *22*, 12. https://doi.org/10.1186/S12896-022-00741-X/FIGURES/4

Garcia-Ruiz, H. (2019). Host factors against plant viruses. *Molecular Plant Pathology*, *20*(11), 1588–1601. https://doi.org/10.1111/mpp.12851

Gavrilescu, M., & Chisti, Y. (2005). Biotechnology - A sustainable alternative for chemical industry. *Biotechnology Advances*, *23*(7–8), 471–499. https://doi.org/10.1016/j.biotechadv.2005.03.004

Gerasymenko, I., Sheludko, Y. V., Navarro Fuertes, I., Schmidts, V., Steinel, L., Haumann, E., & Warzecha, H. (2022). Engineering of a Plant Isoprenyl Diphosphate Synthase for Development of Irregular Coupling Activity. *ChemBioChem*, *23*(1), e202100465. https://doi.org/10.1002/cbic.202100465

Gold, K. M. (2021). Plant Disease Sensing: Studying Plant-Pathogen Interactions at Scale. *MSystems*, *6*(6), e01228-21. https://doi.org/10.1128/msystems.01228-21

Goulson, D. (2013). An overview of the environmental risks posed by neonicotinoid insecticides. *Journal of Applied Ecology*, *50*(4), 977–987. https://doi.org/10.1111/1365-2664.12111

Gunstone, T., Cornelisse, T., Klein, K., Dubey, A., & Donley, N. (2021). Pesticides and Soil Invertebrates: A Hazard Assessment. *Frontiers in Environmental Science*, *9*, 643847. https://doi.org/10.3389/fenvs.2021.643847

Guo, Q., Major, I. T., & Howe, G. A. (2018). Resolution of growth–defense conflict: mechanistic insights from jasmonate signaling. *Current Opinion in Plant Biology*, *44*, 72–81. https://doi.org/10.1016/j.pbi.2018.02.009

Hagström, Å. K., Wang, H.-L., Liénard, M. A., Lassance, J.-M., Johansson, T., & Löfstedt, C. (2013). A moth pheromone brewery: production of (*Z*)-11-hexadecenol by heterologous co-expression of two biosynthetic genes from a noctuid moth in a yeast cell factory. *Microbial Cell Factories*, *12*, 125. https://doi.org/10.1186/1475-2859-12-125

Hayes, B. J., Chen, C., Powell, O., Dinglasan, E., Villiers, K., Kemper, K. E., & Hickey, L. T. (2023). Advancing artificial intelligence to help feed the world. *Nature Biotechnology*, *41*(9), 1188–1189. https://doi.org/10.1038/s41587-023-01898-2

Heck, M. (2018). Insect Transmission of Plant Pathogens: a Systems Biology Perspective. *MSystems*, *3*(2), e00168-17.

Heinrich, M., Hettenhausen, C., Lange, T., Wünsche, H., Fang, J., Baldwin, I. T., & Wu, J. (2013). High levels of jasmonic acid antagonize the biosynthesis of gibberellins and inhibit the growth of *Nicotiana attenuata* stems. *Plant Journal*, *73*(4), 591–606. https://doi.org/10.1111/tpj.12058

Holkenbrink, C., Ding, B.-J., Wang, H.-L., Dam, M. I., Petkevicius, K., Kildegaard, K. R., … Borodina, I. (2020). Production of moth sex pheromones for pest control by yeast fermentation. *Metabolic Engineering*, *62*, 312–321. https://doi.org/10.1016/j.ymben.2020.10.001

Hommay, G., Alliaume, A., Reinbold, C., & Herrbach, E. (2021). Transmission of Grapevine leafroll-associated virus-1 (Ampelovirus) and Grapevine virus A (Vitivirus) by the Cottony Grape Scale, *Pulvinaria vitis* (Hemiptera:Coccidea). *Viruses*, *13*(10), 2081.

Jaiswal, D. K., Gawande, S. J., Soumia, P. S., Krishna, R., Vaishnav, A., & Ade, A. B. (2022). Biocontrol strategies: an eco-smart tool for integrated pest and diseases management. *BMC Microbiology*, *22*, 324. https://doi.org/10.1186/s12866-022-02744-2

Jakab, G., Droz, E., Brigneti, G., Baulcombe, D., & Malnoë, P. (1997). Infectious *in vivo* and *in vitro* transcripts from a full-length cDNA clone of PVY-N605, a Swiss necrotic isolate of potato virus Y. *Journal of General Virology*, *78*(12), 3141–3145. https://doi.org/10.1099/0022-1317-78-12-3141

Jarstfer, M. B., Zhang, D.-L., & Poulter, C. D. (2002). Recombinant squalene synthase. Synthesis of non-head-to-tail isoprenoids in the absence of NADPH. *Journal of the American Chemical Society*, *124*(30), 8834–8845. https://doi.org/10.1021/ja020410i

Juroszek, P., Racca, P., Link, S., Farhumand, J., & Kleinhenz, B. (2020). Overview on the review articles published during the past 30 years relating to the potential climate change effects on plant pathogens and crop disease risks. *Plant Pathology*, *69*(2), 179–193. https://doi.org/10.1111/ppa.13119

Kakoti, B., Deka, B., Roy, S., & Babu, A. (2023). The scale insects: Its status, biology,

ecology and management in tea plantations. *Frontiers in Insect Science*, *2*, 1048299. https://doi.org/10.3389/finsc.2022.1048299

Kežar, A., Kavčič, L., Polák, M., Nováček, J., Gutiérrez-Aguirre, I., Žnidarič, M. T., … Podobnik, M. (2019). Structural basis for the multitasking nature of the potato virus Y coat protein. *Science Advances*, *5*(7), eaaw3808. https://doi.org/10.1126/sciadv.aaw3808

Kim, J. H., Castroverde, C. D. M., Huang, S., Li, C., Hilleary, R., Seroka, A., … He, S. Y. (2022). Increasing the resilience of plant immunity to a warming climate. *Nature*, *607*(7918), 339–344. https://doi.org/10.1038/s41586-022-04902-y

Kobayashi, M., & Kuzuyama, T. (2018). Structural and Mechanistic Insight into Terpene Synthases that Catalyze the Irregular Non-Head-to-Tail Coupling of Prenyl Substrates. *ChemBioChem*, *20(1)*, 29-33. https://doi.org/10.1002/cbic.201800510

Kreuze, J. F., Souza-Dias, J. A. C., Jeevalatha, A., Figueira, A. R., Valkonen, J. P. T., & Jones, R. A. C. (2019). Viral Diseases in Potato. In H. Campos & O. Ortiz (Eds.), *The Potato Crop* (pp. 389–430). Springer Cham.

Kurotani, K. I., Hirakawa, H., Shirasawa, K., Tanizawa, Y., Nakamura, Y., Isobe, S., & Notaguchi, M. (2023). Genome Sequence and Analysis of *Nicotiana benthamiana*, the Model Plant for Interactions between Organisms. *Plant & Cell Physiology*, *64*(2), 248–257. https://doi.org/10.1093/pcp/pcac168

Lassance, J. M., Ding, B.-J., & Löfstedt, C. (2021). Evolution of the codling moth pheromone via an ancient gene duplication. *BMC Biology*, *19*, 83. https://doi.org/10.1186/s12915-021-01001-8

Lassance, J. M., Groot, A. T., Liénard, M. A., Antony, B., Borgwardt, C., Andersson, F., … Löfstedt, C. (2010). Allelic variation in a fatty-acyl reductase gene causes divergence in moth sex pheromones. *Nature*, *466*(7305), 486–489. https://doi.org/10.1038/nature09058

Li, J., Hu, S., Jian, W., Xie, C., & Yang, X. (2021). Plant antimicrobial peptides: structures, functions, and applications. *Botanical Studies*, *62*, 5. https://doi.org/10.1186/s40529-021-00312-x

Liénard, M. A., Strandh, M., Hedenström, E., Johansson, T., & Löfstedt, C. (2008). Key biosynthetic gene subfamily recruited for pheromone production prior to the extensive radiation of Lepidoptera. *BMC Evolutionary Biology*, *8*, 270. https://doi.org/10.1186/1471-2148-8-270

Löfstedt, C., Wahlberg, N., & Millar, J. G. (2016). Evolutionary Patterns of Pheromone Diversity in Lepidoptera. In J. D. Allison & R. T. Carde (Eds.), *Pheromone Communication in Moths* (pp. 43–78). University of California Press.

Low, G., Dalhaus, T., & Meuwissen, M. P. M. (2023). Mixed farming and agroforestry systems: A systematic review on value chain implications. *Agricultural Systems*, *206*, 103606. https://doi.org/10.1016/j.agsy.2023.103606

Lukan, T., Baebler, Š., Pompe-Novak, M., Guček, K., Zagorščak, M., Coll, A., & Gruden, K. (2018). Cell death is not sufficient for the restriction of potato virus Y spread in hypersensitive response-conferred resistance in potato. *Frontiers in Plant Science*, *9*, 168. https://doi.org/10.3389/fpls.2018.00168

Lukan, T., Pompe-Novak, M., Baebler, Š., Tušek-Žnidarič, M., Kladnik, A., Križnik, M.,

… Gruden, K. (2020). Precision transcriptomics of viral foci reveals the spatial regulation of immune-signaling genes and identifies RBOHD as an important player in the incompatible interaction between potato virus Y and potato. *Plant Journal*, *104*(3), 645–661. https://doi.org/10.1111/tpj.14953

Luo, Z., Magsi, F. H., Li, Z., Cai, X., Bian, L., Liu, Y., … Chen, Z. (2020). Development and evaluation of sex pheromone mass trapping technology for *Ectropis grisescens*: A potential integrated pest management strategy. *Insects*, *11*(1), 15. https://doi.org/10.3390/insects11010015

Mansour, R., Belzunces, L. P., Suma, P., Zappalà, L., Mazzeo, G., Grissa-Lebdi, K., … Biondi, A. (2018). Vine and citrus mealybug pest control based on synthetic chemicals. A review. *Agronomy for Sustainable Development*, *38*(4), 37. https://doi.org/10.1007/s13593-018-0513-7

Marco, S., Loredana, M., Riccardo, V., Raffaella, B., Walter, C., & Luca, N. (2022). Microbe-assisted crop improvement: a sustainable weapon to restore holobiont functionality and resilience. *Horticulture Research*, *9*, uhac160. https://doi.org/10.1093/hr/uhac160

Molina-Hidalgo, F. J., Vazquez-Vilar, M., D'Andrea, L., Demurtas, O. C., Fraser, P., Giuliano, G., … Goossens, A. (2021). Engineering Metabolism in *Nicotiana* Species: A Promising Future. *Trends in Biotechnology*, *39*(9), 901–913. https://doi.org/10.1016/j.tibtech.2020.11.012

Montesinos, E. (2007). Antimicrobial peptides and plant disease control. *FEMS Microbiology Letters*, *270*(1), 1–11. https://doi.org/10.1111/j.1574-6968.2007.00683.x

Mora-Vásquez, S., Wells-Abascal, G. G., Espinosa-Leal, C., Cardineau, G. A., & García-Lara, S. (2022). Application of metabolic engineering to enhance the content of alkaloids in medicinal plants. *Metabolic Engineering Communications*, *14*, e00194. https://doi.org/10.1016/J.MEC.2022.E00194

Nagel, R., Schmidt, A., & Peters, R. J. (2019). Isoprenyl diphosphate synthases : the chain length determining step in terpene biosynthesis. *Planta*, *249*, 9–20. https://doi.org/10.1007/s00425-018-3052-1

Nešněrová, P., Šebek, P., Macek, T., & Svatoš, A. (2004). First semi-synthetic preparation of sex pheromones. *Green Chemistry*, *6*(7), 305–307. https://doi.org/10.1039/b406814a

Nicaise, V. (2014). Crop immunity against viruses: Outcomes and future challenges. *Frontiers in Plant Science*, *5*, 660. https://doi.org/10.3389/fpls.2014.00660

Ogawa, T., Emi, K., Koga, K., Yoshimura, T., & Hemmi, H. (2016). A *cis*-prenyltransferase from *Methanosarcina acetivorans* catalyzes both head-to-tail and nonhead-to-tail prenyl condensation. *FEBS Journal*, *283*(12), 2369–2383. https://doi.org/10.1111/febs.13749

Ortiz, A. M. D., Outhwaite, C. L., Dalin, C., & Newbold, T. (2021). A review of the interactions between biodiversity, agriculture, climate change, and international trade: research and policy priorities. *One Earth*, *4*(1), 88–101. https://doi.org/10.1016/j.oneear.2020.12.008

Ortiz, R., Geleta, M., Gustafsson, C., Lager, I., Hofvander, P., Löfstedt, C., … Stymne, S. (2020). Oil crops for the future. *Current Opinion in Plant Biology*, *56*, 181–189.

https://doi.org/10.1016/j.pbi.2019.12.003

Ozaki, T., Zhao, P., Shinada, T., Nishiyama, M., & Kuzuyama, T. (2014). Cyclolavandulyl Skeleton Biosynthesis via Both Condensation and Cyclization Catalyzed by an Unprecedented Member of the cis - Isoprenyl Diphosphate Synthase Superfamily. *Journal of the American Chemical Society*, *136*(13), 4837–4840.

Pasin, F. (2022). Assembly of plant virus agroinfectious clones using biological material or DNA synthesis. *STAR Protocols*, *3*(4), 101716. https://doi.org/10.1016/j.xpro.2022.101716

Patel, R., Mitra, B., Vinchurkar, M., Adami, A., Patkar, R., Giacomozzi, F., … Baghini, M. S. (2022). A review of recent advances in plant-pathogen detection systems. *Heliyon*, *8*(12), e11855. https://doi.org/10.1016/j.heliyon.2022.e11855

Pathak, V. M., Verma, V. K., Rawat, B. S., Kaur, B., Babu, N., Sharma, A., … Cunill, J. M. (2022). Current status of pesticide effects on environment, human health and it's eco-friendly management as bioremediation: A comprehensive review. *Frontiers in Microbiology*, *13*, 962619. https://doi.org/10.3389/fmicb.2022.962619

Petkevicius, K., Löfstedt, C., & Borodina, I. (2020). Insect sex pheromone production in yeasts and plants. *Current Opinion in Biotechnology*, *65*, 259–267. https://doi.org/10.1016/j.copbio.2020.07.011

Pingali, P. L. (2012). Green revolution: Impacts, limits, and the path ahead. *Proceedings of the National Academy of Sciences of the United States of America*, *109*(31), 12302–12308. https://doi.org/10.1073/pnas.0912953109

Puig, A. S., Wurzel, S., Suarez, S., Marelli, J.-P., & Niogret, J. (2021). Mealybug (Hemiptera: Pseudococcidae) species associated with cacao mild mosaic virus and evidence of virus acquisition. *Insects*, *12*(11), 994. https://doi.org/10.3390/insects12110994

Qian, Y., & Huang, S. C. (2020). Improving plant gene regulatory network inference by integrative analysis of multi-omics and high resolution data sets. *Current Opinion in Systems Biology*, *22*, 8–15. https://doi.org/10.1016/j.coisb.2020.07.010

Quesada, C. R., Witte, A., & Sadof, C. S. (2018). Factors influencing insecticide efficacy against armored and soft scales. *HortTechnology*, *28*(3), 267–275. https://doi.org/10.21273/HORTTECH03993-18

Ranawaka, B., An, J., Lorenc, M. T., Jung, H., Sulli, M., Aprea, G., … Waterhouse, P. M. (2023). A multi-omic *Nicotiana benthamiana* resource for fundamental research and biotechnology. *Nature Plants*, *9*(9), 1558–1571. https://doi.org/10.1038/s41477-023-01489-8

Raven, P. H., & Wagner, D. L. (2021). Agricultural intensification and climate change are rapidly decreasing insect biodiversity. *Proceedings of the National Academy of Sciences of the United States of America*, *118*(2), e2002548117. https://doi.org/10.1073/PNAS.2002548117

Ray, D. K., Ramankutty, N., Mueller, N. D., West, P. C., & Foley, J. A. (2012). Recent patterns of crop yield growth and stagnation. *Nature Communications*, *3*, 1293. https://doi.org/10.1038/ncomms2296

Ristaino, J. B., Anderson, P. K., Bebber, D. P., Brauman, K. A., Cunniffe, N. J., Fedoroff, N. V., … Wei, Q. (2021). The persistent threat of emerging plant disease pandemics

to global food security. *Proceedings of the National Academy of Sciences*, *118*(23), e2022239118. https://doi.org/10.1073/pnas.2022239118

Rivera, S. B., Swedlund, B. D., King, G. J., Bell, R. N., Hussey, C. E., Shattuck-Eidens, D. M., … Poulter, C. D. (2001). Chrysanthemyl diphosphate synthase : Isolation of the gene and characterization of the recombinant non-head-to-tail monoterpene synthase from *Chrysanthemum cinerariaefolium*. *Proceedings of the National Academy of Sciences*, *98*(8), 4373–4378.

Rizvi, S. A. H., George, J., Reddy, G. V. P., Zeng, X., & Guerrero, A. (2021). Latest Developments in Insect Sex Pheromone Research and Its Application in Agricultural Pest Management. *Insects*, *12*(6), 484. https://doi.org/10.3390/INSECTS12060484

Roelofs, W. L., Liu, W., Hao, G., Jiao, H., Rooney, A. P., & Linn, C. E. (2002). Evolution of moth sex pheromones via ancestral genes. *Proceedings of the National Academy of Sciences of the United States of America*, *99*(21), 13621–13626. https://doi.org/10.1073/pnas.152445399

Rupar, M., Faurez, F., Tribodet, M., Gutierrez-Aguirre, I., Delaunay, A., Glais, L., … Ravnikar, M. (2015). Fluorescently tagged Potato virus Y: a versatile tool for functional analysis of plant-virus interactions. *Molecular Plant-Microbe Interactions : MPMI*, *28*(7), 739–750. https://doi.org/10.1094/MPMI-07-14-0218-TA

Schneider, L., Rebetez, M., & Rasmann, S. (2022). The effect of climate change on invasive crop pests across biomes. *Current Opinion in Insect Science*, *50*, 100895. https://doi.org/10.1016/j.cois.2022.100895

Sethi, L., Kumari, K., & Dey, N. (2021). Engineering of Plants for Efficient Production of Therapeutics. *Molecular Biotechnology*, *63*(12), 1125–1137. https://doi.org/10.1007/s12033-021-00381-0

Singh, B. K., Delgado-Baquerizo, M., Egidi, E., Guirado, E., Leach, J. E., Liu, H., & Trivedi, P. (2023). Climate change impacts on plant pathogens, food security and paths forward. *Nature Reviews Microbiology*, *21*(10), 640–656. https://doi.org/10.1038/s41579-023-00900-7

Sirirungruang, S., Markel, K., & Shih, P. M. (2022). Plant-based engineering for production of high-valued natural products. *Natural Product Reports*, *39*(7), 1492–1509. https://doi.org/10.1039/d2np00017b

Son, S., & Park, S. R. (2022). Climate change impedes plant immunity mechanisms. *Frontiers in Plant Science*, *13*, 1032820. https://doi.org/10.3389/fpls.2022.1032820

Stare, K., Coll, A., Gutiérrez-Aguirre, I., Žnidarič, M. T., Ravnikar, M., Kežar, A., … Gruden, K. (2020). Generation and in Planta Functional Analysis of Potato Virus Y mutants. *Bio-Protocol*, *10*(14), e3692. https://doi.org/10.21769/BioProtoc.3692

Suckling, D. M., Conlong, D. E., Carpenter, J. E., Bloem, K. A., Rendon, P., & Vreysen, M. J. B. (2017). Global range expansion of pest Lepidoptera requires socially acceptable solutions. *Biological Invasions*, *19*(4), 1107–1119. https://doi.org/10.1007/s10530-016-1325-9

Thimm, O., Bläsing, O., Gibon, Y., Nagel, A., Meyer, S., Krüger, P., … Stitt, M. (2004). MAPMAN: A user-driven tool to display genomics data sets onto diagrams of metabolic pathways and other biological processes. *Plant Journal*, *37*(6), 914–939. https://doi.org/10.1111/j.1365-313X.2004.02016.x

Thulasiram, H. V, Erickson, H. K., & Poulter, C. D. (2007). Chimeras of Two Isoprenoid Synthases Catalyze All Four Coupling Reactions in Isoprenoid Biosynthesis. *Science*, *73*(316), 73–77. https://doi.org/10.1126/science.1137786

Trapani, S., Bhat, E. A., Yvon, M., Lai-Kee-Him, J., Hoh, F., Vernerey, M. S., … Bron, P. (2023). Structure-guided mutagenesis of the capsid protein indicates that a nanovirus requires assembled viral particles for systemic infection. *PLoS Pathogens*, *19*(1), e1011086. https://doi.org/10.1371/journal.ppat.1011086

Tsai, W.-A., Brosnan, C. A., Mitter, N., & Dietzgen, R. G. (2022). Perspectives on plant virus diseases in a climate change scenario of elevated temperatures. *Stress Biology*, *2*(1), 37. https://doi.org/10.1007/s44154-022-00058-x

Tschofen, M., Knopp, D., Hood, E., & Stöger, E. (2016). Plant Molecular Farming: Much More than Medicines. *Annual Review of Analytical Chemistry*, *9*, 271–294. https://doi.org/10.1146/annurev-anchem-071015-041706

Tupec, M., Buček, A., Valterová, I., & Pichová, I. (2017). Biotechnological potential of insect fatty acid-modifying enzymes. *Zeitschrift Fur Naturforschung - Section C*, *72*(9–10), 387–403. https://doi.org/10.1515/znc-2017-0031

Tyczewska, A., Twardowski, T., & Woźniak-Gientka, E. (2023). Agricultural biotechnology for sustainable food security. *Trends in Biotechnology*, *41*(3), 331–341. https://doi.org/10.1016/j.tibtech.2022.12.013

Uranga, M., Aragonés, V., Daròs, J. A., & Pasin, F. (2023). Heritable CRISPR-Cas9 editing of plant genomes using RNA virus vectors. *STAR Protocols*, *4*, 102091. https://doi.org/10.1016/j.xpro.2023.102091

Van Den Berge, K., Hembach, K. M., Soneson, C., Tiberi, S., Clement, L., Love, M. I., … Robinson, M. D. (2019). RNA Sequencing Data: Hitchhiker's Guide to Expression Analysis. *Annual Review of Biomedical Data Science*, *2*, 139–173. https://doi.org/10.1146/annurev-biodatasci-072018-021255

Vazquez-Vilar, M., Selma, S., & Orzaez, D. (2023). The design of synthetic gene circuits in plants: new components, old challenges. *Journal of Experimental Botany*, *74*(13), 3791–3805. https://doi.org/10.1093/jxb/erad167

Velásquez, A. C., Castroverde, C. D. M., & He, S. Y. (2018). Plant–Pathogen Warfare under Changing Climate Conditions. *Current Biology*, *28*(10), R619–R634. https://doi.org/10.1016/j.cub.2018.03.054

Vollheyde, K., Dudley, Q. M., Yang, T., Oz, M. T., Mancinotti, D., Fedi, M. O., … Patron, N. J. (2023). An improved *Nicotiana benthamiana* bioproduction chassis provides novel insights into nicotine biosynthesis. *New Phytologist*, *240*(1), 302–317. https://doi.org/10.1111/nph.19141

Wallrapp, F. H., Pan, J.-J., Ramamoorthy, G., Almonacid, D. E., Hillerich, B. S., Seidel, R., … Poulter, C. D. (2013). Prediction of function for the polyprenyl transferase subgroup in the isoprenoid synthase superfamily. *Proceedings of the National Academy of Sciences*, *110*(13), E1196–E1202. https://doi.org/10.1073/pnas.1300632110

Wang, H.-L., Ding, B.-J., Dai, J.-Q., Nazarenus, T. J., Borges, R., Mafra-Neto, A., … Löfstedt, C. (2022). Insect pest management with sex pheromone precursors from engineered oilseed plants. *Nature Sustainability*, *5*(11), 981–990.

https://doi.org/10.1038/s41893-022-00949-x

Wieczorek, P., Budziszewska, M., Frąckowiak, P., & Obrępalska-Stęplowska, A. (2020). Development of a new tomato torrado virus-based vector tagged with GFP for monitoring virus movement in plants. *Viruses*, *12*(10), 1195. https://doi.org/10.3390/v12101195

Wing, I. S., De Cian, E., & Mistry, M. N. (2021). Global vulnerability of crop yields to climate change. *Journal of Environmental Economics and Management*, *109*, 102462. https://doi.org/10.1016/j.jeem.2021.102462

Witzgall, P., Kirsch, P., & Cork, A. (2010). Sex pheromones and their impact on pest management. *Journal of Chemical Ecology*, *36*, 80–100. https://doi.org/10.1007/s10886-009-9737-y

Xia, Y.-H., Ding, B.-J., Dong, S.-L., Wang, H.-L., Hofvander, P., & Löfstedt, C. (2022). Release of moth pheromone compounds from *Nicotiana benthamiana* upon transient expression of heterologous biosynthetic genes. *BMC Biology*, *20*, 80. https://doi.org/10.1186/s12915-022-01281-8

Xia, Y.-H., Ding, B.-J., Wang, H.-L., Hofvander, P., Jarl-Sunesson, C., & Löfstedt, C. (2020). Production of moth sex pheromone precursors in *Nicotiana* spp.: a worthwhile new approach to pest control. *Journal of Pest Science*, *93*, 1333–1346. https://doi.org/10.1007/s10340-020-01250-6

Xia, Y.-H., Wang, H.-L., Ding, B.-J., Svensson, G. P., Jarl-Sunesson, C., Cahoon, E. B., … Löfstedt, C. (2021). Green Chemistry Production of Codlemone, the Sex Pheromone of the Codling Moth (*Cydia pomonella*), by Metabolic Engineering of the Oilseed Crop Camelina (*Camelina sativa*). *Journal of Chemical Ecology*, *47*(12), 950–967. https://doi.org/10.1007/s10886-021-01316-4

Yang, D. L., Yao, J., Mei, C. S., Tong, X. H., Zeng, L. J., Li, Q., … He, S. Y. (2012). Plant hormone jasmonate prioritizes defense over growth by interfering with gibberellin signaling cascade. *Proceedings of the National Academy of Sciences of the United States of America*, *109*(19), E1192-E1200. https://doi.org/10.1073/PNAS.1201616109

Yang, L.-N., Ren, M., & Zhan, J. (2023). Modeling plant diseases under climate change: evolutionary perspectives. *Trends in Plant Science*, *28*(5), 519–526. https://doi.org/10.1016/j.tplants.2022.12.011

Yang, X., Medford, J. I., Markel, K., Shih, P. M., De Paoli, H. C., Trinh, C. T., … Tuskan, G. A. (2020). Plant Biosystems Design Research Roadmap 1.0. *BioDesign Research*, *2020*, 8051764. https://doi.org/10.34133/2020/8051764

Zaidi, S. S.-A., Mahas, A., Vanderschuren, H., & Mahfouz, M. M. (2020). Engineering crops of the future: CRISPR approaches to develop climate-resilient and disease-resistant plants. *Genome Biology*, *21*, 289. https://doi.org/10.1186/s13059-020-02204-y

Zhang, H., Zhao, Y., & Zhu, J. K. (2020). Thriving under Stress: How Plants Balance Growth and the Stress Response. *Developmental Cell*, *55*(5), 529–543. https://doi.org/10.1016/j.devcel.2020.10.012

Zhao, C., Liu, B., Piao, S., Wang, X., Lobell, D. B., Huang, Y., … Asseng, S. (2017). Temperature increase reduces global yields of major crops in four independent estimates. *Proceedings of the National Academy of Sciences of the United States of*

America, 114(35), 9326–9331. https://doi.org/10.1073/pnas.1701762114

Zhao, Yaling, Yang, X., Zhou, G., & Zhang, T. (2020). Engineering plant virus resistance: from RNA silencing to genome editing strategies. *Plant Biotechnology Journal, 18*(2), 328–336. https://doi.org/10.1111/pbi.13278

Zhao, Yan, Zhu, X., Chen, X., & Zhou, J.-M. (2022). From plant immunity to crop disease resistance. *Journal of Genetics and Genomics, 49*(8), 693–703. https://doi.org/10.1016/j.jgg.2022.06.003

Zou, Y., & Millar, J. G. (2015). Chemistry of the pheromones of mealybug and scale insects. *Natural Product Reports, 32*(7), 1067–1113. https://doi.org/10.1039/c4np00143e

Žunič Kosi, A., Stritih Peljhan, N., Zou, Y., McElfresh, J. S., & Millar, J. G. (2019). A male-produced aggregation-sex pheromone of the beetle *Arhopalus rusticus* (Coleoptera: Cerambycidae, Spondylinae) may be useful in managing this invasive species. *Scientific Reports, 9*, 19570. https://doi.org/10.1038/s41598-019-56094-7

Bibliography

Publications Related to the Thesis

Mateos Fernández, R., Petek, M., Gerasymenko, I., Juteršek, M., Baebler, Š., Kallam, K., … Patron, N. J. (2022). Insect pest management in the age of synthetic biology. *Plant Biotechnology Journal, 20*(1), 25–36. https://doi.org/10.1111/pbi.13685

Mateos-Fernández, R., Moreno-Giménez, E., Gianoglio, S., Quijano-Rubio, A., Gavaldá-García, J., Estellés, L., … Orzáez, D. (2021). Production of Volatile Moth Sex Pheromones in Transgenic *Nicotiana benthamiana* Plants. *BioDesign Research, 2021*, 9891082. https://doi.org/10.34133/2021/9891082

Juteršek, M., Petek, M., Ramšak, Ž., Moreno-Giménez, E., Gianoglio, S., Mateos-Fernández, R., … Baebler, Š. (2022). Transcriptional deregulation of stress-growth balance in *Nicotiana benthamiana* biofactories producing insect sex pheromones. *Frontiers in Plant Science, 13*, 941338. https://doi.org/10.3389/fpls.2022.941338

Juteršek, M., Gerasymenko, I. M., Petek, M., Haumann, E., González, S. V., Kallam, K., … Baebler, Š. (2023). Identification and characterisation of *Planococcus citri cis*- and *trans*-isoprenyl diphosphate synthase genes, supported by short- and long-read transcriptome data. *BioRxiv*. https://doi.org/10.1101/2023.06.09.544309

Lukan, T., Županič, A., Mahkovec Povalej, T., Brunkard, J. O., Kmetič, M., Juteršek, M., … Gruden, K. (2023). Chloroplast redox state changes mark cell-to-cell signaling in the hypersensitive response. *New Phytologist, 237*(2), 548–562. https://doi.org/10.1111/nph.18425

Biography

Mojca Juteršek was born on November 15, 1993, in Ljubljana, Slovenia. She attended primary school in Šmartno pri Litiji and high school in Litija. In 2012, she enrolled in the bachelor study programme Biochemistry at the Faculty of Chemistry and Chemical Technology, University of Ljubljana. Graduating in 2015, she received the Faculty Prešeren Award for her bachelor's thesis describing the use of ribosomal RNA genomic sequences for identification and differentiation of cyanobacteria from the *Synechocystis* genus, completed under the supervision of Prof. Dr. Marko Dolinar (Faculty of Chemistry and Chemical Technology, University of Ljubljana). She continued her studies by enrolling in the master study programme Biochemistry (Faculty of Chemistry and Chemical Technology, University of Ljubljana). In 2018, she defended her master's thesis on the topic of genetic tools for synthetic biology approaches in cyanobacteria. Her work, completed under the supervision of Prof. Dr. Marko Dolinar was also awarded the Faculty Prešeren Award. The results of her undergraduate theses have been published in peer-reviewed journals. In 2018, she enrolled in the PhD programme Nanosciences and Nanotechnologies at the Jožef Stefan International Postgraduate School (Ljubljana, Slovenia) and started working as a young researcher at the Department of Biotechnology and Systems Biology at the National Institute of Biology (Ljubljana, Slovenia) under the supervision of Assist. Prof. Dr. Špela Baebler. She was involved in the European project SUSPHIRE, aiming to develop biotechnological production of insect sex pheromones in plants. Her work included analyses of transcriptomic data from plants and insects with the aim to improve the robustness of biotechnological production in plants and to find insect genes that could be implemented for sex pheromone bioproduction. She was also involved in research concerning crop resilience to viral infections, to which she contributed by constructing a reporter clone of potato virus Y that enables detection of viral spread with confocal microscopy. She attended several workshops, including a training school dedicated to big data analysis (Athens, Greece), a workshop on modelling in systems biology (Heidelberg, Germany), a summer school on environmental signalling in plants (Utrecht, The Netherlands), and a 40-hour training on Python programming language (Ljubljana, Slovenia). She also actively participated at national and international conferences with poster presentations or short talks. She was active at several science popularisation events in Slovenia, such as TEDxUL, Slovenian Science Fair, Science Slam, Plant Fascination Day, and Researchers' Night, and contributed a chapter in a children's book with fascinating plant-related experiments. She was also a member of the organising committee for the 5th Conference on Plant Proteases 2022 in Ljubljana.